Joana Margarida Fernandes Galvão

Evaluation of the potential protective effects of adenosine A3 receptor in retinal ganglion cell degeneration

May 2013

Universidade de Coimbra

Joana Margarida Fernandes Galvão

Evaluation of the potential protective effects of adenosine A3 receptor in retinal ganglion cell degeneration

UNIVERSIDADE DE COIMBRA

Evaluation of the potential protective effect of adenosine A3 receptor against retinal ganglion cell degeneration

Avaliação do potencial efeito protetor dos recetores do tipo A3 da adenosina na degenerescência das células ganglionares da retina

Joana Margarida Fernandes Galvão

Dissertation presented to Faculty of Medicine of the University of Coimbra in partial fulfilment of the requirements for Doctoral degree in Biomedical Sciences.

Tese de Doutoramento apresentada à Faculdade de Medicina da Universidade de Coimbra para prestação de provas para obtenção do grau de Doutor, na especialidade de Ciências Biomédicas.

University of Coimbra

2013

Acknowledgments

I would like to express my sincere gratitude to my supervisor, Doctor Francisco Ambrósio for the continuous support for my PhD study and research, for all the valuable suggestions, patience and helpful discussion of my work. Many thanks for being so understandable and always giving me your wise opinion.

I would also like to thank my co-supervisor Professor Miguel Castelo-Branco for his help to this work.

I would like to express my most sincere gratitude to Professor Francesca Cordeiro which was the mentor of the work done at UCL, London. Many thanks for her support, helpful suggestions, advice and always pushing for new ideas. I would also like to thank Francesca to encouraging me to present my work in international conferences and always being enthusiastic about my work.

To Raquel Santiago, for all her friendly help and teaching in the first year of my PhD, most valuable for all the work I developed in this thesis. Furthermore, I would like to thank her for all the suggestions, and friendship, throughout these four years.

I would like to thank Li Guo for her help with the animal models used in this study. She has been very patient and always very helpful when I needed an extra hand.

To Professor Elena Vecino, from the University of Basque Country, for all her enthusiasm and help in the beginning of this work, and for receiving me in her lab, where I had the opportunity of learning the episcleral vein cauterization animal model of glaucoma used in her lab.

My sincere appreciation is extended to Professor Claire Mitchell from Penn State University, USA, for the discussion and interesting suggestions about my work.

A special thanks to Shereen, Eddie, Mark and Ben for their help, suggestions and support, all of them deserve a mention as they were always there when I had any problem, needed a hand or just for a talk. Many thanks!

I would especially like to thank João Martins for all our discussions from the beginning till the end of this work. For his support and help whenever I need it.

A big thank you to all my Portuguese colleagues at IBILI and my friends at UCL London, for the words, lunch breaks and support day after day, Jenny, Elisa, Abu, Simon, Katarina, Abeir, James, Katie, Ingrid, Tom, Ahmed, Natalie, Zanetta, and all other members of the Institute of Ophthalmology for the good time we spent together over these years.

To all my friends in Portugal and London that had to put up with my boring conversations about my work, their support was most valuable, a special thanks to Inês, Carla and Mariana.

I would like to express my deepest gratitude to my family; my father, my mother, my brother, my auntie, and Ninita for their love and encouragement. Without them this work would have not been possible. Thank you for your patience and unconditional support.

I would like to thank The Foundation for Science and Technology (fellowship SFRH/BD/47947/2008), co-financed by QREN (European Social Fund).

The results presented in this dissertation are published or were submitted for publication in peer-reviewed scientific journals

Galvao J, Davis BM, Cordeiro MF (2013). In vivo imaging of retinal ganglion cells apoptosis. Curr Opin Pharmacol. Feb;13(1):123-7. Doi:10.1016/j.coph.2012.08.007. Epub 2012 Sep 17. PMID: 22995681. I.F. 5.44.

Galvao J, Davis B, Tilley M, Normando E, Duchen M, Cordeiro MF (2013). Unexpected low dose toxicity of the universal solvent, DMSO (accepted for publication at The FASEB Journal, I.F. 5.70).

Galvao J, Elvas F, Martins T, Cordeiro MF, Ambrósio AF, Santiago AR (2013). Activation of adenosine A3 receptor is neuroprotective against the degeneration of retinal ganglion cells (under submission to Neurobiology of Diseases, I.F. 5.6).

Galvao J, Guo L, Santiago AR, Ambrósio AF, Cordeiro MF (2013). Activation of adenosine A3 receptor is neuroprotective to retinal neuronal degeneration in rat models of partial optic nerve transection and ocular hypertension (under submission to Invest Ophthalmol Vis Sci, I.F. 3.44).

Galvao J, Santiago AR, Ambrósio AF. Adenosine in the retina. (Review under preparation).

Table of Contents

Abstract

Glaucoma is a degenerative optic neuropathy, characterized by atrophy of the optic nerve and loss of retinal ganglion cells (RGCs). Increased intraocular pressure (IOP) is the major risk factor for glaucoma, although a significant number of patients continue to lose vision despite successful IOP control. Therefore, novel strategies to save RGCs and prevent vision loss are needed.

Adenosine is a neuromodulator in the central nervous system (CNS) through the activation of four different adenosine receptor (AR) subtypes. The modulation of ARs has been shown to be protective against a broad spectrum of brain insults. While in the retina, adenosine A1R has previously been shown to be neuroprotective against an ischemic insult.

In this study, we aimed to investigate the potential neuroprotective effects of the activation of A3 adenosine receptor (A3R) to protect RGCs. We used different *in vitro* and animal models of retinal degeneration to assess the potential neuroprotective effects of A3R agonist, 2-Cl-IB-MECA. Furthermore, in this study we developed a model of retinal degeneration, using dimethyl sulfoxide (DMSO).

We first demonstrated that DMSO induces retinal cell apoptosis *in vivo* at different concentrations: 1, 2, 4 and 8% (v/v). Toxicity was confirmed *in vitro* in a RGC-5 cell line, at DMSO concentrations above 1%, using annexin-V, TUNEL, AlamarBlue and MTT cell viability assays.

We further identified the mechanism by which DMSO (2-4 %, v/v) induces neuronal death. We found DMSO induces AIF translocation to the nucleus triggering a caspase-3 independent mechanism, involving PARP-1 activation. These results highlight safety concerns of using low concentrations of DMSO (2 - 4%) as a solvent for *in vivo* administration, and we propose the use of DMSO as a quick and easy model for retinal degeneration similar to what is already used with NMDA and staurosporine.

The potential neuroprotective effect of A3R activation was evaluated *in vitro* in both retinal mixed cultures and cultured retinal explants using TUNEL and propidium iodide (PI) assays. Neuroprotective effects were also assessed in two acute animal models of

RGC degeneration, namely an animal model of chemical induced RGC death using *in vivo* imaging with Detection of Apoptosing Retinal Cells (DARC) technique and TUNEL assay, as well as a model of retinal ischemia-reperfusion (I-R) injury using TUNEL assay and Brn3a counts. Furthermore, neuroprotective effects were also assessed in two chronic models of RGC degeneration, namely a model of partial optic nerve transection (pONT), at 7 days after transection, and a model of ocular hypertension (OHT), at 3 weeks after induction of hypertension. In these two models, *in vivo* DARC imaging was used to count annexin v-positive cells after treatment with an A3R agonist and the number of RGC loss was also assessed using Brn3a staining.

The A3R agonist, 2-Cl-IB-MECA, decreased the number of TUNEL- (retinal mixed cultures and retinal explants) and PI-positive cells *in vitro*. Furthermore, TUNEL assay was performed in retinal slices of both DMSO and I-R models and a decrease in the number of TUNEL-positive cells was found after treatment with the A3R agonist. *In vivo* imaging also showed a decrease in the number of fluorescently labelled annexin V-positive cells after treatment with 2-Cl-IB-MECA in the acute model of DMSO-induced cell death, and in the two chronic models of RGC degeneration, pONT and OHT models.

The downregulation of the levels of A3R was shown by immunohistochemistry at GC layer in eyes injured by I-R at 24 h reperfusion, pONT at 7 days and OHT model at 3 weeks.

Our results demonstrate that A3R activation is neuroprotective against RGC death, both *in vitro* and in animal models of RGC degeneration. These results suggest that targeting A3R in RGCs may have great potential in the management of glaucoma.

Resumo

O glaucoma é uma doença ocular degenerativa, caraterizada pela atrofia do nervo ótico e pela perda de células ganglionares da retina (CGR). O aumento da pressão intraocular (PIO) é o principal fator de risco no glaucoma. Apesar do controlo adequado da PIO, um número significativo de doentes continua a perder visão. Por isso, são necessárias novas estratégias para proteger as CGR e evitar a perda de visão.

A adenosina é um neuromodulador do sistema nervoso central (SNC) que atua em quatro tipos de recetores da adenosina. Tem sido demonstrado que a modulação dos recetores da adenosina pode causar efeitos protetores contra um largo espetro de insultos cerebrais. Estudos prévios na retina mostraram que a modulação dos recetores da adenosina do tipo A1 induz efeitos neuroprotetores contra um insulto isquémico.

Neste estudo, que teve como objetivo investigar os potenciais efeitos neuroprotetores resultantes da ativação do recetor de adenosina A3, usando o agonista 2-Cl-IB-MECA, nas CGR, foram utilizados diferentes modelos *in vitro* e modelos animais de degenerescência da retina. Além disso, no presente estudo também foi desenvolvido um modelo de degenerescência da retina utilizando o DMSO.

Começou-se por demonstrar que o DMSO (1, 2, 4 e 8% (v/v)) induz apoptose nas células da retina *in vivo*. A toxicidade do DMSO foi confirmada *in vitro* numa linha de células neuronais da retina (RGC-5) para concentrações superiores a 1% de DMSO. Para isso foram usados ensaios de TUNEL e anexina V, assim como um ensaio de viabilidade celular (MTT). Além disso, elucidou-se o mecanismo pelo qual o DMSO (2-4%) induz morte neuronal, nomeadamente através da translocação de AIF da mitocôndria para o núcleo activando uma via de sinalização celular independente da caspase-3, envolvendo a ativação da PARP-1. Estes resultados evidenciam que o DMSO deve de ser usado com precaução como solvente, mesmo a baixas concentrações (2 - 4%), para a administração *in vivo*. Todavia, propõe-se a utilização de injeção intravítrea de DMSO como um modelo para estudar a degenerescência das células da retina, de modo semelhante aos modelos que utilizam a injeção de NMDA e estaurosporina.

O potencial efeito neuroprotetor conferido pela ativação do recetor da adenosina tipo A3 foi avaliado *in vitro*, quer numa cultura mista de células da retina quer em culturas de explantes de retina, utilizando ensaios de TUNEL e iodeto de propídio. Os efeitos neuroprotetores foram ainda avaliados num modelo animal de morte das CGR induzida por injeção intravítrea de DMSO, utilizando imagiologia *in vivo*, nomeadamente a técnica de deteção da apoptose de células da retina (DARC *Detection of Apoptosing Retinal Cells*). No modelo de isquémia-reperfusão também se realizou o ensaio de TUNEL e procedeu-se à contagem de células imunorreativas a Brn3a. Além disso, os efeitos neuroprotetores foram ainda avaliados em dois modelos crónicos de degenerescência das CGR, em particular no modelo de corte parcial do nervo ótico, sete dias após o corte, e no modelo de hipertensão ocular, 3 semanas após a indução de hipertensão ocular. Em ambos os modelos, após o tratamento com o agonista do recetor da adenosina tipo A3 (2-Cl-IB-MECA), foi usada a técnica de imagiologia DARC para contar as células positivas para anexina V, tendo-se também avaliado o número de CGR utilizando um anticorpo que reconhece o Brn3a, um marcador de células ganglionares de retina.

O agonista dos recetor da adenosina tipo A3, 2-Cl-IB-MECA, diminuiu o número de células marcadas com TUNEL, nas cultura mistas de retina e nos explantes de retina, assim como o número de células positivas para iodeto de propídio. Além disso, o ensaio de TUNEL foi realizado em fatias de retina em ambos os modelos animais, ocorrendo uma diminuição no número de células positivas para TUNEL após o tratamento com o agonista dos recetor da adenosina tipo A3.

Utilizando a técnica de imagiologia DARC *in vivo*, detetou-se um decréscimo no número das células positivas para anexina V, após tratamento com 2-Cl-IB-MECA, quer no modelo de morte celular induzida por DMSO, assim como nos dois modelos crónicos de degenerescência de CGR, nomeadamente no modelo de corte parcial do nervo ótico e no modelo de hipertensão ocular.

A imunorreatividade do recetor da adenosina tipo A3 foi analisada por imunohistoquímica em fatias de retina e detetou-se uma diminuição da

imunorreatividade do recetor da adenosina tipo A3 na camada das CGR nos três modelos animais estudados.

Em resumo, os resultados demonstram que a ativação dos recetor da adenosina tipo A3 induz efeitos neuroprotetores para as CGR, tanto em modelos *in vitro* como em modelos animais de degenerescência das CGR. Estes resultados sugerem que a ativação dos recetor da adenosina tipo A3 poderá ter um grande potencial no tratamento do glaucoma.

Abbreviations

ADP - Adenosine diphosphate

AIF - Apoptosis inducing factor

AMP - Adenosine monophosphate

ARL 67156 - 6-N,N-diethyl-d-beta,gamma-d-ibromomethylene

ATP - Adenosine-5'-triphosphate

CADO - 2-chloroadenosine

cAMP - Cyclic adenosine monophosphate

CBD - Cannabidiol

CHA - Cyclohexyladenosine

CNS - Central nervous system

CGS 21680 – 2 - [4 - (2 - carboxyethyl) phenethylamino] – 5 prime – N - ethylcarboxamidoadenosine

CPA - N6-cyclopentyladenosine

DAPI - 4',6-diamidino-2-phenylindole

DED - Death effector domain

DISC - Death-inducing signalling complex

DMSO - Dimethyl sulfoxide

Endo G - Endonuclease G

ERG - Electroretinogram

ETNA - Erythro-9-(2-hydroxy-3-nonyl) adenine

FADD - FAS-associated death domain

FITC - Fluorescein isothiocyanate

GABA - γ- aminobutyric acid

GAPDH - Glyceraldehyde-3-phosphate dehydrogenase

GCL - Ganglion cell layer

GFAP - Glial fibrillary acidic protein

GPCR - G-protein coupled protein

HPLC - High-performance liquid chromatography

INL - Inner nuclear layer

IOP - Intraocular pressure

IP3-R - Inositol trisphosphate receptor

IPDX - 3-isobutyl-8-pyrrolidinoxanthine

IPL - Inner plexiform layer

KA - Kainate

LPS - Lipopolysaccharide

MOMP - Mitochondrial outer membrane permeabilization

mRNA - messenger RNA

NBI - Nitrobenzylthioinosine / NBTI - S-(p-nitro-benzyl)-6-thioninosine

NBMPR - 6-S-[(4-Nitrophenyl)methyl]-6-thioinosine

NECA - 1-(6–Amino-9*H*–purin–9-yl)–1–deoxy-*N*-ethyl–β–D–ribofuranuronamide or 5'-N-ethylcarboxamidoadenosine

NFL - Nerve fibre layer

NGF - Nerve growth factor

NMDA - N-methyl-D-aspartic acid

ON - Optic nerve

ONH - Optic nerve head

ONL - Outer nuclear layer

PARP - Poly(ADP-ribose) polymerase

PCD - Programmed cell death

PKC - Protein kinase C

PLC - Phospholipase C

pONT - Partial optic nerve transection

RGC - Retinal ganglion cell

RNA - Ribonucleic acid

ROS - Reactive oxygen species

RPE - Retinal pigment epithelium

RT-PCR - Real-time reverse-transcriptase polymerase chain reaction

TNF - Tumour necrosis factor

TUNEL - Terminal transferase dUTP nick end labeling

VEGF - Vascular endothelial growth factor

VSCC - Voltage-sensitive calcium channels

2-CN-Ado - 2-(6-cyano-1-hexyn-1-yl) adenosine

8-PT - 8-phenyltheophylline

8-SPT - 8-(p-sulfophenyl) theophylline

1. CHAPTER ONE: Introduction

Table of Contents

1.1 The Eye

1.1.1 Anatomy of the eye

The eye is composed of various structures, being a highly specialized organ allowing vision. The first structure of the eye is the cornea (the first lens of the eye), which is a transparent external surface that protects the pupil and iris. There is a layer of epithelial cells in the cornea that maintains its transparency due to continuous fluid removal. The iris is a pigmented structure in the centre of the eye composed of circular and radial muscles that control the size of the pupil, thus controlling the amount of light that enters the eye. The capacity to increase or decrease the pupil size and the iris aperture is dependent on changes in the intensity of light. In bright light there is a contraction of the circular muscles to reduce the size of the pupil; in dim light the radial muscles are contracted to dilate the pupil.

The crystalline lens (the second lens of the eye) is a biconvex transparent structure that is located in the centre of the posterior part of the eye and is fixed to the ciliary body on both sides by ligaments called zonule fibers. Together with the cornea it is responsible for refracting the light to the retina in the back of the eye. The capability of contraction or relaxation of the zonule fibers allows the eye to produce sharp images at the level of the retina. These structures (iris, lens and ciliary body) divide the eye into two separated cavities: the anterior chamber, containing the aqueous humour, between the iris and the cornea and posterior chamber of the eye, containing the humour vitreous, from the lens till the retina. The anterior chamber is filled with aqueous humour, produced by the ciliary body, which provides nourishment to the avascular lens and cornea. The posterior cavity is filled with humour vitreous, a transparent gel that occupies most of the volume of the eye and helps holding its spherical shape.

The outermost structure of the eye is a white layer of connective tissue called the sclera. It protects the eyeball and merges itself with the transparent cornea. Between the sclera and the retina lies the choroid, which is composed of blood vessels and connective tissue that nourishes the retina.

Light passes through the cornea and pupil to the crystalline lens, where it is directed through the humour vitreous to reach the retina at the back of the eye (Fig 1.1). The maximum focus of the human eye occurs in the fovea, the central point of the macula, due to the high concentration of photosensitive cones.

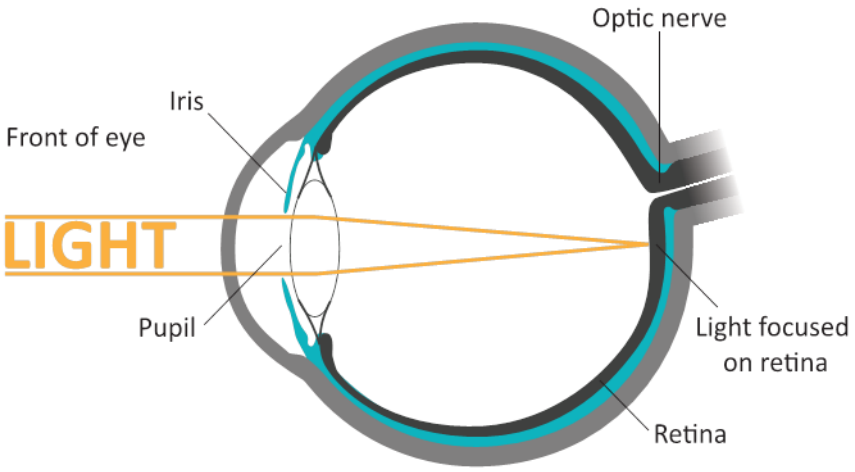

Figure 1.1 - Anatomy of the human eye. Light crosses the cornea, passing through the pupil to the crystalline lens and reaches the retina in the fundus of the eye. Visual information is processed in the retina and sent to the brain through the optic nerve.

1.1.2 Retina

The retina is a layer of neuronal tissue at the back of the eye, and is responsible for transforming the light impulses (photons) reaching the photoreceptors into neurochemical information that will then be transmitted to the visual cortex via the optic nerve. The retina is composed of different cell types: neurons [photoreceptors (rods and cones), bipolar, horizontal, amacrine and ganglion cells], glial cells, vascular cells and epithelial cells. These cells form different layers of the retina (Fig 1.2). The first non-neuronal layer is the retinal pigmented epithelium (RPE), which is in close contact with the choroid through the Bruch's membrane, and is responsible mainly for light absorption and support of photoreceptors, as well as supplying nutrients to the retina (Kevany and Palczewski, 2010). The outer segments of the photoreceptors are next, followed by the inner segments. The nuclei of photoreceptors are located adjacently and represent the outer nuclear layer (ONL). The next layer is designated outer plexiform layer (OPL) and corresponds to the connection between photoreceptors and bipolar and horizontal cells. These three layers correspond to the different parts of the photoreceptors (rods and cones). The inner nuclear layer (INL) represents the region where the nuclei of the bipolar, horizontal and amacrine cells are located. The next layer, the inner plexiform layer, is where bipolar, amacrine and ganglion cells communicate with each other. The ganglion cell layer (GCL) is where the nuclei of retinal ganglion cells (RGCs) are located; their axons represent the nerve fibre layer (NFL), and are the innermost layer of the retina. The axons of the RGCs are joined together to form the optic nerve, via which processed visual information reaches the brain. Müller cells, which represent 90% of the glial cells in the retina, span the entire retina and interact with all cells in this tissue (Pascale et al., 2012).

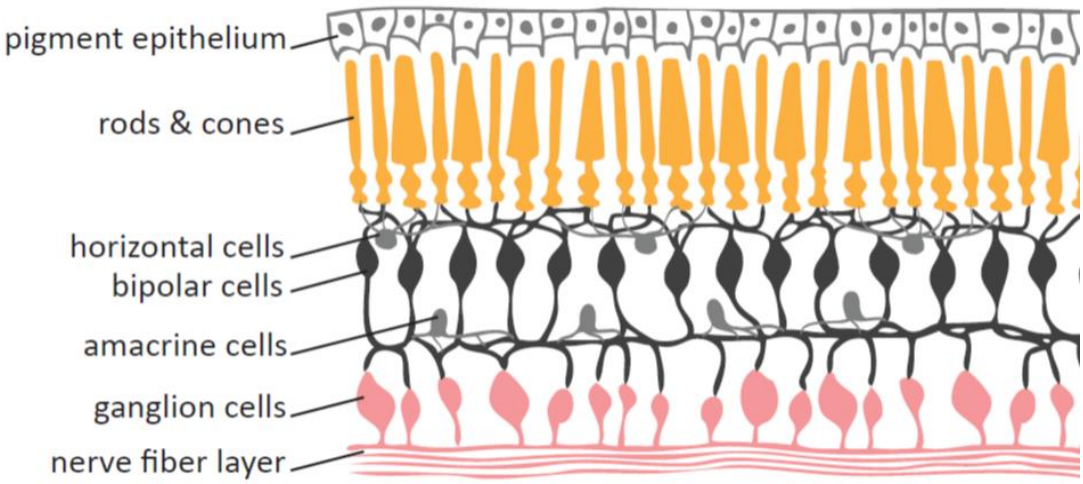

Figure 1.2 - Schematic representation of the retina anatomy. Representation of retinal neuronal cells, from top to bottom: retinal pigmented epithelium, rods and cones photoreceptors (orange), horizontal cells (light grey), bipolar cells (grey), amacrine cells (pale grey) and ganglion cells (pink).

1.1.3 Retinal visual pathway

The neuronal cells in the retina communicate with each other, directly or indirectly, to process visual information. There are two main pathways: the vertical pathway initiates with light being detected by photoreceptors, which in turn sends impulses to bipolar cells, and finally to ganglion cells (Fig 1.3). The lateral pathway occurs both at the level of the outer retina, involving horizontal cells, photoreceptors and bipolar cells, and at the level of the inner retina, involving amacrine cells, bipolar cells and ganglion cells. The vertical pathway is mainly glutamatergic, being excitatory, whereas the lateral pathway is mainly GABAergic or glycinergic, having an inhibitory control of the vertical pathway (Wu, 2010). The stimulation of the visual pigments by light activates the heterotrimeric G-protein transducin, leading to hyperpolarization of photoreceptors due to decrease in cGMP levels. As a consequence of hyperpolarization, less glutamate is released to the bipolar cells, inducing depolarization in the ON bipolar cells (ON cells are depolarized by onset of light, while OFF cells are hyperpolarized by light and depolarized when light is

turned off). Depolarized bipolar cells release glutamate to activate RGCs (Pascale et al., 2012).

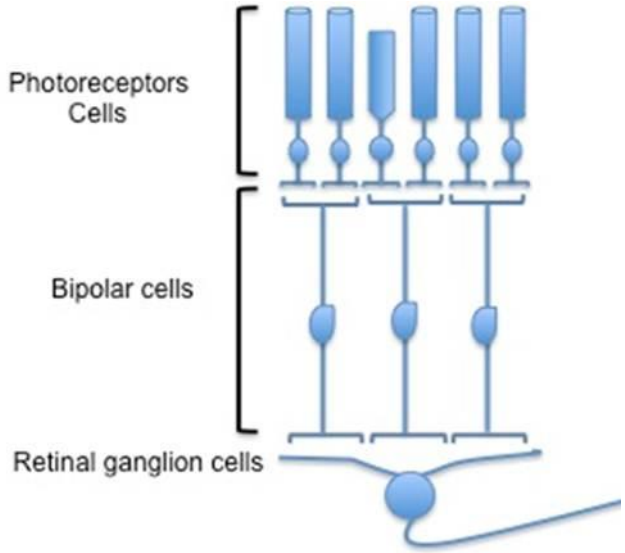

Figure 1.3 - Schematic image of the cells involved in the vertical pathway. Photoreceptors detect the light and communicate with bipolar cells, which in turn communicate with RGCs whose axons then deliver visual information to the brain.

1.1.4 Retinal Ganglion cells

There are 15-20 types of RGCs in the mammalian retina (Sivyer et al., 2011; Wong et al., 2012). RGCs (Fig 1.4) are located in the inner retina, and communicate directly with bipolar and amacrine cells. RGCs are the first cells of the retina where action potentials are generated. RGCs axons are grouped together to form the optic nerve, delivering information to the brain's visual centres, the lateral geniculate nucleus and the superior colliculus. RGCs can be grouped by their response to light: ON, OFF and ON-OFF ganglion cells. RGCs exhibit different physiological properties correlated with their morphology type (Wong et al., 2012). The two most common RGC types are midget cells (or 'P cells'), and the parasol cells (or 'M cells'). P cells are of smaller size with smaller dendritic trees and cell bodies, and they represent 80% of the total RGCs (Pascale et al., 2012).

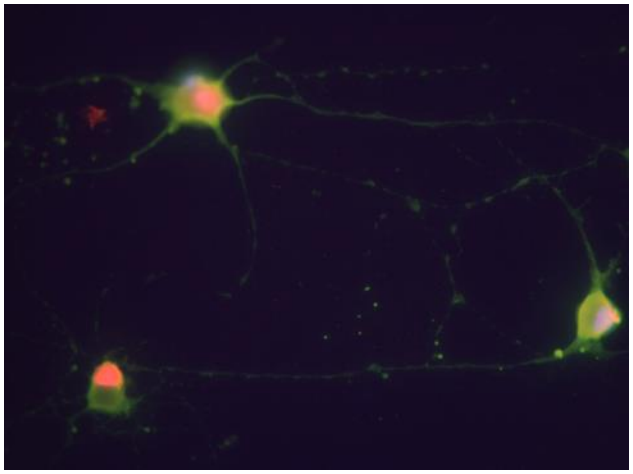

Figure 1.4 - Isolated rat RGCs in culture. RGCs were identified with an antibody that recognizes Brn3a (red), a transcription factor that in the retina is specifically expressed by these cells. Neurites (green) were visualized with an antibody against GluN1 (a subunit of NMDA glutamate receptor). Nuclei were counterstained with DAPI (blue).

1.2 Glaucoma

Glaucoma is a leading cause of irreversible blindness, affecting more than 60 million people worldwide with 10% of those blind in 2010 (Quigley and Broman, 2006; Quigley, 2011). Glaucoma compromises a group of neurodegenerative ocular disorders with characteristics of slow optic nerve cupping and progressive degeneration and death of RGCs (Fechtner and Weinreb, 1994). It is recognised to be an optic neuropathy, present when at least one of the eyes has optic nerve damage and visual field loss (structural and functional defects) (Quigley, 2011). One of the clinical measurements of the disease is the comparison of the cup (a central depression created by the entrance of nerve fibres from RGCs on the optic disc) to the overall size of the optic disc; this establishes the cup-to-disc ratio (Fig 1.5). As the disease progresses, more RGCs are affected and the number of fibres decreases, resulting in an increase of the size of the cup and the cup-to-disc ratio (Quigley, 2011) (Fig 1.5). The excavation and enlargement of the optic cup, characteristic of glaucoma neuropathy, is associated with loss of both axons from RGCs and connective tissue of the optic disc (Burgoyne et al., 2005). Furthermore, the axonal

loss from RGCs also leads to thinning of the NFL that can be detected by clinical examination or by imaging methods such as optical coherence tomography or scanning laser polarimetry. Visual function loss is also assessed by a visual field test to determine both functional and structural injury (Quigley, 2011).

A diverse range of factors has been implicated in this pathology, but the primary cause of glaucoma is still unknown. Nevertheless, several risk factors have been identified, including elevated intraocular pressure (IOP – being the major risk factor for glaucoma), greater cup-to-disc ratio, thinner central corneal measurement, age, ethnicity, and a family history of glaucoma (Varma et al., 2011). Different genes are associated with the different variants of the disease, which include primary open angle glaucoma (MYOC, WDR36, OPTN, NTF4), normal tension glaucoma (OPTN), pseudoexfoliative glaucoma (LOXL1), and congenital glaucoma (LTBP2, CYP1B1). However, many patients with open angle glaucoma do not have any of the mutations or polymorphisms (Chang and Goldberg, 2012).

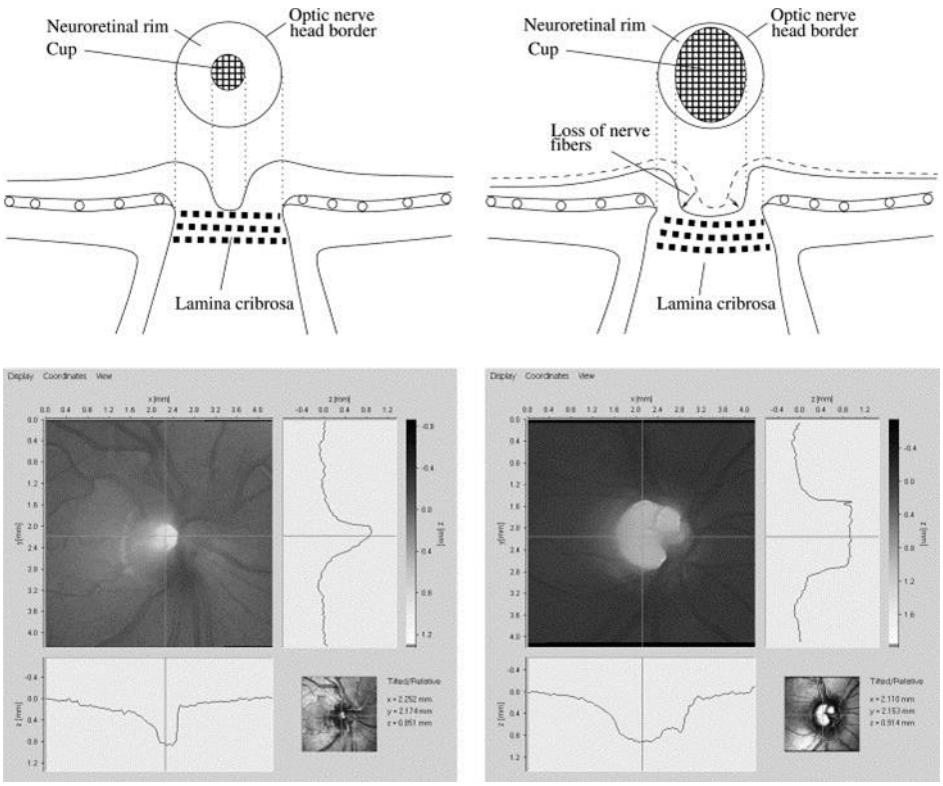

Figure 1.5 - Optic nerve head in normal (A) and glaucomatous (B) eyes. Optic disc changes with cupping and loss of nerve fibre layer can be detected in the eye affected with glaucoma. Heidelberg retina tomography images. Adapted from Chrastek et al., Automated segmentation of the optic nerve head for diagnosis of glaucoma. Medical imaging Analysis. 2005 Aug;9(4):297-314. Epub 2005 Apr 8.

The prevalence of glaucoma increases with age. As the average age of the population increases, so does the number of cases of glaucoma, with approximately 80 million people expected to be affected by glaucoma in 2020 (Quigley and Broman, 2006; Quigley, 2005). In 2010, 2.65% of the global population above 40 years old had glaucoma (Varma et al., 2011), and women are more affected than men, representing 59% of the cases in 2010. Glaucoma prevalence also varies between ethnic groups, with Asians being the most affected with 47% of those with glaucoma by 2010. Glaucoma is also the number one cause of blindness in African-Americans, with a 4 to 5 fold higher incidence than Caucasians and occurs, on average, 10 years earlier (Tielsch et al., 1991). In 2020, it is predicted that of all of those with glaucoma, 74% will have primary open-angle glaucoma, representing 58.6 million people, and 21 million will have primary angle-

closure glaucoma. Of those, 11.1 million are expected to be bilaterally blind by 2020 (Quigley, 2005).

At the onset of the disease one may not exhibit any symptoms, however, up to 20-40% of RGCs are lost before visual field defects are detected using standard clinical tests. This could mean a 10 year delay between the onset and diagnosis (Kerrigan-Baumrind et al., 2000; Khaw et al., 2004). Lowering of the IOP has demonstrated to attenuate the death of RGCs (Heijl et al., 2002; Leske et al., 2003) and is still to date the only pharmacology and surgical treatment available. However, there is evidence that lowering the IOP does not always stop disease progression, being an unmet necessity to develop new treatments for this disease.

There are two main types of glaucoma, open-angle glaucoma and angle-closure glaucoma. Both are associated with similar changes in optic disc and visual field although with different features (Boland et al., 2008).

1.2.1 Primary open angle glaucoma (POAG)

Primary open angle glaucoma is the most common form of glaucoma. It is a slow progressive neuropathy, characterized by excavation or abnormal deepening of the optic disc connective tissue (Quigley, 2011). It is most often bilateral, but asymmetric as it affects selectively the upper and lower axons passing through the optic disc.

The mean age for onset of the disease is 60 years old, and the frequency increases with age as well as with family history. Reports from The Ocular Hypertension Treatment Study (OHTS) show that untreated patients with POAG have 16% probability of becoming unilaterally blind within 10 years (Kass et al., 2002).

Patients with normal tension glaucoma represent about 50% of POAG patients and the disease progression of visual field loss is similar to those patients with elevated IOP (Heijl et al., 2002). Normal tension glaucoma is similar to POAG such as optic disc cupping, thinning of the nerve fibre layer and loss of RGCs, but IOP is 21 mmHg or below (considered to be normal values) (Shields, 2008).

1.2.2 Primary angle closure glaucoma (PACG)

Primary angle closure glaucoma occurs when there is a blockage at the level of the trabecular meshwork that prevents aqueous humour outflow and leads to an acute increase of pressure. Formerly, diagnosis for patients with PACG was based on the knowledge of an acute increase in IOP accompanied by a sudden decrease in vision. Nevertheless, it is now known that this does not occur in 75% of patients with PACG (Yip and Foster, 2006). In acute cases of PACG, pressure in the eye rises quickly due to physical blockage of the aqueous humour outflow. In these cases the cornea becomes waterlogged, causing a decrease in visual acuity (Khaw et al., 2004). PACG can be distinguished from POAG by examining the angle between the iris and the cornea. Therefore, for the diagnosis of angle-closure glaucoma it is important to establish the angle formed between the iris and the cornea and the blockage of the trabecular meshwork by gonioscopy (Quigley, 2011). The degree of vision loss in PACG can be twice as fast as in POAG, meaning that half of the blind patients have PACG (Foster and Johnson, 2001). The major risk factor for PACG are small eyes although other risk factors include: age, being a woman (due to smaller eyes) and Asian and Indian ethnic groups (Quigley, 2011).

1.2.3 Ocular hypertension (OHT)

Most patients with ocular hypertension (high IOP) will not develop primary open angle glaucoma (Friedman et al., 2004; Stuart, 2012). Ocular hypertension patients are reported to have an increase in intraocular pressure without other manifestations of glaucoma, such as optic disc damage or cupping, RGC loss or decrease in nerve fibre layer. The probability of those with OHT developing glaucoma is 9.5% in untreated patient eyes in 5 years (Weinreb et al., 2004).

1.2.4 Aqueous humour production and outflow and intraocular pressure

The aqueous humour is secreted posteriorly to the iris by the ciliary body and then flows to the anterior chamber of the eye in which it is retained. It is an aqueous solution with

electrolytes, organic solutes, proteins and growth factors that supply nutrients to the nonvascularized tissues of the anterior chamber (Fautsch and Johnson, 2006; Weinreb and Khaw, 2004). The primordial pathway by which aqueous humour exits the eye is through the trabecular meshwork into the Schlemm's canal and into the episcleral veins; alternatively it can exit through the ciliary muscles – called the uveoscleral pathway (Fautsch and Johnson, 2006) (Fig 1.6).

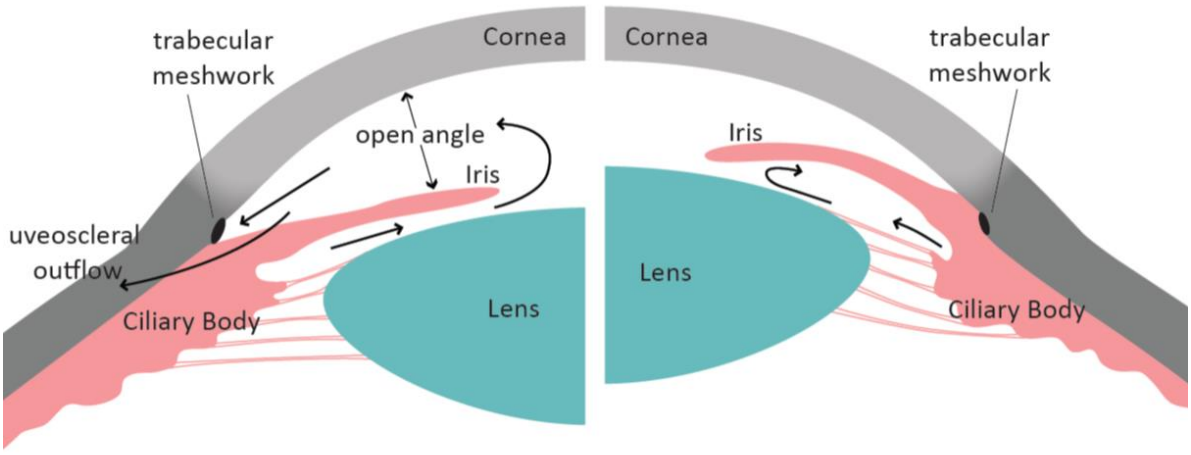

Figure 1.6 - Aqueous humour flow in the eye. The aqueous humour that fills the anterior chamber is produced by the ciliary body and flows between the iris and lens, through the pupil and to the drainage angle at the junction of the iris and the cornea. Aqueous fluid exits the eye through trabecular meshwork and into the Schlemm's canal, in the drainage angle. Blockage to the trabecular meshwork leads to increase in intraocular pressure in the eye. left image represents open-angle glaucoma patient; Right image represents a structural blockage in angle-closure glaucoma.

The intraocular pressure is a result of the balance between the production of aqueous humour inside the eye, and its drainage out of the eye through the trabecular meshwork. Each human eye produces about 2 µl of aqueous humour per minute, representing an average of 70 litres in a lifetime (Khaw et al., 2004). The normal

pressure of the human eye is between 10 to 21 mm Hg, but can exceed 70 mm Hg in acute cases. In general, patients with glaucoma ranging from 20 to 30 mm Hg have damage over several years of disease progression, while patients with 40 to 50 mm Hg have rapid visual field loss (Khaw et al., 2004). Measurement of IOP by tonometry must take into account the cornea thickness, as thicker corneas lead to higher IOPs whereas the contrary is true for thinner corneas (Quigley, 2011).

It is important to accurately measure IOP as it is the major risk factor in glaucoma. Measurement IOP in animals can be categorized as invasive or non-invasive. Invasive technics can damage the cornea and include the servo-null micropipette system (Avila et al., 2001) and the microcannulation technique. Non-invasive methods include pneumotonometer, modification of the Goldmann applanation tonometer, Tono-Pen and Tono-Lab rebound tonometer (Pang and Clark, 2007). The invasive methods involve perforation of the cornea by an electrode or transducer, and due to this fact IOP measurements cannot be done more than once a week to allow the corneal wound to heal; moreover, the animals need to be anesthetized. Hence, these methods are now used less due to very good adaptation of the non-invasive methods for rodents. The most used methods for measuring IOP in rodents are the Tono-Pen and the Tono-Lab tonometer. Tono-Pen records the pressure using an electronic sensor as the tip touches the cornea of the local anesthetized eye (Pang and Clark, 2007). Correction factors have to be applied when measuring the pressure to rodent, as they have different corneal diameter, curvature and thickness compared to humans (Pang et al., 2005a, 2005b). In Tono-Lab rebound tonometer a magnetic probe is propelled toward the cornea, touches it and rebounds. IOP can be measured due to the level of deceleration of the probe after impacting the eye. The use of Tono-Lab tonometer does not need external correlation factors as they are already incorporated into the readings (Kontiola, 1997; Pang and Clark, 2007). Both these techniques can be used with nonsedated conscious rats and mice, which is an important point as anaesthetized animals have generally lower IOP (Jia et al., 2000).

IOP is an important factor in glaucoma, and so far it is the only risk factor that can be managed by medication or surgery. In fact, on The Ocular Hypertension Study, treatment to reduce IOP reduces the risk of developing glaucomatous damage from 5%

to 10% over a period of 5 years. This was also true for patients with a relatively low IOP (normal-tension glaucoma), and with a slow visual field loss progression (Glaucoma and Group, 1998). In the Early Manifest Glaucoma Treatment Trial (EMGT), the estimate risk of glaucoma progression was reduced by 10% for each 1 mm Hg of IOP reduced during the period of the study (Heijl et al., 2002).

1.2.5 Animal Models of Glaucoma

To better understand the mechanism of glaucoma and how RGCs die in glaucoma, different animal models have been developed. The most commonly used animals are rats and mice due to the large genome conservation from that of humans (Paigen, 1995), and due to the low cost, availability, and ease of housing and handling. The retinas of these animals are similar to those of humans, but rodents do not possess maculae in their retinas. The optic nerve head of these animals is slightly different from humans, as they have cellular lamina and astrocytes that are vertically oriented and interlocking around the nerve fibre bundles, instead of lamina cribrosa seen in primates (May and Lütjen-Drecoll, 2002; Morrison et al., 1995). Nevertheless, the optic nerve head and optic nerve composition present in rodents is similar to that of primates. Moreover, the eyes of these animals are affected similarly to glaucoma patients in response to glaucoma-related injury (Weinreb and Khaw, 2004).

Models of retinal ganglion cell degeneration

The cells most affected in glaucoma are the RGCs, and vision loss in patients occurs due to RGC death. Different models have been developed to understand the mechanism by which RGCs undergo apoptosis. There are different models to induce RGCs degeneration and they can be induced by intravitreal (IVT) injection or by surgical procedures. IVT injection models are easy and rapid models to induce RGC death, and IVT injection of staurosporin (SSP), kainate (KA), or N-methyl-D-aspartic acid (NMDA) are toxins commonly used to induce RGC death.

An IVT injection of 100 nM staurosporin was shown to induce neuronal cell death through apoptosis soon after 24h post-injection (Koh et al., 1995). More recently,

Cordeiro and colleagues have shown a quick model of RGC death with IVT injection of SSP having an effect after 2h treatment, with apoptosis detected by annexin V staining *in vivo* (Cordeiro et al., 2004).

Excitotoxicity has also been implicated in glaucoma. IVT injection of NMDA or KA is reported to induce neurotoxicity in the rat inner retina without altering the IOP (Siliprandi et al. 1992; Johnson and Tomarev, 2010). These models have been used to study the excitotoxic mechanism affecting RGCs. NMDA induces a dose dependent decrease in RGCs (8 to 200 nmoles) with an increase in TUNEL- (Terminal deoxynucleotidyl transferase dUTP nick end labelling) positive cells in the inner retina and a decrease in inner retinal thickness (Lam et al., 1999; Siliprandi et al., 1992). IVT injection of NMDA leads to a decrease of more than 80% of RGCs and axons, as assessed by retrograde labelling with retrograde tracer horseradish-peroxidase (Pang and Clark, 2007; Vorwerk et al., 1996).

Surgically induced degeneration can be achieved by direct damage to the optic nerve (axons of RGCs). These models aim to mimic changes that occur at the level of the optic nerve, such as loss of retrograde transport, reported to occur early in glaucoma patients. Different models, differing in the severity of damage, have been developed to induce damage to the optic nerve: optic nerve transection, optic nerve crush, and partial optic nerve transection. Mechanical injury to RGC axons leads to degeneration and loss of RGCs. The optic nerve is accessed through the sclera, and the optic nerve is crushed, or totally or partially transected with care not to damage the central retinal artery and without disrupting normal blood supply (Johnson and Tomarev, 2010). RGC loss depends upon the degree of damage applied to the optic nerve, with increased damage associated with total optic nerve transection. Total transection of the optic nerve was reported to induce 50% of RGC loss at 1 week and 80% to 100% loss after 2 weeks (Levkovitch-Verbin, 2004; Pang and Clark, 2007). The damage induced by optic nerve crush is smaller compared with total optic nerve transection, and is considered to be more similar to the neuropathy in glaucoma. In this model, there was 47% of RGC survival after one week and 27% RGC survival after 2 weeks with complete RGC loss occurring after 30 days. Others report 90% RGC survival after 2 weeks and 80% RGC survival after 4 weeks (Johnson and Tomarev, 2010). Reproducibility is considered the

main issue regarding these models, with observed different degrees of damage depending on the operator (Levkovitch-Verbin, 2004). The partial optic nerve transection model was developed as the first model of secondary degeneration and it is considered to be less severe to RGCs. The initial cut to the optic nerve causes the primary degeneration, secondary degeneration occurs later and is due to the loss of RGCs from the initial damage (Levkovitch-Verbin, 2004).

Surgical glaucoma models

Since IOP is one of the principal risk factors for the development of glaucoma in humans, experimental approach to recreate the disease has been to induce elevated IOP in animals. Currently there are 3 widely used methods to increase IOP in order to model glaucoma.

The model known as hypertonic model or Morrison's model, involves the injection of hypertonic saline solution (1.8 M NaCl) into the episcleral veins of the rat eye, producing scarring of the tissue which blocks the outflow of the aqueous humour (Morrison et al., 1997). Due to the proximity of the limbal venous plexus to the aqueous humour outflow network, retrograde delivery of saline solution is forced to the Schlemm's canal, trabecular meshwork and anterior chamber angle, resulting in a sustained IOP increase. The increase of IOP is directly correlated with the number of episcleral veins injected. IOP was reported to be increased for as long as 200 days after injection (Morrison et al., 1997). A range of IOP between 20-30 mm Hg in the operated eye is expected to last 3-4 months (Nickells, 2007). In this model, it is reported that the degree of RGC death is associated with the level of IOP (Pang and Clark, 2007). The morphologic changes in the optic nerve are similar to those observed in glaucoma patients and IOP-dependent progressive cupping of the optic disc was shown by scanning laser tomography (Chauhan et al., 2002).

In the episcleral cauterization/ligation model, IOP is increased by cauterizing/ligating two or more episcleral veins of the eye, by congesting the uveal vasculature (Shareef et al., 1995; Yu et al., 2006b). On the episcleral vein cauterization model, an average of 28 mm Hg IOP elevation can be registered on the first week. A 14%, 25% and 30% decrease in RGCs was seen respectively at 4, 6 and 8 weeks after increased IOP (Laquis et al.,

1998). The degree of RGC loss was reported to be 4% per week. In this model, the increase in RGC loss was correlated with an increase in the number of TUNEL-positive cells (Garcia-Valenzuela et al., 1995).

A third method, known as microbeads model, relies on the injection of microbeads (polystyrene or magnetic) into the anterior chamber of the eye, creating occlusion of the iridocorneal angle and increasing IOP by blockage of the aqueous humour outflow (Samsel et al., 2011; Sappington et al., 2010). A single injection of beads is reported to induce a sustained 30% increase in the IOP for 2 weeks, with mean IOP at approximately 30 mm Hg (Sappington et al., 2010). In this model, the level of RGC loss produced by IOP increase was between 23-36%, which is in accordance with the percentage of RGC loss detected in the models mentioned above (Samsel et al., 2011).

Laser glaucoma models

There are two major laser-induced glaucoma models, the translimbal laser photocoagulation and the laser trabecular photocoagulation (LTP). Both use laser treatment to damage the trabecular meshwork blocking the outflow of the aqueous humour (Levkovitch-Verbin, 2004; Ueda et al., 1998). Usually repeated laser treatments are required to maintain high IOP. These methods produce scarring of the structures involved in the outflow pathway of the aqueous humour, which leads to an increase in resistance to the drainage of the aqueous humour, increasing the IOP in the eye. The LTP model uses the injection of India ink one week prior the laser to increase the damage made to the trabecular meshwork due to light absorption of the ink at the level of this structure (Ueda et al., 1998). Following laser treatment, increased IOP peaks between 34-40 mm Hg for at least 3 weeks. Axonal loss in this model is about 20% after 3 weeks, 25% at 6 weeks and about 50% loss at 9 weeks (Levkovitch-Verbin, 2004).

Spontaneous glaucoma models

DBA/2J substrains of inbred mice were observed as spontaneously developing glaucoma at 6 months of age (John et al., 1998). This occurs due to the development of iris abnormalities, pigment dispersion and iris atrophy, and leads to scarification of the trabecular meshwork (John et al., 1998). These animals have IOP between 20 and 30 mm

Hg by 8 to 9 months of age, although some reported IOP increase at just 4 months of age (Nickells, 2007; X. Zhou et al., 2005). By 10-12 months there is loss of RGCs (Nickells, 2007). Ocular hypertension in these animals is accompanied by RGC death, optic nerve atrophy and cupping, and visual deficits (Libby et al., 2005a), with the retinal degeneration being specific to RGCs (Jakobs et al., 2005). At the same time, there is an age-dependent increase in the damage to the optic nerve after increased IOP (John et al., 1998; Libby et al., 2005a). The DBA/2J mouse is one of the best-characterized rodent glaucoma models. Nevertheless, to evaluate neuroprotective drugs, animals need to be treated for extended periods of time as the models develop for several months. Moreover, due to the fact that the rate of disease is not uniform on both eyes of the same animal, experimental groups require a large number of animals to overcome the intrinsic variability (Pang and Clark, 2007). Notwithstanding, this is a valuable model in glaucoma research as it is considered to most accurately recreate the human disease.

Each of these models has their own strengths and limitations, being therefore important to use the appropriate model for a particular response and to use more than one model to characterize each response. The use of rodent models, due to their accessibility, is also important to allow a proof of principal for testing potential therapeutic approaches prior to testing in primates and humans.

1.2.6 Current treatments in glaucoma

One of the major risk factors of glaucoma is the increase in IOP, and nowadays the most common treatments for glaucoma focus on decreasing the IOP. In fact, in controlled clinical trials, treatment for lowering IOP was reported to be beneficial for patients suspected to have glaucoma even before detection of the initial damage (Kass et al., 2002). Furthermore, treatment for lowering IOP is effective and always recommended even in patients with normal tension (Glaucoma and Group, 1998; Heijl et al., 2002). Thus, effective reduction of IOP significantly prevents glaucoma progression in 80-90% of patients (Glaucoma and Group, 1998).

There are five different pharmacological therapies to decrease IOP in humans: miotics, adrenergic agonists, carbonic anhydrase inhibitors, beta-blockers and prostaglandins.

The more common treatments for glaucoma are eye drops using α2-adrenergic agonists or prostaglandin analogues (Realini, 2011).

Miotics are a group of drugs that constringe the pupil, to allow the drainage of aqueous humour decreasing the constringent of the angle between iris and the cornea. They are currently used in glaucoma surgery (Realini, 2011).

Carbonic anhydrase inhibitors reduces IOP by reducing aqueous humour formation (Weinreb and Khaw, 2004). The most used in clinic are acetazolamide (oral), dorzolamide and brinzolamide (topical). The topical formulations have fewer side effects than the oral ones, but are less effective in lowering IOP.

Beta-blockers (β-blockers) are propranolol, timolol (levobunalol, metipranolol, and carteolol) and bataxolol. β-blockers also reduce IOP by decreasing aqueous humour secretion/production. Care must be taken when using β-blockers as they have substantial respiration and cardiovascular side effects (Diggory et al., 1996).

The α2 adrenergic agonists (brimonidine and apraclonidine) lower IOP by reducing secretion of aqueous humour and increasing aqueous humour drainage (Toris et al., 1999). They are less effective at lowering IOP compared with prostaglandin analogues (Einarson et al., 2000). Side effects include oral dryness, ocular hyperemia, ocular discomfort, headache and fatigue (Novack et al., 2002).

Currently, the prostaglandin analogues are the safest and most effective drugs to treat glaucoma, and are latanoprost, travoprost, bimatoprost, unoprostone, and tafluprost (Realini, 2011). Prostaglandins reduce IOP by increasing the outflow of aqueous humour through the uveoscleral pathway. This occurs due to changes induced in the extracellular matrix, which reduce outflow resistance at the ciliary body allowing aqueous humour flowing through this route (Sagara et al., 1999; Weinreb et al., 2002). They are the most used due to their once-a-day application, minimum side effects and effectiveness at lowering intraocular pressure (Weinreb and Khaw, 2004).

Other forms to lower IOP are by laser or surgical treatment. Laser treatments include trabeculoplasty, cyclophotocoagulation (CPC) and peripheral iridotomy. Surgical procedures include trabeculectomy.

In primary open angle glaucoma the most common laser treatment is the trabeculoplasty. This laser treatment is delivered to the trabecular meshwork to increase aqueous humour drainage and lower IOP with minimum risks and side effects. Patients older than 40 years and with increased trabecular pigmentation respond better to this treatment. Nevertheless, although patients have decreased pressure in the first months the effect gradually lessens (Weinreb and Khaw, 2004).

CPC is a laser treatment that destroys part of the ciliary body in order to decrease the production of aqueous humour. It is normally used when both therapy and surgery have failed. It has a temporary effect and often needs to be repeated (Gupta and Weinreb, 1997).

Peripheral iridotomy is a laser procedure that creates a hole in the iris to open an angle between the cornea and the iris most commonly used for the treatment of primary angle closure glaucoma (Realini, 2011).

In trabeculectomy part of the trabecular meshwork is removed creating a hole to increase the leaking of aqueous humour from the anterior chamber. It is rarely used as a primary treatment nowadays due to regularly different post-surgical complications (Edmunds et al., 2002).

It is known that the average progressive visual field loss reduces by half when pressure is decreased by 20-40% (Quigley, 2011). However, patients with rapid rates of deterioration need increased treatment attention to prevent vision loss, and decreased IOP per se might not be enough. Furthermore, patients have difficulties complying with the large number of times they have to apply the drop therapy and the success of surgical rates is still not satisfying. The bioavailability of topical drops into the eye is very low, sometimes not reaching 5% (Loch et al., 2012; Rittenhouse et al., 1998). The half-time of topical drops in precornea is about 1 minute due to tear film and cleaning by frequent blinking (Wei et al., 2002). Even with controlled IOP, disease progression and loss of RGCs still occurs in some patients. It is of most importance that other pharmacologic approaches could be developed to prevent RGC loss. Research on neuroprotection in glaucoma has increased in the last few years with different candidates to protect RGCs.

1.2.7 Neuroprotection in glaucoma

A strategy by which one treats a disease by preventing neuronal death is termed neuroprotection. Various strategies have been proposed to prevent or delay RGC death in glaucoma, with the ultimate goal of prolonging visual function. The approaches to prevent RGC death are based in pharmacological agents, stem cells, and gene therapy. The aim of neuroprotective agents is to target the multiple pathogenic mechanisms that cause the death of RGCs in glaucoma.

Pharmacological approach

Neuroprotection based on pharmacological approaches has been mainly focused on excitoxicity, neurotrophins depletion, mitochondrial dysfunction and oxidative stress.

Excitotoxicity is reported to occur in glaucoma, with increased glutamate levels in the vitreous humour of patients with glaucoma (Dreyer et al., 1996). Blocking glutamate excitotoxicity is one of the most studied approaches to protect RGCs. Memantine is an uncompetitive NMDA receptor antagonist, that binds to NMDA receptors when glutamate has previously been bound to it. It is known as an 'open channel blocker' because it only binds to the NMDA ion channel when it is already open (Chang and Goldberg, 2012; Danesh-Meyer, 2011). Memantine is protective against RGC loss in different animal models of RGC death (Hare et al., 2001; Lagreze et al., 1998; WoldeMussie et al., 2002). Memantine was the first proposed neuroprotectant to reach a large, parallel, randomized, phase III clinical trial. The clinical trial for human glaucoma (NCT00168350) failed to meet the primary efficacy end point with the report still to be published by Allergan, Inc. (Irvine, CA) (Osborne, 2008).

Brimonidine is an α2 adrenergic agonist currently used to decrease IOP. Systemic administration of brimonidine is approved for lowering IOP in glaucoma and it was reported that it protects RGCs in a rat model of ocular hypertension (Hare et al., 2001; Hernández et al., 2008). The mode of action of brimonidine is still unclear. It has been shown that brimonidine protects RGCs by inhibiting NMDA receptor function and upregulating brain-derived neurotrophic factor (Dong et al., 2008; Hernández et al., 2008; Lee et al., 2012). Others have reported neuroprotective effects through the

inhibition of apoptotic cascade (Lai et al., 2002). Recently, in the Low Tension Glaucoma Treatment Study, despite similar effects with timolol on lowering IOP, patients that received brimonidine showed less visual field progression compared with patients with timolol (Krupin et al., 2011).

Deficit in axonal transport is known to occur early in glaucoma patients. This will lead to deprivation of neurotrophins such as brain-derived neurotrophic factor (BDNF) and nerve growth factor (NGF). Neurotrophins activate survival signals and also inhibit apoptotic events. Neurotrophins act through the activation of tropomyosin-related kinase (Trk) and p75 neurotrophin receptors. BDNF has been widely tested as neuroprotective in RGCs and in different models of RGC insult (Klöcker et al., 1998; Weber and Harman, 2008). Moreover, combination with other substances has been used to potentiate its effects (Fu et al., 2009). NGF was identified as neuroprotective in an ocular hypertensive model, reducing apoptosis to RGCs (Colafrancesco et al., 2011; Lambiase et al., 2009). RGC survival *in vivo* was also demonstrated for ciliary neurotrophic factor (CNTF), neurotrophin-4 (NT-4), basic fibroblast growth factor-2 (FGF-2) and neurturin (Grozdanic et al., 2010; Parrilla-Reverter et al., 2009). Neuroprotective approach that utilizes neurotrophins pathways would lead to an increase in their endogenous expression, to an increase of exogenous supplies, or to the modulatation of neurotrophin receptors at the level of RGCs (Danesh-Meyer, 2011). However, prolonged treatments lead to a decrease in the expression of neurotrophin receptors reducing the effectiveness of the treatment, and this has to be taken into account when designing clinical approaches (Baltmr et al., 2010).

Mitochondria play a critical role in cell homeostasis. They are responsible for energy production through oxidative phosphorylation, maintenance of intracellular calcium levels, as well as the production of reactive oxygen species (ROS). RGC axons, at the level of optic nerve head, before they become myelinated, are very rich in mitochondria (Carelli et al., 2004). Mitochondrial membrane permeabilization and decrease in mitochondrial membrane potential have been implicated in RGC death in glaucoma (Mittag et al., 2000; Tatton et al., 2001; Tezel and Yang, 2004). Neuroprotective approaches that target mitochondria have been used to protect RGCs. Coenzyme Q10, nicotinamide, creatine and lipoic acid have all been successfully used to target

mitochondrial dysfunction in RGC death (Beal, 2003; Chidlow et al., 2002; Juravleva et al., 2011; Nakajima et al., 2008). Regarding the number of mitochondria present on RGCs, targeting mitochondria dysfunction could be a valuable approach to protect RGCs against a glaucomatous insult.

Oxidative stress is caused by the imbalance of production and breakdown of ROS and has been recognize to be involved in glaucoma injury of RGCs (Kanamori et al., 2010). Superoxide dismutase-1 and heme oxygenase act as antioxidant enzymes and were shown to attenuate RGC death after axonal or ischemia-reperfusion injury (Kanamori et al., 2010; Sun et al., 2010).

Other pharmacological approaches for RGC neuroprotection have been studied in different models of RGC death. Beta-blockers such as betaxolol and timolol have activity as calcium blockers, reducing excessive influx of calcium and protecting RGCs (Chidlow et al., 2000; Osborne et al., 1999; Schuettauf et al., 2002; Setoguchi et al., 1995). Nitric oxide (NO) synthase inhibitors were also reported to prevent loss of RGCs (Neufeld, 2004, 2002; Neufeld et al., 1999).

Stem cells transplantation

More recently, other approaches have been used to target RGC neuroprotection, namely stem cell transplantation. Glial cell transplantation, specifically olfactory ensheathing cells (OECs), has been used to protect RGCs. OECs produce several neutrophic factors (CNTF, BDNF, NGF and glial cell line-derived neurotrophic factor (GDNF)) reported to be beneficial to RGCs (Lipson et al., 2003; Woodhall et al., 2001). Co-culture of OECs with retinal explants protects RGC, with conditioned media having no protective effects, thus demonstrating a contact-dependent neuroprotection of these cells (Dai et al., 2010). *In vivo,* OECs protect RGCs after optic nerve trauma due to local increase in BDNF production (Wu et al., 2010). OEC transplantation to other models of optic nerve injury also show protective effects to RGC axons and function (Li et al., 2008; Liu et al., 2010). Schwann cells were also shown to increase RGC survival both *in vitro* and *in vivo* after optic nerve transection (Bampton et al., 2005; Li et al., 2004). Furthermore, mesenchymal stem cells (MSC) are multipotent and capable of differentiating into different cell types. They can be isolated from the human umbilical

cord and adult bone marrow (Johnson and Martin, 2013). MSC transplantation protects RGC from ocular hypertension by episcleral vein ligation, by photocoagulation, from ischemia, optic nerve crush and optic nerve transection (Harper et al., 2011; Johnson et al., 2010; Levkovitch-Verbin et al., 2010; Li et al., 2009; Yu et al., 2006a; Zhao et al., 2011). Further studies are important to assess the degree of integration of these cells *in vivo* and their long term effect in RGC neuroprotection.

Gene therapy

Gene therapy in glaucoma targets the mechanisms underlying RGC degeneration and promotes RGC survival.

Adenoviral (Ad) approaches a main disadvantage of strong cytotoxic and immune reactions, although the use of helper dependent Ad has considerable reduced immune response. This has been used intravitreally to promote transgene expression of neurotrophic factors to Müller cells to protect RGCs (Di Polo et al., 1998; Isenmann et al., 1998; Lamartina and Cimino, 2007; Reichel et al., 1998). Moreover, Ad-mediated heme oxygenase gene transfer protects RGCs against ischemia-reperfusion and pressure induced ischemia (Hegazy et al., 2000; Peng et al., 2008).

Adeno-associated viral (AAV) vectors have been successfully used intravitreally to protect RGCs (Ali et al., 1998; Cheng et al., 2002; Harvey, 2002), although RGC specific promoters have not yet been used. This approach mediates long-term transgene expression that can last for several years with low immunogenicity (Stieger et al., 2009).

The use of Ad.BDNF and AAV.BDNF promotes RGC survival after optic nerve transection (Di Polo et al., 1998; Leaver et al., 2006). In experimental glaucoma, AAV.BDNF protects RGCs, although it does not affect axonal regrowth (Harvey et al., 2009; Martin, 2003). AAV.CNTF was also reported to be protective to RGC, with 15% increase in the number of RGC axons compared to the control, in a laser-induced ocular hypertension, and 7% increase of RGC survival in axotomized RGCs (Pease et al., 2009; van Adel et al., 2005). The neuroprotective effects of neurotrophic factors are known to supress intrinsic apoptotic cascade by activating intracellular survival signals. AAV targeting mitogen activated protein kinase/extracellular signal-regulated kinase kinase 1 results in robust

survival of RGC in a rat model of ocular hypertension (Pernet et al., 2005; Y. Zhou et al., 2005). AAV-mediated gene expression of Bcl-XL and OPA-1 shows neuroprotective effects to RGC death after axotomy or spontaneous glaucoma (Ju et al., 2010; Malik et al., 2005). Furthermore AAV-Nogo receptor (myelin-associated growth inhibitor molecules) and AAV vector for C3 ribosyltranferase (RhoA inhibitor) were reported to promote axonal regrowth important in different pathologies such the case of glaucoma (RGC axonal growth) (Fischer et al., 2004; Lehmann et al., 1999).

DNA and RNA based approaches have been used to modify RGC gene expression. Albeit DNA plasmids are easy to prepare, they are not easily uptaken by cells resulting in a modest protection of RGCs (Caprioli et al., 2009; Isenmann et al., 1999). Nevertheless, siRNA can be injected intravitreally and be effectively delivered to RGCs soon after administration (Wilson and Di Polo, 2012). siRNA knockdown to c-Jun, Bax, Apaf-1 and potassium channels all showed effective protective effects against RGC death (Lingor et al., 2005).

RGCs are known to die through apoptosis after caspase activation (Huang et al., 2005a; Kerrigan et al., 1997; McKinnon et al., 2002; Qu et al., 2010; Quigley, 1999). Targeting the caspase cascade to prevent cell death has proven to have modest success. The exception is the use of siRNA to knockdown caspase-2 expression in RGCs. IVT injection of caspase-2 inhibitors have shown robust neuroprotection of RGCs in optic nerve crush or cut (Ahmed et al., 2011). This approach is currently under Phase I clinical trial for non-arteritic anterior ischemic optic neuropathy (ID NCT01064505).

1.2.8 Retinal ganglion cell death

The mechanism by which RGCs are damaged in glaucoma is still unknown, but there are several hypotheses regarding where the damage starts in the eye. Three main theories have been proposed: mechanical, vascular and biochemical (Weber and Harman, 2008). Mechanical mechanism is based on the fact that elevated IOP is a major risk factor for this disease and it is considered that elevated IOP by itself acts directly on damaging RGCs. This would make the optic nerve head the primordial site for damage initiation. The elevation of IOP would result in damage to RGCs through compression of their

axons, which is in accordance with the focal area where there is optic nerve cupping, with further loss of RGCs. In glaucoma, loss of visual field occurs initially to the peripheral vision and not across the visual field although RGC cell bodies are adjacent to each other and more numerous than in the periphery, suggesting that the dysfunction does not initiate in the retina (Chang and Goldberg, 2012). Furthermore, at the optic nerve head the axons are particularly vulnerable because they are unmyelinated at the lamina cribrosa. Nevertheless, it remains unanswered whether it first affects axons, glial cells, vascular or a combination between the three. Notwithstanding, normal tension glaucoma patients also have similar damage to RGCs and optic nerve cupping although the compression factor might not be present. In these patients, one hypothesis is that their RGCs might be more sensitive to lower pressure values.

A number of mechanisms by which RGC death has been proposed includes excitotoxicity, ischemia, damage of axonal transport, withdrawal of trophic factors, reactive oxygen species, and loss of electrical activity (Chang and Goldberg, 2012). Whatever the early events involved in glaucoma, RGCs are known to die as a result of caspase activation, through mitochondrial-mediated apoptosis (Huang et al., 2005a; Kerrigan et al., 1997; McKinnon et al., 2002; Qu et al., 2010; Quigley, 1999). Nevertheless, deletion of the pro-apoptotic gene bax in the DBA/2J mouse model shows only a protective effect on the cell body of RGC with no further protection regarding axonal loss (Libby et al., 2005b). Deficit in axonal transport due to optic nerve head (ONH) blockage was first reported in the 1970s (Anderson and Hendrickson, 1974; Minckler et al., 1977). Blockage of the retrograde transport of pro-survival factors to the cell body, such as BDNF, is known to trigger apoptosis (Pease et al., 2000). The general path of vision loss is correlated with anatomical features of the ONH, suggesting that the initial damage is axogenic and moving from the ONH to the retina (Quigley, 1999). Transport blockade could be correlated with metabolic abnormalities to the molecular motors and/or cytoskeleton that would produce transport deficits (Morfini et al., 2009).

Axonal degeneration can occur either by wallerian degeneration or dying back (Coleman, 2005). Wallerian degeneration typically results from a trauma to axon, as it is a synchronised process that affects the entire axon. In the dying back mechanism, the degeneration of the axon occurs from distal to proximal, as it is a progressive cascade

that is initiated at the synaptic terminals. RGC synaptic elimination has been reported in glaucoma both early (Fu et al., 2009; Stevens et al., 2007) and later in the disease, well after other functional deficits occur (Georgiou et al., 2010). An insult of wallerian degeneration to the optic nerve head would result in axonal degeneration through the entire axon (Salinas-Navarro et al., 2010). Nevertheless, degenerative diseases are initiated by distal axonopathy followed by dying back (Coleman, 2005).

Increased glia reactivity occurs at the level of the optic nerve head, which could induce changes in the extracellular matrix of the lamina (Fuchshofer et al., 2005; Son et al., 2010). These changes could be due to dying oligodendrocytes in response to inflammatory cytokines from microglia and astrocytes (Nakazawa et al., 2006; Tezel et al., 2001). NOS-2 (Nitric oxide synthase - 2) immunoreactivity has been reported to be increased in the retina and optic nerve of human and rats' eyes (Liu and Neufeld, 2001; Shareef et al., 1999).

Oxidative stress has also been implicated in glaucoma. And it is known that with aging the CNS becomes increasingly susceptible to oxidative damage to the DNA and to proteins (Cakatay et al., 2001). In fact, catalase, gluthathione peroxidase, superoxide dismutase, and malondialdehyde are important anti-oxidative markers elevated in the aqueous humour of patients with glaucoma (Ferreira et al., 2004; Ghanem et al., 2010). In the retinas of DBA/2J mouse ceruloplasmin, an important antioxidant, is upregulated (Steele et al., 2006). In cultures of rat retinas and optic nerve head, ROS lead to activation of glial cell and upregulation of MCH class II (Tezel et al., 2008). ROS can directly damage lipids, proteins and nucleic acids as well as impair mitochondrial respiration depolarization leading to cell death. In addition, ROS promotes Ca^{2+} release from internal stores.

It has been proposed that vascular insufficiency is involved in glaucoma. The pressure would result in a decrease blood supply and episodic ischemia of retinal neurons leading to RGC death and axon loss (Flammer et al., 1999; Gherghel et al., 2004). Another component associated with glaucoma is ischemic reperfusion due to compromise vascular circulation at the level of the ONH (Osborne et al., 2004).

1.3 Neuronal cell death

1.3.1 Mitochondria

Mitochondria are very important organelles of all cells, responsible for energy (ATP) production, and for the control of cell death. In healthy cells, mitochondrial has two membranes: the inner membrane (IM), highly selected and impermeable, and the outer membrane (OM) which is more permeable. The existence of an impermeable inner membrane allows the formation of a proton gradient between the mitochondrial matrix and the intermembrane space that allows for oxidative respirations to occur through the respiratory chain on the inner membrane. The charge imbalance between the matrix and the intermembrane space creates an electrochemical gradient across the IM that is responsible for the mitochondrial membrane potential ($\Delta\Psi m$). The proton gradient is then used for the production of ATP by the complex V. Dysregulation of the mitochondrial homeostasis is responsible for apoptosis cell death.

1.3.2 Apoptosis

Apoptosis in an endogenous programmed cell death that plays an essential role in homeostasis and in the normal development of all multicellular organisms. Apoptosis is characterized by sequential morphologic and biochemical changes, namely, cell shrinkage, membrane blebbing, pyknotic nuclei (chromatin condensation) and karyorhexix (nuclear fragmentation) (Kroemer et al., 2005). Biochemical changes include phosphatidylserine (PS) translocation from the inner leaflet to the outer leaflet of plasma membrane, nuclear fragmentation and protease activation (Zamzami et al., 1996). The final step of apoptosis includes phagocytic clearance in the absence of inflammation (Fadok and Chimini, 2001; Fadok et al., 2001). Dysregulation of apoptosis is responsible for a plethora of autoimmune and neurodegenerative diseases (Green and Kroemer, 2004; Kroemer et al., 2007; Zamzami et al., 1996).

There are two main apoptotic pathways, the extrinsic and the intrinsic pathways, caspase dependent or independent. The activation of a specific class of proteases called

caspases ("cysteine protease cleaving after Asp") are required for the more common form of apoptosis. However, not all caspases are required to induce apoptosis. There are two groups of caspases: caspase executers – caspase-3, -6, and -7 (Fuentes-Prior and Salvesen, 2004); and initiator caspases-8, -9, and -10 that can downstream activate executer caspases (Fig 1.7).

Extrinsic pathway

The extrinsic pathway, also known as the death receptor pathway, is characterized by the binding of extracellular ligands belonging to the tumour necrosis factor (TNF) receptor superfamily, such as tumour necrosis factor itself, TNF-related apoptosis-inducing ligand (TRAIL) and FAS/CD95 ligand (Galluzzi et al., 2012). The binding of any of these ligands causes the recruitment of Fas-associated death domain (FADD) allowing the complex to attract several molecules of procaspase-8, forming 'death-inducing signalling complex' (DISC) which leads to activation of caspase-8 and caspase 10 (Galluzzi et al., 2012; Hengartner, 2000; Kroemer et al., 2007; Muzio et al., 1998). Finally, caspase-8 activates the effector caspases -3, -6 or -7 resulting in various apoptotic substrates and nuclear fragmentation (Reed, 2000) (Fig 1.7).

Intrinsic pathway

The intrinsic pathway, also known as mitochondrial pathway, is activated after loss of pro survival signals inside the cell or from neighbouring cells and result into activation of intracellular cascade of events. In vertebrates, cell death occurs mainly via the intrinsic pathway and can be caspase-dependent or -independent (Galluzzi et al., 2012; Green and Kroemer, 2004) (Fig 1.7).

Caspase-dependent

Caspase-dependent pathway occurs due to mitochondria dysregulation leading to cytochrome C release from mitochondria. Cytochrome C is released to the cytosol where it binds to apoptosis protease activating factor 1 (APAF-1) in the presence of ATP/dATP to form the apoptosome. The release of cytochrome c from mitochondria occurs after mitochondrial outer membrane permeabilization (MOMP). The apoptosome activates

caspase-9, which in turn activates executer caspase-3 leading to cell death (Galluzzi et al., 2012; Kroemer et al., 2007) (Fig 1.7).

Caspase-independent

Caspase-independent pathway occurs after mitochondrial membrane permeabilization and the release of apoptosis inducing factor (AIF) and endonuclease G (Endo G) from the mitochondria (Fig 1.7). AIF (67 kDa) and Endo G (35 kDa) mitochondrial intermembrane flavoprotein (Susin et al., 1999). After an apoptotic insult, AIF is translocated to the nucleus where it induces large scale DNA-fragmentation leading to cell death (Daugas et al., 2000; Galluzzi et al., 2012).

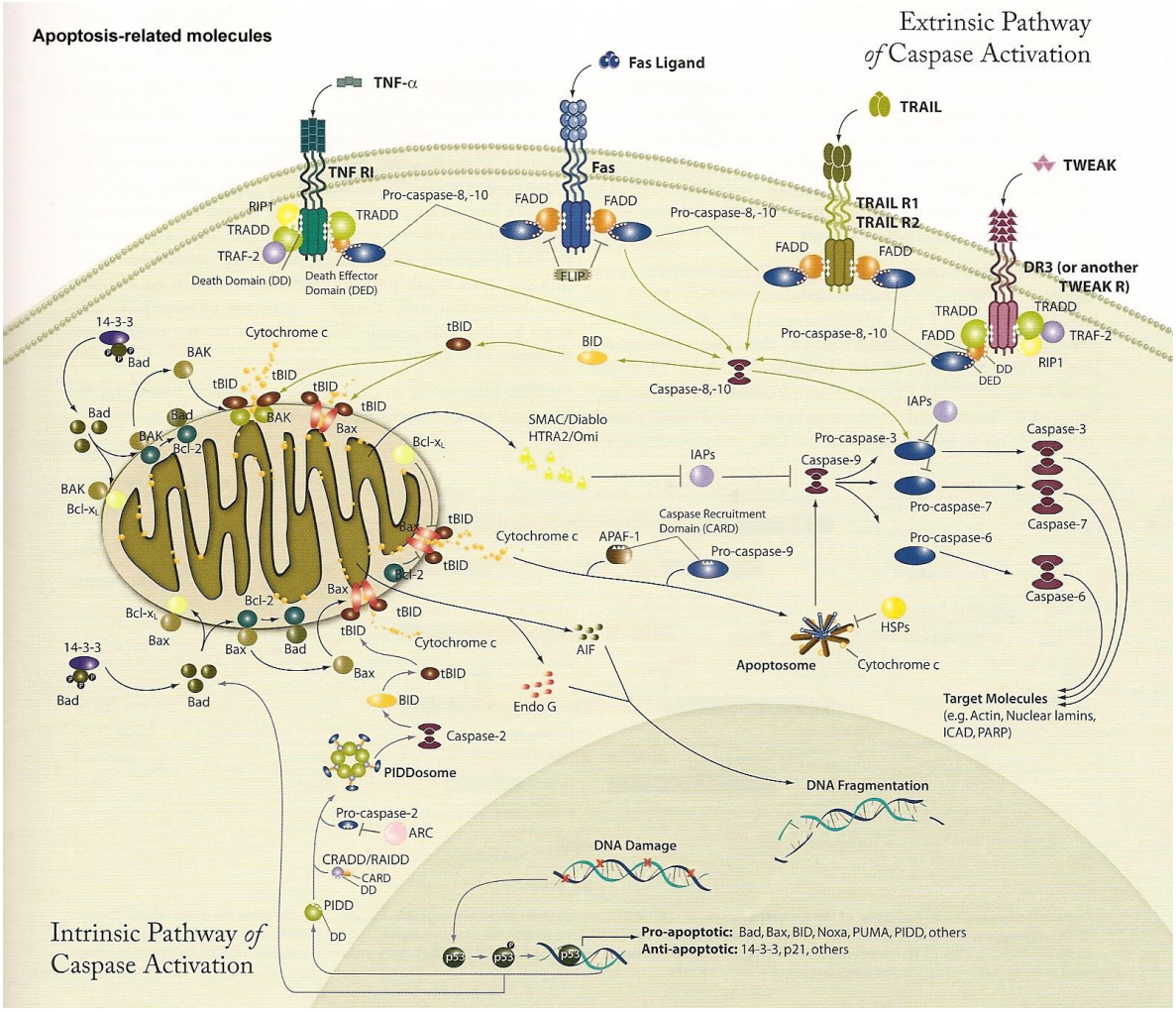

Figure 1.7 - Extrinsic and intrinsic apoptotic pathways. From www.hixonparvo.info%2Fmodel.html&ei=qlOiUdvbGaXJ0AWdoIH4BA&psig=AFQjCNG8N7S3wusMPVT2ojSew_0-Hc3uTw&ust=1369673457991153

1.3.3 Necrosis

Necrosis is ATP-independent cell death in response to a strong toxic insult. It is accompanied by an intracellular ATP depletion and is characterized by the following features: mitochondria and endoplasmic reticulum swelling, DNA destruction and loss of plasma membrane integrity (Haeberlein, 2004). The main features of necrosis include cell volume increase (oncosis), and rupture of the plasma membrane with the release of all cell organelles. Due to the release of cell organelles, necrosis is accompanied by local inflammation (Kroemer et al., 2007).

1.3.4 Detection of apoptosis *in vivo*

The DARC Technology

Annexin V is a phospholipid binding protein with the ability to bind to negatively charged phosphatidylserine (PS) with high affinity in the presence of Ca^{2+} (Meers and Mealy, 1993). During apoptosis, PS, which is ordinarily located in the inner leaflet of the plasma membrane of mammalian cells, is translocated to the outer leaflet and exposed to the extracellular domain. Fluorescently conjugated annexin V has been used in cell biology for the detection of apoptotic cells (FITC-annexin V) (Vermes et al., 1995). More recently, radiolabelled Annexin V has been used to detect apoptosis in vivo. Over 30 clinical studies have been performed using Technetium-99m (99m Tc) labeled annexin V (Table 1.1) to detect apoptosis in acute myocardial infarction, acute cardiac allograft rejection, cerebral hypoxia, ischemic brain injury, hepatitis, breast cancer, lung cancer, lymphoma, and sarcoma (Blankenberg and Strauss, 2001; Flotats and Carrió, 2003; Mountz et al., 2002; Narula et al., 2001; Reutelingsperger et al., 2002; Zhao et al., 2001).

Table 1.1 - Clinical trials using intravenous Annexin.

Technique	No. of patients	Imaging agent	Dose	Year	Ref
I/R injury, Angiotensin II Receptor blocker	20	Tc-99m–HYNIC annexin A5	0.1mg; 400MBq	2011	(Meijer et al., 2011)
Cardiomyopathy/dysplasia	6	Tc-99m–HYNIC annexin A5	0.15mg; 600MBq	2011	(Campian et al., 2011)
Forearm Ischaemia model	12		?	2010 NCT00691613	
Cancer	11	Tc-99m–labeled annexin A5	0.15mg; 600MBq	2009	(Rottey et al., 2009)
Statin Therapy in I/R injury	60	(HYNIC)-Anx	0.1mg; 400MBq	2009	(Meijer et al., 2009)
Cardiac I/R Injury, Rosuvastatin	65	Tc-99m–labeled annexin A5	0.1mg; 400MBq	2008	(Meijer et al., 2009)
Head & Neck cancer	24	99mTc-ethylenedicystein Anx	0.18-0.26mg; 714-1032MBq	2008	(Cordeiro et al., 2011)
Breast cancer	10	(HYNIC)-Anx	0.23-0.27; 925-1073MBq	2008	(Cordeiro et al., 2011)
Outcome prediction cancer treatment	38	(HYNIC)-Anx	0.15-0.28mg; 616-1117MBq	2008	(Cordeiro et al., 2011)
AMPD1 Gene Ischemic Tolerance	20	Tc-99m–labeled annexin A5	0.1mg; 400MBq	2007	(Riksen et al., 2007)
Diabetes	20	Tc-99m–HYNIC annexin A5	?	2007 NCT00184821	
Ischaemia	20	Tc-99m–labeled annexin A5	0.1mg; 400MBq	2007	(Cordeiro et al., 2011)
Crohn's Disease	14		0.11mg; 450MBq	2007	(Cordeiro et al., 2011)
Heart failure *Healthy*	9 2	(HYNIC)-Anx	0.25mg iv	2007	(Cordeiro et al., 2011)
Lung cancer	16	(HYNIC)-Anx	0.17-0.28mg; 690-1116MBq	2007	(Cordeiro et al., 2011)
Treatment-induced normal tissue	18	(HYNIC)-Anx	0.17-0.28mg; 676-1117MBq	2006	(Cordeiro et al., 2011)
Acute stroke	12	(HYNIC)-Anx	0.25mg iv	2006	(Cordeiro et al., 2011)
Dementia	12	(HYNIC)-Anx	0.14-0.19mg; 555-740MBq	2006	(Cordeiro et al., 2011)
Ischaemic Preconditioning	42	Tc-99m–labeled annexin A5	0275mg	2006	(Riksen et al., 2006)
Health *Ischaemic muscle pre-conditioning*	44	(HYNIC)-Anx	0.1mg ischaemic infusion	2005	(Cordeiro et al., 2011)
I/R Injury limited by dipyridamole	32	Tc-99m-HYNIC Annexin A5	0.1mg	2005	(Riksen et al., 2005)
Follicular lymphoma	11	(HYNIC)-Anx	0.11-0.25mg; 482-1013MBq	2004	(Cordeiro et al., 2011)
Head & Neck cancer	28	(HYNIC)-Anx	0.25mg?	2004	(Cordeiro et al., 2011)
Head & Neck cancer	18	(HYNIC)-Anx	0.25mg?	2004	(Cordeiro

					et al., 2011)
Head & Neck cancer	13	(HYNIC)-Anx	0.25mg?	2004	(Cordeiro et al., 2011)
Atherosclerosis	4	(HYNIC)-Anx	0.15-0.2mg; 600-800MBq	2004	(Cordeiro et al., 2011)
Head & Neck cancer	33	B-Anx	0.1-0.28mg; 387-117MBq	2004	(Cordeiro et al., 2011)
Myocardial infarction	9	^{123}I-rh-Anx	c. 1mg iv	2003	(Cordeiro et al., 2011)
Healthy	6	(HYNIC)-Anx	940µg iv	2003	(Cordeiro et al., 2011)
Head & Neck cancer	20	Anx	0.14±0.03mg; 550±110MBq	2003	(Cordeiro et al., 2011)
Healthy	6	99mTc-hydrazinonicotinamido (HYNIC)-Anx	25µg iv	2003	(Cordeiro et al., 2011)
Myocardial infarct ***Heart failure*** ***Other heart diseases*** ***Healthy***	12 4 3 1	I-Anx (99m)Tc-(4,5-bis (thiocetamido)pentanoyl)-Anx BAnx	1.0mg iv in 2.5ml	2003	(Cordeiro et al., 2011)
Lung cancer ***Lymphoma*** ***Breast cancer***	10 3 2	I-Anx	1.0mg iv	2002	(Cordeiro et al., 2011)
Cardiac tumour	1	I-Anx	?	2001	(Cordeiro et al., 2011)
Cardiac allograft rejection	18	I-Anx	0.5-1.0mg iv in 10ml	2001	(Cordeiro et al., 2011)
Acute myocardial infartation	7	Tc 99m–labeled annexin-V	1.0mg iv	2000	(Cordeiro et al., 2011)

In vivo imaging of apoptotic RGCs was first described using the DARC technology (Detection of Apoptosing Retinal Cells) (Cordeiro et al., 2004). DARC is a non-invasive technique that uses the unique optical properties of the eye, to allow direct visualization of apoptotic cells in the retina. This technique utilizes fluorescently conjugated annexin V that binds PS retaining its functionality (Fig 1.8). This enables real-time detection of single RGCs undergoing apoptosis (annexin V-positive cells) in the eye when visualized using a wide-angle confocal laser-scanning ophthalmoscope (cLSO) (Belhocine and Blankenberg, 2006; Fischer and Schulze-Osthoff, 2006) (Fig 1.9).

Different studies have been successfully performed using DARC technology for the determination of RGC apoptosis in vivo using experimental models (Cordeiro et al., 2010, 2004; Guo and Cordeiro, 2008; Guo et al., 2007, 2006; Maass et al., 2007; Schmitz-Valckenberg et al., 2008), demonstrating the potential of this technique, not only for the

determination of glaucoma pathogenesis but also to gauge the potential neuroprotective effects of novel drug candidates and their therapeutic efficacy. DARC will soon be tested in a glaucoma Phase I clinical trial (ISRCTN59484478). It is hoped the DARC technology will give a 'snapshot' of the number of cells undergoing apoptosis at a given time point and repeated imaging will be used as an indicator of disease progression.

Annexin V is an endogenous protein ubiquitously expressed in humans. This protein is located mainly inside the cell and does not incite an immunological reaction, although patients with antiphospholipid syndrome or lupus may have anti-annexin V antibodies.

Intravenous application of annexin V radiolabelled has been used in over 30 clinical trials to date which show annexin V to be well tolerated intravenously (Table 1.1), with an ability to cross the intact blood brain barrier (D'Arceuil et al., 2000). The first DARC clinical trials will therefore involve intravenous administration of fluorescently conjugated annexin V. Intravenous injection is an accepted route in ophthalmology and is currently used for diagnostic imaging tests such as fluorescein and indocyanine green angiography. The ultimate goal of DARC, however, is the production of a non-invasive topically active formulation.

Since it was first described (Cordeiro et al., 2004), the DARC technique has evolved to incorporate annexin V conjugated to an infrared probe. This was done to overcome fundus autofluorescence and improve signal-to-noise ratio. The DARC technology is initially planned to identify abnormal glaucomatous RGC degeneration. Experimental glaucoma studies have demonstrated that apoptosis is specific to RGC layer (Jakobs et al., 2005; Quigley et al., 1995; Shareef et al., 1995). However, large population based studies will be required to establish DARC as a valuable marker of disease progression, differentiating pathological from age-related events.

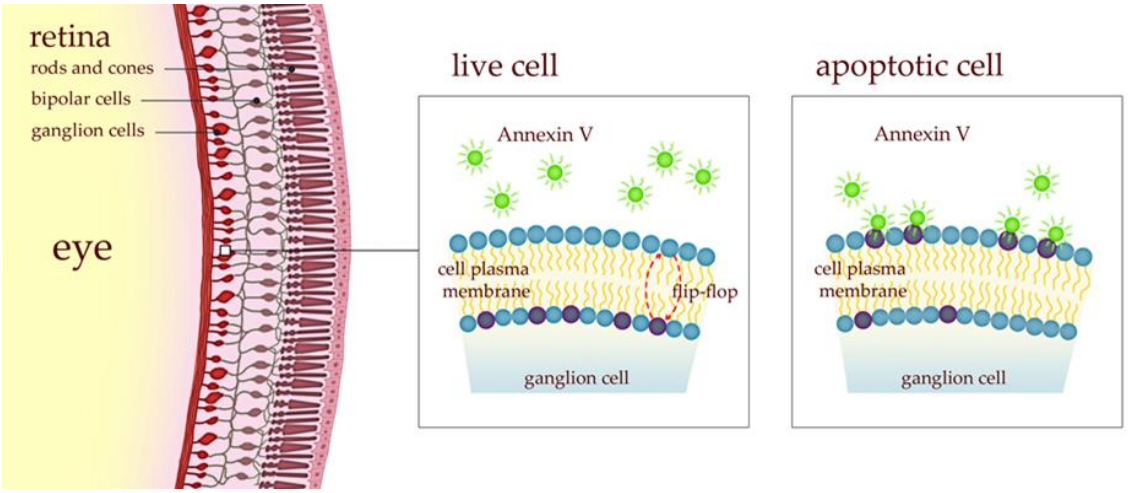

Figure 1.8 - Schematic representation of the DARC technic. Annexin V labelled with a fluorescent marker injected intravitreally binds to RGCs undergoing apoptosis. In the presence of calcium, Annexin V binds specifically to phosphatidilserine that flipped from the inner membrane of the cell to the outer membrane when cells are in the process of apoptosis.

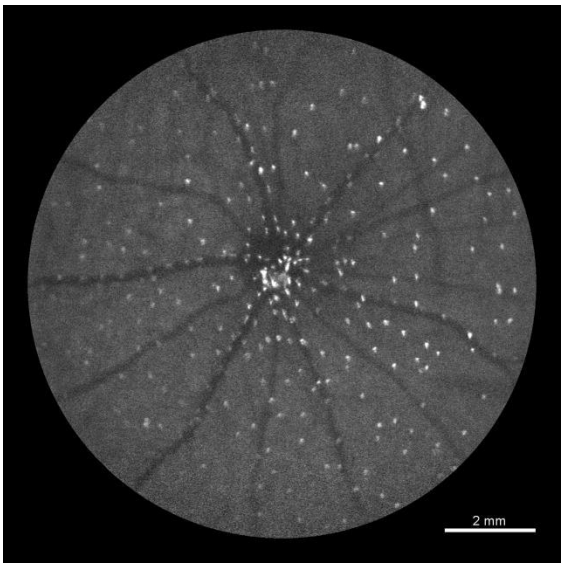

Figure 1.9 - The *in vivo* retinal image of a Dark Agouti rat with chemically induced apoptosis captured using a wide-field lens, two hours after intravitreal administration of fluorescent labelled annexin V. Each white spot represents an individual RGC undergoing apoptosis. The DARC technique can provide a snapshot of the level of RGC apoptosis at any given timepoint.

1.4 Adenosine

1.4.1 Adenosine family

Adenosine is a ubiquitous nucleoside known to be important in cell homeostasis. It is composed of a molecule of adenine attached to a ribose molecule. Adenosine is a neuromodulator in the Central Nervous System (CNS) and can exert both pre- and postsynaptic actions in the same synapse (Ribeiro et al., 2003). Extracellular adenosine can result from the hydrolysis of released adenine nucleotides, such as ATP, AMP, and ADP, through the activation of different ectoenzymes, or through the release of adenosine itself, which is known to occur in different cell types (Perez et al., 1988). Adenosine is rapidly metabolized by adenosine kinase to 5'-AMP and, in a lesser degree, by adenosine deaminase (ADA) to inosine (Parkinson et al., 2005). Inosine can be transformed to hypoxanthine that is then oxidized to xanthine and xanthine to uric acid by xanthine dehydrogenase (Fig 1.10). Most of the extracellular adenosine formed comes either from ATP released by cells, from cAMP, or from AMP, which are metabolized, respectively, by ATPases, phosphodiesterases, and 5'-nucleotidases (CD73), with ATPase localized in the innermost process of Müller cells (Kreutzberg and Hussain, 1982) (Fig 1.10). Extracellular adenosine can also derive from intracellular adenosine through their release by purine nucleoside transporters. There are two major subclasses of nucleoside transporters, the concentrative (CNTs, sodium-dependent), and the equilibrative (ENTs, sodium independent). These former ones also divide into sensitive (es or ENT1) or insensitive (ei or ENT2) to nitrobenzylthioinosine (NBTI) (Visser et al., 2002). Equilibrative nucleoside transporters transport adenosine depending on its gradient, facilitating adenosine influx or efflux depending on adenosine concentration. If there is a high concentration of adenosine outside the cell, ENTs mediate the influx of adenosine. If there is a higher concentration of adenosine inside the cell, ENTs will facilitate their efflux. In contrast, CNTs transport adenosine into the cell at the same time as sodium ions (Parkinson et al., 2005).

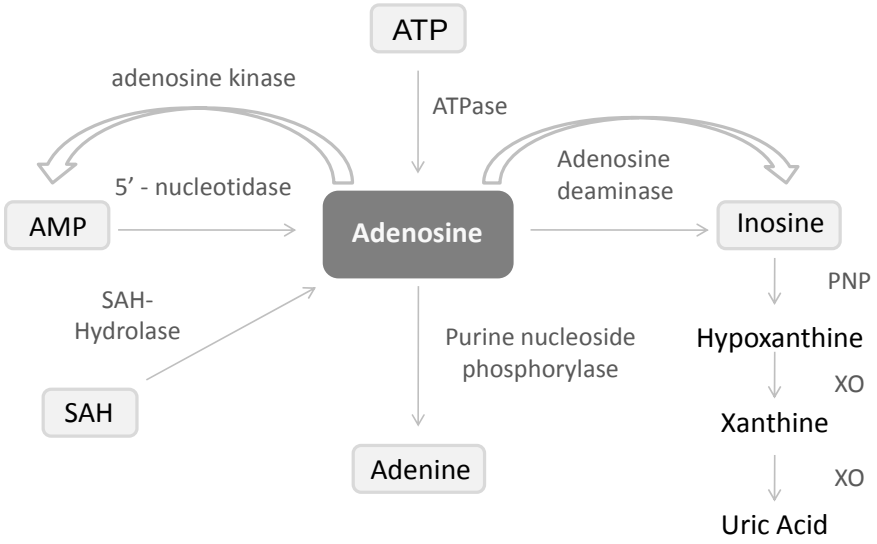

PNP – Purine nucleoside phosphorylase
XO – Xanthine oxidase
5'NT – 5' nucleotidase
ADA – Adenosine deaminase
SAH - S-adenosylhomocysteine

Figure 1.10 - Adenosine metabolism. Adenosine is rapidly metabolised to AMP, inosine, or adenine and transported by the nucleoside transporters to or from inside the cells.

1.4.2 Adenosine receptors

Adenosine acts through the activation of four different receptors, called P1 receptors, which belong to the superfamily of G-protein-coupled receptors (GPCRs), either inhibiting adenylate cyclase (A1 and A3) or stimulating it (A2). A2 receptors (A2R) can be divided into A2a (A2aR) and A2b (A2bR) according to their affinity to [H^3] NECA (non-specific agonist), with the former having a high affinity and the latter a low affinity (Bruns et al., 1986) (Fig 1.11). All four receptors have been characterized and cloned. The A1 adenosine receptor (A1R) is a 36 kDa protein normally associated to adenylate cyclase but it is also known to be coupled to phospholipase C (Palmer and Stiles, 1995). The A2 adenosine receptor is a 45 KDa protein that is responsible for stimulating adenylate cyclase after being activated, leading to increased levels of cAMP. The

activation of A3 adenosine receptor (A3R) is known to decrease cAMP levels in the cell (Jacobson and Gao, 2006). Different agonists and antagonists can be used to modulate the activity of each receptor (Table 1.2). The main strategy to design them was through modifications on the molecule of adenosine, with modification on the N^6, 2-position (adenine moiety) or on the ribose moiety (3', 4' or 5' position). A1R can be antagonised by modified xanthines or non-xanthines. The A1R and A2aR can be generally antagonized by methylxanthines such as caffeine and theophylline (Olah and Stiles, 1992). A2b adenosine receptor (A2bR) is the less represented in the body and is the least known receptor. Agonists or antagonists for this receptor are in small number (Jacobson and Gao, 2006). It has been reported that adenosine arising from adenine nucleotides acts preferentially through A2aR while released adenosine acts preferentially through A1R (Ribeiro et al., 2003). One way of increasing adenosine concentration outside the cells could be by manipulating its metabolism and transport, either by inhibiting its transport or stimulating/inhibiting the enzymes responsible for the adenosine metabolism, or even both.

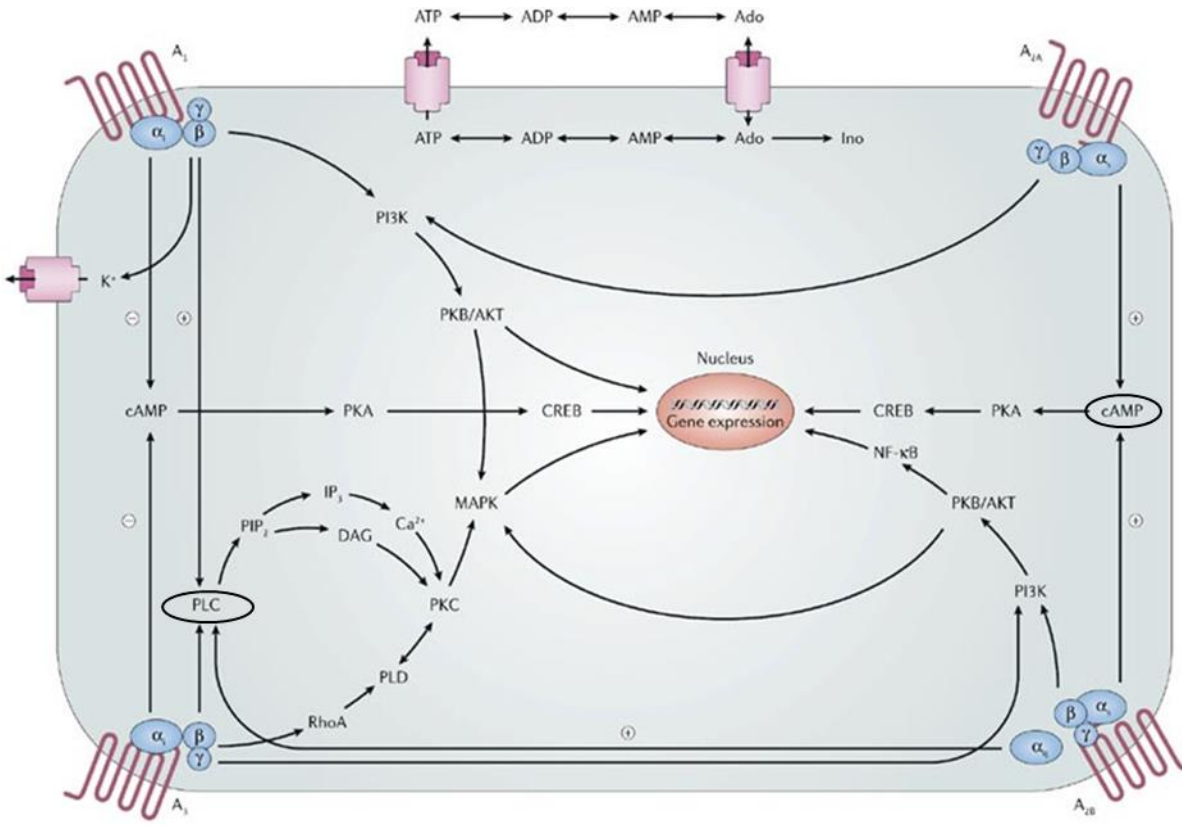

Figure 1.11 - Adenosine receptors pathways. Ligand binding to the A1 and A3 adenosine receptors (ARs) inhibits adenylyl cyclase activity through activation of pertussis toxin-sensitive Gi proteins and results in increased activity of phospholipase C (PLC). Ligand biding to A2A and A2B adenosine receptors increases adenylyl cyclase activity through activation of Gs proteins. All four subtypes of ARs can couple to mitogen-activated protein kinase (MAPK), giving them a role in cell growth, survival, death and differentiation. (CREB - cAMP response element binding protein; DAG - diacylglycerol; IP3 - inositol 1,4,5-trisphosphate; PI3K - phosphatidylinositol 3-kinase; PIP2 -phosphatidylinositol-4,5-bisphosphate; PK - protein kinase; PLD - phospholipase D; NF-κB - nuclear factor-KB. Image adapted from Jacobson and Goa, Adenosine Receptors and Therapeutic Targets, Nat Rev Drug Discov. 2006 Mar;5(3):247-64..

Table 1.2 - Adenosine receptors agonist and antagonists.

Adenosine receptor subtype	Compound name	Ki (nM) A1R	A2aR	A2bR	A3R	Refs
A1 Agonist						
	ADAC	0.85	210	N.A.	13.3	Gao et al., 2003
	AMP579	5.1	56	N.A.	N.A.	Yan et al., 2003
	CCPA	0.83	2,270	18,800	38	Gao et al., 2003; Yan et al., 2003
	CPA	2.3	794	18,600	72	Gao et al., 2003; Yan et al., 2003
	CVT-510 (Tecadenoson)	6.5	2,315	N.A.	N.A.	Yan et al., 2003; Ellenbogen et al., 2005
	GR79236	3.1	1,300	N.A.	N.A.	Knutsen L., 1999
	NNC-21-0136	10	630	N.A.	N.A.	Knutsen L., 1999
	S(–)-ENBA	0.38	>10,000	>10,000	915	Gao et al., 2003; Yan et al., 2003
	SDZ WAG 994	23	25,000	>1,000	N.A.	Yan et al., 2003
	Selodenoson	1.1	306	N.A.	N.A.	Yan et al., 2003
Antagonist						
	BG9719	0.43	1,051	172	3,870	Moro et al., 2006
	BG9928	29	4,720	690	42,110	Auchampach et al., 2004
	DPCPX	3.9	129	56	3,980	Moro et al., 2006
	FK453	18	1300	980	>10,000	Harada et al., 2001
	FR194921	2.9	>10,000	N.A.	>10,000	Maemoto et al., 2004

	KW3902	1.3	380	N.A	N.A.	Moro et al., 2006
	WRC-0571	1.7	105	N.A.	7,940	Martin et al., 1996
A2a Agonist						
	ATL-146e	77	0.5	N.A.	45	Rieger et al., 2001; Yan et al., 2003
	Binodenoson	48,000	270	430,000	903	Gao et al., 2003
	CGS 21680	289	27	>10,000	67	Klotz et al., 1998; Gao et al., 2003
	CV-3146	>10,000	290	>10,000	>10,000	Palle et al., 2003
	DPMA	168	153	>10,000	106	Gao et al., 2003
	NECA	14	20	140	25	Klotz et al., 1998; Gao et al., 2003
Antagonist						
	CSC	28,000	54	N.A.	N.A.	Moro et al., 2006
	KW6002	2,830	36	1,800	>3,000	Weiss et al., 2003
	SCH 442416	1,110	0.048	>10,000	>10,000	Moresco et al., 2005
	SCH 58261	725	5.0	1,110	1,200	Jacobson and Goa 2006
	'Schering compound'	82.4	0.8	N.A.	N.A.	Matasi et al., 2005
	VER 6947	17	1.1	112	1,470	Weiss et al., 2003
	VER 7835	170	1.7	141	1,931	Weiss et al., 2003
	ZM241,385	774	1.6	75	743	Moro et al., 2006
A2b Agonist						
	LUF5835	4.4	21	10	104	Beukers et al., 2004
Antagonist						
	MRE 2029-F20	245	>1,000	3.0	>1,000	Gessi et al., 2005
	MRS1754	403	503	1.45	570	Ji et al., 2001
	OSIP-339391	37	328	0.5	450	Stewart et al., 2004, Gessi et al.,2006
A3 Agonist						
	Cl-IB-MECA	220	5,400	>100,000	1.4	Gao et al., 2003; Tchilibon et al., 2005
	CP-608039	7,300	N.A.	N.A.	5.8	Tracey et al., 2003
	IB-MECA	51	2,900	11,000	1.8	Klotz et al., 1998; Tchilibon et al., 2005
	LJ568	193	223	N.A.	0.38	Jeong et al., 2003

1.4.3 Adenosine related therapy

The therapeutic use of adenosine has been focused on heart and lung diseases and the central nervous system (CNS). Currently there are 381 clinical trials using adenosine either in process or already concluded (clinicaltrial.gov search from October 2013). Adenosine is already approved to treat paroxysmal supraventricular tachycardia (PSVT), and is associated with accessory bypass tracts (Wolff-Parkinson-White Syndrome). It is used as an antiarrhythmic drug as Adenocard (6 mg/2 ml solution for injection vials) or as Adenoscan (30 mg/10 ml solution for infusion vials).

The research based in pharmacology activation or inhibition of one of the four different adenosine receptors is vast and encompasses diseases such as asthma, diabetes, renal failure, heart diseases, Huntington's disease, Parkinson's disease, hypertension, liver disorders and others (Table 1.3).

Adenosine receptors have been targeted for the treatment of various nervous system disorders.

In dementia and anxiety disorders, the A1R antagonist, FR194921, was orally administered to treat these diseases (Maemoto et al., 2004). Activation of A1Rs reduce acute pain, post-operative pain, headaches and migraines as well as reducing hypersensitivity followed peripheral inflammation (Giffin et al., 2003; Li et al., 2003; Zambrowicz, 2003).

Adenosine has been tested for treatment of Parkinson's disease due to interactions between A2aR and dopamine receptor D_2, with antagonist effects observed in striatum (Ferre et al., 1991). A2aR antagonists show relief in Parkinson's disease symptoms, and also decreasing neurodegeneration of dopaminergic cells (Xu et al., 2005). Furthermore, KW-6002 (A2aR antagonist) finished the Phase III of clinical trial and BIIB014 is in Phase II clinical trial for Parkinson's disease with still no results presented (Hauser et al., 2003; Hauser, 2011; Matasi et al., 2005; Weiss et al., 2003).

The A2aR knockout mice are protected against neuronal cell death induced by ischemia (Chen et al., 1999; Monopoli et al., 1998). A1R agonists are also protective in different models of ischemia (Knutsen et al., 1999; Von Lubitz et al., 1996). Moreover, A3R agonist

(IB-MECA) was reported to be cerebroprotective against ischemia in a gerbil model (Von Lubitz et al., 1994).

Adenosine was also found to be an endogenous sleep-promoting substance (Porkka-Heiskanen, 1997; Porkka-Heiskanen et al., 2002), with A2aR having key roles in the involvement of adenosine effects on promoting sleep (Urade, 2003). The wakefulness effects of caffeine were also reported to be mediated by A2aR and not A1R (Huang et al., 2005b).

Table 1.3 - Adenosine receptors as targets for potential therapeutic approaches. Adapted from Gessi S., Adenosine receptor targeting in health and disease. Expert Opinion Investigative Drugs. 2011 Dec;20(12):1591-609. doi: 10.1517/13543784.2011.627853. Epub 2011 Oct 22.

Receptor	Pathology		Drug	Mechanism of action	Phase	Reference
A1						Gessi et al., 2011
	Cardiovascular disease	Arrhythmia, atrial fibrillation	Capadenoson	Agonist	Phase II	Gessi et al., 2011
			Selodenoson	Agonist	Phase II	Gessi et al., 2011
			Tecadenoson	Agonist	Phase III	Gessi et al., 2011
		Heart failure, congestive	Derenofylline	Antagonist	Phase II	Gessi et al., 2011
			Tonapofylline	Antagonist	Phase III	Gessi et al., 2011
	Respiratory disorders	Asthma	Doxofylline	Antagonist	Launched 1987	Gessi et al., 2011
			Theophylline	Antagonist	Launched 1987	Gessi et al., 2011
		COPD	Theophylline	Antagonist	Phase II	Gessi et al., 2011
	Renal disorders	Renal failure	Rolofylline	Antagonist	Phase III	Gessi et al., 2011
			Derenofylline	Antagonist	Phase II	Gessi et al., 2011
	Endocrine disorders	Diabetes	CVT-3619	Partial agonist	Phase I	Gessi et al., 2011
	Eye disorders	Glaucoma	Pj-875	Agonist	Phase II	Gessi et al., 2011
	Metabolic disease	Lipoprotein disorders	CVT-3619	Partial agonist	Phase I	Gessi et al., 2011
	Pain	Neuropathic pain	T-62	Allosteric enhancer	Phase II	Gessi et al., 2011
A2a						Gessi et al., 2011
	Neurological disorders	Huntington's disease	[^{123}]MNI-420	Antagonist	Phase I	Gessi et al., 2011
		Parkinson's disease	Istadefylline	Antagonist	Preregistered	Gessi et al., 2011
			Preladenant	Antagonist	Phase III	Gessi et al., 2011
			ST-1535	Antagonist	Phase I	Gessi et al., 2011
			SYN-115	Antagonist	Phase II	Gessi et al., 2011
			^{123}]MNI-420	Antagonist	Phase I	Gessi et al., 2011
	Cardiovascular diseases	Coronary artery disease diagnosis	Regadenoson	Agonist	Launched 2008	Gessi et al., 2011
			Apadenoson	Agonist	Phase III	Gessi et

						al., 2011
			Binodenoson	Agonist	Preregistered	Gessi et al., 2011
		Hypertention	YT-146	Agonist	Phase II	Gessi et al., 2011
		Sickle cell disease	Regadenoson	Agonist	Phase I	Gessi et al., 2011
	Respiratory disorders	COPD	Apadenoson	Agonist	Phase I	Gessi et al., 2011
		Asthma	Apadenoson	Agonist	Phase I	Gessi et al., 2011
	Dermatological disorders	Ulcer, diabetic	Sonedenoson	Agonist	Phase II	Gessi et al., 2011
A2b						Gessi et al., 2011
	Respiratory disorders	Asthma	CVT-6883	Antagonist	Phase I	Gessi et al., 2011
			GS-6201	Antagonist	Phase I	Gessi et al., 2011
	Gastrointestinal disorders	Diarrhea	CVT-6883	Antagonist	Phase I	Gessi et al., 2011
	Cardiovascular disorders		CVT-6883	Antagonist	Phase I	Gessi et al., 2011
A3	Musculoskeletal and connective tissue disorders	Osteoarthritis	CF-101	Agonist	Phase II	Gessi et al., 2011
		Rheumatoid arthritis	CF-101	Agonist	Phase I	Gessi et al., 2011
	Cancer	Hepatocellular carcinoma	CF-102	Agonist	Phase II	Bar-Yehuda et al., 2008
	Eye disorders	Dry eyes	CF-101	Agonist	Phase II	Avni et al., 2010
		Glaucoma	CF-101	Agonist	Phase II	Gessi et al., 2011
		Uveitis	CF-101	Agonist	Phase I	Gessi et al., 2011
	Gastrointestinal disorders	Liver disorders	CF-102	Agonist	Phase I	Gessi et al., 2011
		Hepatitis C	CF-102	Agonist	Phase II	Gessi et al., 2011
	Dermatological disorders	Psoriasis	CF-101	Agonist	Phase III	Gessi et al., 2011

1.4.4 Localization of adenosine in the retina

Endogenous adenosine, adenosine receptors, enzymes of the adenosine metabolism and adenosine transporters have been identified in the retina. The A1R was the first receptor to be identified. Using the A1R agonist ^{3}H-CHA, it was found that RGCs, as well as in superior colliculus and lateral geniculate nucleus (retinal ganglion cell projections to the brain) had a high density of labelled A1R (Blazynski et al., 1989; Goodman et al., 1983). Northern blot analysis for A1R and RT-PCR for A2aR detected mRNA levels of both receptors at superior colliculus, with higher levels of A1R compared to A2a (Ishikawa et al., 1997). Braas and colleagues also identified a similar distribution of A1R in the retina. By immunocytochemistry and autoradiographic analysis using ^{3}H-PIA and ^{125}I H-PIA, the majority of staining was observed in retinal ganglion cells, nerve fiber layer and inner plexiform layer of the rat and guinea pig retina. This staining was associated with RGCs soma, axons and dendritic tree. In monkey and human retina the binding of ^{3}H-PIA and ^{125}I H-PIA was predominantly localized in RGCs, although in monkeys there was more diffuse binding through the nerve fiber layer and outer plexiform layer, while in humans the binding was throughout the entire retina (Braas et al., 1987). A1R agonist labelled with silver grains appeared in retinal pigmented epithelium as well as in the outer and inner segment layers of photoreceptors, which was different from what was found before.

Binding sites for both A1R and A2R were assessed using ^{3}H NECA. Since NECA is known to bind both A1R and A2R, the use of R-PIA, an A1R agonist, which would be competitive for A1 adenosine receptor ligand sites, would displace ^{3}H NECA from A1R. Results using these agonists, NECA and R-PIA, localized the A2R to the outer retina. A2R was also localized by autoradiography in photoreceptors (Blazynski, 1990). In the rat retina, the levels of mRNA for adenosine receptors assessed by in situ hybridization, indicate the presence of A1R mainly in GCL and some cells of inner nuclear layer (probably amacrine cells), while A2aR expression was predominantly seen at the inner nuclear layer and less prominent at GCL and outer nuclear layer (Ghiardi et al., 1999; Kvanta et al., 1997). The expression of mRNAs for A1R, A2aR and A2bR was also localized to epithelial cells in the rat eye (Kvanta et al., 1997). The mRNA for A3R was not detected in the retina by Kvanta and colleagues (1997) but was subsequently identified in RGCs (Zhang et al., 2006). This

molecular identification was functionally confirmed in isolated purified retinal ganglion cells using the agonist Cl-IB-MECA (Zhang et al., 2006).

The different enzymes of the adenosine metabolism were also shown to be present in the retina. For example, 5'-nucleotidase, an enzyme responsible for the hydrolysis of AMP (adenosine monophosphate) to adenosine was present between photoreceptors and horizontal cells (Kreutzberg and Hussain, 1982; Scott, 1967), as well as on certain domains of Müller cells (Kreutzberg and Hussain, 1982), in mouse (Braun et al., 1995) and canine retinas (Lutty et al., 2000). ADA, which removes the amine group from adenosine, converting it to inosine was also identified in the rat retina by immunohistochemical analysis mostly in the retinal ganglion cell layer and inner plexiform layer (Senba et al., 1986). The staining in GCL was not altered after optic nerve transection, consistent with displaced amacrine cells labelling and not ganglion cells (Blazynski and Perez, 1991).

Nucleoside transporters are also expressed in the rabbit retina and ARPE-19 (human retinal pigment epithelial cell line) (Majumdar et al., 2004). It has been reported that [^{3}H] adenosine uptake and its inhibition by Nitrobenzylthioinosine (NBMPR) take place in the rabbit retinal ganglion cell and inner nuclear layers (Blazynski and Perez, 1991) as well as on chick embryo primary cultures of retinal neurons and photoreceptors (Paes de Carvalho et al., 1990). Adenosine nucleoside transporters were also found in murine retinal microglia (Liou et al., 2008).

1.4.5 Adenosine in the ganglion cell layer

There are about 15-20 different functional classes of RGCs, based on their receptive field and their linear or nonlinear summation properties (Sivyer et al., 2011; Wassle and Boycott, 1991; Wong et al., 2012). A1 and A3 adenosine receptors are expressed in RGC. However, the expression of A2aR by RGCs is controversial, with some claiming it is present and others claiming it is present only in the outer retina.

The A1 adenosine receptor agonist, CHA, inhibits Ca^{2+} currents in salamander RGCs, and this effect was completely abolished in the presence of the A1 adenosine receptor

antagonist DPCPX (Sun et al., 2002). This inhibitory effect of adenosine on Ca^{2+} currents was reported to be due to the inhibition of the N-type Ca^{2+} channels, but not the L-type, as ω-conotoxin-GVIA (N-type VSCC blocker) had a similar effect as CHA itself (Sun et al., 2002). Others have reported the same Ca^{2+} effects, where adenosine was reported to reduce the intracellular Ca^{2+} increase evoked by glutamate on isolated rat RGCs. This effect was mediated by the A1 adenosine receptor as DPCPX (A_1 antagonist), but not DMPX (A2a antagonist), blocked the adenosine effect. Furthermore, results obtained in intact rat retina during exposure to NMDA (Hartwick et al., 2004). Moreover, Clark and colleagues have demonstrated that adenosine evokes hyperpolarisation of RGCs, mediated by the activation of A1 adenosine receptors, which leads to the opening of the inwardly rectifying K^+ channels and to an increase of IP3-R (Inositol trisphosphate receptor) dependent release of Ca^{2+} from internal stores leading to the opening of small conductance Ca^{2+} - activating K^+ channels (Clark et al., 2009). More recently, stimulation of adenosine A3R in isolated ganglion cells led to a decrease in P2X7-induced Ca^{2+} levels and cell death (Zhang et al., 2006). Furthermore, *in vivo* studies corroborate these experiments, showing neuroprotective effects of A3R activation to P2X7 induced cell death (Hu et al., 2010).

1.5 Aims of the present study

Glaucoma is a leading cause of irreversible blindness with more than 60 million people affected worldwide (Quigley and Broman, 2006). The therapeutic approach for this disease is the decrease in intraocular pressure (IOP), even though the decrease of IOP does not stop disease progression, which is due to the death of RGCs. At the present moment, there are no pharmacologic tools to prevent RGC death. There is an unmet need to find new approaches to prevent RGC death and vision loss in glaucoma.

Previous work has shown that adenosine protects against ischemia both in brain and heart. Adenosine receptors have been considered potential therapeutic targets in neurodegenerative diseases, such as stroke, traumatic brain injury, Alzheimer's disease, Parkinson's disease, Huntington's disease and multiple sclerosis. In the retina, adenosine and three of its four receptors have been identified at the level of retinal ganglion cells, including the A3 adenosine receptors, which might have relevance at the RGC level.

The aim of this study was to evaluate the potential neuroprotective effect of adenosine A3 receptor activation against RGC death, using the A3 receptor agonist, 2-Cl-IB-MECA. Different models have been used in this study both *in vitro* and *in vivo* to assess the potential neuroprotective role of the A3 adenosine receptor agonist in RGCs, and thus devise a potential new treatment for glaucoma.

In Chapter 2, the mechanism by which DMSO triggers cell death is unveiled. A new model of short term RGC death was established.

In Chapter 3, the neuroprotective effect of the A3 adenosine receptor agonist was evaluated *in vitro* in a mixed primary culture of retinal cells and in an organotypic culture of the retina. The model established in chapter 2 and in an ischemic/reperfusion model was used to assess A3 adenosine receptor agonist as a neuroprotective agent. Changes seen *in vivo* were validated histologically on the same retinas.

In Chapter 4, the neuroprotective effect of the A3 adenosine receptor agonist was evaluated *in vivo* in a model of partial optic nerve transection and in a glaucoma model,

the chronic ocular hypertension model. As before, the changes observed *in vivo* were validated histologically on the same retinas.

1.6 References

Ahmed, Z., Kalinski, H., Berry, M., Almasieh, M., Ashush, H., Slager, N., Brafman, A., Spivak, I., Prasad, N., Mett, I., Shalom, E., Alpert, E., Di Polo, A., Feinstein, E., Logan, A., 2011. Ocular neuroprotection by siRNA targeting caspase-2. Cell Death Dis. 2, e173.

Ali, R.R., Reichel, M.B., Alwis, M.A.H.E.S.H.D.E., Kanuga, N., Kinnn, C., Levinsky, R.O.L.A.N.D.J., Hunt, D.M., Bhattacharya, S.S., Thrasher, A.J., 1998. Brief Report Adeno-Associated Virus Gene Transfer to Mouse Retina 86, 81–86.

Anderson, D.R., Hendrickson, A., 1974. Effect of intraocular pressure on rapid axoplasmic transport in monkey optic nerve. Invest. Ophthalmol. 13, 771–83.

Avila, M.Y., Carré, D. a, Stone, R. a, Civan, M.M., 2001. Reliable measurement of mouse intraocular pressure by a servo-null micropipette system. Invest. Ophthalmol. Vis. Sci. 42, 1841–6.

Baltmr, A., Duggan, J., Nizari, S., Salt, T.E., Cordeiro, M.F., 2010. Neuroprotection in glaucoma - Is there a future role? Exp. Eye Res. 91, 554–66.

Bampton, E.T.W., Ma, C.H., Tolkovsky, A.M., Taylor, J.S.H., 2005. Osteonectin is a Schwann cell-secreted factor that promotes retinal ganglion cell survival and process outgrowth. Eur. J. Neurosci. 21, 2611–23.

Beal, M.F., 2003. Bioenergetic Approaches for Neuroprotection in Parkinson ' s Disease. Ann Neurol 53, 39–48.

Belhocine, Z.T., Blankenberg, F.G., 2006. The Imaging of Apoptosis with the Radiolabelled Annexin A5: A New Tool in Translational Research. Curr. Clin. Pharmacol. 1, 129–137.

Blankenberg, F.G., Strauss, H.W., 2001. Will imaging of apoptosis play a role in clinical care? A tale of mice and men. Apoptosis 6, 117–23.

Blazynski, C., 1990. Discrete distributions of adenosine receptors in mammalian retina. J. Neurochem. 54, 648–55.

Blazynski, C., Cohen, a I., Früh, B., Niemeyer, G., 1989. Adenosine: autoradiographic localization and electrophysiologic effects in the cat retina. Invest. Ophthalmol. Vis. Sci. 30, 2533–6.

Blazynski, C., Perez, M.T., 1991. Adenosine in vertebrate retina: localization, receptor characterization, and function. Cell. Mol. Neurobiol. 11, 463–84.

Boland, M. V, Zhang, L., Broman, A.T., Jampel, H.D., Quigley, H. a, 2008. Comparison of optic nerve head topography and visual field in eyes with open-angle and angle-closure glaucoma. Ophthalmology 115, 239–245.e2.

Braas, K.M., Zarbin, M.A., Snyder, S.H., 1987. Endogenous adenosine and adenosine receptors localized to ganglion cells of the retina. Proc. Natl. Acad. Sci. U. S. A. 84, 3906–10.

Braun, N., Brendel, P., Zimmermann, H., 1995. Distribution of 5'-nucleotidase in the developing mouse retina. Brain Res. Dev. Brain Res. 88, 79–86.

Bruns, R., Lu, G., Pugsley, T., 1986. Characterization of the A2 Adenosine [3H] NECA in Rat Striatal Membranes Receptor Labeled by. Mol. Pharmacol. 29, 331–346.

Burgoyne, C.F., Downs, J.C., Bellezza, A.J., Suh, J.-K.F., Hart, R.T., 2005. The optic nerve head as a biomechanical structure: a new paradigm for understanding the role of IOP-related stress and strain in the pathophysiology of glaucomatous optic nerve head damage. Prog. Retin. Eye Res. 24, 39–73.

Cakatay, U., Telci, A., Kayalì, R., Tekeli, F., Akçay, T., Sivas, A., 2001. Relation of oxidative protein damage and nitrotyrosine levels in the aging rat brain. Exp. Gerontol. 36, 221–9.

Campian, M.E., Tan, H.L., van Moerkerken, A.F., Tukkie, R., van Eck-Smit, B.L.F., Verberne, H.J., 2011. Imaging of programmed cell death in arrhythmogenic right ventricle cardiomyopathy/dysplasia. Eur. J. Nucl. Med. Mol. Imaging 38, 1500–6.

Caprioli, J., Munemasa, Y., Kwong, J.M.K., Piri, N., 2009. Overexpression of thioredoxins 1 and 2 increases retinal ganglion cell survival after pharmacologically induced oxidative stress, optic nerve transection, and in experimental glaucoma. Trans. Am. Ophthalmol. Soc. 107, 161–5.

Carelli, V., Ross-Cisneros, F.N., Sadun, A. a, 2004. Mitochondrial dysfunction as a cause of optic neuropathies. Prog. Retin. Eye Res. 23, 53–89.

Chang, E.E., Goldberg, 2012. Glaucoma 2.0: neuroprotection, neuroregeneration, neuroenhancement. Ophthalmology 119, 979–86.

Chauhan, B.C., Pan, J., Archibald, M.L., LeVatte, T.L., Kelly, M.E.M., Tremblay, F., 2002. Effect of intraocular pressure on optic disc topography, electroretinography, and axonal loss in a chronic pressure-induced rat model of optic nerve damage. Invest. Ophthalmol. Vis. Sci. 43, 2969–76.

Chen, J.F., Huang, Z., Ma, J., Zhu, J., Moratalla, R., Standaert, D., Moskowitz, M. a, Fink, J.S., Schwarzschild, M. a, 1999. A(2A) adenosine receptor deficiency attenuates brain injury induced by transient focal ischemia in mice. J. Neurosci. 19, 9192–200.

Cheng, L., Chaidhawangul, S., Wong-Staal, F., Gilbert, J., Poeschla, E., Toyoguchi, M., El-Bradey, M., Bergeron-Lynn, G., Soules, K. a, Freeman, W.R., 2002. Human immunodeficiency virus type 2 (HIV-2) vector-mediated in vivo gene transfer into adult rabbit retina. Curr. Eye Res. 24, 196–201.

Chidlow, G., Melena, J., Osborne, N.N., 2000. Betaxolol, a beta(1)-adrenoceptor antagonist, reduces Na(+) influx into cortical synaptosomes by direct interaction with Na(+) channels: comparison with other beta-adrenoceptor antagonists. Br. J. Pharmacol. 130, 759–66.

Chidlow, G., Schmidt, K.-G., Wood, J.P.M., Melena, J., Osborne, N.N., 2002. Alpha-lipoic acid protects the retina against ischemia-reperfusion. Neuropharmacology 43, 1015–25.

Clark, B.D., Kurth-Nelson, Z.L., Newman, E.A., 2009. Adenosine-evoked hyperpolarization of retinal ganglion cells is mediated by G-protein-coupled inwardly rectifying K+ and small conductance Ca2+-activated K+ channel activation. J. Neurosci. 29, 11237–45.

Colafrancesco, V., Parisi, V., Sposato, V., Rossi, S., Russo, M.A., Coassin, M., Lambiase, A., Aloe, L., 2011. Ocular application of nerve growth factor protects degenerating retinal ganglion cells in a rat model of glaucoma. J. Glaucoma 20, 100–8.

Coleman, M., 2005. Axon degeneration mechanisms: commonality amid diversity. Nat. Rev. Neurosci. 6, 889–98.

Cordeiro, M.F., Guo, L., Coxon, K.M., Duggan, J., Nizari, S., Normando, E.M., Sensi, S.L., Sillito, a M., Fitzke, F.W., Salt, T.E., Moss, S.E., 2010. Imaging multiple phases of neurodegeneration: a novel approach to assessing cell death in vivo. Cell Death Dis. 1, e3.

Cordeiro, M.F., Guo, L., Luong, V., Harding, G., Wang, W., Jones, H.E., Moss, S.E., Sillito, A.M., Fitzke, F.W., 2004. Real-time imaging of single nerve cell apoptosis in retinal neurodegeneration. Proc. Natl. Acad. Sci. U. S. A. 101, 13352–6.

Cordeiro, M.F., Migdal, C., Bloom, P., Fitzke, F.W., Moss, S.E., 2011. Imaging apoptosis in the eye. Eye (Lond). 25, 545–53.

D'Arceuil, H., Rhine, W., de Crespigny, A., Yenari, M., Tait, J.F., Strauss, W.H., Engelhorn, T., Kastrup, A., Moseley, M., Blankenberg, F.G., Traystman, R.J., 2000. 99mTc Annexin V Imaging of Neonatal Hypoxic Brain Injury Editorial Comment. Stroke 31, 2692–2700.

Dai, C., Qin Yin, Z., Li, Y., Raisman, G., Li, D., 2010. Survival of retinal ganglion cells in slice culture provides a rapid screen for olfactory ensheathing cell preparations. Brain Res. 1354, 40–6.

Danesh-Meyer, H. V, 2011. Neuroprotection in glaucoma: recent and future directions. Curr. Opin. Ophthalmol. 22, 78–86.

Daugas, E., Susin, S.A., Zamzami, N., Ferri, K.F., Irinopoulou, T., Larochette, N., Prévost, M.-C., Leber, B., Andrews, D., Penninger, J., Kroemer, G., 2000. Mitochondrio-nuclear translocation of AIF in apoptosis and necrosis. FASEB 14, 729–739.

Di Polo, a, Aigner, L.J., Dunn, R.J., Bray, G.M., Aguayo, a J., 1998. Prolonged delivery of brain-derived neurotrophic factor by adenovirus-infected Müller cells temporarily rescues injured retinal ganglion cells. Proc. Natl. Acad. Sci. U. S. A. 95, 3978–83.

Diggory, P., Cassels-Brown, A., Fernandez, C., 1996. Topical beta-blockade with intrinsic sympathomimetic activity offers no advantage for the respiratory and cardiovascular function of elderly people. Age Ageing 25, 424–8.

Dong, C.-J., Guo, Y., Agey, P., Wheeler, L., Hare, W. a, 2008. Alpha2 adrenergic modulation of NMDA receptor function as a major mechanism of RGC protection in experimental glaucoma and retinal excitotoxicity. Invest. Ophthalmol. Vis. Sci. 49, 4515–22.

Dreyer, E.B., Zurakowski, D., Robert, A., Podos, S.M., Lipton, S.A., 1996. Elevated glutamate levels in the vitreous body of humans and monkeys with glaucoma. Arch Ophthalmol. 114, 299–305.

Edmunds, B., Thompson, J.R., Salmon, J.F., Wormald, R.P., 2002. The National Survey of Trabeculectomy. III. Early and late complications. Eye (Lond). 16, 297–303.

Einarson, T.R., Kulin, N. a, Tingey, D., Iskedjian, M., 2000. Meta-analysis of the effect of latanoprost and brimonidine on intraocular pressure in the treatment of glaucoma. Clin. Ther. 22, 1502–15.

Fadok, V. a, Chimini, G., 2001. The phagocytosis of apoptotic cells. Semin. Immunol. 13, 365–72.

Fadok, V. a, de Cathelineau A, Daleke, D.L., Henson, P.M., Bratton, D.L., 2001. Loss of phospholipid asymmetry and surface exposure of phosphatidylserine is required for phagocytosis of apoptotic cells by macrophages and fibroblasts. J. Biol. Chem. 276, 1071–7.

Fautsch, M., Johnson, D., 2006. Aqueous humor outflow: what do we know? where will it lead us? Invest. Ophthalmol. Vis. Sci. 47, 4181–4187.

Fechtner, R., Weinreb, R.N., 1994. MAJOR REVIEW Mechanisms of Optic Nerve Damage in Primary Open Angle Glaucoma. Surv. Ophthalmol. 39.

Ferre, S., von Euler, G., Johansson, B., Fredholm, B.B., Fuxe, K., 1991. Stimulation of high-affinity adenosine A2 receptors decreases the affinity of dopamine D2 receptors in rat striatal membranes. Proc. Natl. Acad. Sci. U. S. A. 88, 7238–41.

Ferreira, S.M., Lerner, S.F., Brunzini, R., Evelson, P. a., Llesuy, S.F., 2004. Oxidative stress markers in aqueous humor of glaucoma patients. Am. J. Ophthalmol. 137, 62–69.

Fischer, D., Petkova, V., Thanos, S., Benowitz, L.I., 2004. Switching mature retinal ganglion cells to a robust growth state in vivo: gene expression and synergy with RhoA inactivation. J. Neurosci. 24, 8726–40.

Fischer, U., Schulze-Osthoff, K., 2006. New Approaches and Therapeutics Targeting Apoptosis in Disease. Pharmacol. Rev. 57, 187–215.

Flammer, J., Haeflinger, I., Orgul, S., Resink, T., 1999. Vascular dysregulation: A principal risk factor for glaucoma damage? Journal of Glaucoma.

Flotats, A., Carrió, I., 2003. Non-invasive in vivo imaging of myocardial apoptosis and necrosis. Eur. J. Nucl. Med. Mol. Imaging 30, 615–30.

Foster, P.J., Johnson, G.J., 2001. Glaucoma in China : how big is the problem ? Br J Ophthalmol. 1277–1282.

Friedman, D.S., Wilson, M.R., Liebmann, J.M., Fechtner, R.D., Weinreb, R.N., 2004. An evidence-based assessment of risk factors for the progression of ocular hypertension and glaucoma. Am. J. Ophthalmol. 138, S19–31.

Fu, Q.-L., Li, X., Yip, H.K., Shao, Z., Wu, W., Mi, S., So, K.-F., 2009. Combined effect of brain-derived neurotrophic factor and LINGO-1 fusion protein on long-term survival of retinal ganglion cells in chronic glaucoma. Neuroscience 162, 375–82.

Fuchshofer, R., Birke, M., Welge-Lussen, U., Kook, D., Lütjen-Drecoll, E., 2005. Transforming growth factor-beta 2 modulated extracellular matrix component expression in cultured human optic nerve head astrocytes. Invest. Ophthalmol. Vis. Sci. 46, 568–78.

Fuentes-Prior, P., Salvesen, G.S., 2004. The protein structures that shape caspase activity, specificity, activation and inhibition. Biochem. J. 384, 201–32.

Galluzzi, L., Vitale, I., Abrams, J.M., Alnemri, E.S., Baehrecke, E.H., Blagosklonny, M. V, Dawson, T.M., Dawson, V.L., El-Deiry, W.S., Fulda, S., Gottlieb, E., Green, D.R., Hengartner, M.O., Kepp, O., Knight, R. a, Kumar, S., Lipton, S. a, Lu, X., Madeo, F., Malorni, W., Mehlen, P., Nuñez, G., Peter, M.E., Piacentini, M., Rubinsztein, D.C., Shi, Y., Simon, H.-U., Vandenabeele, P., White, E., Yuan, J., Zhivotovsky, B., Melino, G., Kroemer, G., 2012. Molecular definitions of cell death subroutines: recommendations of the Nomenclature Committee on Cell Death 2012. Cell Death Differ. 19, 107–20.

Garcia-Valenzuela, E., Shareef, S., Walsh, J., Sharma, S.C., 1995. Programmed cell death of retinal ganglion cells during experimental glaucoma. Exp. Eye Res. 61, 33–44.

Georgiou, a L., Guo, L., Cordeiro, M.F., Salt, T.E., 2010. Changes in NMDA receptor contribution to synaptic transmission in the brain in a rat model of glaucoma. Neurobiol. Dis. 39, 344–51.

Ghanem, A. a, Arafa, L.F., El-Baz, A., 2010. Oxidative stress markers in patients with primary open-angle glaucoma. Curr. Eye Res. 35, 295–301.

Gherghel, Gherghel, D., Orgül, S., Prünte, C., Gugleta, K., Lübeck, P., Gekkieva, M., 2004. Interocular differences in optic disc topographic parameters in normal subjects. Curr. Eye Res. 20, 276–282.

Ghiardi, G.J., Gidday, J.M., Roth, S., 1999. The purine nucleoside adenosine in retinal ischemia-reperfusion. Inj. Vis. Res. 39, 2519–2535.

Giffin, N.J., Kowacs, F., Libri, V., Williams, P., Goadsby, P.J., Kaube, H., 2003. Effect of the adenosine A1 receptor agonist GR79236 on trigeminal nociception with blink reflex recordings in healthy human subjects. Cephalalgia 23, 287–92.

Glaucoma, C.N., Group, S., 1998. The Effectiveness of Intraocular Pressure Reduction in the Treatment of Normal-Tension Glaucoma. Am. J. Ophthalmol. 126, 498–505.

Goodman, R.R., Kuhar, M.J., Hester, L., Snyder, S.H., 1983. Adenosine receptors: autoradiographic evidence for their location on axon terminals of excitatory neurons. Science 220, 967–9.

Green, D.R., Kroemer, G., 2004. The pathophysiology of mitochondrial cell death. Science 305, 626–9.

Grozdanic, S.D., Lazic, T., Kuehn, M.H., Harper, M.M., Kardon, R.H., Kwon, Y.H., Lavik, E.B., Sakaguchi, D.S., 2010. Exogenous modulation of intrinsic optic nerve neuroprotective activity. Graefes Arch. Clin. Exp. Ophthalmol. 248, 1105–16.

Guo, L., Cordeiro, M.F., 2008. Assessment of neuroprotection in the retina with DARC. Prog. Brain Res. 173, 437–50.

Guo, L., Salt, T.E., Luong, V., Wood, N., Cheung, W., Maass, A., Ferrari, G., Russo-Marie, F., Sillito, A.M., Cheetham, M.E., Moss, S.E., Fitzke, F.W., Cordeiro, M.F., 2007. Targeting amyloid-beta in glaucoma treatment. Proc. Natl. Acad. Sci. U. S. A. 104, 13444–9.

Guo, L., Salt, T.E., Maass, A., Luong, V., Moss, S.E., Fitzke, F.W., Cordeiro, M.F., 2006. Assessment of neuroprotective effects of glutamate modulation on glaucoma-related retinal ganglion cell apoptosis in vivo. Invest. Ophthalmol. Vis. Sci. 47, 626–33.

Gupta, N., Weinreb, R., 1997. Diode laser transscleral cyclophotocoagulation. J. Glaucoma 6, 426–429.

Haeberlein, S.L.B., 2004. Mitochondrial function in apoptotic neuronal cell death. Neurochem. Res. 29, 521–30.

Hare, W., WoldeMussie, E., Lai, R., Ton, H., Ruiz, G., Feldmann, B., Wijono, M., Chun, T., Wheeler, L., 2001. Efficacy and safety of memantine, an NMDA-type open-channel blocker, for reduction of retinal injury associated with experimental glaucoma in rat and monkey. Surv. Ophthalmol. 45 Suppl 3, S284–9; discussion S295–6.

Harper, M.M., Grozdanic, S.D., Blits, B., Kuehn, M.H., Zamzow, D., Buss, J.E., Kardon, R.H., Sakaguchi, D.S., 2011. Transplantation of BDNF-secreting mesenchymal stem cells provides neuroprotection in chronically hypertensive rat eyes. Invest. Ophthalmol. Vis. Sci. 52, 4506–15.

Hartwick, A.T.E., Lalonde, M.R., Barnes, S., Baldridge, W.H., 2004. Adenosine A1-receptor modulation of glutamate-induced calcium influx in rat retinal ganglion cells. Invest. Ophthalmol. Vis. Sci. 45, 3740–8.

Harvey, a, 2002. Intravitreal Injection of Adeno-associated Viral Vectors Results in the Transduction of Different Types of Retinal Neurons in Neonatal and Adult Rats: A Comparison with Lentiviral Vectors. Mol. Cell. Neurosci. 21, 141–157.

Harvey, A.R., Hellström, M., Rodger, J., 2009. Gene therapy and transplantation in the retinofugal pathway. Prog. Brain Res. 175, 151–61.

Hauser, R. a, 2011. Future treatments for Parkinson's disease: surfing the PD pipeline. Int. J. Neurosci. 121 Suppl , 53–62.

Hauser, R. a., Hubble, J.P., Truong, D.D., 2003. Randomized trial of the adenosine A2A receptor antagonist istradefylline in advanced PD. Neurology 61, 297–303.

Hegazy, K. a, Dunn, M.W., Sharma, S.C., 2000. Functional human heme oxygenase has a neuroprotective effect on adult rat ganglion cells after pressure-induced ischemia. Neuroreport 11, 1185–9.

Heijl, A., Leske, M., Bengtsson, Bo, Hyman, L., Bengtsson, Boel, Hussein, M., 2002. Reduction of Intraocular Pressure and Glaucoma Progression. Arch Ophthalmol. 20, 9–12.

Hengartner, M.O., 2000. The biochemistry of apoptosis. Nature 407, 770–6.

Hernández, M., Urcola, J.H., Vecino, E., 2008. Retinal ganglion cell neuroprotection in a rat model of glaucoma following brimonidine, latanoprost or combined treatments. Exp. Eye Res. 86, 798–806.

Hu, H., Lu, W., Zhang, M., Zhang, X., Argall, A.J., Patel, S., Lee, G.E., Kim, Y.-C., Jacobson, K. a, Laties, A.M., Mitchell, C.H., 2010. Stimulation of the P2X7 receptor kills rat retinal ganglion cells in vivo. Exp. Eye Res. 91, 425–32.

Huang, Dobberfuhl, A., Filippopoulos, T., Ingelsson, M., Fileta, J.B., Poulin, N.R., Grosskreutz, C.L., 2005a. Transcriptional up-regulation and activation of initiating caspases in experimental glaucoma. Am. J. Pathol. 167, 673–81.

Huang, U, W.-M., Eguchi, N., Chen, J.-F., Schwarzschild, M. a, Fredholm, B.B., Urade, Y., Hayaishi, O., 2005b. Adenosine A2A, but not A1, receptors mediate the arousal effect of caffeine. Nat. Neurosci. 8, 858–9.

Isenmann, S., Engel, S., Gillardon, F., Bähr, M., 1999. Bax antisense oligonucleotides reduce axotomy-induced retinal ganglion cell death in vivo by reduction of Bax protein expression. Cell Death Differ. 6, 673–82.

Isenmann, S., Klöcker, N., Gravel, C., Bähr, M., 1998. Short communication: protection of axotomized retinal ganglion cells by adenovirally delivered BDNF in vivo. Eur. J. Neurosci. 10, 2751–6.

Ishikawa, S., Saijoh, K., Okada, Y., 1997. Endogenous adenosine facilitates neurotransmission via A2A adenosine receptors in the rat superior colliculus in vivo. Brain Res. 757, 268–75.

Jacobson, Gao, Z., 2006. Adenosine receptors as therapeutic targets. Nat. Rev. Drug Discov. 5, 247–264.

Jakobs, T.C., Libby, R.T., Ben, Y., John, S.W.M., Masland, R.H., 2005. Retinal ganglion cell degeneration is topological but not cell type specific in DBA/2J mice. J. Cell Biol. 171, 313–25.

Jia, L., Cepurna, W.O., Johnson, E.C., Morrison, J.C., 2000. Effect of general anesthetics on IOP in rats with experimental aqueous outflow obstruction. Invest. Ophthalmol. Vis. Sci. 41, 3415–9.

John, S.W., Smith, R.S., Savinova, O. V, Hawes, N.L., Chang, B., Turnbull, D., Davisson, M., Roderick, T.H., Heckenlively, J.R., 1998. Essential iris atrophy, pigment dispersion, and glaucoma in DBA/2J mice. Invest. Ophthalmol. Vis. Sci. 39, 951–62.

Johnson, Bull, N.D., Hunt, D.P., Marina, N., Tomarev, S.I., Martin, K.R., 2010. Neuroprotective effects of intravitreal mesenchymal stem cell transplantation in experimental glaucoma. Invest. Ophthalmol. Vis. Sci. 51, 2051–9.

Johnson, T. V, Martin, K.R., 2013. Cell transplantation approaches to retinal ganglion cell neuroprotection in glaucoma. Curr. Opin. Pharmacol. 13, 78–82.

Johnson, T. V, Tomarev, S.I., 2010. Rodent models of glaucoma. Brain Res. Bull. 81, 349–58.

Ju, W.-K., Kim, K.-Y., Duong-Polk, K.X., Lindsey, J.D., Ellisman, M.H., Weinreb, R.N., 2010. Increased optic atrophy type 1 expression protects retinal ganglion cells in a mouse model of glaucoma. Mol. Vis. 16, 1331–42.

Juravleva, E., Barbakadze, T., Mikeladze, D., Kekelidze, T., 2011. Creatine enhances survival of glutamate-treated neuronal/glial cells, modulates Ras/NF-kappaB

signaling, and increases the generation of reactive oxygen species. J. Neurosci. Res. 79, 224–30.

Kanamori, A., Catrinescu, M.-M., Mahammed, A., Gross, Z., Levin, L. a, 2010. Neuroprotection against superoxide anion radical by metallocorroles in cellular and murine models of optic neuropathy. J. Neurochem. 114, 488–98.

Kass, M., Miller, J.P., Ii, R.K.P., Wilson, M.R., Gordon, M.O., 2002. The Ocular Hypertension Treatment Study. Arch Ophthalmol. 120.

Kerrigan, Zack, D.J., Smith, S.D., Quigley, H.A., Pease, M.E., 1997. TUNEL-Positive Ganglion Cells in Human Primary Open-angle Glaucoma. Arch Ophthalmol. 115, 1031–1035.

Kerrigan-Baumrind, L. a, Quigley, H. a, Pease, M.E., Kerrigan, D.F., Mitchell, R.S., 2000. Number of ganglion cells in glaucoma eyes compared with threshold visual field tests in the same persons. Invest. Ophthalmol. Vis. Sci. 41, 741–8.

Kevany, B.M., Palczewski, K., 2010. Phagocytosis of retinal rod and cone photoreceptors. Physiology (Bethesda). 25, 8–15.

Khaw, P.T., Shah, P., Elkington, A.R., 2004. Glaucoma — 1 : Diagnosis Primary open angle glaucoma. BMJ 528, 97–99.

Klöcker, N., Cellerino, A., Bähr, M., 1998. Free radical scavenging and inhibition of nitric oxide synthase potentiates the neurotrophic effects of brain-derived neurotrophic factor on axotomized retinal ganglion cells In vivo. J. Neurosci. 18, 1038–46.

Knutsen, L.J.S., Lau, J., Petersen, H., Thomsen, C., Weis, J.U., Shalmi, M., Judge, M.E., Hansen, A.J., Sheardown, M.J., 1999. N-Substituted Adenosines as Novel Neuroprotective A 1 Agonists with Diminished Hypotensive Effects. J. Med. C 3463–3477.

Koh, J., Wie, M., Gwag, B., 1995. Staurosporine-induced neuronal apoptosis. Exp. Neurol. 135, 153–159.

Kontiola, A., 1997. A new electromechanical method for measuring intraocular pressure The probe is set in motion by a very weak compression spring or by an ex- 265–276.

Kreutzberg, G.W., Hussain, S.T., 1982. Cytochemical heterogeneity of the glial plasma membrane: 5'-nucleotidase in retinal Müller cells. J. Neurocytol. 11, 53–64.

Kroemer, El-Deiry, W.S., Golstein, P., Peter, M.E., Vaux, D., Vandenabeele, P., Zhivotovsky, B., Blagosklonny, M. V, Malorni, W., Knight, R. a, Piacentini, M., Nagata, S., Melino, G., 2005. Classification of cell death: recommendations of the Nomenclature Committee on Cell Death. Cell Death Differ. 12 Suppl 2, 1463–7.

Kroemer, G., Galluzzi, L., Brenner, C., 2007. Mitochondrial Membrane Permeabilization in Cell Death 99–163.

Krupin, T., Liebmann, J.M., Greenfield, D.S., Ritch, R., Gardiner, S., 2011. A Randomized Trial of Brimonidine Versus Timolol in Preserving Visual Function: Results From the Low-pressure Glaucoma Treatment Study. Am. J. Ophthalmol. 1–11.

Kvanta, a, Seregard, S., Sejersen, S., Kull, B., Fredholm, B.B., 1997. Localization of adenosine receptor messenger RNAs in the rat eye. Exp. Eye Res. 65, 595–602.

Lagreze, W.A., Knorle, R., Bach, M., 1998. Retinal Ischemia. Invest. Ophthalmol. Vis. Sci. 39.

Lai, R.K., Chun, T., Hasson, D., Lee, S., Mehrbod, F., Wheeler, L., 2002. Alpha-2 adrenoceptor agonist protects retinal function after acute retinal ischemic injury in the rat. Vis. Neurosci. 19, 175–85.

Lam, T.T., Abler, A.S., Kwong, J.M.K., Tso, M.O.M., 1999. in Rat Retina. Invest. Ophthalmol. Vis. Sci. 40, 2391–2397.

Lamartina, S., Cimino, M., 2007. Helper dependent adenovirus for the gene therapy of proliferative retinopathies: stable gene transfer, regulated gene expression and therapeutic efficacy. J. Gene Med. 9, 862–874.

Lambiase, A., Aloe, L., Centofanti, M., Parisi, V., Mantelli, F., Colafrancesco, V., Manni, G.L., Bucci, M.G., Bonini, S., Levi-Montalcini, R., 2009. Experimental and clinical evidence of neuroprotection by nerve growth factor eye drops: Implications for glaucoma. Proc. Natl. Acad. Sci. U. S. A. 106, 13469–13474.

Laquis, S., Chaudhary, P., Sharma, S.C., 1998. The patterns of retinal ganglion cell death in hypertensive eyes. Brain Res. 784, 100–4.

Leaver, S.G., Cui, Q., Plant, G.W., Arulpragasam, A., Hisheh, S., Verhaagen, J., Harvey, a R., 2006. AAV-mediated expression of CNTF promotes long-term survival and regeneration of adult rat retinal ganglion cells. Gene Ther. 13, 1328–41.

Lee, D., Kim, K.-Y., Noh, Y.H., Chai, S., Lindsey, J.D., Ellisman, M.H., Weinreb, R.N., Ju, W.-K., 2012. Brimonidine blocks glutamate excitotoxicity-induced oxidative stress and preserves mitochondrial transcription factor a in ischemic retinal injury. PLoS One 7, e47098.

Lehmann, M., Fournier, A., Selles-Navarro, I., Dergham, P., Sebok, A., Leclerc, N., Tigyi, G., McKerracher, L., 1999. Inactivation of Rho signaling pathway promotes CNS axon regeneration. J. Neurosci. 19, 7537–47.

Leske, M., Heijl, A., Hussein, M., Bengtsson, B., Hyman, L., Komaroff, E., 2003. Factors for Glaucoma Progression and the Effect of Treatment. Arch Ophthalmol. 121.

Levkovitch-Verbin, H., 2004. Animal models of optic nerve diseases. Eye (Lond). 18, 1066–74.

Levkovitch-Verbin, H., Sadan, O., Vander, S., Rosner, M., Barhum, Y., Melamed, E., Offen, D., Melamed, S., 2010. Intravitreal injections of neurotrophic factors secreting mesenchymal stem cells are neuroprotective in rat eyes following optic nerve transection. Invest. Ophthalmol. Vis. Sci. 51, 6394–400.

Li, Hu, B., Tay, D., So, K.-F., Yip, H.K.-F., 2004. Intravitreal transplants of Schwann cells and fibroblasts promote the survival of axotomized retinal ganglion cells in rats. Brain Res. 1029, 56–64.

Li, Li, D., Khaw, P.T., Raisman, G., 2008. Neuroscience Letters Transplanted olfactory ensheathing cells incorporated into the optic nerve head ensheathe retinal ganglion cell axons : Possible relevance to glaucoma. Neurosci. Lett. 440, 251–254.

Li, Li, X., Yuan, J., 2009. Effects of bone-marrow mesenchymal stem cells transplanted into vitreous cavity of rat injured by ischemia/reperfusion. Graefes Arch. Clin. Exp. Ophthalmol. 247, 503–14.

Li, X., Conklin, D., Pan, H., Eisenach, J., 2003. Allosteric adenosine receptor modulation reduces hypersensitivity following peripheral inflammation by a central mechanism. J. Pharmacol. Exp. Ther. 305, 950–955.

Libby, R.T., Anderson, M.G., Pang, I.-H., Robinson, Z.H., Savinova, O. V, Cosma, I.M., Snow, A., Wilson, L. a, Smith, R.S., Clark, A.F., John, S.W.M., 2005a. Inherited glaucoma in DBA/2J mice: pertinent disease features for studying the neurodegeneration. Vis. Neurosci. 22, 637–48.

Libby, R.T., Li, Y., Savinova, O. V, Barter, J., Smith, R.S., Nickells, R.W., John, S.W.M., 2005b. Susceptibility to neurodegeneration in a glaucoma is modified by Bax gene dosage. PLoS Genet. 1, 17–26.

Lingor, P., Koeberle, P., Kügler, S., Bähr, M., 2005. Down-regulation of apoptosis mediators by RNAi inhibits axotomy-induced retinal ganglion cell death in vivo. Brain 128, 550–8.

Liou, G., Auchampach, J., Hillard, C., Zhu, G., Yousufzai, B., Mian, S., Khan, S., Khalifa, Y., 2008. Medication of Cannabidiol anti-inflammation in the Retina by Equilibrative Nucleoside Transporter and A2a Adenosine Receptor. Invest. Ophthalmol. Vis. Sci. 49, 5526–5531.

Lipson, A.C., Widenfalk, J., Lindqvist, E., Ebendal, T., Olson, L., 2003. Neurotrophic properties of olfactory ensheathing glia. Exp. Neurol. 180, 167–171.

Liu, B., Neufeld, A., 2001. Nitric oxide synthase-2 in human optic nerve head astrocytes induced by elevated pressure in vitro. Arch. Ophthalmol. 119, 240–5.

Liu, Gong, Z., Liu, L., Sun, H., 2010. Combined effect of olfactory ensheathing cell (OEC) transplantation and glial cell line-derived neurotrophic factor (GDNF) intravitreal injection on optic nerve injury in rats. Mol. Vis. 16, 2903–10.

Loch, C., Zakelj, S., Kristl, A., Nagel, S., Guthoff, R., Weitschies, W., Seidlitz, A., 2012. Determination of permeability coefficients of ophthalmic drugs through different layers of porcine, rabbit and bovine eyes. Eur. J. Pharm. Sci. 47, 131–8.

Lutty, G. a, Merges, C., McLeod, D.S., 2000. 5' Nucleotidase and Adenosine During Retinal Vasculogenesis and Oxygen-Induced Retinopathy. Invest. Ophthalmol. Vis. Sci. 41, 218–29.

Maass, A., von Leithner, P.L., Luong, V., Guo, L., Salt, T.E., Fitzke, F.W., Cordeiro, M.F., 2007. Assessment of rat and mouse RGC apoptosis imaging in vivo with different scanning laser ophthalmoscopes. Curr. Eye Res. 32, 851–61.

Maemoto, T., Tada, M., Mihara, T., Ueyama, N., Matsuoka, H., Harada, K., 2004. Full Paper Pharmacological Characterization of FR194921 , a New Potent , Selective , and Orally Active Antagonist for Central Adenosine A 1 Receptors 52, 42–52.

Majumdar, S., Macha, S., Pal, D., Mitra, A.K., 2004. Mechanism of ganciclovir uptake by rabbit retina and human retinal pigmented epithelium cell line ARPE-19. Curr. Eye Res. 29, 127–36.

Malik, J.M.I., Shevtsova, Z., Bähr, M., Kügler, S., 2005. Long-term in vivo inhibition of CNS neurodegeneration by Bcl-XL gene transfer. Mol. Ther. 11, 373–81.

Martin, K.R.G., 2003. Gene Therapy with Brain-Derived Neurotrophic Factor As a Protection: Retinal Ganglion Cells in a Rat Glaucoma Model. Invest. Ophthalmol. Vis. Sci. 44, 4357–4365.

Matasi, J.J., Caldwell, J.P., Hao, J., Neustadt, B., Arik, L., Foster, C.J., Lachowicz, J., Tulshian, D.B., 2005. The discovery and synthesis of novel adenosine receptor (A2A) antagonists. Bioorg. Med. Chem. Lett. 15, 1333–1336.

May, C.A., Lütjen-Drecoll, E., 2002. Morphology of the murine optic nerve. Invest. Ophthalmol. Vis. Sci. 43, 2206–12.

McKinnon, Lehman, D.M., Kerrigan-Baumrind, L. a, Merges, C. a, Pease, M.E., Kerrigan, D.F., Ransom, N.L., Tahzib, N.G., Reitsamer, H. a, Levkovitch-Verbin, H., Quigley, H. a, Zack, D.J., 2002. Caspase activation and amyloid precursor protein cleavage in rat ocular hypertension. Invest. Ophthalmol. Vis. Sci. 43, 1077–87.

Meers, P., Mealy, T., 1993. Calcium-dependent annexin V binding to phospholipids: stoichiometry, specificity, and the role of negative charge. Biochemistry 32, 11711–21.

Meijer, P., Oyen, W.J.G., Dekker, D., van den Broek, P.H.H., Wouters, C.W., Boerman, O.C., Scheffer, G.J., Smits, P., Rongen, G. a, 2009. Rosuvastatin increases extracellular adenosine formation in humans in vivo: a new perspective on cardiovascular protection. Arterioscler. Thromb. Vasc. Biol. 29, 963–8.

Meijer, P., Wouters, C.W., Oyen, W.J., Boerman, O.C., Scheffer, G.J., Smits, P., Rongen, G. a, 2011. Angiotensin II type 1 receptor blockade does not enhance apoptotic cell death during ischemia and reperfusion in humans in vivo. J. Cardiovasc. Pharmacol. 57, 702–6.

Minckler, D.S., Bunt, a H., Johanson, G.W., 1977. Orthograde and retrograde axoplasmic transport during acute ocular hypertension in the monkey. Invest. Ophthalmol. Vis. Sci. 16, 426–41.

Mittag, T.W., Danias, J., Pohorenec, G., Yuan, H.M., Burakgazi, E., Chalmers-Redman, R., Podos, S.M., Tatton, W.G., 2000. Retinal damage after 3 to 4 months of elevated intraocular pressure in a rat glaucoma model. Invest. Ophthalmol. Vis. Sci. 41, 3451–9.

Monopoli, a, Lozza, G., Forlani, A., Mattavelli, A., Ongini, E., 1998. Blockade of adenosine A2A receptors by SCH 58261 results in neuroprotective effects in cerebral ischaemia in rats. Neuroreport 9, 3955–9.

Morfini, G. a, Burns, M., Binder, L.I., Kanaan, N.M., LaPointe, N., Bosco, D. a, Brown, R.H., Brown, H., Tiwari, A., Hayward, L., Edgar, J., Nave, K.-A., Garberrn, J., Atagi, Y., Song, Y., Pigino, G., Brady, S.T., 2009. Axonal transport defects in neurodegenerative diseases. J. Neurosci. 29, 12776–86.

Morrison, J., Farrell, S., Johnson, E., Deppmeier, L., Moore, C.G., Grossmann, E., 1995. Structure and composition of the rodent lamina cribrosa. Exp. Eye Res. 60, 127–35.

Morrison, Moore, C.G., Deppmeier, L.M., Gold, B.G., Meshul, C.K., Johnson, E.C., 1997. A rat model of chronic pressure-induced optic nerve damage. Exp. Eye Res. 64, 85–96.

Mountz, J.D., Hsu, H.-C., Wu, Q., Liu, H.-G., Zhang, H.-G., Mountz, J.M., 2002. Molecular imaging: new applications for biochemistry. J. Cell. Biochem. Suppl. 39, 162–71.

Muzio, M., Stockwell, B.R., Stennicke, H.R., Salvesen, G.S., Dixit, V.M., 1998. An induced proximity model for caspase-8 activation. J. Biol. Chem. 273, 2926–30.

Nakajima, Y., Inokuchi, Y., Nishi, M., Shimazawa, M., Otsubo, K., Hara, H., 2008. Coenzyme Q10 protects retinal cells against oxidative stress in vitro and in vivo. Brain Res. 1226, 226–33.

Nakazawa, T., Nakazawa, C., Matsubara, A., Noda, K., Hisatomi, T., She, H., Michaud, N., Hafezi-Moghadam, A., Miller, J.W., Benowitz, L.I., 2006. Tumor necrosis factor-alpha mediates oligodendrocyte death and delayed retinal ganglion cell loss in a mouse model of glaucoma. J. Neurosci. 26, 12633–41.

Narula, J., Acio, E.R., Narula, N., Samuels, L.E., Fyfe, B., Wood, D., Fitzpatrick, J.M., Raghunath, P.N., Tomaszewski, J.E., Kelly, C., Steinmetz, N., Green, A., Tait, J.F., Leppo, J., Blankenberg, F.G., Jain, D., Strauss, H.W., 2001. Annexin-V imaging for noninvasive detection of cardiac allograft rejection. Nat. Med. 7, 1347–52.

Neufeld, A., 2002. Loss of Retinal Ganglion Cells Following Retinal Ischemia: The Role of Inducible Nitric Oxide Synthase. Exp. Eye Res. 75, 521–528.

Neufeld, A., 2004. Pharmacologic neuroprotection with an inhibitor of nitric oxide synthase for the treatment of glaucoma. Brain Res. Bull. 62, 455–9.

Neufeld, A., Sawada, A., Becker, B., 1999. Inhibition of nitric-oxide synthase 2 by aminoguanidine provides neuroprotection of retinal ganglion cells in a rat model of chronic glaucoma. Proc. Natl. Acad. Sci. U. S. A. 96, 9944–8.

Nickells, R.W., 2007. Ganglion cell death in glaucoma: from mice to men. Vet. Ophthalmol. 10 Suppl 1, 88–94.

Novack, G.D., O'Donnell, M.J., Molloy, D.W., 2002. New glaucoma medications in the geriatric population: efficacy and safety. J. Am. Geriatr. Soc. 50, 956–62.

Olah, M., Stiles, G.L., 1992. Adenosine Receptors. Annu Rev Physiol 54, 211–225.

Osborne, N.N., 2008. Pathogenesis of ganglion "cell death" in glaucoma and neuroprotection: focus on ganglion cell axonal mitochondria. Prog. Brain Res. 173, 339–52.

Osborne, N.N., Chidlow, G., Layton, C.J., Wood, J.P.M., Casson, R.J., Melena, J., 2004. Optic nerve and neuroprotection strategies. Eye (Lond). 18, 1075–84.

Osborne, N.N., DeSantis, L., Bae, J.H., Ugarte, M., Wood, J.P., Nash, M.S., Chidlow, G., 1999. Topically applied betaxolol attenuates NMDA-induced toxicity to ganglion cells and the effects of ischaemia to the retina. Exp. Eye Res. 69, 331–42.

Paes de Carvalho, R., Braas, K.M., Snyder, S.H., Adler, R., 1990. Analysis of adenosine immunoreactivity, uptake, and release in purified cultures of developing chick embryo retinal neurons and photoreceptors. J. Neurochem. 55, 1603–11.

Paigen, K., 1995. A miracle enough: the power of mice. Nat. Med. 1, 215–220.

Palmer, T.M., Stiles, G.L., 1995. Adenosine receptors. Neuropharmacology 34, 683–94.

Pang, I.-H., Clark, A.F., 2007. Rodent models for glaucoma retinopathy and optic neuropathy. J. Glaucoma 16, 483–505.

Pang, I.-H., Wang, W.-H., Clark, A.F., 2005a. Acute effects of glaucoma medications on rat intraocular pressure. Exp. Eye Res. 80, 207–14.

Pang, I.-H., Wang, W.-H., Millar, J.C., Clark, A.F., 2005b. Measurement of mouse intraocular pressure with the Tono-Pen. Exp. Eye Res. 81, 359–60.

Parkinson, F.E., Xiong, W., Zamzow, C.R., 2005. Astrocytes and neurons: different roles in regulating adenosine levels. Neurol. Res. 27, 153–60.

Parrilla-Reverter, G., Agudo, M., Sobrado-Calvo, P., Salinas-Navarro, M., Villegas-Pérez, M.P., Vidal-Sanz, M., 2009. Effects of different neurotrophic factors on the survival of retinal ganglion cells after a complete intraorbital nerve crush injury: a quantitative in vivo study. Exp. Eye Res. 89, 32–41.

Pascale, A., Drago, F., Govoni, S., 2012. Protecting the retinal neurons from glaucoma: lowering ocular pressure is not enough. Pharmacol. Res. 66, 19–32.

Pease, M.E., McKinnon, S.J., Quigley, H. a, Kerrigan-Baumrind, L. a, Zack, D.J., 2000. Obstructed axonal transport of BDNF and its receptor TrkB in experimental glaucoma. Invest. Ophthalmol. Vis. Sci. 41, 764–74.

Pease, M.E., Zack, D.J., Berlinicke, C., Bloom, K., Cone, F., Wang, Y., Klein, R.L., Hauswirth, W.W., Quigley, H. a, 2009. Effect of CNTF on retinal ganglion cell survival in experimental glaucoma. Invest. Ophthalmol. Vis. Sci. 50, 2194–200.

Peng, P.-H., Ko, M.-L., Chen, C.-F., Juan, S.-H., 2008. Haem oxygenase-1 gene transfer protects retinal ganglion cells from ischaemia/reperfusion injury. Clin. Sci. (Lond). 115, 335–42.

Perez, M.T., Arnér, K., Ehinger, B., 1988. Stimulation-evoked release of purines from the rabbit retina. Neurochem. Int. 13, 307–18.

Pernet, V., Hauswirth, W.W., Di Polo, A., 2005. Extracellular signal-regulated kinase 1/2 mediates survival, but not axon regeneration, of adult injured central nervous system neurons in vivo. J. Neurochem. 93, 72–83.

Porkka-Heiskanen, T., 1997. Adenosine: A Mediator of the Sleep-Inducing Effects of Prolonged Wakefulness. Science (80-.). 276, 1265–1268.

Porkka-Heiskanen, T., Alanko, L., Kalinchuk, A., Stenberg, D., 2002. Adenosine and sleep. Sleep Med. Rev. 6, 321–332.

Qu, J., Wang, D., Grosskreutz, C.L., 2010. Mechanisms of retinal ganglion cell injury and defense in glaucoma. Exp. Eye Res. 91, 48–53.

Quigley, 2011. Glaucoma. Lancet 377, 1367–77.

Quigley, Broman, 2006. The number of people with glaucoma worldwide in 2010 and 2020. Br. J. Ophthalmol. 90, 262–7.

Quigley, H., 1999. Neuronal death in glaucoma. Prog. Retin. Eye Res. 18, 39–57.

Quigley, H., 2005. Letters to the editor. J. Am. Vet. Med. Assoc. 241, 1275–6.

Quigley, H., Nickells, R.W., Kerrigan, L., Pease, M.E., Thibault, D.J., Zack, D.J., 1995. Retinal ganglion cell death in experimental glaucoma and after axotomy occurs by apoptosis. Invest. Ophthalmol. Vis. Sci. 36, 774–86.

Realini, T., 2011. A history of glaucoma pharmacology. Optom. Vis. Sci. 88, 36–8.

Reed, J.C., 2000. Mechanisms of apoptosis. Am. J. Pathol. 157, 1415–30.

Reichel, M.B., Ali, R.R., Thrasher, a J., Hunt, D.M., Bhattacharya, S.S., Baker, D., 1998. Immune responses limit adenovirally mediated gene expression in the adult mouse eye. Gene Ther. 5, 1038–46.

Reutelingsperger, C.P.M., Dumont, E., Thimister, P.W., van Genderen, H., Kenis, H., van de Eijnde, S., Heidendal, G., Hofstra, L., 2002. Visualization of cell death in vivo with the annexin A5 imaging protocol. J. Immunol. Methods 265, 123–32.

Ribeiro, J., Sebastiao, A., Mendonca, A., 2003. Adenosine receptors in the nervous system: pathophysiological implications. Prog. Neurobiol. 68, 377–392.

Riksen, N.P., Franke, B., Oyen, W.J.G., Borm, G.F., van den Broek, P., Boerman, O.C., Smits, P., Rongen, G. a, 2007. Augmented hyperaemia and reduced tissue injury in response to ischaemia in subjects with the 34C > T variant of the AMPD1 gene. Eur. Heart J. 28, 1085–91.

Riksen, N.P., Oyen, W.J.G., Ramakers, B.P., Van den Broek, P.H.H., Engbersen, R., Boerman, O.C., Smits, P., Rongen, G. a, 2005. Oral therapy with dipyridamole limits ischemia-reperfusion injury in humans. Clin. Pharmacol. Ther. 78, 52–9.

Riksen, N.P., Zhou, Z., Oyen, W.J.G., Jaspers, R., Ramakers, B.P., Brouwer, R.M.H.J., Boerman, O.C., Steinmetz, N., Smits, P., Rongen, G. a, 2006. Caffeine prevents protection in two human models of ischemic preconditioning. J. Am. Coll. Cardiol. 48, 700–7.

Rittenhouse, K.D., Peiffer, R.L., Pollack, G.M., 1998. Evaluation of microdialysis sampling of aqueous humor for in vivo models of ocular absorption and disposition. J. Pharm. Biomed. Anal. 16, 951–9.

Rottey, S., Van Den Bossche, B., Slegers, G., Van Belle, S., Van De Wiele, C., 2009. Influence of chemotherapy on the biodistribution of [99mTc] hydrazinonicotina mide annexin V in cancer patients. Q J Nucl Med Mol Imagig 53, 127–132.

Sagara, T., Gaton, D.D., Lindsey, J.D., Gabelt, B.T., Kaufman, P.L., Weinreb, R.N., 1999. Topical prostaglandin F2alpha treatment reduces collagen types I, III, and IV in the monkey uveoscleral outflow pathway. Arch. Ophthalmol. 117, 794–801.

Salinas-Navarro, M., Alarcón-Martínez, L., Valiente-Soriano, F.J., Jiménez-López, M., Mayor-Torroglosa, S., Avilés-Trigueros, M., Villegas-Pérez, M.P., Vidal-Sanz, M., 2010. Ocular hypertension impairs optic nerve axonal transport leading to progressive retinal ganglion cell degeneration. Exp. Eye Res. 90, 168–83.

Samsel, P. a, Kisiswa, L., Erichsen, J.T., Cross, S.D., Morgan, J.E., 2011. A novel method for the induction of experimental glaucoma using magnetic microspheres. Invest. Ophthalmol. Vis. Sci. 52, 1671–5.

Sappington, R.M., Carlson, B.J., Crish, S.D., Calkins, D.J., 2010. The microbead occlusion model: a paradigm for induced ocular hypertension in rats and mice. Invest. Ophthalmol. Vis. Sci. 51, 207–16.

Schmitz-Valckenberg, S., Guo, L., Maass, A., Cheung, W., Vugler, A., Moss, S.E., Munro, P.M.G., Fitzke, F.W., Cordeiro, M.F., 2008. Real-time in vivo imaging of retinal cell apoptosis after laser exposure. Invest. Ophthalmol. Vis. Sci. 49, 2773–80.

Schuettauf, F., Quinto, K., Naskar, R., Zurakowski, D., 2002. Effects of anti-glaucoma medications on ganglion cell survival: the DBA/2J mouse model. Vision Res. 42, 2333–7.

Scott, T., 1967. The distribution of 5’ Nucleotidase in the brain of the Mouse. J. Comp. Neurol. 129, 97–114.

Senba, E., Daddona, P.E., Nagy, J.I., 1986. Immunohistochemical localization of adenosine deaminase in the retina of the rat. Brain Res. Bull. 17, 209–17.

Setoguchi, M., Ohya, Y., Abe, I., Fujishima, M., 1995. antagonist , on voltage-dependent calcium channels in guinea-pig artery and vein. Br. J. Pharmacol. 115, 198–202.

Shareef, S., Sawada, A., Neufeld, A., 1999. Isoforms of Nitric Oxide Synthase in the Optic Nerves Intraocular Pressure AND 40, 2884–2891.

Shareef, S.R., Garcia-Valenzuela, E., Salierno, A., Walsh, J., Sharma, S.C., 1995. Chronic ocular hypertension following episcleral venous occlusion in rats. Exp. Eye Res. 61, 379–82.

Shields, M., 2008. Normal-tension glaucoma: is it different from primary open-angle glaucoma? Curr. Opin. Ophthalmol. 19, 85–8.

Siliprandi, R., Canella, R., Carmignoto, G., Schiavo, N., Zanellato, A., Zanoni, R., Vantini, G., 1992. N-methyl-D-aspartate-induced neurotoxicity in the adult rat retina. Vis. Neurosci. 8, 567–73.

Sivyer, B., Venkataramani, S., Taylor, W.R., Vaney, D.I., 2011. A novel type of complex ganglion cell in rabbit retina. J. Comp. Neurol. 519, 3128–38.

Son, J.L., Soto, I., Oglesby, E., Lopez-Roca, T., Pease, M.E., Quigley, H. a, Marsh-Armstrong, N., 2010. Glaucomatous optic nerve injury involves early astrocyte reactivity and late oligodendrocyte loss. Glia 58, 780–9.

Steele, M.R., Inman, D.M., Calkins, D.J., Horner, P.J., Vetter, M.L., 2006. Microarray analysis of retinal gene expression in the DBA/2J model of glaucoma. Invest. Ophthalmol. Vis. Sci. 47, 977–85.

Stevens, B., Allen, N.J., Vazquez, L.E., Howell, G.R., Christopherson, K.S., Nouri, N., Micheva, K.D., Mehalow, A.K., Huberman, A.D., Stafford, B., Sher, A., Litke, A.M., Lambris, J.D., Smith, S.J., John, S.W.M., Barres, B. a, 2007. The classical complement cascade mediates CNS synapse elimination. Cell 131, 1164–78.

Stieger, K., Schroeder, J., Provost, N., Mendes-Madeira, A., Belbellaa, B., Le Meur, G., Weber, M., Deschamps, J.-Y., Lorenz, B., Moullier, P., Rolling, F., 2009. Detection of intact rAAV particles up to 6 years after successful gene transfer in the retina of dogs and primates. Mol. Ther. 17, 516–23.

Stuart, A., 2012. Landmark Glaucoma Studies. EyeNet 49–55.

Sun, M.-H., Pang, J.-H.S., Chen, S.-L., Han, W.-H., Ho, T.-C., Chen, K.-J., Kao, L.-Y., Lin, K.-K., Tsao, Y.-P., 2010. Retinal protection from acute glaucoma-induced ischemia-reperfusion injury through pharmacologic induction of heme oxygenase-1. Invest. Ophthalmol. Vis. Sci. 51, 4798–808.

Sun, X., Barnes, S., Baldridge, W.H., 2002. Adenosine inhibits calcium channel currents via A1 receptors on salamander retinal ganglion cells in a mini-slice preparation. J. Neurochem. 81, 550–6.

Susin, S. a, Lorenzo, H.K., Zamzami, N., Marzo, I., Snow, B.E., Brothers, G.M., Mangion, J., Jacotot, E., Costantini, P., Loeffler, M., Larochette, N., Goodlett, D.R., Aebersold, R., Siderovski, D.P., Penninger, J.M., Kroemer, G., 1999. Molecular characterization of mitochondrial apoptosis-inducing factor. Nature 397, 441–6.

Tatton, W.G., Chalmers-Redman, R.M., Sud, A., Podos, S.M., Mittag, T.W., 2001. Maintaining mitochondrial membrane impermeability. an opportunity for new therapy in glaucoma? Surv. Ophthalmol. 45 Suppl 3, S277–83; discussuin S295–6.

Tezel, G., Li, L.Y., Patil, R. V, Wax, M.B., 2001. TNF-alpha and TNF-alpha receptor-1 in the retina of normal and glaucomatous eyes. Invest. Ophthalmol. Vis. Sci. 42, 1787–94.

Tezel, G., Yang, X., 2004. Caspase-independent component of retinal ganglion cell death, in vitro. Invest. Ophthalmol. Vis. Sci. 45, 4049–59.

Tezel, G., Yang, X., Luo, C., Peng, Y., Sun, S.L., 2008. Mechanisms of Immune System Activation in Glaucoma: Oxidative Stress-Stimulated Antigen Presentation by the Retina and Optic Nerve Head Glia. Invest. Ophthalmol. Vis. Sci. 48, 705–714.

Tielsch, J., Sommer, A., Katz, J., 1991. Racial variations in the prevalence of primary open-angle glaucoma. JAMA 266, 369–374.

Toris, C.B., Camras, C.B., Yablonski, M.E., 1999. Acute versus chronic effects of brimonidine on aqueous humor dynamics in ocular hypertensive patients. Am. J. Ophthalmol. 128, 8–14.

Ueda, J., Sawaguchi, S., Hanyu, T., Yaoeda, K., Fukuchi, T., Abe, H., Ozawa, H., 1998. Experimental glaucoma model in the rat induced by laser trabecular photocoagulation after an intracameral injection of India ink. Jpn. J. Ophthalmol. 42, 337–344.

Urade, Y., 2003. IV . ADENOSINE A2A RECEPTORS IN NONLOCOMOTOR FEATURES OF PARKINSON ' S DISEASE Minireview : Sleep regulation in adenosine A 2A receptor-deficient mice. Neurology 21680.

Van Adel, B. a, Arnold, J.M., Phipps, J., Doering, L.C., Ball, a K., 2005. Ciliary neurotrophic factor protects retinal ganglion cells from axotomy-induced apoptosis via modulation of retinal glia in vivo. J. Neurobiol. 63, 215–34.

Varma, R., Lee, P.P., Goldberg, I., Kotak, S., 2011. An assessment of the health and economic burdens of glaucoma. Am. J. Ophthalmol. 152, 515–22.

Vermes, I., Haanen, C., Steffens-Nakken, H., Reutelingsperger, C., 1995. A novel assay for apoptosis. Flow cytometric detection of phosphatidylserine expression on early apoptotic cells using fluorescein labelled Annexin V. J. Immunol. Methods 184, 39–51.

Visser, W.F., van Roermund, C.W.T., Waterham, H.R., Wanders, R.J. a, 2002. Identification of human PMP34 as a peroxisomal ATP transporter. Biochem. Biophys. Res. Commun. 299, 494–7.

Von Lubitz, D.K., Beenhakker, M., Lin, R., Carter, M.F., Paul, I.A., Bischofberger, N., Jacobson, K.A., 1996. Reduction of postischemic brain damage and memory deficits following treatment with selective adenosine A1 receptor agonist. Eur. J. Pharmacol. 302, 43–48.

Von Lubitz, D.K., Lin, R.C., Popik, P., Carter, M.F., Jacobson, K. a, 1994. Adenosine A3 receptor stimulation and cerebral ischemia. Eur. J. Pharmacol. 263, 59–67.

Vorwerk, C.K., Kreutz, M., Dreyer, E.B., Sabel, B.A., 1996. Systemic L-Kynurenine Administration Partially Protects Against NMDA , But Not Kainate-Induced Degeneration of Retinal Ganglion Cells , and Reduces Visual Discrimination Deficits in Adult Rats. Invest. Ophthalmol. Vis. Sci. 37, 2382–2392.

Wassle, H., Boycott, B., 1991. Functional architecture of the mammalian striatum: mouse vascular and striosome organization and their anatomic relationships. Physiol. Rev. 71, 447–480.

Weber, A.J., Harman, C.D., 2008. BDNF preserves the dendritic morphology of alpha and beta ganglion cells in the cat retina after optic nerve injury. Invest. Ophthalmol. Vis. Sci. 49, 2456–63.

Wei, G., Xu, H., Ding, P.T., Li, S.M., Zheng, J.M., 2002. Thermosetting gels with modulated gelation temperature for ophthalmic use: the rheological and gamma scintigraphic studies. J. Control. Release 83, 65–74.

Weinreb, R.N., Friedman, D.S., Fechtner, R.D., Cioffi, G. a, Coleman, A.L., Girkin, C. a, Liebmann, J.M., Singh, K., Wilson, M.R., Wilson, R., Kannel, W.B., 2004. Risk assessment in the management of patients with ocular hypertension. Am. J. Ophthalmol. 138, 458–67.

Weinreb, R.N., Khaw, P.T., 2004. Primary open-angle glaucoma. Lancet 363, 1711–20.

Weinreb, R.N., Toris, C.B., Gabelt, B.T., Lindsey, J.D., Kaufman, P.L., 2002. Effects of prostaglandins on the aqueous humor outflow pathways. Surv. Ophthalmol. 47 Suppl 1, S53–64.

Weiss, S., Benwell, K., Cliffe, I., 2003. Discovery of nonxanthine adenosine A2A receptor antagonists for the treatment of Parkinson's disease. Neurology 61.

Wilson, a M., Di Polo, A., 2012. Gene therapy for retinal ganglion cell neuroprotection in glaucoma. Gene Ther. 19, 127–36.

WoldeMussie, E., Yoles, E., Schwartz, M., Ruiz, G., Wheeler, L. a, 2002. Neuroprotective effect of memantine in different retinal injury models in rats. J. Glaucoma 11, 474–80.

Wong, R.C.S., Cloherty, S.L., Ibbotson, M.R., O'Brien, B.J., 2012. Intrinsic physiological properties of rat retinal ganglion cells with a comparative analysis. J. Neurophysiol. 108, 2008–23.

Woodhall, E., West, a K., Chuah, M.I., 2001. Cultured olfactory ensheathing cells express nerve growth factor, brain-derived neurotrophic factor, glia cell line-derived neurotrophic factor and their receptors. Brain Res. Mol. Brain Res. 88, 203–13.

Wu, Fan, D.-G., Tadmori, I., Yang, H., Furman, M., Jiao, X.-Y., Young, W., Sun, D., You, S.-W., 2010. Death of axotomized retinal ganglion cells delayed after intraoptic nerve transplantation of olfactory ensheathing cells in adult rats. Cell Transplant. 19, 159–66.

Wu, S., 2010. Synaptic organization of the vertebrate retina: general principles and species-specific variations: the Friedenwald lecture. Invest. Ophthalmol. Vis. Sci. 51, 1263–74.

Xu, K., Bastia, E., Schwarzschild, M., 2005. Therapeutic potential of adenosine A(2A) receptor antagonists in Parkinson's disease. Pharmacol. Ther. 105, 267–310.

Yip, J.L.Y., Foster, P.J., 2006. Ethnic differences in primary angle-closure glaucoma. Curr. Opin. Ophthalmol. 17, 175–80.

Yu, S., Tanabe, T., Dezawa, M., Ishikawa, H., Yoshimura, N., 2006a. Effects of bone marrow stromal cell injection in an experimental glaucoma model. Biochem. Biophys. Res. Commun. 344, 1071–9.

Yu, S., Tanabe, T., Yoshimura, N., 2006b. A rat model of glaucoma induced by episcleral vein ligation. Exp. Eye Res. 83, 758–70.

Zambrowicz, B., 2003. Predicting drug efficacy: knockouts model pipeline drugs of the pharmaceutical industry. Curr. Opin. Pharmacol. 3, 563–570.

Zamzami, N., Susin, S. a, Marchetti, P., Hirsch, T., Gómez-Monterrey, I., Castedo, M., Kroemer, G., 1996. Mitochondrial control of nuclear apoptosis. J. Exp. Med. 183, 1533–44.

Zhang, Budak, M.T., Lu, W., Khurana, T.S., Zhang, X., Laties, A.M., Mitchell, C.H., 2006. Identification of the A3 adenosine receptor in rat retinal ganglion cells. Mol. Vis. 12, 937–48.

Zhao, Li, Yunqin, Tang, L., Li, Yuehua, Fan, F., Jiang, B., 2011. Protective effects of human umbilical cord blood stem cell intravitreal transplantation against optic nerve injury in rats. Graefes Arch. Clin. Exp. Ophthalmol. 249, 1021–8.

Zhao, M., Beauregard, D. a, Loizou, L., Davletov, B., Brindle, K.M., 2001. Non-invasive detection of apoptosis using magnetic resonance imaging and a targeted contrast agent. Nat. Med. 7, 1241–4.

Zhou, X., Li, F., Kong, L., Tomita, H., Li, C., Cao, W., 2005. Involvement of inflammation, degradation, and apoptosis in a mouse model of glaucoma. J. Biol. Chem. 280, 31240–8.

Zhou, Y., Pernet, V., Hauswirth, W.W., Di Polo, A., 2005. Activation of the extracellular signal-regulated kinase 1/2 pathway by AAV gene transfer protects retinal ganglion cells in glaucoma. Mol. Ther. 12, 402–12.

2. CHAPTER TWO: Unexpected Low Dose Toxicity of the Universal Solvent, DMSO

Table of Contents

2.1 Abstract

Dimethyl sulfoxide (DMSO) is an important aprotic solvent that can solubilise a wide variety of otherwise poorly soluble polar and non-polar molecules. This, coupled with its apparent low toxicity at concentrations below 10%, has led to its ubiquitous use and widespread applications. Here, we demonstrate that DMSO induces retinal apoptosis *in vivo* at low concentrations (5 µl intravitreally (IVT) dosed DMSO in rat from a stock concentration of 1, 2, 4 and 8% (v/v)). Toxicity was confirmed *in vitro* in a retinal neuronal cell line, at DMSO concentrations > 1% (v/v), using annexin V, TUNEL, MTT and AlamarBlue cell viability assays. DMSO concentrations > 10% (v/v) have recently been reported to cause cellular toxicity through plasma membrane pore formation. Here, we show the mechanism by which low concentrations (2 – 4% DMSO) induce neuronal death is through AIF translocation to the nucleus and stimulation of a caspase-3 independent mechanism, involving PARP activation. These results highlight safety concerns of using low concentrations of DMSO as a solvent for *in vivo* administration, and in biological assays. We recommend that methods other than DMSO are employed for solubilizing drugs, but where no alternative exists, researchers compute absolute DMSO final concentrations, and include an untreated control group in addition to DMSO vehicle control to check for solvent toxicity.

Keywords: neuronal apoptosis, retina, DARC, toxicity, AIF.

2.2 Introduction

Dimethyl sulfoxide ($(CH_3)_2SO$ - DMSO) is an organic polar aprotic molecule widely used as a solvent for the dissolution of small hydrophobic drug molecules due to its amphipathic nature (Szmant, 1975). DMSO is commonly utilised for cell cryopreservation because of its membrane penetrating and water displacement properties. Due to its broad solubilising capability, DMSO is employed as a solvent for many drug types, and is often used as the vehicle control-of-choice for both *in vitro* and *in vivo* studies (Li and Lo, 2010; Modesitt and Parsons, 2010; Sankpal et al., 2012). While some studies recognise that DMSO can be toxic (Hanslick et al., 2009; Julien et al., 2012), so ubiquitous is the use of this solvent, that the concentration of DMSO used is often unreported (Modesitt and Parsons, 2010; Sankpal et al., 2012). A similar disregard for its potency is observed *in vivo*, where systemic DMSO injections have been used as vehicle controls for: peripheral nerve regeneration (Sun et al., 2012), silencing gene expression (Pelzel et al., 2012, 2010), inhibition of tumour growth (Lin et al., 2011), and compression-induced muscle damage (Teng et al., 2011). In the eye, DMSO has also been used as a topical vehicle control (Avila et al., 2002a), including a clinical study in 1975 in which 50% (v/v) DMSO was applied topically twice daily for two years (Hill, 1973). Furthermore, subconjunctival administration of 80% (v/v) DMSO was used as a control for both rapamycin treatment (Piña et al., 2011) and following trabeculectomy (Lüke et al., 2010). Most often, however, DMSO is administered intravitreally (IVT) as a vehicle control in animal studies, including for: curcumin (5 pmol, 20 pmol) (Burugula et al., 2011), rotenone (0.2 mg/kg in DMSO, with DMSO vehicle controls) (Rojas et al., 2008a, 2008b), 2-(6-cyano-1-hexyn-1-yl)adenosine (2-CN-Ado, 50% (v/v) DMSO) (Konno et al., 2007) and Histone H4 deacetylation DMSO (1 µl) (Pelzel et al., 2010).

Apoptosis, or programmed cell death, plays an essential role in homeostasis and the normal development of all multicellular organisms; in fact dysregulation of this process is responsible for a plethora of autoimmune and neurodegenerative diseases (Fischer and Schulze-osthoff, 2005). Mitochondria play a central role in the regulation of apoptosis and are involved in the release or interaction with different pro- and anti-

apoptotic proteins that trigger both caspase-dependent and caspase-independent cell death (Hengartner, 2000; Reed, 2000).

In vitro, DMSO is reported to induce apoptosis at concentrations greater than 10% (v/v), due to plasma membrane pore formation (de Ménorval et al., 2012; Notman et al., 2006). Moreover, DMSO has been previously reported to induce cell death through caspase 9 in the EL-4 cell line and caspase 3 activation both in vitro in a cochlear cell line, and in vivo in the developing central nervous system (Hanslick et al., 2009; Liu et al., 2001; Qi et al., 2008).

This study aims to establish whether the use of DMSO as a vehicle control in ocular drug delivery is fit for purpose. This was investigated by evaluating its effects in the retina in vivo and in vitro, at DMSO concentrations less than 10% (v/v).

2.3 Materials and Methods

2.3.1 Animals

Adult, male, Dark Agouti rats (Harlan Laboratories, UK) weighing 150 g to 200 g were housed in an air-conditioned, 21°C environment with a 12 h light/dark cycle (50 lux), where food and water was available *ad libitum*. All the experimental and animal care procedures were approved by the UK Home Office and in compliance with the ARVO Statement for the Use of Animals in Ophthalmic and Vision Research.

2.3.2 Intravitreal injections

All animals were anesthetised by intraperitoneal injection using a mixture of ketamine (37.5%)/medetomidine (25% Dormitor; Pfizer Animal Health, Exton, PA, USA) solution (0.75 ml ketamine, 0.5 ml medetomidine, and 0.75 ml sterile water) at 0.2 ml/100 g as previously described (Cordeiro et al., 2004). Animals were randomly assigned to DMSO treatment (5µl stock at 0, 1, 2, 4, 8, 10, 15 and 25% (minimum of n=4 eyes per concentration)). A final volume of 5 µl DMSO and fluorescently-labelled annexin V (Anx-F) was administered IVT (Cordeiro et al., 2004) using a 34G needle attached to a 5 µl Hamilton syringe (Hamilton, Reno, NV, USA) under direct microscopic visualisation. The needle was inserted through the sclera superiorly, 1 mm behind the limbus, at an angle of 45° (Cordeiro et al., 2004), and caution was taken to avoid contact with the lens.

2.3.3 *In vivo* Imaging of RGC apoptosis

Eyes were imaged using an HRA Spectralis (Heidelberg Retinal Angiograph) (Heidelberg Engineering, Germany) as previously described (Cordeiro et al., 2004). Preliminary experiments established the effects of DMSO to be optimal 2 hours after IVT injections. Pupils were dilated with one drop each of phenylephrine hydrochloride 2.5% and cyclopentolate hydrochloride 1.0%, and corneal clarity was preserved with regular lubrication. During image acquisition, the HRA Spectralis was focused on the retinal nerve fibre layer, as identified in the reflectance mode. The images were collected and analysed using a recently validated MatLab script (Validation and refinement of an

automated technique of counting apoptosing retinal cells imaged with DARC, Mukhtar et al., ARVO Annual Meeting 2012).

2.3.4 Cell culture

A transformed RGC-5 cell line was used in this study, which was a kind gift from Dr. Neeraj Agarwal (Department of Cell Biology and Genetics, UNT Health Science Center, Fort Worth, TX, USA). This cell line has been characterised as expressing RGC proteins Thy-1 and Brn-3c (Krishnamoorthy et al., 2001), and we have confirmed them to express the RGC marker Brn3a as well as the neuronal marker β3 tubulin (Burugula et al., 2011; Nadal-Nicolás et al., 2009). The original cell line was transformed with Ψ2 E1A virus and developed from postnatal Sprague Dawley rats (Krishnamoorthy et al., 2001), but recent controversy has suggested they are from mice (Van Bergen et al., 2009). However, they remain the only cell line that resembles RGCs, and are repeatedly used in this manner (Balaiya et al., 2012; Liu et al., 2013). RGC-5 were grown in Dulbecco's modified Eagle's medium (DMEM; Invitrogen), supplemented with 10% heated-inactivated fetal bovine serum (Invitrogen), 100 U/ml penicillin, and 100mg/ml streptomycin.

2.3.5 *In vitro* imaging of externalisation of phosphatidylserine RGC-5 apoptosis

RGC-5s were seeded at $1x10^4$ cells/well in a 96 well plate. Cells were incubated for 24 h (37 °C, 5% CO_2) before treatment with varying final concentrations of DMSO (0%, 1%, 2%, 4%, and 8% (v/v)) diluted in tissue culture medium for 2 hours, after which the DMSO was removed. Cells were next incubated with 150 ng/ml Anx-F for 30 minutes. After this time, the Anx-F was removed and cells were washed three times (10 mM HEPES, 150 mM sodium chloride, 2 mM calcium chloride, pH 7.4). Anx-F fluorescence was recorded in the same buffer using an ODYSSEY Li-cor, and the results expressed as fluorescence intensities normalised to controls (0% DMSO (v/v)).

2.3.6 Oxygen consumption measurement

The mitochondria respiration rates were measured using polarographic oxygen sensors in a 2-chamber Oroboros Oxygraph (Oxygraph 2-k, Oroboros Instruments, Obergurgl,

Austria) with electromagnetic stirrers and thermostatically maintained at 37°C. The cells were grown to 100% confluency in a T75 flask. They were washed twice with warm PBS, trypsinised and centrifuged for 2 minutes at 1000 x g. The pellet of cells was gently re-suspended in DMEM/HEPES (DMEM without Sodium Bicarbonate ($NaHCO_3$), Glucose 5.5mM, HEPES 20 mM) and kept in a 37°C water bath. 2.5 ml of medium containing approximately 1 million cells was used for each experiment. The cells were transferred to a cuvette, which made contact with the O_2 membrane and different final concentartions of DMSO (1, 2 and 4% (v/v)) were added. The system was then closed and, after it reached equilibrium, the levels of oxygen were recorded. Sequentially concentrations of: ATP-synthase specific inhibitor, oligomycin (5mM), was added to prevent reverse pumping of protons by the ATPase; coupled respiration was assessed followed by uncoupling with FCCP (carbonylcyanide p-trifluoromethoxyphenylhydrazone) (1mM); uncoupled respiration was next assessed by inhibition at complex III by antimycin A (1mg/ml); finally, ascorbate and N,N,N',N'-tetramethyl-p-phenylenediamine (TMPD) (0.8M) were added to determine the capacity of cytochrome c oxidase (complex IV), as previous described (Brand and Nicholls, 2011). The oxygen consumption was normalized to the number of cells in each cuvette and to the basal control levels.

2.3.7 Cell treatment with DMSO

RGC-5 cells were plated in a T75 flask (for western blot extracts), on glass coverslips on a 12 well plate (for immunocytochemistry), on glass coverslips on a 6 well plate (for live cell imaging) or in 96 well plates (for the AlamarBlue assay) and then treated with different final concentrations of DMSO (0, 1, 2, 4 and 8% v/v) for 24 hours, as in previous studies (Burugula et al., 2011; Pelzel et al., 2012, 2010; Sankpal et al., 2012).

2.3.8 *In vitro* cell viability and apoptosis assays

TUNEL, propidium iodide (PI) and Hoechst assays were used to assess the effects of DMSO on RGC-5. For Hoechst staining, cells were grown to 80% confluency and separate wells treated with DMSO at 0, 1%, 2%, 4%, 8% and 10% final concentrations (Burugula et al., 2011; Pelzel et al., 2012, 2010; Sankpal et al., 2012). The cells were then fixed with

4% paraformaldehyde (PFA) for 30 minutes and stained with the cell permeable dye Hoechst 33342 (Molecular Probes, Eugene, OR, USA) at 5 µg/ml after 5 minutes incubation at room temperature. Nuclear morphology was evaluated with a fluorescent microscope (Leica DM IRB, Germany) to allow assessment of apoptosis characterised by bright staining and chromatin condensation (Santiago et al., 2007). Condensed nuclei were counted using ImageJ (NIH - National Institute of Health, Bethesda, MD, USA) and were presented as a percentage of the total number of cells in the field. For the simultaneous detection of apoptosis and necrosis, three markers were used. Cells were grown on glass coverslips to 80% confluence, and treated with a 10 µM caspase-3 inhibitor in accordance with the manufacturer's protocol (Z-DEV-FMK, R&D Systems, UK) (Kumi-Diaka and Butler, 2000) before adding DMSO at final concentrations of 1%, 2%, 4% and 8%. The cells were then washed twice with fresh cold PBS for 5 minutes each time, and incubated for 10 minutes on ice with both PI (Invitrogen, Paisley, UK) at 5 µg/ml and Hoechst 33342 (Molecular Probes, Eugene, OR) at 10 µg/ml. The 5 minute wash was repeated twice as before with fresh cold PBS, and the cells were fixed with 4% PFA in PBS for 30 minutes at 4°C. After washing again, the cells were permeabilised with 0.2% triton X-100 (Sigma-Aldrich, St. Louis, MO, USA). To distinguish fragmented nuclei a TUNEL kit (DeadEnd^{TM} Fluorometric TUNEL System Promega, Wisconsin, USA) was used following the manufacturer's protocol.

The images were acquired on a Leica confocal scanning microscope SP2 (Leica Microsystems GmbH, Wetzlar, Germany) using a 40x oil objective lens coupled to a Kr/Ar laser (488 nm), a He/Ne laser (543 nm) and a blue diode (405 nm). The total number of cells, as well as the number of apoptotic and necrotic cells were counted using ImageJ software (ImageJ 1.44p, NIH - National Institute of Health, Bethesda, MD, USA). The percentage of apoptotic cells was calculated for each concentration in relation to the total number of cells and compared with the control. Cells stained with PI were co-localised with TUNEL, as described previously for final stage of apoptosis (Elmore, 2007).

2.3.9 Western Blot Analysis of Mitochondrial Proteins

Cells were grown to 80% confluence and treated for 24 hours in DMSO (1, 2 and 4 %). For total extracts, cells were washed twice using fresh cold PBS (Sigma-Aldrich, St. Louis,

MO, USA) and lysate using RIPA buffer (Sigma-Aldrich, St. Louis, MO, USA) for 10 minutes at 4°C on a plate shaker. Cells were dissociated using a P 1000 micropipette and stored at -20°C for futher analysis.

For analysis of the mitochondrial, nuclear and cytosolic fractions, cells were treated using a Qproteome® Mitochondria Isolation kit according to the manufacturer's protocol (Quiagen, Hilden, Germany). The samples were stored at -20°C for further analysis.

The total protein content of samples was quantified using the bicinchoninic acid assay (BCA; Thermo Fisher Scientific, Rockford, IL, USA). Equal amounts of protein (20 µg or 40 µg) were loaded on 12% gels after denaturation with 4x concentrated sample buffer (30 % (v/v) glycerol, 0.6 M dithiothreitol (DTT), 10 % (w/v) sodium dodecyl sulfate (SDS), 715 mM Tris-HCL (pH 6.8) and 0.012 % bromophenol blue), and were heat inactivated at 95°C for 5 minutes. The samples were separated by sodium dodecyl sulfate polyacrylamide gel electrophoresis (SDS-PAGE) and then electro-transferred to polyvinylidene difluoride (PVDF) membranes (GE HealthCare, UK). After blocking for 1 hour at room temperature with 5% non-fat milk in Tris-buffered saline (20 mM Tris, 140 mM Nach, pH 7.6) containing 0.1 % Tween 20 (TBS-T), the membranes were incubated overnight at 4°C with primary antibodies against AIF 1:200 (SC-9416, Santa Cruz Biotechnology), Bax 1:200 (sc-6236, Santa Cruz Biotechnology), caspase-3 (BD Transduction laboratoty), cleaved caspase-3 (Asp175, Cell Signalling Technology), and PARP 1:500 (Cell Signaling Technology). After washing three times (15 minutes with TBS-T), the membranes were incubated for 2 h at room temperature with their respective alkaline phosphatase-linked secondary antibody (Cell Signaling technology, DAKO) in TBS-T containing 5% non-fat milk. The membranes were then washed three times (15 minutes in TBS-T), and protein bands revealed with enhanced chemiluminescent substrate (ECL, GE HealthCare, UK). The membranes were then re-probed and tested for α-tubulin (DM1A, Cell Signalling Technology) or VDAC (Cell Signalling Technology) immunoreactivity as loading controls.

2.3.10 DMSO is toxic to retinal ganglion cells *in vivo*

Live cell imaging was performed using a Zeiss LSM 510 (Zeiss, Germany). Experiments were carried out at 37°C. The cells were washed twice with PBS, and growth medium

was replaced by HEPES saline solution (156 mM NaCl, 3 mM KCl, 2 mM MgSO4, 1.25 mM KH2PO4, 2 mM CaCl, 10 mM Glucose, 10 mM HEPES, pH 7.35). Fluo-4 was loaded 45 minutes before the beginning of the experiment to final concentrations of 2 µM. Fluo-4 was excited using a Kr/Ar laser at 488 nm. Images were acquired every 15 minutes for 2 hours, and were later analysed using ImageJ software.

2.3.11 Measurement of NADH autofluorescence

As before, live cell imaging was performed using a Zeiss LSM 510 (Zeiss, Germany). Experiments were carried out at 37°C. The cells were washed twice with PBS, and growth medium was replaced by HEPES saline solution. NADH autofluorescence after excitation with UV laser at 351 nm was measured every 2 minutes for 20 minutes and quantified using ImageJ software.

2.3.12 AlamarBlue assay

Cell viability using a PARP inhibitor or Calpain inhibitor at the same time as DMSO was assessed using the AlamarBlue (Invitrogen) viability assay, following preliminary experiments to identify the most appropriate concentrations. RGC-5 were plated in a 96 well plate at 4000 cell/ml and the cells were pre-treated for 1 hour with either a PARP inhibitor (10µM, PARP Inhibitor III, DPQ, Merck Millipore, UK) or calpain inhibitor (1µM, Calpeptine, Merck Millipore, UK). 2% DMSO was added to the cells with the inhibitors and incubated for 24 hours. 10 µl of filtered AlamarBlue solution was added to each 100 µl well plate and incubated for 2.30 hours according to manufacture protocol. The fluorescence was read at 585 nm with results presented as a percentage of the control.

2.3.13 Statistical analysis

Graphical data for mean values were represented with SEM. Statistical comparisons between different concentrations of DMSO animals and controls were performed using the One-Way ANOVA followed by Dunnett or Bonferroni post-hoc test using GraphPad Prism. Differences were considered significant for $p < 0.05$.

2.4 Results

2.4.1 DMSO is toxic to retinal ganglion cells *in vivo*

To evaluate the effects of DMSO on rat retinal ganglion cells (RGCs) *in vivo*, IVT injections (5 µl) of various stock concentrations of DMSO (0, 1, 2, 4, 8, 10, 15 and 25% (v/v)) were administered to Dark Agouti rats with Anx-F. Dosing of high stock concentrations of DMSO (≥ 10% (v/v)) resulted in lens toxicity, causing opacity and poor visualisation of the retina. DMSO was found to be toxic at all stock concentrations dosed < 10% (v/v) (effective vitreal concentration 0.1, 0.2, 0.4, 0.7, 0.9 and 1.4 % (v/v)) 2h post intravitreal administration, inducing significant ($p<0.01$, one-way ANOVA) RGC apoptosis as detected by Anx-F-positive cells (Fig 2.1, white spots indicate apoptosing cells on the retina, present after dosing DMSO stock concentrations of 1% (B), 2% (C), 4% (D), and 8% (v/v) (E)). This occurred in a dose-dependent manner, with RGC apoptosis increasing by 585%, 717%, 877% and 1620% compared to control with dosing 1%, 2%, 4% and 8% stock DMSO concentrations (v/v) respectively (Fig 2.1F).

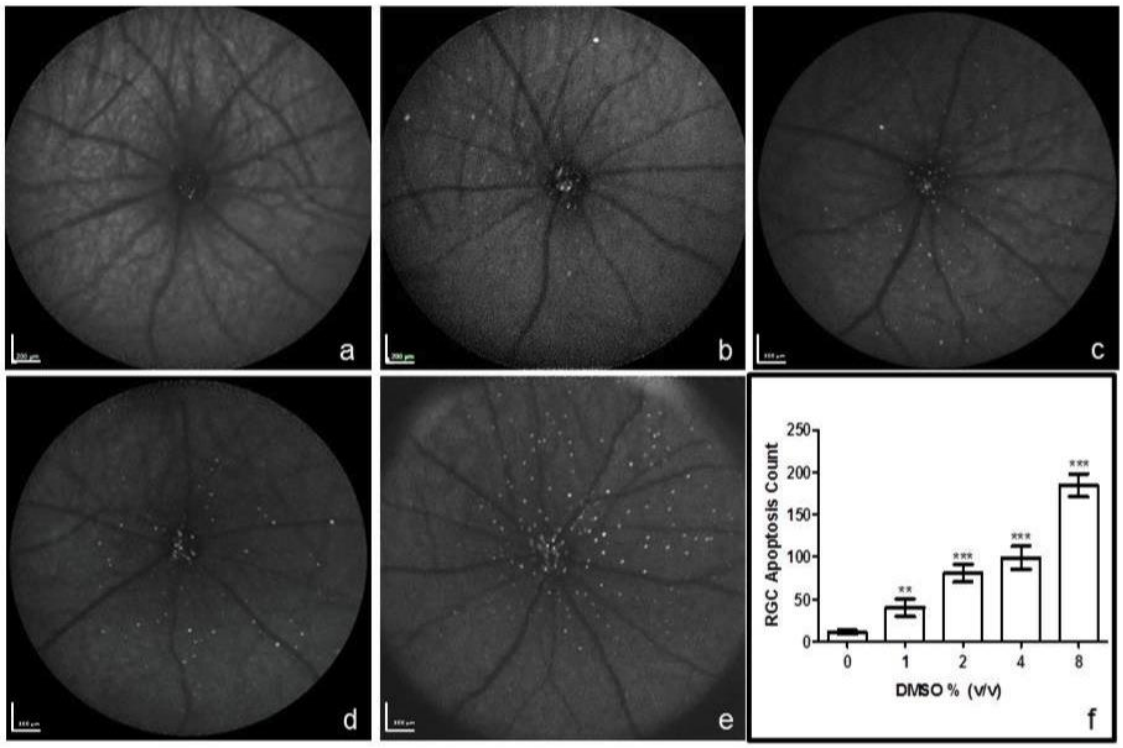

Figure 2.1 - DMSO toxicity *in vivo*: effects on RGC apoptosis. *In vivo* DARC (Detection of Apoptosing Retinal Cells) images obtained using a HRA Spectralis (Heidelberg Engineering, Germany), show the effects of 5 µl of intravitreally administered DMSO at indicated stock concentrations of 0%, 1%, 2%, 4% or 8% (v/v) on RGC apoptosis 2 hours following intravitreal injection of fluorescently-labelled annexin V (Anx-F). The white spots represent apoptotic RGCs labeled by Anx-F. (A-E) Wide-angle *in vivo* retinal images: PBS control (A), 1% DMSO (v/v) (B), 2% DMSO (v/v) (C), 4% DMSO (v/v) (D), 8 % DMSO (v/v) (E). Statistical analysis of the number of Anx-F positive cells after IVT injection of PBS or DMSO; *, $p<0.05$; **, $p < 0.01$; ***, $p < 0.001$), error bars represent SEM (f). Scale bar 200 µm.

2.4.2 DMSO is toxic to retinal ganglion cells *in vitro*

Having established that low concentrations of DMSO were toxic in the retina *in vivo,* we next investigated the toxicity of DMSO *in vitro*. RGC-5 cell viability and apoptosis were determined using Hoechst 33342 nucleic staining following a 24 hour treatment with 1, 2, 4, 8 or 10% DMSO (v/v). Hoechst 33342 staining is dull in normal cells, but much

stronger when the chromatin is condensed in apoptotic cells, allowing for both total and pyknotic cell counts to be made. DMSO was found to induce cell loss and apoptosis in a dose dependent manner (Fig 2.2 A-H). The total number of cells fell by 24%, 50%, 70%, 92%, and 98% respectively, with significance at 1% ($p<0.05$) and at concentrations ≥ 2% DMSO ($p<0.005$) compared to control (Fig 2.2A). Similarly, the number of pyknotic nuclei increased by 100%, 550%, 1725% and 2025% (percentage of total cells) compared to control (2, 4, 8 and 10% DMSO, respectively), with a significant increase noted at 1 ($p<0.05$), 2 ($p<0.01$) and 4% ($p<0.001$, one-way ANOVA) DMSO (v/v) (Fig 2.2B). These effects are clearly seen in the representative Hoechst 33342 images (Fig 2.2) at DMSO final concentrations of 0 (C), 1% (D), 2% (E), 4% (F), 8% (G), and 10% DMSO (H).

Cell viability was further assessed using an MTT assay after 24h treatment with 1, 2, 4, 8 and 10% DMSO (v/v). A decrease in cell viability was observed with final concentrations above 1% DMSO (v/v) ($p<0.001$, one-way ANOVA), being 35%, 68%, 76% and 90.5%, respectively for 2, 4, 8, and 10% DMSO (v/v) (Fig 2.2I). The IC50 was also calculated after 24h and was found to be at 2.14% DMSO (v/v) (Fig 2.2J).

As apoptosis is associated with phosphatidylserine (PS) externalisation, we next investigated whether DMSO can induce PS externalisation *in vitro*. RGC-5 cells were treated with varying final concentrations of DMSO (0%, 1%, 2%, 4%, 8%) for 2 hours and incubated with Anx-F for 30 min. Treatment of RGC-5 cells with final concentrations of DMSO ≥ 2% (v/v) were found to result in significant ($p<0.05$, t-test) phosphatidylserine externalisation compared to untreated controls in a dose dependent manner (Fig 2.2K).

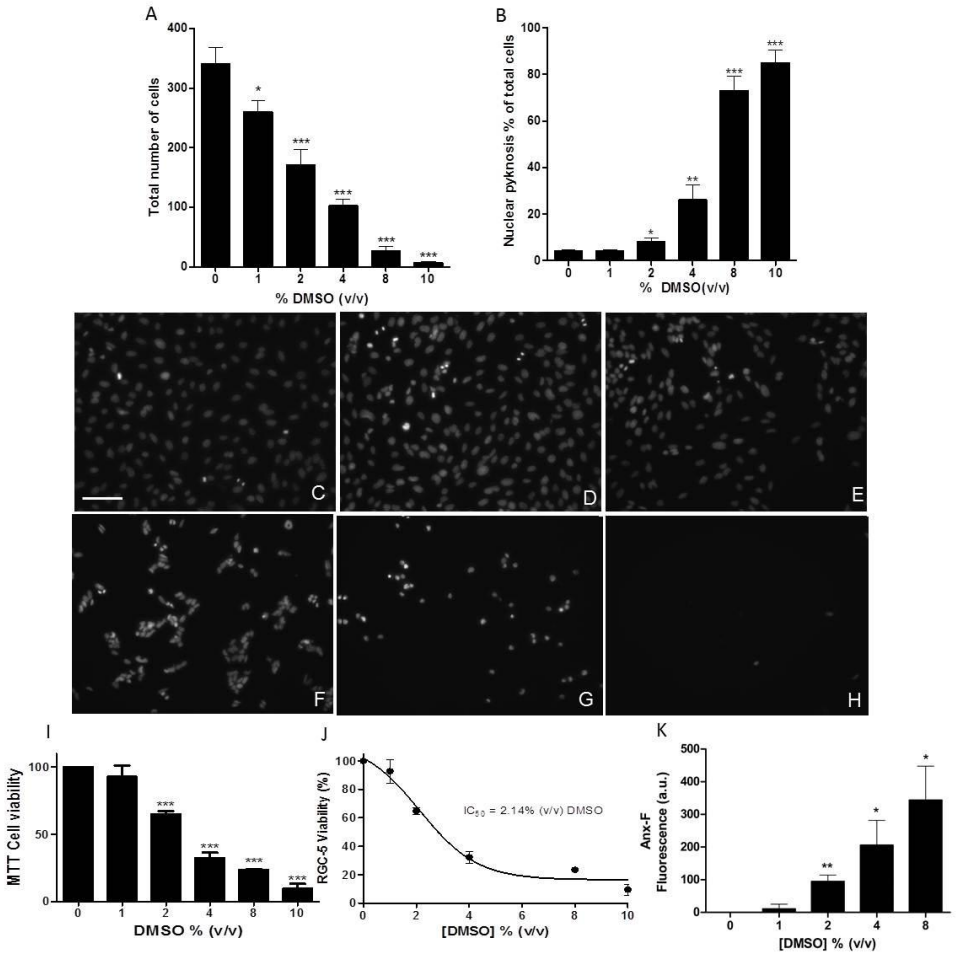

Figure 2.2 - DMSO toxicity *in vitro:* effects on RGC viability and apoptosis. Effects of DMSO after 24 h treatment, at final concentrations of 0%, 1%, 2%, 4%, 8% and 10%. DMSO increases chromatin condensation and decreases total cell count in a dose dependent manner. Cell viability was determined by nucleic morphology with Hoechst 33342 nucleic staining. Total cells and apoptotic cells per field were counted using ImageJ for each concentration. (A) Total number of cells per image at t = 24 h. (B) Number of cells with pyknotic nuclei, represented as a percentage of total cells. (C-H) Representative images: Control (C), 1% DMSO (D), 2% DMSO (E), 4% DMSO (F), 8% DMSO (G), 10% DMSO (H). An MTT assay was performed after 24 h treatment of RGC-5 with different final concentrations of DMSO (0, 1, 2, 4, 8, 10% v/v) (I). A significant decrease in cell viability was observed with final concentrations above 1% DMSO (v/v, (I)). The IC50 occurs at 2.14% (v/v DMSO) (J). After 2 h treatment, (0%, 1%, 2%, 4%, 8% (v/v) DMSO), RGC-5s exhibited a significant increase in phosphatidylserine externalisation reported after 30 min incubation with the fluorescent conjugated annexin V (Anx-F, n=3, ± SEM) (K). Statistical analysis using one-way ANOVA followed by Dunnett's multiple comparison test. Error bars represent SEM. Statistical analysis *, $p<0.05$; **, $p < 0.01$; ***, $p < 0.001$. Scale bar 100 µm.

2.4.3 DMSO inhibits mitochondrial oxygen consumption and leads to intracellular calcium increase.

Mitochondria play a crucial role in the control of apoptotic events. Having established that DMSO induces cell death, we next investigated if this was related to changes in mitochondrial function. Measurement of RGC-5 cellular oxygen consumption following DMSO application showed significantly reduced basal oxygen consumption after addition of 1, 2 and 4% DMSO ($p<0.001$) (Fig 2.3A). Moreover, application of oligomycin decreased oxygen consumption due to inhibition of oxidative phosphorylation, and addition of 4 % DMSO (v/v) showed a further decrease in oxygen respiration levels (Fig 2.3B). Application of the uncoupler, FCCP, is known to increase oxygen consumption levels (maximal respiration); however this increase was shown to be significantly and decreased at 2 and 4 % DMSO compared with control ($p<0.001$) (Fig 2.3C). Finally, antimycin A, a complex III inhibitor, was added demonstrating that the oxygen consumption was due to mitochondria respiration (supplementary data). The levels of NADH were next investigated to assess the redox state of the mitochondrial NAD system by recording changes in NADH fluorescence. NADH levels were quantified but were shown not to be significant affected by the addition of 2 and 4% DMSO (v/v) (Fig 2.3D). Next, calcium levels were investigated using Fluo-4 AM. Changes in intracellular calcium were quantified after 2 hours of application (Fig 2.3E). This demonstrated that an increase in intracellular calcium concentration ($[Ca^{2+}]_c$) was induced by DMSO at both 2 and 4% (v/v) final concentrations, and this was statistically significant ($p<0.001$) compared to control. The development of changes in intracellular calcium were recorded using live cell imaging for a period of two hours, with single cell (Fig 2.3 F-H) and average traces (Fig 2.3 I-K) clearly showing an increase in intracellular calcium transients exposed to 2 and 4% DMSO over time (Fig 2.3 F-K). To assess the involvement of the mPTP in DMSO-induced cell death, we also tested if the mPTP inhibitor Cyclosporine A (CsA) had an impact on DMSO-induced cell death. CsA did not decrease cell death in any of the DMSO final concentrations tested indicating that DMSO induced cell death is mPTP independent (data not shown).

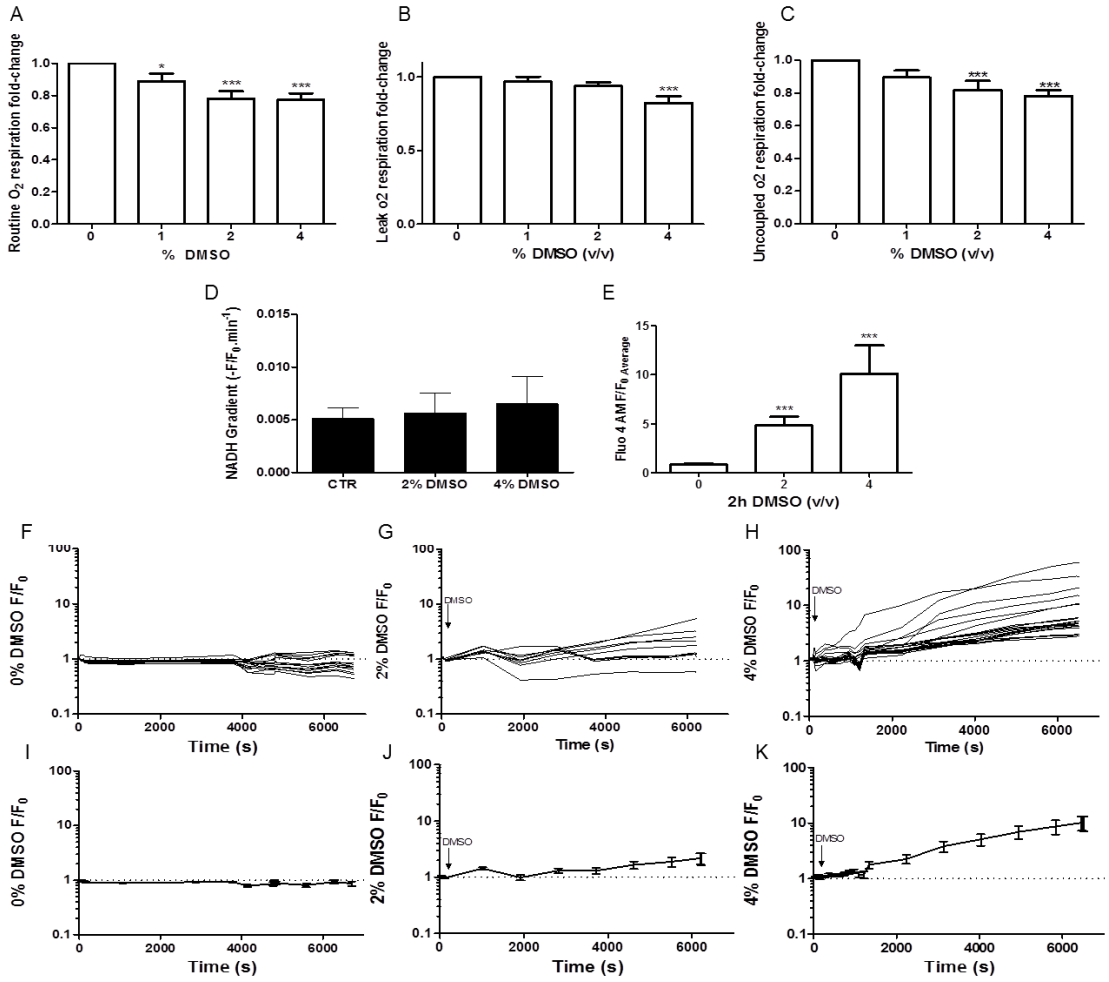

Figure 2.3 - Effects of DMSO induced apoptosis involves mitochondrial dysfunction. Oxygen consumption was measured in RGC-5 cells. There is significant inhibition of mitochondrial respiration at final concentrations of 1, 2 and 4% DMSO (*p<0.05; ***p<0.001) (A). DMSO was found to significantly decrease respiration levels after addition of the ATP synthase inhibitor, oligomycin at a final concentration of 4% DMSO only (***p<0.001) (B). Moreover, addition of the uncoupler FCCP, induced a decrease in respiration at both 2 and 4% DMSO (***p<0.001) (C). NADH levels were evaluated using live cell imaging for a period of 20 min. Graph represents the gradient of each curve which was shown not to be significant with 2 and 4% DMSO (v/v) (D). Fluo-4 AM analysis assessing intracellular calcium was performed (E-K). Average of F/Fo single cells at the endpoint of the experiment for each concentration (2 h), shows that DMSO at both 2 and 4% final concentrations causes a significant increase in $[Ca^{2+}]_c$ in RGC-5, ***p< 0.001 t-test analysis (E). This change is clearly shown in the raw data of calcium levels with single cell (F-H), and average (I-K) analysis of the raw data for control (F, I), 2% (G, J) and 4% (H, K) DMSO F/Fo respectively. Error bars represent SEM.

2.4.4 Apoptosis induced by DMSO is caspase-3 independent

Having established that DMSO induces apoptosis at low concentrations, we next investigated if this involved caspase-3. RGC-5 cells were incubated with the caspase-3 inhibitor Z-DEVD-fmk inhibitor (10 µM) and DMSO (0, 1, 2, 4 and 8% (v/v)) for 24 hours. Apoptosis and cell death were determined using Hoechst, TUNEL and PI staining (Fig 2.4A - D). Firstly, the presence of the caspase-3 inhibitor had no effect on the level of RGC-5 loss (Fig 2.4A) with decreasing cell viability still occurring with increasing final concentrations of DMSO, as assessed using Hoechst (Fig 2.4A, D). Similarly, Z-DEVD-fmk did not appear to influence the number of TUNEL positive cells, with increased apoptosis continuing to be associated with increasing final concentrations of DMSO (Fig 2.4B, D). Finally, the number of PI-positive cells increased with increasing DMSO final concentrations, until 8% DMSO when the majority of cells were stained with PI, with no effect by caspase-3 inhibition (Fig 2.4C, D). The findings were further supported by Western blot analysis which showed no caspase-3 activity in RGCs at any of the DMSO final concentrations tested (Fig 2.4E), strongly suggesting that the pathway by which DMSO triggers cell death is caspase-3 independent.

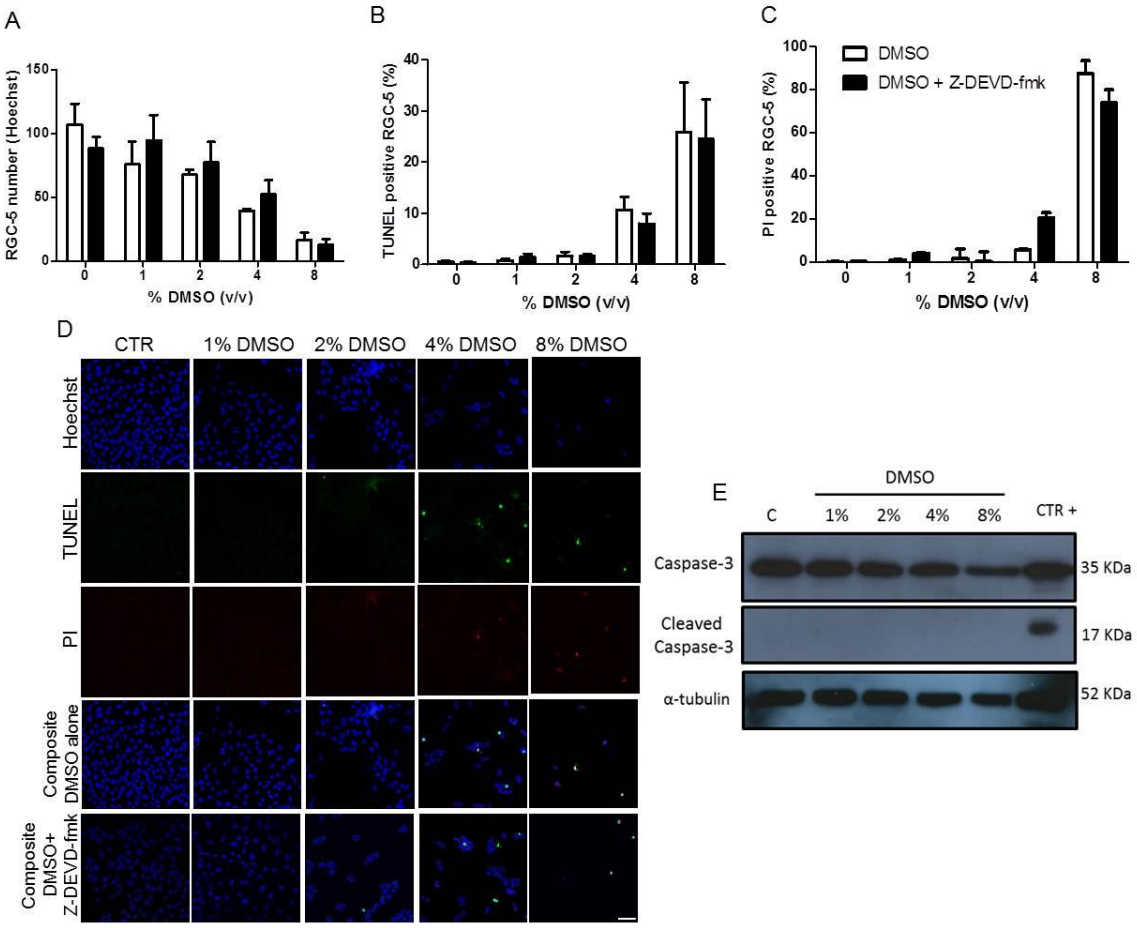

Figure 2.4 - DMSO induced cell death in RGC–5 cells is caspase-3 independent. RGC-5 cells were treated with 10 µM caspase-3 inhibitor Z-DEVD-fmk before a 24 h treatment with DMSO (1%, 2%, 4%, and 8%). DMSO was found to decrease the total number of cells while increasing the number of TUNEL and PI positive cells in a dose dependent manner (A-D). The caspase-3 inhibitor Z-DEVD-fmk did not have a significant effect on the total number (A, D, Hoechst blue), TUNEL-stained (B, D, TUNEL green) or PI-positive (C, D, PI red) cells, compared with DMSO treatment alone. Error bars represent SEM. Scale bar 100 µm (D). Assessment of the levels of caspase-3 and cleaved caspase-3 in DMSO-treated RGC-5 cells were achieved by Western blot (E). No detection of activated caspase-3 was seen at any of the DMSO final concentrations (1%, 2%, 4%, and 8%) tested (E). A positive control and a loading control (α-tubulin) were used.

2.4.5 DMSO induces cell death by nuclear translocation of AIF, and translocation of Bax to mitochondria

To determine the pathway by which DMSO induces cell death, concentrations of the pro-apoptotic proteins AIF and Bax were evaluated in mitochondrial, nuclear and cytosolic fractions of RGC-5 cells treated with DMSO. Western blot analysis showed that after 24h treatment, there was a gradual decline in the levels of mitochondrial AIF (Fig 2.5A, B) with increasing final concentrations of DMSO, whilst a concomitant increase in nuclear AIF (Fig 2.5A, C) was observed at equivalent concentrations. This is in accordance with AIF translocation from the mitochondria to the nucleus during apoptosis. VDAC and α-tubulin were used as loading controls for the mitochondrial and cytosolic fractions respectively (A). Immunocytochemistry analysis was performed using an AIF antibody after 24h exposure to different final concentrations of DMSO (Fig 2.5D). From concentrations above 1% DMSO (v/v), more AIF is seen in the nucleus, as demonstrated by the co-localization plots with AIF and nuclear staining (Hoechst) (Fig 2.5D). This is in keeping with AIF translocation from the mitochondria to the nucleus, as revealed by Western blots analysis in Fig 2.5 A – C. The level of pro-apoptotic Bax was evaluated similarly to AIF using Western blots. Mitochondrial Bax (Fig 2.5A, E) was increased at 2 and 4% DMSO and this was paralleled by a corresponding decrease in cytosolic Bax at the same concentrations (Fig 2.5A, F). This is in accordance with Bax oligomerization at the mitochondrial level. This data strongly supports the fact that DMSO induces AIF translocation from mitochondria to the nucleus through Bax-induced mitochondria permeabilisation.

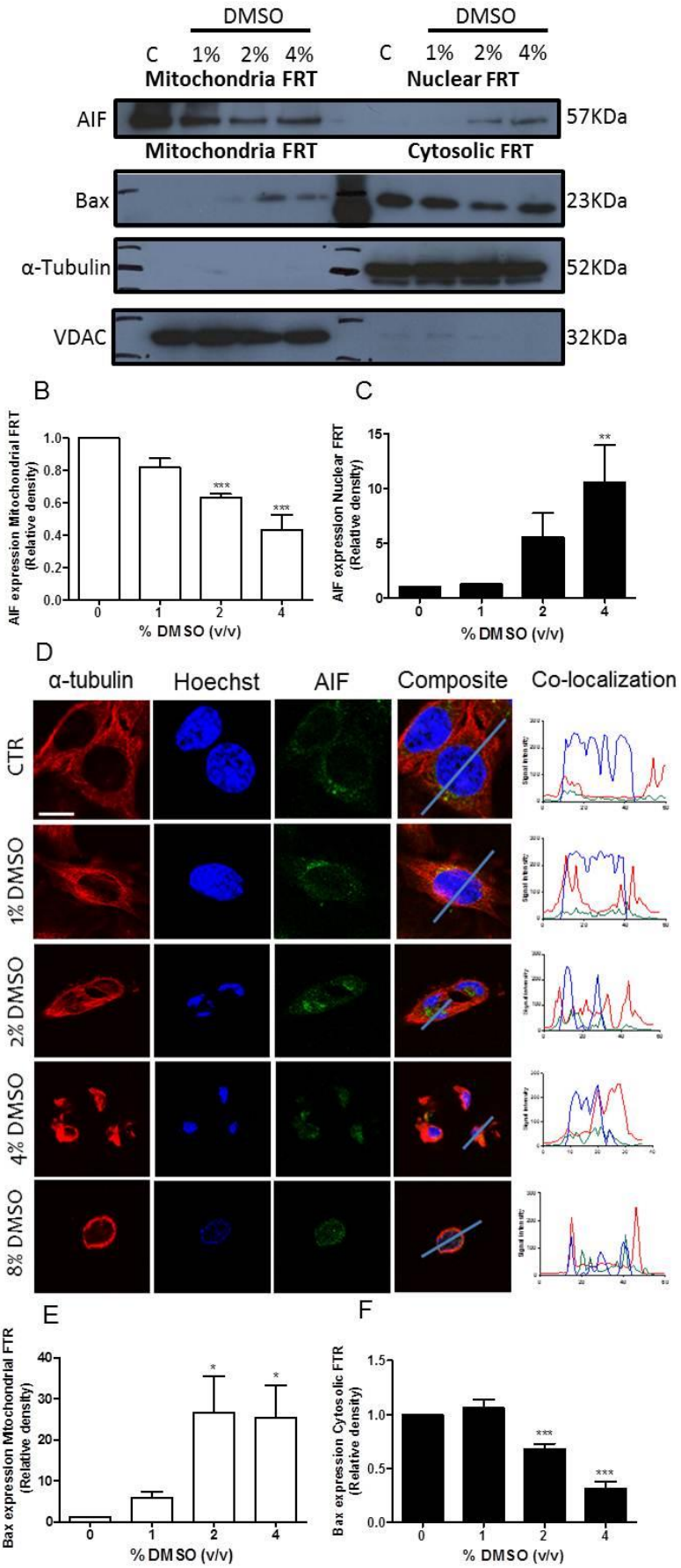
DMSO
DMSO
C 1% 2% 4%
C 1% 2% 4%
Mitochondria FRT
Nuclear FRT
AIF
57KDa
Mitochondria FRT
Cytosolic FRT
Bax
23KDa
α-Tubulin
52KDa
VDAC
32KDa
B
C
AIF expression Mitochondrial FRT (Relative density)
% DMSO (v/v)
AIF expression Nuclear FRT (Relative density)
% DMSO (v/v)
D
α-tubulin
Hoechst
AIF
Composite
Co-localization
CTR
1% DMSO
2% DMSO
4% DMSO
8% DMSO
E
F
Bax expression Mitochondrial FTR (Relative density)
% DMSO (v/v)
Bax expression Cytosolic FTR (Relative density)
% DMSO (v/v)

Figure 2.5 - DMSO induces cell death through AIF translocation from mitochondria to the nucleus and Bax translocation to mitochondria. Western blot analysis shows that AIF translocation from the mitochondria (A, B) to the nucleus (A, C) occurs after 24 h, following 2% and 4% DMSO treatment (v/v). Levels of AIF were decreased in mitochondria fractions with increasing DMSO final concentrations (A, B), while increasing AIF in nuclear fractions (A, C). Immunocytochemistry images show immunoreactivity against AIF (Green), α-tubulin (Red), and Hoechst (Blue) at different final concentrations of DMSO after 24 h treatment. Signal intensity profiles show co-localization of AIF and Hoechst at 2, 4 and 8% DMSO (F), confirming concentration-dependent AIF translocation to nucleus. (Scale bar 20 µm.) Similarly, the levels of Bax change: with increasing DMSO final concentrations, levels of Bax increased in mitochondrial fractions (A, E) while decreasing in cytosolic fractions (A, F). VDAC and α-tubulin were used as loading controls for the mitochondrial and cytosolic fractions respectively. Western blot quantification of protein levels in mitochondrial, cytosolic and nuclear fractions (*, $p < 0.05$; **, $p < 0.01$; ***, $p < 0.001$), error bars represent SEM (B-C, D-E).

2.4.6 DMSO causes PARP-1 activation

As AIF translocation has been associated with the activation of PARP-1 (Abeti and Duchen, 2012; van Wijk and Hageman, 2005), we next assessed the levels of PARP-1 expression in whole cell extracts of RGC-5 cells by Western blot, after 24h after treatment with DMSO (0%, 1% 2%, 4%, 8% v/v). The anti-PARP-1 antibody used detects both the full length (116 kDa) and cleaved (activated) form (86 kDa) (Fig 2.6A). We detected cleaved PARP-1 at 2, 4 and 8% v/v DMSO final concentrations and this was found to be statistically significant compared to control, 2% ($p<0.05$), >4% ($p<0.001$) (Fig 2.6B). This suggests that PARP-1 activation is involved in the pathway by which DMSO induces cell death.

To further evaluate the involvement of PARP and calpains on the proposed pathway we used PARP and calpain inhibitors to investigate DMSO-induced cell death with the AlamarBlue cell viability assay. Both the PARP inhibitor (***$p<0.001$; Fig 2.6C) and Calpain inhibitor (*$p<0.05$; Fig 2.6D), induced significant inhibition of DMSO-induced cell death with 1 h pre-treatment and 24 hours treatment of 2% DMSO. These results

strongly suggest the involvement of both PARP-1 and Calpain in DMSO-induced cell death.

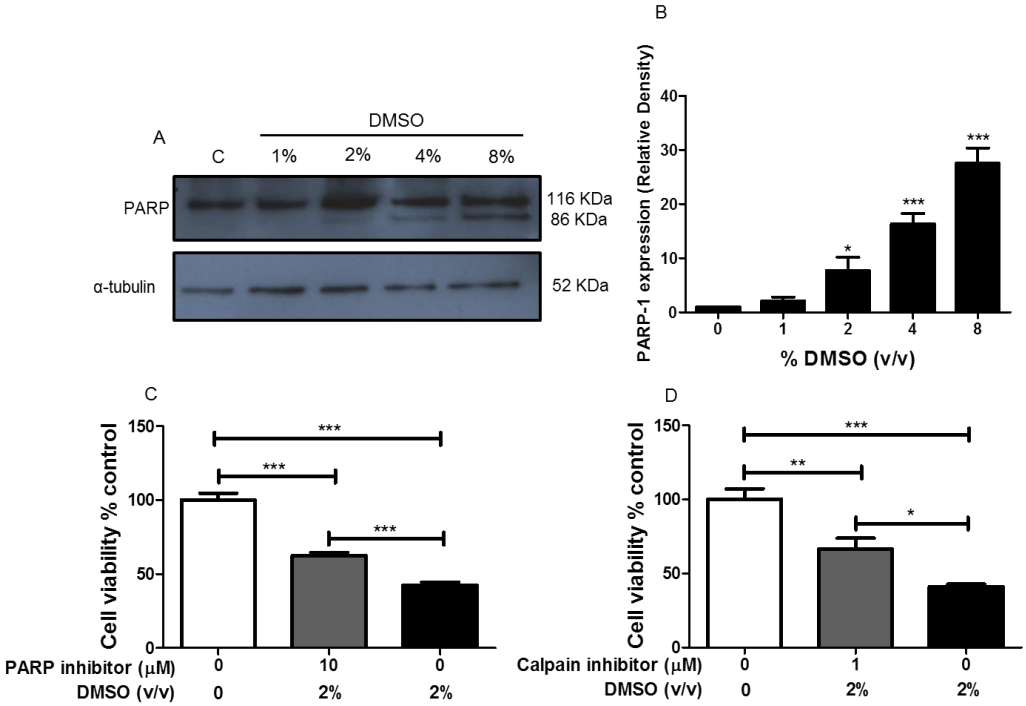

Figure 2.6 - DMSO induces PARP activation. Activation of PARP-1 after 24 h treatment. Western blot analysis shows PARP-1 activation at 2, 4, and 8% of DMSO 24 h treatment. α-tubulin was used as the loading control (Fig 6A). Statistical analysis identified a significant increase in the levels of PARP-1 activation after exposure of RGC-5 cell to 2, 4 and 8% v/v DMSO (Fig 6B). Cell viability assay using AlamarBlue was performed after pre-treatment of cells with PARP (Fig 6C) or Calpain (Fig 6D) inhibitors with 2% DMSO compared to 2% DMSO alone. Statistical analysis shows a significant reduction in cell death with PARP (Fig 6C, $p<0.001$) or calpain (Fig 6D, $p<0.05$) inhibitor treatments, although levels did not return to control ($p<0.001$). * $p< 0.05$; **$p<0.01$; *** $p< 0.001$ compared with controls. Error bars represent SEM.

2.5 Discussion

Our findings have shown that final concentrations of DMSO as low as 0.1% (v/v) are toxic *in vivo* (1%, 2%, 4% and 8% ((v/v) stock; 5 µl injected volume) causing significant retinal apoptosis. This is different to what has been previously reported, and the widely accepted belief that DMSO is well tolerated at concentrations below 10 % (v/v) (Burugula et al., 2011; Konno et al., 2007; Pelzel et al., 2010; Rojas et al., 2008a, 2008b). In previous IVT *in vivo* studies (Aita et al., 2005; Avila et al., 2002a, 2002b; Hill, 1973; Konno et al., 2007; Li and Lo, 2010; Lin et al., 2011; Lüke et al., 2010; Modesitt and Parsons, 2010; Piña et al., 2011; Sankpal et al., 2012; Sun et al., 2012; Teng et al., 2011), the stock concentrations of DMSO administered are reported, although we have also quantified corresponding final vitreous concentration of 0.1, 0.2, 0.4, 0.7, 0.9, 1.4 and 2.3 % (v/v) based on the DA rat vitreous volume of 55µl. DMSO toxicity is also present *in vitro*, as demonstrated using RGC-5 and DMSO (1-8 % (v/v)) with several methods including: fluorescently labelled annexin V, TUNEL, PI, MTT and Hoechst retinal ganglion cell viability assays. The effective concentrations of DMSO required to induce toxicity were greater *in vitro* than *in vivo*. The can be readily explained as it is well documented that cell lines are more resistant to insults than primary cell cultures (Ekwall et al., 1990). High concentrations of DMSO (> 10% (v/v)) have previously been shown to induce toxicity (Aita et al., 2005; Hanslick et al., 2009; Julien et al., 2012) through plasma membrane pore formation (de Ménorval et al., 2012; Notman et al., 2006). In the present study, we describe a new mechanism by which DMSO induces neuronal death at significantly lower concentrations than previous reported. Cell death is induced through AIF translocation to the nucleus and stimulation of a caspase-3 independent pathway of apoptosis, involving PARP activation. Our proposed pathway (Fig 2.7) is initiated by inhibition of mitochondrial respiration with stimulation of intracellular calcium transients. This is followed by phosphatidylserine externalisation on the cell membrane. Next, Bax oligomerization induces mitochondrial permeabilization, which in turn is followed by AIF translocation, PARP activation and finally, cell death.

DMSO is used widely in the eye as a vehicle control (Avila et al., 2002a; Burugula et al., 2011; Huang et al., 2008; Konno et al., 2007; Lüke et al., 2010; Pelzel et al., 2012, 2010;

Piña et al., 2011; Rojas et al., 2008a, 2008b), and there are several studies claiming no adverse effects (Daniels et al., 1990; Li et al., 2000; Perche et al., 2007). It has been used topically (1-50% (v/v)) (Avila et al., 2002a; Hill, 1973), subconjunctivally (80-100% (v/v)) (14), and intravitreally (up to 100% (v/v)) (Burugula et al., 2011; Rojas et al., 2008b), but most often, its absolute concentration is not reported (Burugula et al., 2011; Lüke et al., 2010; Pelzel et al., 2012, 2010; Rojas et al., 2008b). There is some functional, although no structural evidence that retinal toxicity is induced by low concentrations (0.6-8% (v/v)) of DMSO, but this study was based only on electrophysiology data (Tsai et al., 2009).

However, DMSO has been reported to induce apoptosis in vivo elsewhere in the body. After intraperitoneal (IP) application to mice, apoptosis was reported in the developing central nervous system at 10 ml/kg of DMSO (100% (v/v)) (6). Moreover, IP injections of 4 ml/kg of DMSO (10% (v/v)) have been found to induce Tau hyperphosphorylation in the brains of C57/129 mice (Julien et al., 2012). We believe our data suggests that DMSO could be used as a new, inexpensive model for retinal neuron cell death and neurodegeneration in vivo, with the opportunity of providing a rapid assessment of neuroprotective strategies.

In vitro, DMSO is reported to induce apoptosis at concentrations greater than 10 % (v/v), due to plasma membrane pore formation (de Ménorval et al., 2012; Notman et al., 2006). Although rare, there are a few reports of effects of DMSO at low concentrations causing toxicity in cell types other than neurons. In EL-4 lymphoma cells, for example, 2.5% (v/v) DMSO was reported to induce apoptosis through a mitochondrial-mediated, caspase-3 and -9 dependent pathway, associated with down-regulation of Bcl-2, loss of mitochondrial membrane potential and release of cytochrome c from the mitochondria to the cytoplasm (Liu et al., 2001). Elsewhere, exposure of U937 (monocytes) to 1% (v/v) DMSO for 48 h was reported to have no effect on apoptotic signalling proteins (Bcl-2, FADD [Fas-Associated protein with Death Domain], caspase-3 and -8, IAPs [Inhibitor of apoptosis proteins] or cFLIP(L) [Cellular FLICE-inhibitory Protein]). Finally, treatment of U937 cells in this way was found to lead to an increased sensitivity to receptor mediated apoptosis (Vondrácek et al., 2006). In ocular tissues, 48h incubation with 1% (v/v) DMSO to human lens epithelial cells has been reported to decrease cell viability (MTT assay)

and increase cellular apoptosis (TUNEL assay) (Cao et al., 2007). In ARPE 19 (human retinal pigment epithelial cell line), there is a significant increase in caspase-3/7 activity after 24 h treatment with 1 mg/ml and 0.5 mg/ml DMSO (0.11% (v/v) and 0.055% (v/v) respectively) although the same was not observed on r28 (retinal precursor cell line) (Zacharias et al., 2011).

The present study suggests that DMSO induces apoptosis via inhibiting mitochondrial respiration and increasing intracellular calcium. DMSO crosses biological membranes (Yu and Quinn, 1994) and has been reported to induce apoptosis through mitochondrial depolarization as visualised using JC-1 (Liu et al., 2001). The results of the present study suggest a similar process occurs in RGCs, as inhibition of mitochondrial respiration was observed after 1%, 2% and 4% (v/v) DMSO application (Fig 2.3). Mitochondria play a crucial role in many models of cell death, and determine the irreversibility of cell injury (Reed, 2000). However, there are several issues to consider with regard to the effects of DMSO on mitochondrial respiration. Analysis of the fraction of respiration that is ATP-dependent revealed a significant decrease ($p<0.001$) in this parameter at 2 and 4 % DMSO (v/v), suggesting an effect of DMSO on ATP synthase activity. Measurement of maximal mitochondrial respiration was provided by FCCP, which is an uncoupler of the electron transport chain and oxidative phosphorylation. Both 2 and 4% DMSO reduced maximal respiratory capacity in response to uncoupler, providing further evidence of a direct effect of DMSO on the mitochondrial membrane. This observation is in broad agreement with previous observations in intact and permeabilized neurons (Clerc and Polster, 2012). We found that after DMSO application, mitochondrial respiration was decreased while PARP was activated. The association between PARP activation and inhibition of mitochondrial respiration is well documented and inhibition of mitochondria respiration is reported to precede or proceed PARP activation (Andrabi et al., 2008; Sun et al., 2013). PARP activation and NAD+ depletion can cause decreased mitochondrial respiration, and would reduce both basal and maximal respiratory capacity in conjunction with a decrease in NADH. Our results, however, did not show any significant change in NADH, suggesting that changes in mitochondrial respiration induced by DMSO precede PARP activation. Moreover, changes in the lipid content of the mitochondrial membrane are reported to affect mitochondrial respiration, and as

DMSO has been suggested to interfere with lipid structure, this could provide an alternative explanation for the effects observed in the present study. Furthermore, on analysis of complex IV activity, our results indicated that the inhibitory effects observed were not due to complex IV inhibition. As all 3 mitochondrial parameters measured (basal respiration, ATP-dependent and FCCP) decreased in the presence of DMSO, this implies mitochondrial function is directly impaired upon addition of DMSO. An increase in intracellular calcium was observed after DMSO application (Fig 2.7). DMSO induced cytoplasmic calcium influx has previously been reported in isolated Balanus eburneus photoreceptors after application of 5% (v/v) of DMSO, which is in accordance with our results (Brown and Rydqvist, 1990). Calcium cell dysregulation is associated with cell death particularly in muscle and neuronal cells (Osellame et al., 2012). Whilst increased intracellular calcium leads to mitochondrial Ca^{2+} uptake, upregulation of the TCA cycle and increased oxidative phosphorylation (Duchen, 2012; Osellame et al., 2012), Ca^{2+} overload may induce formation of the mitochondrial permeability transition pore (mPTP) and necrosis (Duchen, 2012; Halestrap, 1999). However, our results suggest that DMSO induced cell death is mPTP independent. Furthermore, as shown in Figure 2.5, DMSO induced cell death increased expression of Bax in mitochondrial extracts at final concentrations of 2% and 4%, but not 1% (v/v), up to 24 h after exposure. This observation is in agreement with the existing literature where 1% DMSO treatment for up to 40 h in U937 cells (the human myeloid leukemia cell line) did not show changes in Bax levels (Vondrácek et al., 2006). Likewise, in an *in vivo* model, Dalton's lymphoma mice mRNA levels were assessed and the levels of Bax increased with the concomitant decrease of the Bcl-2/Bax ratio after DMSO treatment (7.5 g/kg i.p.) (Koiri and Trigun, 2011).

Our results show that DMSO induced cell death is caspase-3 independent. This differs from results obtained previously in hepatocytes (Banič et al., 2011) and in vivo in the central nervous system (Hanslick et al., 2009). In this study, results obtained in the brain of mice treated with DMSO show caspase-3 activation in brain slices of different regions of the brain (Hanslick et al., 2009). At first glance, the data presented in this study appear to contradict these findings. However, Hanslick et al postulate that a possible source of the detected caspase-3 activation could be astrocytes or other glia-like cells, as

white matter was predominantly stained. Since caspase-3 activation was not co-localized with a neuronal marker in their study, further work is needed to confirm this hypothesis.

DMSO-induced RGC-5 cell death appeared AIF dependent as DMSO induced a significant degree of AIF translocation from mitochondria to the nucleus 24 h after exposure to 2% or 4% (v/v) DMSO. A number of cytotoxic drugs used to induce cell death, NMDA (N-Methyl-D-aspartic acid), glutamate, MNNG (Methylnitronitrosoguanidine), H2O2 (Hydrogen peroxide), serum withdraw, staurosporine, glucocorticoids, adriamycin, cis-platin, ceramide and etoposide (topoisomerase II inhibitor) have been shown to cause cleavage of AIF and its release from mitochondria, and translocation to the nucleus (Daugas et al., 2000; Delavallée et al., 2011; Lorenzo et al., 1999; Yu et al., 2002). This is however, to our knowledge, the first occasion that AIF release and translocation from the mitochondria to the nucleus following treatment with DMSO has been reported. AIF has been previously linked to the activation of PARP-1 in the pathway to cell death (Daugas et al., 2000; Hong et al., 2004; Lorenzo et al., 1999). Figure 2.5 and 2.6 indicate that a simultaneous increase in PARP-1 activation 24 h after exposure to 2%, 4% and 8% DMSO (v/v) and nuclear AIF after 2% and 4% DMSO (v/v). Increased PARP expression has also been described in vivo, following DMSO treatment in Dalton's lymphoma mice (Koiri and Trigun, 2011).

AIF and PARP-1 activation have been previously implicated in caspase-independent cell death, through a newly proposed pathway of cell death: Parthanatos (Wang et al., 2011, 2009a). Parthanatos is a form of apoptosis associated with rapid activation of PARP-1 with early accumulation of poly(ADP-ribose) (PAR) polymers, mitochondria depolarization, loss of NAD and ATP, late caspase-3 activation (although not necessary for cell death), propidium iodide (PI) cell permeabilization within 18-24 hours of onset and calpain independent AIF activation (Andrabi et al., 2008, 2006; Wang et al., 2009b; Yu et al., 2006, 2002). In this study, we see PARP-1 activation, AIF translocation and mitochondrial respiration inhibition in accordance with what is described for Parthanatos cell death. Despite being a strong candidate, particularly as we do not see caspase-3 activation during the 24 h treatment, we do not believe that we are observing the Parthanatos pathway of cell death in response to low concentrations of DMSO. PI staining is a good indicator of plasma membrane permeabilization, and our results

showed that there was little evidence of this below 8% (24 h) despite the observed cell death (Fig 2.4). In addition, it has been noted that inhibition of PARP-1 dependent cell death by CsA after MNNG treatment affects Parthanatos (van Wijk and Hageman, 2005); our data indicates that CsA does not decrease cell death after DMSO treatment (data not shown). Since there is no evidence for mPTP involvement in response to low concentrations (< 8% v/v) of DMSO, no changes to NADH levels and no PI staining within 24 hours of the DMSO insult, this suggests that low concentrations of DMSO induced a cell death pathway which differs from the Parthanatos pathway (Fig 2.7).

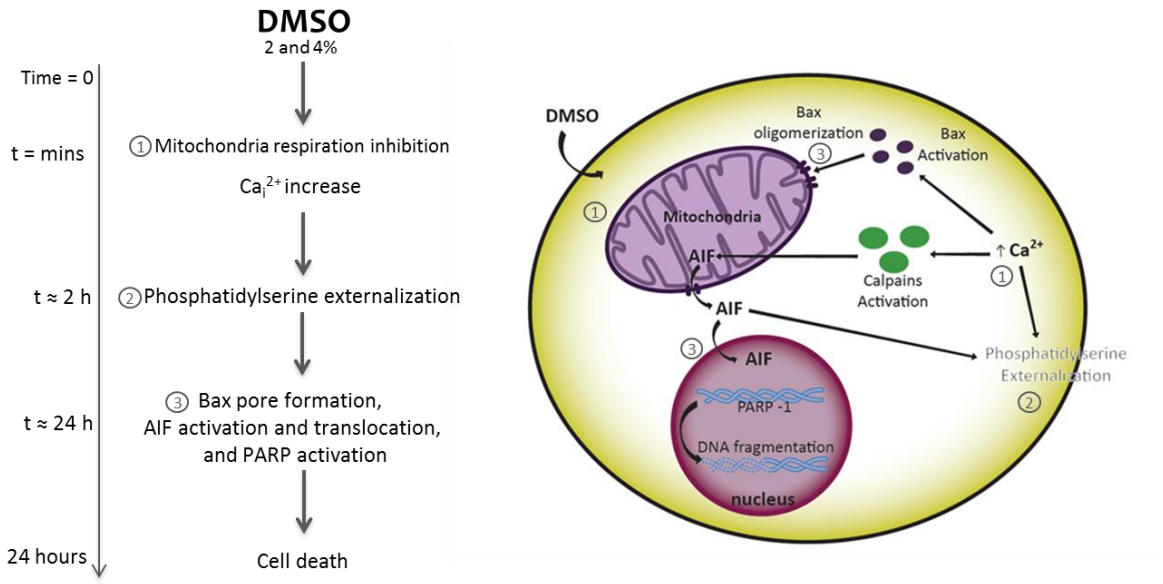

Figure 2.7 - Proposed pathway for the induction of neuronal cell death in the eye by low doses of DMSO. DMSO (2-4% v/v) inhibits mitochondrial respiration, and stimulates intracellular calcium transients. This leads to phosphatidylserine externalisation and the earliest stages of apoptosis. Bax oligomerization induces mitochondrial permeabilization, and AIF activation and translocation. Apoptosis continues through PARP activation resulting in cell death. Timeline shown is based on *in vitro* results.

AIF and Bax have been implicated in the Fas induced cell death pathway (Austin and Fehlings, 2008). Furthermore, Fas levels were reported to be elevated after DMSO treatment in the human myeloid leukemia cell line (Vondrácek et al., 2006). In the eye, Fas mediated cell death has been reported though activation of Fas/FasL to glia (Gregory et al., 2011; Ju et al., 2006) and in vitro RGC-5 apoptosis has been shown to occur in co-culture with activated T-cells (Wax et al., 2009). Neither glial or T-cells were present in our in vitro study, which is therefore unlikely to involve Fas.

We propose that the mechanism by which DMSO induces cell death (Fig 2.7) involves inhibition of mitochondrial respiration leading to decreased oxygen consumption within minutes of application. Moreover, elevation of cytosolic calcium and phosphatidylserine externalization occur. Calcium has been implicated in phosphatidylserine flipping previously (Lee et al., 2013; Mirnikjoo et al., 2009a, 2009b) and is known to induce calpain activation (Norberg et al., 2010; Polster et al., 2005). Calpain acts to induce the

release and redistribution of AIF to the nucleus (Norberg et al., 2010; Polster et al., 2005). This could occur through Bax-translocation from the cytosol to the mitochondria (Er et al., 2006; Vieira and Kroemer, 2003). Increased levels of Bax in mitochondrial fractions and decreased levels in the cytosolic fractions are in accordance with Bax oligomerization and pore formation indicating that AIF translocation from mitochondria is via Bax pore formation (Fig 2.5). AIF has also been implicated in phosphatidylserine externalization through the interaction with scramblase Scrm-1 (Wang et al., 2007). AIF can in addiction translocate to the nucleus and cause DNA fragmentation and activation of PARP-1 (Fig 2.5 and 2.6) leading to cell death (Fig 2.2).

DMSO is a universal solvent routinely used in experimental and biological disciplines, and is widely accepted to be non-toxic at concentrations below 10% (v/v) (Avila et al., 2002a; Burugula et al., 2011; Huang et al., 2008; Konno et al., 2007; Lüke et al., 2010; Pelzel et al., 2010; Piña et al., 2011; Rojas et al., 2008a, 2008b). It is often used to solubilise drug molecules that are otherwise poorly soluble. Our finding that at concentrations below 10% (v/v), DMSO is toxic is unexpected. These results underline safety concerns of using low concentrations of DMSO as a solvent for in vivo administration of numerous molecules, which we show not to be safe. We believe that the scientific community should question the use of DMSO in biological assays, with particular relevance to delivery to neuronal cells. Finally, due to the broad number of drugs dissolved in DMSO, we believe these results have widespread implications, not only in the eye and in neuroscience, but also throughout the whole body.

Given the ubiquitous use of DMSO in biological assays, we would like to highlight to the scientific community the implications of our results. We recommend that other methods (such as micelle/liposomal formulations) are used in preference to DMSO for solubilizing drugs, but where no alternative exists, absolute DMSO concentrations are calculated and reported. We recommend that the percentage of DMSO used to dissolve drugs should be kept to a minimum (injection of less than 1% (v/v) solutions in vivo), and an untreated control group is included in addition to DMSO vehicle control to check for solvent toxicity.

2.6 Acknowledgements

This study was supported by Foundation for Science and Technology, Portugal (FCT fellowship SFRH/BD/47947/2008) and FEDER. We would like to thank Dr. Lisa Turner for proof reading, Dr. Will Kotiadis, Dr. Ronan Astin and Dr. Goncalo Pereira on mitochondrial respiration electrode, Dr. António Francisco Ambrósio and Dr. Ana Raquel Santiago for general advice. Conflict of Interest: M F Cordeiro – Patent application.

2.7 References

Abeti, R., Duchen, M.R., 2012. Activation of PARP by oxidative stress induced by β-amyloid: implications for Alzheimer's disease. Neurochem. Res. 37, 2589–96.

Aita, K., Irie, H., Tanuma, Y., Toida, S., Okuma, Y., Mori, S., Shiga, J., 2005. Apoptosis in murine lymphoid organs following intraperitoneal administration of dimethyl sulfoxide (DMSO). Exp. Mol. Pathol. 79, 265–71.

Andrabi, S. a, Dawson, T.M., Dawson, V.L., 2008. Mitochondrial and nuclear cross talk in cell death: parthanatos. Ann. N. Y. Acad. Sci. 1147, 233–41.

Andrabi, S. a, Kim, N.S., Yu, S.-W., Wang, H., Koh, D.W., Sasaki, M., Klaus, J. a, Otsuka, T., Zhang, Z., Koehler, R.C., Hurn, P.D., Poirier, G.G., Dawson, V.L., Dawson, T.M., 2006. Poly(ADP-ribose) (PAR) polymer is a death signal. Proc. Natl. Acad. Sci. U. S. A. 103, 18308–13.

Austin, J.W., Fehlings, M.G., 2008. Molecular mechanisms of Fas-mediated cell death in oligodendrocytes. J. Neurotrauma 25, 411–26.

Avila, M.Y., Seidler, R.W., Stone, R. a, Civan, M.M., 2002a. Inhibitors of NHE-1 Na+/H+ exchange reduce mouse intraocular pressure. Invest. Ophthalmol. Vis. Sci. 43, 1897–902.

Avila, M.Y., Stone, R. a, Civan, M.M., 2002b. Knockout of A3 adenosine receptors reduces mouse intraocular pressure. Invest. Ophthalmol. Vis. Sci. 43, 3021–6.

Balaiya, S., Ferguson, L.R., Chalam, K. V, 2012. Evaluation of sirtuin role in neuroprotection of retinal ganglion cells in hypoxia. Invest. Ophthalmol. Vis. Sci. 53, 4315–22.

Banič, B., Nipič, D., Suput, D., Milisav, I., 2011. DMSO modulates the pathway of apoptosis triggering. Cell. Mol. Biol. Lett. 16, 328–41.

Brand, M.D., Nicholls, D.G., 2011. Assessing mitochondrial dysfunction in cells. Biochem. J. 435, 297–312.

Brown, H.M., Rydqvist, B., 1990. Dimethyl sulfoxide elevates intracellular Ca 2 + and mimics effects of increased light intensity in a photoreceptor. Pflugers Arch. 415, 395–398.

Burugula, B., Ganesh, B.S., Chintala, S.K., 2011. Curcumin attenuates staurosporine-mediated death of retinal ganglion cells. Invest. Ophthalmol. Vis. Sci. 52, 4263–73.

Cao, X.-G., Li, X.-X., Bao, Y.-Z., Xing, N.-Z., Chen, Y., 2007. Responses of human lens epithelial cells to quercetin and DMSO. Invest. Ophthalmol. Vis. Sci. 48, 3714–8.

Clerc, P., Polster, B.M., 2012. Investigation of mitochondrial dysfunction by sequential microplate-based respiration measurements from intact and permeabilized neurons. PLoS One 7, e34465.

Cordeiro, M.F., Guo, L., Luong, V., Harding, G., Wang, W., Jones, H.E., Moss, S.E., Sillito, A.M., Fitzke, F.W., 2004. Real-time imaging of single nerve cell apoptosis in retinal neurodegeneration. Proc. Natl. Acad. Sci. U. S. A. 101, 13352–6.

Daniels, S.A., Coonley, K.G., Yoshizumi, M.O., 1990. Taxol treatment of experimental proliferative vitreoretinopathy. Graefes Arch. Clin. Exp. Ophthalmol. 228, 513–516.

Daugas, E., Susin, S.A., Zamzami, N., Ferri, K.F., Irinopoulou, T., Larochette, N., Prévost, M.-C., Leber, B., Andrews, D., Penninger, J., Kroemer, G., 2000. Mitochondrio-nuclear translocation of AIF in apoptosis and necrosis. FASEB 14, 729–739.

De Ménorval, M.-A., Mir, L.M., Fernández, M.L., Reigada, R., 2012. Effects of dimethyl sulfoxide in cholesterol-containing lipid membranes: a comparative study of experiments in silico and with cells. PLoS One 7, e41733.

Delavallée, L., Cabon, L., Galán-Malo, P., Lorenzo, H.K., Susin, S. a, 2011. AIF-mediated caspase-independent necroptosis: a new chance for targeted therapeutics. IUBMB Life 63, 221–32.

Duchen, M.R., 2012. Mitochondria, calcium-dependent neuronal death and neurodegenerative disease. Pflugers Arch. 464, 111–21.

Ekwall, B., Silano, V., Zucco, F., 1990. Toxicity Tests with Mammalian Cell Cultures. Short-term Toxic. tests non-genotoxic Eff. 75–98.

Elmore, S., 2007. Apoptosis: a review of programmed cell death. Toxicol. Pathol. 35, 495–516.

Er, E., Oliver, L., Cartron, P.-F., Juin, P., Manon, S., Vallette, F.M., 2006. Mitochondria as the target of the pro-apoptotic protein Bax. Biochim. Biophys. Acta 1757, 1301–11.

Fischer, U.T.E., Schulze-osthoff, K., 2005. New Approaches and Therapeutics Targeting Apoptosis in Disease 57, 187–215.

Gregory, M.S., Hackett, C.G., Abernathy, E.F., Lee, K.S., Saff, R.R., Hohlbaum, A.M., Moody, K.-S.L., Hobson, M.W., Jones, A., Kolovou, P., Karray, S., Giani, A., John, S.W.M., Chen, D.F., Marshak-Rothstein, A., Ksander, B.R., 2011. Opposing roles for membrane bound and soluble Fas ligand in glaucoma-associated retinal ganglion cell death. PLoS One 6, e17659.

Halestrap, a P., 1999. The mitochondrial permeability transition: its molecular mechanism and role in reperfusion injury. Biochem. Soc. Symp. 66, 181–203.

Hanslick, J.L., Lau, K., Noguchi, K.K., Olney, J.W., Zorumski, C.F., Mennerick, S., Farber, N.B., 2009. Dimethyl sulfoxide (DMSO) produces widespread apoptosis in the developing central nervous system. Neurobiol. Dis. 34, 1–10.

Hengartner, M.O., 2000. The biochemistry of apoptosis. Nature 407, 770–6.

Hill, R. V, 1973. Dimethyl Sulfoxide in the treatment of Retinal Disease. Ann. N. Y. Acad. Sci. 485–490.

Hong, S.J., Dawson, T.M., Dawson, V.L., 2004. Nuclear and mitochondrial conversations in cell death: PARP-1 and AIF signaling. Trends Pharmacol. Sci. 25, 259–64.

Huang, Y., Li, Z., Wang, N., van Rooijen, N., Cui, Q., 2008. Roles of PI3K and JAK pathways in viability of retinal ganglion cells after acute elevation of intraocular pressure in rats with different autoimmune backgrounds. BMC Neurosci. 9, 78.

Ju, K.R., Kim, H.S., Kim, J.H., Lee, N.Y., Park, C.K., 2006. Retinal glial cell responses and Fas/FasL activation in rats with chronic ocular hypertension. Brain Res. 1122, 209–21.

Julien, C., Marcouiller, F., Bretteville, A., El Khoury, N.B., Baillargeon, J., Hébert, S.S., Planel, E., 2012. Dimethyl sulfoxide induces both direct and indirect tau hyperphosphorylation. PLoS One 7, e40020.

Koiri, R.K., Trigun, S.K., 2011. Dimethyl sulfoxide activates tumor necrosis factorα-p53 mediated apoptosis and down regulates D-fructose-6-phosphate-2-kinase and lactate dehydrogenase-5 in Dalton's lymphoma in vivo. Leuk. Res. 35, 950–6.

Konno, T., Uchibori, T., Nagai, A., Kogi, K., Nakahata, N., 2007. Effect of 2-(6-cyano-1-hexyn-1-yl)adenosine on ocular blood flow in rabbits. Life Sci. 80, 1115–22.

Krishnamoorthy, R.R., Agarwal, P., Prasanna, G., Vopat, K., Lambert, W., Sheedlo, H.J., Pang, I.H., Shade, D., Wordinger, R.J., Yorio, T., Clark, a F., Agarwal, N., 2001. Characterization of a transformed rat retinal ganglion cell line. Brain Res. Mol. Brain Res. 86, 1–12.

Kumi-Diaka, J., Butler, A., 2000. Caspase-3 protease activation during the process of genistein-induced apoptosis in TM4 testicular cells. Biol. Cell 92, 115–24.

Lee, Meng, X.W., Flatten, K.S., Loegering, D. a, Kaufmann, S.H., 2013. Phosphatidylserine exposure during apoptosis reflects bidirectional trafficking between plasma membrane and cytoplasm. Cell Death Differ. 20, 64–76.

Li, B., Yang, C., Rosenbaum, D.M., Roth, S., 2000. Signal transduction mechanisms involved in ischemic preconditioning in the rat retina in vivo. Exp. Eye Res. 70, 755–65.

Li, Lo, A.C.Y., 2010. Lutein Protects RGC-5 Cells Against Hypoxia and Oxidative Stress. Int. J. Mol. Sci. 11, 2109–17.

Lin, Yang, J., Lin, J., Lai, K., Lu, H., 2011. Rutin Inhibits Human Leukemia Tumor Growth in a Murine Xenograft Model In Vivo 1–5.

Liu, B., Sun, X., Suyeoka, G., Garcia, J.G.N., Leiderman, Y.I., 2013. TGFβ signaling induces expression of Gadd45b in retinal ganglion cells. Invest. Ophthalmol. Vis. Sci. 54, 1061–9.

Liu, Yoshikawa, H., Nakajima, Y., Tasaka, K., 2001. Involvement of mitochondrial permeability transition and caspase-9 activation in dimethyl sulfoxide-induced apoptosis of EL-4 lymphoma cells. Int. Immunopharmacol. 1, 63–74.

Lorenzo, Susin, S. a, Penninger, J., Kroemer, G., 1999. Apoptosis inducing factor (AIF): a phylogenetically old, caspase-independent effector of cell death. Cell Death Differ. 6, 516–24.

Lüke, Nassar, K., Lüke, M., Tura, A., Merz, H., Giannis, A., Grisanti, S., 2010. The effect of adjuvant dimethylenastron, a mitotic Kinesin Eg5 inhibitor, in experimental glaucoma filtration surgery. Curr. Eye Res. 35, 1090–8.

Mirnikjoo, B., Balasubramanian, K., Schroit, A.J., 2009a. Mobilization of lysosomal calcium regulates the externalization of phosphatidylserine during apoptosis. J. Biol. Chem. 284, 6918–23.

Mirnikjoo, B., Balasubramanian, K., Schroit, A.J., 2009b. Suicidal membrane repair regulates phosphatidylserine externalization during apoptosis. J. Biol. Chem. 284, 22512–6.

Modesitt, S.C., Parsons, S.J., 2010. In vitro and in vivo histone deacetylase inhibitor therapy with vorinostat and paclitaxel in ovarian cancer models: does timing matter? Gynecol. Oncol. 119, 351–7.

Nadal-Nicolás, F.M., Jiménez-López, M., Sobrado-Calvo, P., Nieto-López, L., Cánovas-Martínez, I., Salinas-Navarro, M., Vidal-Sanz, M., Agudo, M., 2009. Brn3a as a marker of retinal ganglion cells: qualitative and quantitative time course studies in naive and optic nerve-injured retinas. Invest. Ophthalmol. Vis. Sci. 50, 3860–8.

Norberg, E., Orrenius, S., Zhivotovsky, B., 2010. Mitochondrial regulation of cell death: processing of apoptosis-inducing factor (AIF). Biochem. Biophys. Res. Commun. 396, 95–100.

Notman, R., Noro, M., O'Malley, B., Anwar, J., 2006. Molecular basis for dimethylsulfoxide (DMSO) action on lipid membranes. J. Am. Chem. Soc. 128, 13982–3.

Osellame, L.D., Blacker, T.S., Duchen, M.R., 2012. Cellular and molecular mechanisms of mitochondrial function. Best Pract. Res. Clin. Endocrinol. Metab. 26, 711–23.

Pelzel, H.R., Schlamp, C.L., Nickells, R.W., 2010. Histone H4 deacetylation plays a critical role in early gene silencing during neuronal apoptosis. BMC Neurosci. 11, 62.

Pelzel, H.R., Schlamp, C.L., Waclawski, M., Shaw, M.K., Nickells, R.W., 2012. Silencing of Fem1cR3 gene expression in the DBA/2J mouse precedes retinal ganglion cell death and is associated with histone deacetylase activity. Invest. Ophthalmol. Vis. Sci. 53, 1428–35.

Perche, O., Doly, M., Ranchon-Cole, I., 2007. Caspase-dependent apoptosis in light-induced retinal degeneration. Invest. Ophthalmol. Vis. Sci. 48, 2753–9.

Piña, Y., Decatur, C., Murray, T., Houston, S., Gologorsky, D., Cavalcante, M., Cavalcante, L., Hernandez, E., Celdran, M., Feuer, W., Lampidis, T., 2011. Advanced retinoblastoma treatment: targeting hypoxia by inhibition of the mammalian target of rapamycin (mTOR) in LH(BETA)T(AG) retinal tumors. Clin. Ophthalmol. 5, 337–43.

Polster, B.M., Basañez, G., Etxebarria, A., Hardwick, J.M., Nicholls, D.G., 2005. Calpain I induces cleavage and release of apoptosis-inducing factor from isolated mitochondria. J. Biol. Chem. 280, 6447–54.

Qi, W., Ding, D., Salvi, R.J., 2008. Cytotoxic effects of dimethyl sulphoxide (DMSO) on cochlear organotypic cultures. Hear. Res. 236, 52–60.

Reed, J.C., 2000. Mechanisms of apoptosis. Am. J. Pathol. 157, 1415–30.

Rojas, J.C., Lee, J., John, J.M., Gonzalez-Lima, F., 2008a. Neuroprotective effects of near-infrared light in an in vivo model of mitochondrial optic neuropathy. J. Neurosci. 28, 13511–21.

Rojas, J.C., Saavedra, J. a, Gonzalez-Lima, F., 2008b. Neuroprotective effects of memantine in a mouse model of retinal degeneration induced by rotenone. Brain Res. 1215, 208–17.

Sankpal, U.T., Abdelrahim, M., Connelly, S.F., Lee, C.M., Madero-Visbal, R., Colon, J., Smith, J., Safe, S., Maliakal, P., Basha, R., 2012. Small molecule tolfenamic acid inhibits PC-3 cell proliferation and invasion in vitro, and tumor growth in orthotopic mouse model for prostate cancer. Prostate.

Santiago, A.R., Cristóvão, A.J., Santos, P.F., Carvalho, C.M., Ambrósio, A.F., 2007. High glucose induces caspase-independent cell death in retinal neural cells. Neurobiol. Dis. 25, 464–72.

Sun, C., Guo, X.-X., Zhu, D., Xiao, C., Bai, X., Li, Y., Zhan, Z., Li, X.-L., Song, Z.-G., Jin, Y.-H., 2013. Apoptosis is Induced in Cancer Cells via the Mitochondrial Pathway by the Novel Xylocydine-Derived Compound JRS-15. Int. J. Mol. Sci. 14, 850–70.

Sun, H.H., Saheb-Al-Zamani, M., Yan, Y., Hunter, D. a, Mackinnon, S.E., Johnson, P.J., 2012. Geldanamycin Accelerated Peripheral Nerve Regeneration in Comparison to FK-506 In Vivo. Neuroscience 223, 114–123.

Szmant, H.H., 1975. Physical properties of dimethyl sulfoxide and its function in biological systems. Ann. N. Y. Acad. Sci. 243, 20–3.

Teng, B.T., Tam, E.W., Benzie, I.F., Siu, P.M., 2011. Protective effect of caspase inhibition on compression-induced muscle damage. J. Physiol. 589, 3349–69.

Tsai, T.I., Bui, B. V, Vingrys, A.J., 2009. Dimethyl sulphoxide dose-response on rat retinal function. Doc. Ophthalmol. 119, 199–207.

Van Bergen, N.J., Wood, J.P.M., Chidlow, G., Trounce, I. a, Casson, R.J., Ju, W.-K., Weinreb, R.N., Crowston, J.G., 2009. Recharacterization of the RGC-5 retinal ganglion cell line. Invest. Ophthalmol. Vis. Sci. 50, 4267–72.

Van Wijk, S.J.L., Hageman, G.J., 2005. Poly(ADP-ribose) polymerase-1 mediated caspase-independent cell death after ischemia/reperfusion. Free Radic. Biol. Med. 39, 81–90.

Vieira, H., Kroemer, G., 2003. Mitochondria as targets of apoptosis regulation by nitric oxide. IUBMB Life 55, 613–6.

Vondrácek, J., Soucek, K., Sheard, M. a, Chramostová, K., Andrysík, Z., Hofmanová, J., Kozubík, A., 2006. Dimethyl sulfoxide potentiates death receptor-mediated apoptosis in the human myeloid leukemia U937 cell line through enhancement of mitochondrial membrane depolarization. Leuk. Res. 30, 81–9.

Wang, Dawson, V.L., Dawson, T.M., 2009a. Poly(ADP-ribose) signals to mitochondrial AIF: a key event in parthanatos. Exp. Neurol. 218, 193–202.

Wang, Kim, N.S., Haince, J.-F., Kang, H.C., David, K.K., Andrabi, S. a, Poirier, G.G., Dawson, V.L., Dawson, T.M., 2011. Poly(ADP-ribose) (PAR) binding to apoptosis-inducing factor is critical for PAR polymerase-1-dependent cell death (parthanatos). Sci. Signal. 4, ra20.

Wang, Kim, N.S., Li, X., Greer, P. a, Koehler, R.C., Dawson, V.L., Dawson, T.M., 2009b. Calpain activation is not required for AIF translocation in PARP-1-dependent cell death (parthanatos). J. Neurochem. 110, 687–96.

Wang, Wang, J., Gengyo-Ando, K., Gu, L., Sun, C.-L., Yang, C., Shi, Yong, Kobayashi, T., Shi, Yigong, Mitani, S., Xie, X.-S., Xue, D., 2007. C. elegans mitochondrial factor WAH-1 promotes phosphatidylserine externalization in apoptotic cells through phospholipid scramblase SCRM-1. Nat. Cell Biol. 9, 541–9.

Wax, M.B., Tezel, G., Yang, J., Peng, G., Patil, R. V, Agarwal, N., Sappington, R.M., Calkins, D.J., 2009. Induced autoimmunity to heat shock proteins elicits glaucomatous loss

of retinal ganglion cell neurons via activated T cell-derived Fas-ligand. J. Neurosci. 28, 12085–12096.

Yu, Andrabi, S. a, Wang, H., Kim, N.S., Poirier, G.G., Dawson, T.M., Dawson, V.L., 2006. Apoptosis-inducing factor mediates poly(ADP-ribose) (PAR) polymer-induced cell death. Proc. Natl. Acad. Sci. U. S. A. 103, 18314–9.

Yu, Quinn, P.J., 1994. Dimethyl sulphoxide: a review of its applications in cell biology. Biosci. Rep. 14, 259–81.

Yu, Wang, H., Poitras, M.F., Coombs, C., Bowers, W.J., Federoff, H.J., Poirier, G.G., Dawson, T.M., Dawson, V.L., 2002. Mediation of poly(ADP-ribose) polymerase-1-dependent cell death by apoptosis-inducing factor. Science 297, 259–63.

Zacharias, L.C., Estrago-franco, M.F., Ramirez, C., Kenney, M.C., 2011. The Effects of Commercially Available Preservative-Free. J. Ocul. Pharmacol. Ther. 27.

3. CHAPTER THREE: Activation of adenosine A3 receptor is neuroprotective against the degeneration of retinal ganglion cells

Table of Contents

3.1 Abstract

Glaucoma is a degenerative optic neuropathy, characterized by atrophy of the optic nerve and loss of retinal ganglion cells (RGCs). To prevent vision loss novel strategies to save RGCs are needed besides lowering increased intraocular pressure (IOP), the major risk factor for glaucoma. Adenosine is a neuromodulator in the central nervous system (CNS). The modulation of adenosine receptors (AR) has been shown to be protective against a broad spectrum of brain insults and ischemic insult in the retina. The potential neuroprotective effect of A3R activation was evaluated in vitro, in retinal neural mixed culture and retinal organotypic cultures using TUNEL and propidium iodide (PI) assays. Moreover, neuroprotective effects were also assessed after intravitreal injection 2-Cl-IB-MECA (5 µM) in two different animal models, DMSO-induced RGC death and ischemia-reperfusion (I-R) injury. Cell death was quantified with *in vivo* imaging using Detection of Apoptosing Retinal Cells (DARC) and by TUNEL assay. The survival of RGCs was assessed by quantification of Brn3a-positive cells.

The A3R agonist, 2-Cl-IB-MECA, decreased the number of TUNEL- and PI-positive cells *in vitro* in retinal mixed cultures and retinal organotypic cultures. *In vivo* imaging showed a decrease in the number of fluorescently labelled annexin V-positive cells after DMSO-induced cell death when 2-Cl-IB-MECA was injected into the vitreous. Furthermore, treatment with A3R agonist decreased the number of TUNEL-positive cells in DMSO and I-R models and inhibited the decrease in the number of Brn3a-positive cells induced by I-R injury.

Our results demonstrate that A3R activation is neuroprotective to RGCs, both *in vitro* and in animal models of RGC degeneration. These results suggest that targeting A3R in RGCs may have great potential in the management of glaucoma.

3.2 Introduction

Glaucoma is a progressive, non-curable disease and a leading cause of irreversible blindness worldwide (Quigley and Broman, 2006). By 2020, 80 million people are predicted to be affected by glaucoma and of those 11.1 million are expected to be bilaterally blind (Quigley and Broman, 2006). The prevalence of glaucoma increases with age, representing by 2010, 2.65% of the global population above 40 years old (Varma et al., 2011). Although the primary causes and the mechanism of the pathogenesis of glaucoma are still unclear, elevated intraocular pressure (IOP) is an important risk factor, namely for optic nerve head damage and retinal ganglion cell (RGC) death (Quigley, 2011; Weber and Harman, 2008). A number of mechanisms have been proposed and include, excitotoxicity, ischemia, reactive oxygen species, withdrawal of trophic factors and axonal transport damage (Chang and Goldberg, 2012; Coxon et al., 2010). Excitotoxicity is reported to occur in glaucoma, with glutamate levels reported to be increased in the vitreous of patients with this disease (Dreyer et al., 1996). Ischemic vascular insufficiency has also been proposed to be involved in glaucoma. Increased IOP results in a decreased blood supply and episodic ischemia of retinal neurons leading to RGC death and axon loss (Flammer et al., 1999; Gherghel et al., 2004). This is associated with ischemic reperfusion due to compromised vascular circulation at the level of the optic nerve head (ONH) (Osborne et al., 2004). Lowering of IOP has been demonstrated to attenuate RGC death (Heijl et al., 2002; Leske et al., 2003) and is still to date the only pharmacological treatment available. However, it is known that lowering IOP does not always stop disease progression (Baltmr et al., 2010; Chang and Goldberg, 2012). Therefore, new and more effective treatments are necessary, and neuroprotection of RGCs is considered to offer potential as an additional therapy.

Adenosine, a purine nucleoside, is a neuromodulator in CNS. It acts through the activation of inhibitory (A1 and A3) and facilitatory (A2A and A2B) receptors. Adenosine has been claimed one of the most promising neuroprotective agents in CNS (Cunha, 2005). The modulation of adenosine receptors (ARs) has been shown to be protective against a broad spectrum of brain insults. Pharmacological modulation of ARs is

currently in clinical trials for a diverse number of CNS diseases, such as Parkinson's and Huntington's diseases (Gessi et al., 2011).

A3R was the last adenosine receptor to be discovered and cloned (Zhou et al., 1992), it is a G protein-coupled to Gi/Gq being involved in a variety of different intracellular signalling pathways. Activation of A3R is reported to inhibit adenylyl cyclase activity through Gi proteins. While in the rat brain, stimulation of A3R through Gq proteins was reported to activate phospholipase C (PLC). Reports in the brain show that chronic activation of A3R by CF-101 (IB-MECA) has significant protective effects after an ischemic insult. Moreover, knock-out mice for A3R have increased neurodegeneration in the brain in response to hypoxia (Fedorova et al., 2011). In the retina of several species, the highest adenosine immunoreactivity occurs in RGCL and throughout the inner plexiform layer (IPL), where RGC make synapses with bipolar and amacrine cells (Blazynski, 1990; Ghiardi et al., 1999; Kvanta et al., 1997). A3R mRNA has been identified in RGCs, and functionally confirmed in immunopurified isolated RGCs using the selective agonist 2-Cl-IB-MECA (Zhang et al., 2006a). Previous reports demonstrated that A3R activation attenuates calcium rise in RGCs after glutamate, NMDA, or P2X activation (Zhang et al., 2010, 2006b). The aim of the present work was to evaluate the protective effects of an A3R agonist, 2-Cl-IB-MECA in the retina, using *in vitro* models and animal models of retinal degeneration. To the best of our knowledge, this is the first report showing the protective effects of the activation of A3R in a vast number of models of retinal degeneration both *in vitro* and *in vivo*.

3.3 Materials and Methods

3.3.1 Animals

Adult male Wistar (250-300 g, Charles River, France) or Dark Agouti (250-300 g, Harlan Laboratories, UK) rats were housed in a temperature- and humidity-controlled environment and were provided with standard rodent diet and water *ad libitum* while kept on a 12-h light/12-h dark cycle. All procedures involving the animals were in agreement to the ARVO Statement for the Use of Animals in Ophthalmic and Vision Research.

3.3.2 Primary rat retinal neural cell cultures

Retinal neural cell culture was prepared as previously described (Santiago et al., 2007). Briefly, 3 to 5 days old Wistar rat pups were decapitated, and the retinas were dissected, in Ca^{2+} and Mg^{2+} free Hank's balanced salt solution (HBSS; in mM: 137 NaCl, 5.4 KCl, 0.45 KH_2PO_4, 0.34 Na_2HPO_3, 5 glucose; pH 7.4). Retinas were digested with 0.05% trypsin (w/v) for 15 min at 37 °C. The dissociated cells were pelleted by centrifugation and resuspended in Eagle's minimum essential medium (MEM) supplemented with 26 mM $NaHCO_3$, 25 mM HEPES, 10% heat-inactivated fetal bovine serum, penicillin (100 U/ml) and streptomycin (100 µg/ml). Cells were plated at a density of 2.0 x 10^6 cells/cm^2 on glass coverslips coated with poly-D-lysine (0.1 mg/ml). The cells were maintained at 37 °C in a humidified atmosphere of 5% CO_2.

After 6 days in culture, cells were incubated with 1 µM 2-Cl-IB-MECA (A3R agonist), 1 µM MRS 1191 (A3R antagonist), or both, 30 min before incubation with kainic acid (KA) and cyclothiazide (CTZ) to prevent AMPA receptor desensitization, for 24 h.

3.3.3 Cultures of rat retinal ganglion cells

RGCs were purified from the retinas of 3-4 days old Wistar rat pups by sequential immunopanning, as previously described (Barres et al., 1988a), with some modifications as follows. Dissected retinas were incubated for 30 min at 37 °C in Earl's Balanced Salt Solution (EBSS) containing papain (16.5 U/ml; Worthington Biochemical, USA), 1.65 mM L-cysteine, and 124 U/ml deoxyribonuclease I (DNase I). The resulting cell suspension

was mechanically triturated in ovomucoid (1.5 mg/ml), bovine albumin serum (BSA; 1.5 mg/ml) and DNase I (124 U/ml) in EBSS. The cell suspension was further triturated in a solution containing ovomucoid (1.5 mg/ml), BSA (1.5 mg/ml), DNase I (124 U/ml) and a rabbit anti-rat macrophage antiserum (Accurate Chemical, USA), and incubated for 10 min. Cells were pelleted by centrifugation, and resuspended in EBSS containing ovomucoid (5 mg/ml) and BSA (10 mg/ml) and then centrifuged again. The pelleted cells were resuspended in Dulbecco's Phosphate Buffered Saline (DPBS) with BSA (0.2 mg/ml) and insulin (5 μg/ml), followed by incubation on the panning plates, as described previously (Barres et al., 1988b). Briefly, cells were incubated in 150 mm dishes coated with affinity-purified goat anti-rabbit IgG (H+L) antibody (5.3 μg/ml; Rockland Immunochemicals, USA). Non-adherent cells were removed to a 100 mm dish coated with affinity-purified goat anti-mouse IgM antibody (6.7 μg/ml; Rockland Immunochemicals, USA) and mouse anti-rat Thy1.1 antibody (T11D7e; ATCC, USA). After 30 min, the non-adherent cells were washed with Ca^{2+}- and Mg^{2+}-free DPBS, and the adherent RGCs were detached with a 0.125% trypsin solution in EBSS. Trypsinization was stopped with FBS (30%) in Neurobasal-A (Gibco, USA), and the cell suspension was centrifuged to obtain a cell pellet.

RGCs were plated at a density of 30,000 cells/cm^2 on 10-mm glass coverslips coated with poly-D-lysine (10 μg/ml) and laminin (10 μg/ml), and cultured in Neurobasal-A media containing B27 supplement (1x), insulin (5 μg/ml), sodium pyruvate (1 mM), Sato/Bottenstein supplement (1x), triiodothyronine (40 ng/ml), L-glutamine (2 mM), N-acetylcysteine (5 mg/ml), inosine (100 μM), ciliary neurotrophic factor (20 ng/ml), brain-derived neurotrophic factor (25 ng/ml), forskolin (5 μM), basic fibroblast growth factor (10 ng/ml) and gentamicin (50 μg/ml). Cells were cultured for 16 h at 37 °C in a humidified environment of 5% CO_2.

3.3.4 Retinal organotypic culture

Retinas of 8-9 weeks old male Wistar rats were dissected in ice cold HBSS (pH 7.2) and flat-mounted onto 30 mm diameter culture plate inserts with a 0.4 μm pore size (Millicell, Millipore, USA), with the retinal ganglion cell layer facing upward. The retinal organotypic tissue was cultured in six-well plates containing Neurobasal-A media

supplemented with B27 (1x), L-glutamine (2 mM) and gentamicin (50 µg/ml), and maintained for 4 days *in vitro* (DIV) in a humidified incubator at 37 °C and 5% CO_2.

When present, 2-Cl-IB-MECA (1 µM) was added at day 1 (DIV1) and again 1 h before the incubation with 300 µM N-Methyl-D-aspartic acid (NMDA; Sigma-Aldrich, USA) at day 2 (DIV2). MRS1191 (1 µM; Tocris Bioscience, UK) was added 30 min before the treatment with A3R agonist.

3.3.5 RGC death triggered by DMSO injection into the vitreous

Dark Agouti rats were anesthetized with an intraperitoneal injection of ketamine (37.5%)/medetomidine (25% Dormitor; Pfizer Animal Health, USA) at 0.2ml/100g as previously described (Cordeiro et al., 2004). Animal eyes were randomly divided into 4 experimental groups: 8% DMSO (v/v), control, DMSO+2-Cl-IB-MECA, and 2-Cl-IB-MECA. A solution containing DMSO (8% v/v), or PBS (vehicle, control), and fluorescently labeled annexin V was injected in the vitreous using a 34-G needle attached to a 5-µl Hamilton syringe (Hamilton, USA), in a total volume of 5 µl. The A3R agonist, 2-Cl-IB-MECA (1.2 µM, 5µl injected), or PBS was injected intravitreally 30 min before DMSO injection. All agents were injected into the vitreous under microscopic visualization, and the needle was inserted through the sclera superiorly, 1 mm behind the limbus, at an angle of 45° (Cordeiro et al., 2004). Caution was taken to avoid contact with the lens.

3.3.6 Retinal ischemia-reperfusion

Wistar rats were anesthetized by isoflurane inhalation using a gas anesthetizing system (VetEquip, USA). Then, oxybuprocaine (4 mg/ml; Laboratórios Edol, Portugal) anaesthetic was applied topically to the eyes and the pupils were dilated with tropicamide (10 mg/ml; Laboratórios Edol, Portugal).

Both eyes were injected intravitreally with 5 µl 2-Cl-IB-MECA (1.2 µM) or with 5 µl sterile saline solution (vehicle, 0.9% sodium chloride; Fresenius Kabi, Portugal) 2 h before ischemia. The anterior chamber of the left eye was cannulated with a 30-gauge needle connected to a reservoir infusing a sterile saline solution. Retinal ischemia was induced by retinal blood flow blockade due to an increase in IOP to approximately 90 mmHg

(TonoLab, Icare, Finland) for 60 min. The contralateral eye served as the non-ischemic control. The observed whitening of the iris and the loss of the red reflex confirmed retinal ischemia. The needle was withdrawn after 60 min, and reperfusion was confirmed by the re-appearance of the red reflex. Fusidic acid (10 mg/g; Leo Pharmaceutical, Denmark) treatment was applied in the conjunctival sac at the end of the experiment. The animals were allowed to recover for 24 h before sacrifice.

3.3.7 *In Vivo* Imaging of RGC apoptosis

Dark Agouti rats were imaged using a Heidelberg Retinal Angiograph (HRA) spectralis (Heidelberg Engineering, Germany) 2 h after intravitreal injection of fluorescently labeled annexin V, as previously described (Cordeiro et al., 2004). To optimize visualization, eyes drop lubricant viscotears® Liquid Gel (Novartis, UK) was regularly used. Pupils were dilated with 2.5% phenylephrine hydrochloride and 1.0% cyclopentolate hydrochloride (Bausch & Lomb, France). During image acquisition, HRA spectralis was focused on the retinal nerve fiber layer, as identified in the reflectance mode. The images were collected and the number of spots was counted using MatLab (MathWorks, USA).

3.3.8 Histological preparation

Preparation of paraffin sections

The eyes of Dark Agouty rats were enucleated immediately after sacrifice and then fixed in 4% (w/v) paraformaldehyde (PFA) and kept at 4 °C until further processing. The eyes in 4% PFA were dissected in phosphate buffered saline (PBS) and the cornea, lens and vitreous were gently removed. The eyecups were then transferred to a paraffin-embedding machine (Leica TP1020, Leica Microsystems GmbH, Germany) where they were submitted to overnight cycles of ethanol (70%, 90% and 100%), xylene and finally paraffin. The paraffin blocks were then cut using a microtome (Leica Microsystems GmbH, Germany) into 7 µm thickness sections.

Frozen retinal sections

Wistar rats, under deep anesthesia (75 mg/kg ketamine and 10 mg/kg xylazine), were transcardially perfused with PBS (pH 7.4), followed by 4% (w/v) PFA in PBS. The eyes

were enucleated, washed in PBS and then transferred to PFA for 1 h. The cornea, lens and pupil were removed and the eyecup was further fixed for 1 h in 4% PFA. After washing in PBS, the eyes were cryopreserved by placing the eye cup in 15% (w/v) sucrose in PBS for 1 h and then in 30% (w/v) sucrose in PBS overnight at 4°C. Finally, the eyecup was embedded in tissue-freezing medium (OCT; Shandon, USA), the frozen blocks were cut in a cryostat into 10 µm thickness sections and the cryosections were then collected on SuperFrost Plus glass slides (Menzel-Glaser, Germany) and stored at -20 °C.

3.3.9 Immunofluorescence labelling

Cultured RGCs

RGCs were fixed in 4% PFA, washed with PBS and permeabilized in 1% Triton X-100 for 5 min at room temperature (RT). Cells were incubated in a 3% BSA and 0.2% Tween 20 blocking solution for 1 h at RT to prevent unspecific binding. After washing, cells were incubated with primary antibodies (Table 1) in blocking solution for 90 min at RT. After washing, they were incubated with the corresponding secondary antibody in blocking solution for 1h at RT (Table 1). The nuclei were stained with DAPI (Life Technologies, USA) diluted 1:2000. The coverslips were mounted on glass slides using Glycergel mounting medium (Dako, Denmark) and visualized in a laser scanning confocal microscope (Zeiss LSM 710, Germany).

Antibody	Sample	Dilution used	Supplier	Species
Anti-Brn3a	Cultured RGCs	1:25	Millipore, USA	Mouse
	Cultured Retinal Explants	1:500		
	Frozen/Paraffin Retinal Sections	1:200		
Anti-A3R	Cultured RGCs	1:200	Sigma Aldrich, USA	Rabbit
	Cultured Retinal Explants	1:200		
	Frozen/Paraffin Retinal Sections	1:200		
Alexa Fluor® 568 anti-mouse IgG	Cultured RGCs	1:200	Life Technologies, USA	Goat
	Cultured Retinal Explants			
	Frozen Retinal Sections			
Alexa Fluor® 488 anti-rabbit IgG	Cultured RGCs Cultured Retinal Explants	1:200	Life Technologies, USA	Goat
	Frozen/Paraffin Retinal Sections			

Table 3.1 - List of antibodies used in immunofluorescence labeling

Retinal organotypic Cultured

Organotypic retinal cultures were fixed in ice-cold absolute ethanol at 4 °C. After washing with PBS, the tissue was incubated in a blocking solution containing 3% BSA, 10% normal goat serum (NGS) and 0.1% Triton X-100 for 1 h at RT. Organotypic retinal tissue was then kept for 2 days at 4°C with primary antibodies (Table 1) in blocking solution, and then they were incubated overnight at 4°C with the corresponding secondary antibody in blocking solution (Table 1). The nuclei were stained with DAPI (1:1000). The organotypic retinal cultures were flat-mounted on slides and coverslipped using Glycergel mounting medium (Dako, Denmark) and visualized in a laser scanning confocal microscope (Zeiss LSM 710, Germany).

Frozen Retinal Sections

Retinal sections were placed overnight at RT. After fixing with ice-cold acetone for 10 min at -20°C, the sections were hydrated in PBS until OCT was removed. Sections were permeabilized in 0.25% Triton X-100 for 30 min at RT, and blocked in 1% BSA and 10% NGS solution for 30 min in a humidified atmosphere at RT. Sections were then incubated overnight at 4°C in a humidified atmosphere with primary antibodies (Table 1) in 1% BSA solution. After washing, sections were incubated with the corresponding secondary antibody in 1% BSA solution for 1 h at RT (Table 1). The nuclei were stained with DAPI (1:2000). The sections were mounted using Glycergel mounting medium (Dako, Denmark) and visualized in a laser scanning confocal microscope (Zeiss LSM 710, Germany).

Paraffin Retinal Sections

Paraffin sections were placed on the heat pad to allow paraffin to melt. In order to allow deparaffinization and rehydration of the sections, sequential 5 min incubations of xylene (3x) and descending ethanol series (100%, 90% and 70%) were performed. To allow antigen unmasking, sections were incubated in citric buffer for 5 min in a microwave (600 watts). The slices where then washed in water for 5 min and in Tris-Buffered Saline (TBS) containing 0.1% Tween-20 (TBST; 137 mM sodium chloride, 20 mM Tris, 0.1% Tween-20, pH 7.6) for 5 min. To block any unspecific binding the slices were incubated for 1 h at RT in a humidified chamber in 5% NGS prepared in TBST containing 0.5% BSA

and 0.1% NaN3. Sections were incubated with the primary antibody (Table 1) overnight in a humidity chamber at 4 °C. The slices were washed for 5 min in TBST, and then incubated with the secondary antibody (Table 1) for 1 h at RT. Nuclei were stained with DAPI (1:2500). The slices were then washed and mounted in PBS/glycerol. Fluorescence images were acquired using confocal microscope (Leica SP2, Leica Microsystems GmbH, Germany).

3.3.10 Propidium iodide uptake assay

Retinal organotypic cultures were incubated with propidium iodide (PI; 2 µM) at 48 h (DIV 2) and 96 h (DIV 4) to assess RGC death. Representative images in the four retinal quadrants of each retina were acquired in a fluorescence microscope (Leica DM IRE2, Germany) using the 10x objective. PI-positive cells per retinal quadrant were counted at DIV2 (before incubation with NMDA) and at DIV4. The extent of cell death was expressed as the ratio between PI-positive cells at DIV4 and DIV2.

3.3.11 TdT-mediated dUTP nick-end labeling assay

Rat retinal neuronal culture

Rat retinal neuronal cells were fixed in 4% PFA at 4°C. After washing with PBS, the cells were incubated in a blocking solution containing 3% BSA and 0.1% Triton X-100 for 1 h at RT. Terminal deoxynucleotidyl transferase-mediated dUTP nick-end labelling (TUNEL) assay was used in the rat retinal neuronal culture according to the manufacturer instructions (Promega, USA). Nuclei were counterstained with DAPI (1:1000). The coverslip with the cells were mounted on slides with Glycergel mounting medium. Fluorescence images from each condition were taken using a laser scanning confocal microscope (Zeiss LSM 710, Germany).

Retinal organotypic Cultured

Retinal organotypic tissue was fixed in ice-cold absolute ethanol at 4°C. After washing with PBS, the tissue was incubated in a blocking solution containing 3% BSA, 10% NGS and 0.1% Triton X-100 for 1 h at RT. Terminal deoxynucleotidyl transferase-mediated dUTP nick-end labelling (TUNEL) assay was used in the organotypic retinal tissue according to the manufacturer instructions (Promega, USA). Nuclei were counterstained

with DAPI (1:1000). The organotypic retinal culture was flat-mounted on slides and coverslipped with Glycergel mounting medium. Fluorescence images from the four quadrants in each retina were taken using a laser scanning confocal microscope (Zeiss LSM 710, Germany) under 40x magnification. Twelve images per retina (3 per retinal quadrant) were randomly acquired. The number of TUNEL-positive cells was counted and the results were presented as TUNEL-positive cells/mm^2 for each condition (normalized to the control condition).

Frozen/Paraffin Retinal Sections

After immunostaining with anti-Brn3a antibody and the corresponding secondary antibody, TUNEL assay was performed in retinal sections (frozen/paraffin) according to the manufacturer instructions (Promega, USA). Nuclei were counterstained with DAPI (1:2000). The sections were mounted using Glycergel mounting medium (Dako, Denmark) and visualized in a fluorescence microscope (Leica DM IRE2, Germany or Leica SP2, Germany). From each eye, 3 images were randomly acquired from each retinal section (4 from each animal). In each image, the number of TUNEL-positive cells in the outer nuclear layer (ONL), inner nuclear layer (INL) and retinal ganglion cell layer (GCL) was counted. The number of Brn3a immunoreactive cell bodies was counted in the same images. The number of TUNEL-positive cells was counted and the results were presented as TUNEL-positive cells/mm^2 for each condition (normalized to the control condition).

3.4 Results

3.4.1 Activation of A3 receptor protects retinal cells from excitotoxicity-induced cell death in mixed cultures

The potential neuroprotective effect induced by A3R activation was assessed with TUNEL assay (Fig 3.1) in a primary retinal mixed culture, well established in our lab (Santiago et al., 2007). Retinal cultures were incubated with the selective A3R agonist (2-Cl-IB-MECA, 1 μM) and/or antagonist (MRS1191, 1 μM), 45 min before the exposure to kainate (KA, 100 μM) in the presence of cyclothiazide (CTZ, 30 μM), used to prevent AMPA/KA receptor desensitization. Incubation with KA+CTZ for 24h significantly increased the number of TUNEL-positive cells, as compared to control cells (272.7±24.5% of the control, ***$p<0.001$). When cells were pre-treated with 2-Cl-IB-MECA, the number of TUNEL-positive cells was similar to the control (118.7±4.4% of the control). Furthermore, the protective effect of 2-Cl-IB-MECA was lost when MRS1191 was also present. With similar number of TUNEL-positive cells to the KA+CTZ condition. Incubation of cells with 2-Cl-IB-MECA, MRS1191 or both did not significantly change the number of TUNEL-positive cells compared with the control (Fig 3.1).

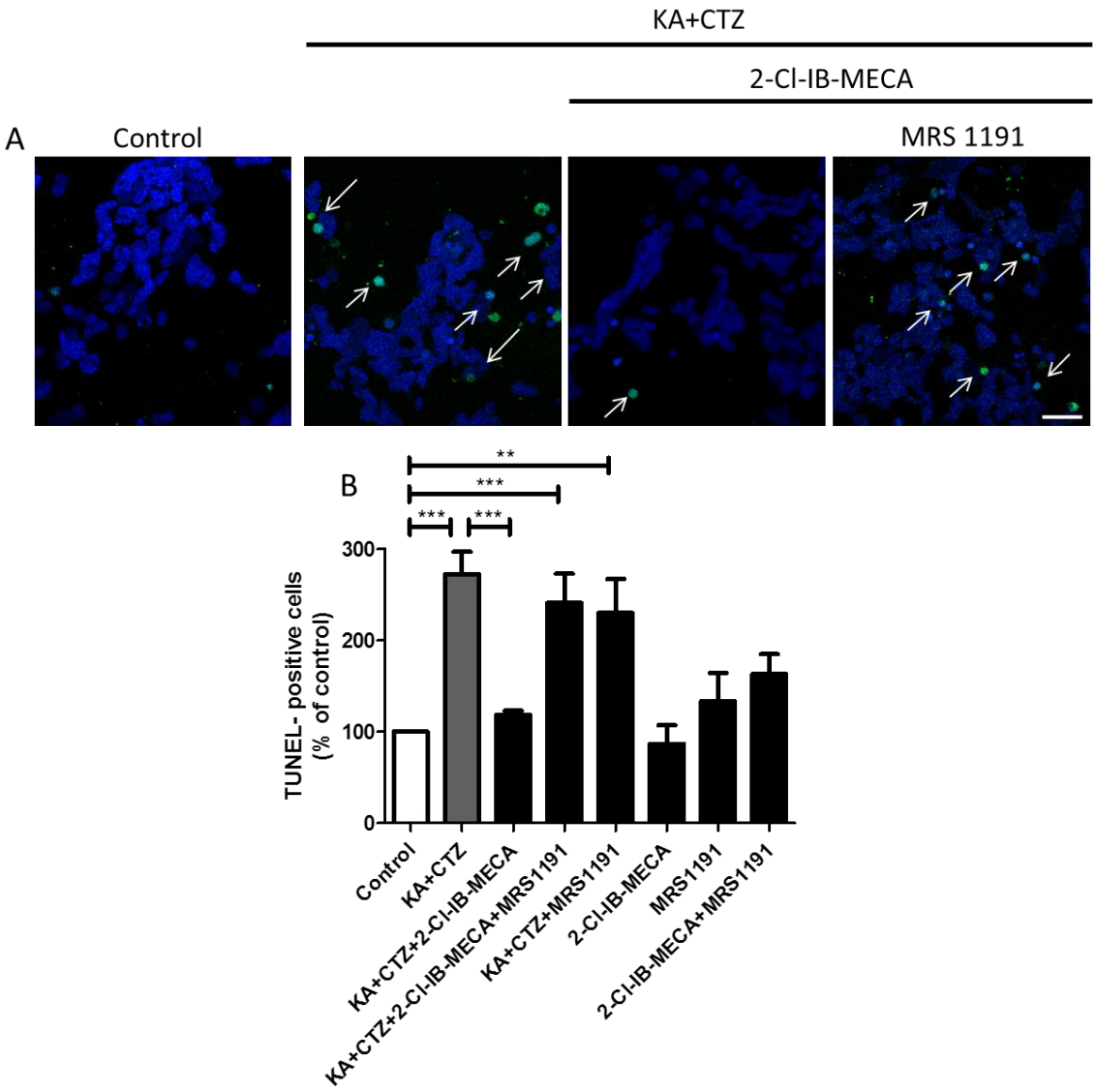

Figure 3.1 - A3 adenosine receptor activation protects retinal mixed neural cell cultures against excitotoxic-induced cell death. Retinal cell death was quantified by the TUNEL assay. After 6 days in culture, retinal cells were treated with 2-Cl-IB-MECA 30 min before exposure to KA+CTZ. TUNEL assay was performed 24h after the insult. The results represent the mean ± SEM of 7-9 independent experiments, and are expressed as percentage of control. Statistical analysis was performed using ANOVA followed by Bonferroni post-test. ***p<0.001, significantly different (KA+CTZ, KA+CTZ+MRS1191 and KA+CTZ+2-Cl-IB-MECA+MRS1191) compared with control; ***p<0.001, significantly different (KA+CTZ+2-Cl-IB-MECA) compared with KA+CTZ.

3.4.2 Retinal ganglion cells express the A3 adenosine receptor

The expression of A3R in RGCs was assessed by immunofluorescence in immunopurified RGC cultures (Fig 3.2, top), retinal organotypic cultures (Fig 3.2, middle), and retinal cryosections (Fig 3.2, bottom). In the retina, the transcription factor Brn3a is only expressed in RGCs (Nadal-Nicolás et al., 2009). Therefore, RGCs were identified using an antibody that recognizes Brn3a. In culture, all RGCs were immunoreactive for A3R (Fig 3.2, top). However, in mixed *in vitro* systems, only some RGCs were immunoreactive to A3R (Fig 3.2, middle and bottom), indicating that not all RGCs express A3R.

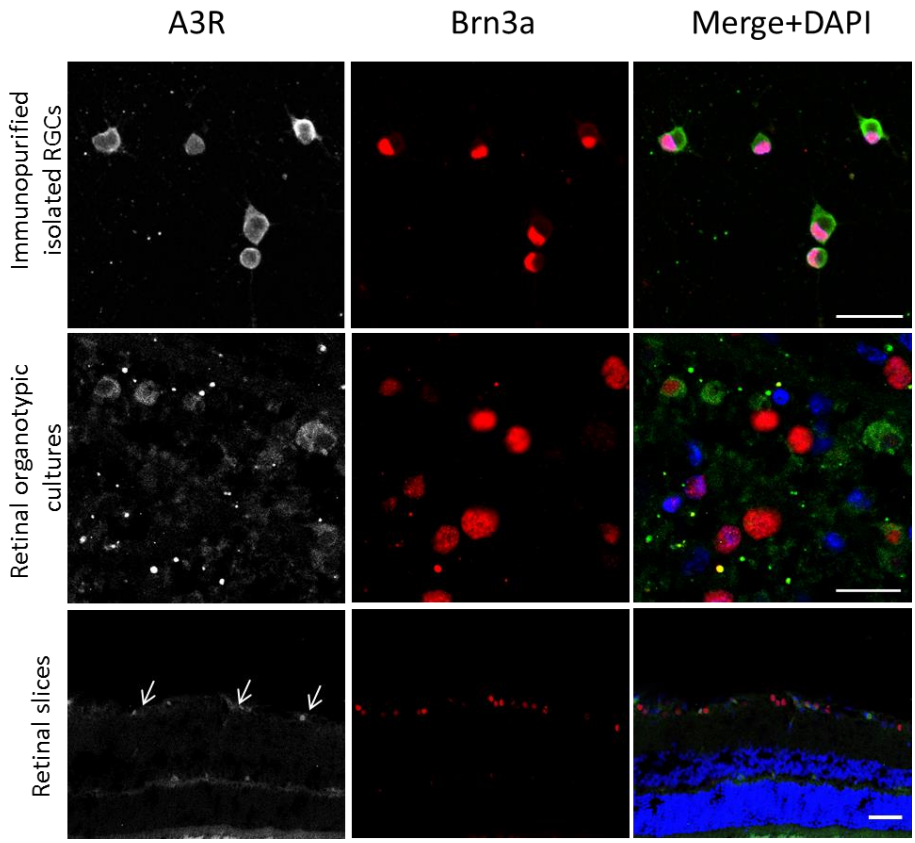

Figure 3.2 - A3 adenosine receptor is expressed in retinal ganglion cells. Immunocytochemistry against A3R (green) and Brn3a (RGC marker; red) was performed in purified retinal ganglion cells (Top), retinal organotypic cultures (Middle) and retinal slices (Bottom). Nuclei were counterstained with DAPI (blue). Top panel, purified RGCs isolated from Wistar rat pups; Middle panel, retinal organotypic culture from young adult Wistar rats; Bottom panel, retinal slices from Dark Agouti rats. A3R immunoreactivity was co-localized with Brn3a indicating the expression of this receptor in RGCs. Scale bar 20 µm.

3.4.3 A3 receptor activation protects retinal cells against excitotoxicity-induced cell death in retinal organotypic cultures

The neuroprotective effect of A3R activation against cell death induced by excitotoxicity was investigated by exposing a retinal organotypic cultures to NMDA (300 µM) for 48 h, in the presence and/or absence of A3R agonist and/or antagonist. Cell death was assessed with PI incorporation (Fig 3.3 A) and TUNEL (Fig 3.3 B and C) assays. When retinal organotypic cultures were exposed to NMDA for 48h, there was a significant increase in the PI-positive cells ratio, compared to control (3.3±0.3 vs. 1.4±0.1; ***p<0.001). Pre-treatment with 2-Cl-IB-MECA (1 µM) prevented the increase in the ratio of PI-positive cells induced by NMDA (1.3±0.1 vs 1.4±0.1). This protective effect was eliminated when the A3R antagonist (MRS1191; 1 µM) was also present. Moreover, incubation of NMDA with MRS 1191 was not different from NMDA alone, showing that blocking A3R does not interfere in NMDA induced cell death. Incubation with 2-Cl-IB-MECA, MRS1191, or vehicle (0.00001% DMSO, v/v) alone did not change the ratio DIV4/DIV2 for PI-positive cells. Similarly, upon exposure to NMDA there was a significant increase in the number of TUNEL-positive cells in the GCL compared to the control (17 fold increase). The presence of 2-Cl-IB-MECA (1 µM) partially prevented the increase in the number of TUNEL-positive cells (8.3 fold increase), indicating a decrease in cell death (**p<0.01). The number of TUNEL-positive cells after treatment with A3R agonist and NMDA was significantly different from control (**p<0.01) in accordance with the partial protection observed. Moreover, pre-incubation with the A3R antagonist abolished the protective effect of 2-Cl-IB-MECA (16 fold increase, ***p<0.001).

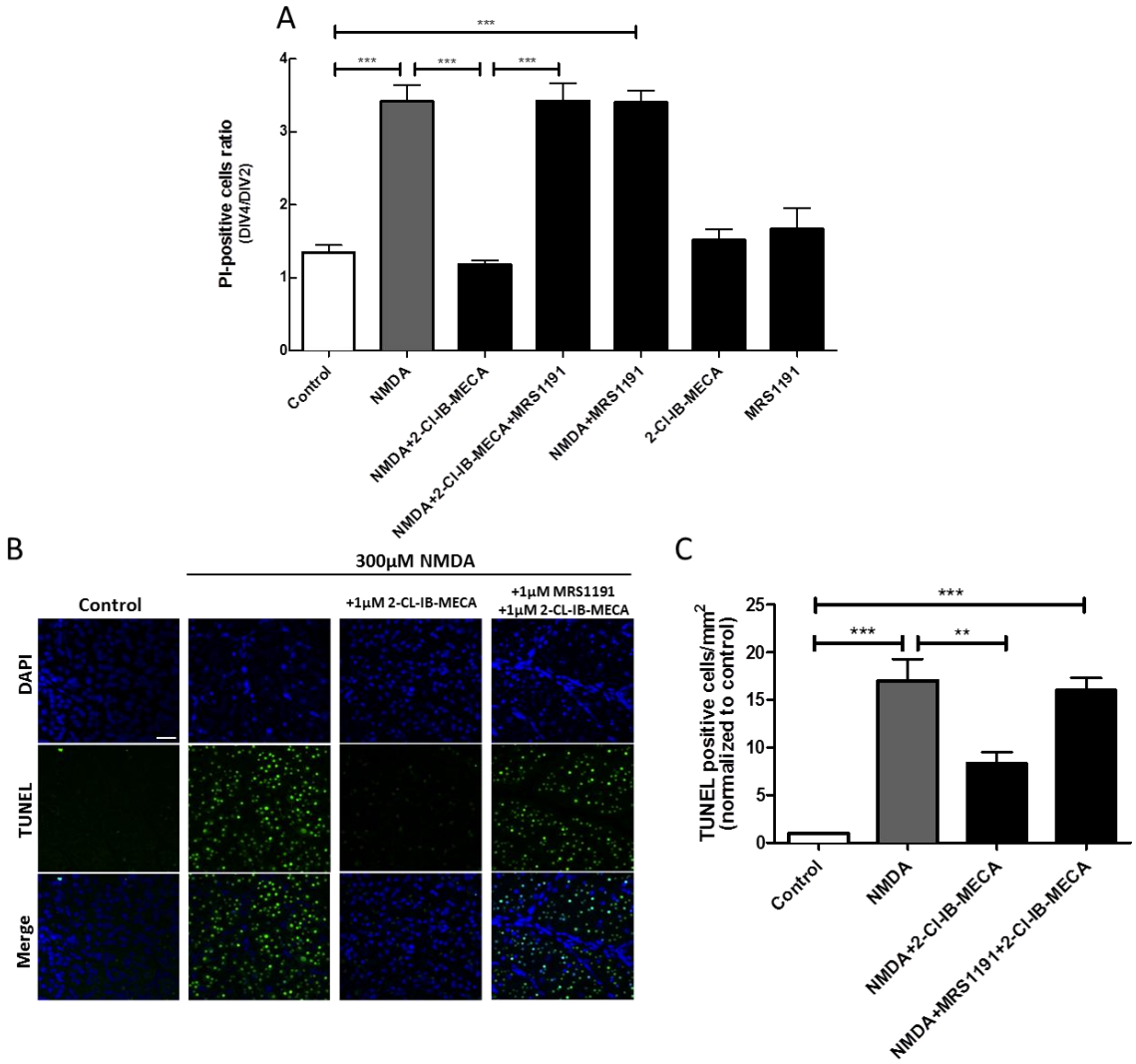

Figure 3.3 - A3 adenosine receptor agonist protects cells against excitotoxic-induced cell death in retinal organotypic cultures. Cell death in retinal organotypic cultures was quantified by PI and TUNEL assays. At DIV4 and DIV2, retinal organotypic cultures were treated with 2-Cl-IB-MECA (DIV1) before exposure to NMDA. Cell death was assessed with propidium iodide (PI) staining in live cells. The results represent the mean ± SEM, and represent the ratio of PI-positive cells at DIV4 and DIV2 in the ganglion cell layer; ***p<0.001, compared with control; **p<0.01, compared with NMDA; *p<0.05, compared with NMDA+2-Cl-IB-MECA, One-way ANOVA test followed by Bonferroni post test (A). Cell death was assessed with TUNEL assay: green staining indicates TUNEL-positive cells (B). The results represent the mean ± SEM, and represent the number of TUNEL-positive cells per mm^2 in the ganglion cell layer; ***p<0.001, compared with control; **p<0.01, compared with NMDA. One-way ANOVA test followed by Bonferroni post-test (C).

3.4.4 A3 receptor agonist protects RGCs in an animal model of DMSO induced RGC apoptosis

After establishing that activation of A3R protects RGCs against cell death induced by excitotoxicity using *in vitro* models, we investigated whether A3R activation could also have protective effects in the retina in an animal model of RGC degeneration. Death of RGCs was induced by an intravitreal injection of DMSO (8%, v/v), and 2-Cl-IB-MECA (1.2 µM, 6 µM and 12 µM; 5µl concentration injected) was injected into the vitreous 30 min prior DMSO injection. Death of RGCs was assessed *in vivo* with fluorescently labelled annexin V, using DARC imaging, as previously well characterized (Cordeiro et al., 2004). Intravitreal injection of DMSO significantly increased the number of annexin V-positive cells (178.8±16.3), as compared to the control (15.3±5.3) (Fig 3.4), indicating an increase in RGC apoptosis induced by DMSO. Injection of 2-Cl-IB-MECA, significantly reduced DMSO-induced RGC apoptosis by 74%, 66% and 70%, at 1.2 µM, 6 µM and 12 µM, respectively, compared to the DMSO-treated eyes (***$p<0.001$). The number of RGCs undergoing apoptosis in eyes treated with 2-Cl-IB-MECA alone was not significantly different compared to control (PBS).

Furthermore, to confirm DARC imaging results, TUNEL assay was performed in retinal slices of the same eyes (Fig 3.5). DMSO induced a significant increase in the number of TUNEL-positive cells (6.7±0.8 TUNEL-positive cells/mm^2) compared with the control (1.9±0.4 TUNEL-positive cells/mm^2). Treatment with 2-Cl-IB-MECA significantly decreased the number of TUNEL-positive cells (1.4±0.5 TUNEL-positive cells/mm^2; ***$p<0.001$) compared to the insult (Fig 3.5).

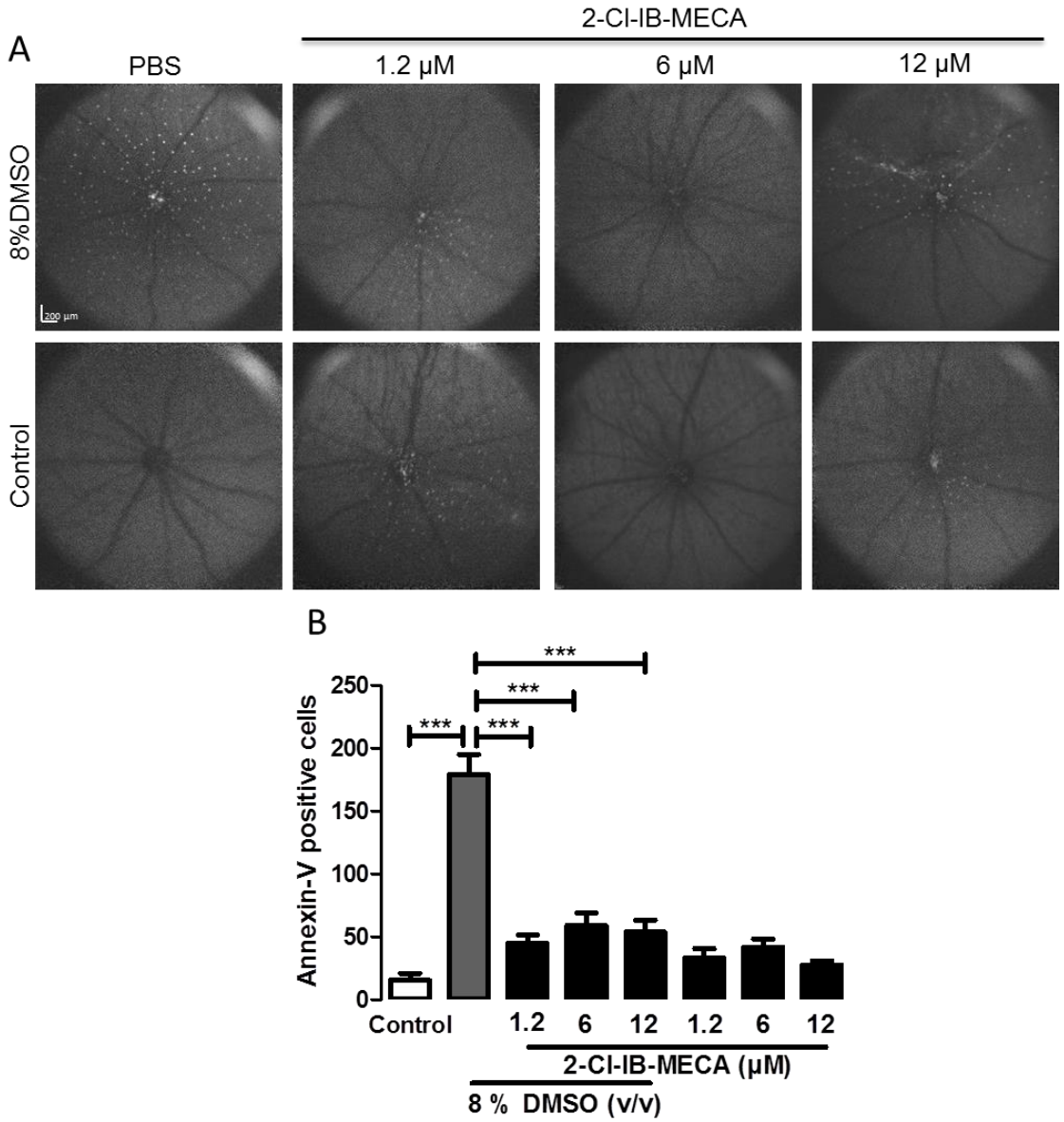

Figure 3.4 - A3 adenosine receptor agonist prevents apoptosis in a model of DMSO induced cell death. Analysis of *in vivo* cell death after an intravitreal injection of PBS, DMSO, DMSO with A3R agonist (1.2 µM, 6 µM or 12 µM) or A3R agonist alone (1.2 µM, 6 µM and 12 µM). *In vivo* DARC images (A) using Heidelberg retinal angiography Spectralis (HRA Spectralis, Heidelberg Engineering, Germany) show cells undergoing apoptosis at the level of RGCs, 2 h following injection of fluorescently-labelled annexin V. Results were compared with vehicle alone (PBS). Wide-angle retinal images show white spots, which represent single cells undergoing apoptosis (A). Statistical analysis represent the mean ± SEM and the number of cells labelled with annexin V. ***p<0.001, compared with control; ***p<0.001, compared with DMSO (8% v/v); One-way ANOVA test followed by Bonferroni post-test (B).

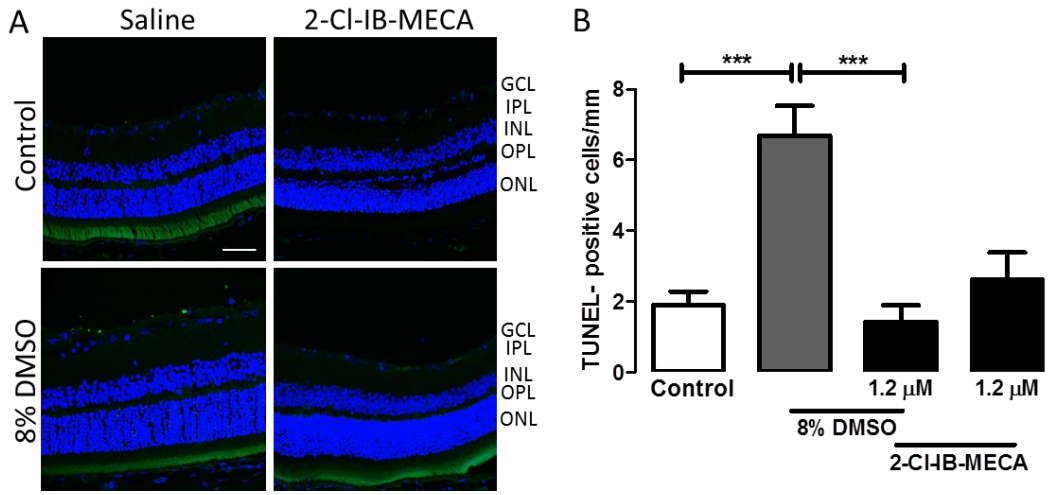

Figure 3.5 - A3 adenosine receptor agonist protects RGCs after DMSO-induced cell death. Cell death was quantified by TUNEL assay in retinal slices. The number of TUNEL-positive cells, in green, was counted at the level of RGCs. The results represent the mean ± SEM. Statistical analysis using one-way ANOVA followed Bonferroni's post-test show significant changes ***p<0.001, compared with control; ***p<0.001, compared with DMSO (8% v/v). Scale bar: 20 μm.

3.4.5 A3 receptor agonist protects RGCs in a model of ischemia-reperfusion injury

According with the results obtained on the DMSO-induced RGC apoptosis model, we next used the lowest concentration that afforded protective effects *in vivo*. We hypothesized that degeneration affecting RGC also decreases A3R expression at the level of GCL. To evaluate this, immunohistochemistry against A3R and Brn3a was performed in retinal slices of eyes subjected to I-R (ischemia-reperfusion) injury and control group (Fig 3.6 A). Retinal I-R injury significantly decreased A3R immunoreactivity, especially in the GCL, compared to control (**p<0.01). Treatment with A3R agonist prevented the decrease in A3R immunoreactivity (Fig 3.6 A and B).

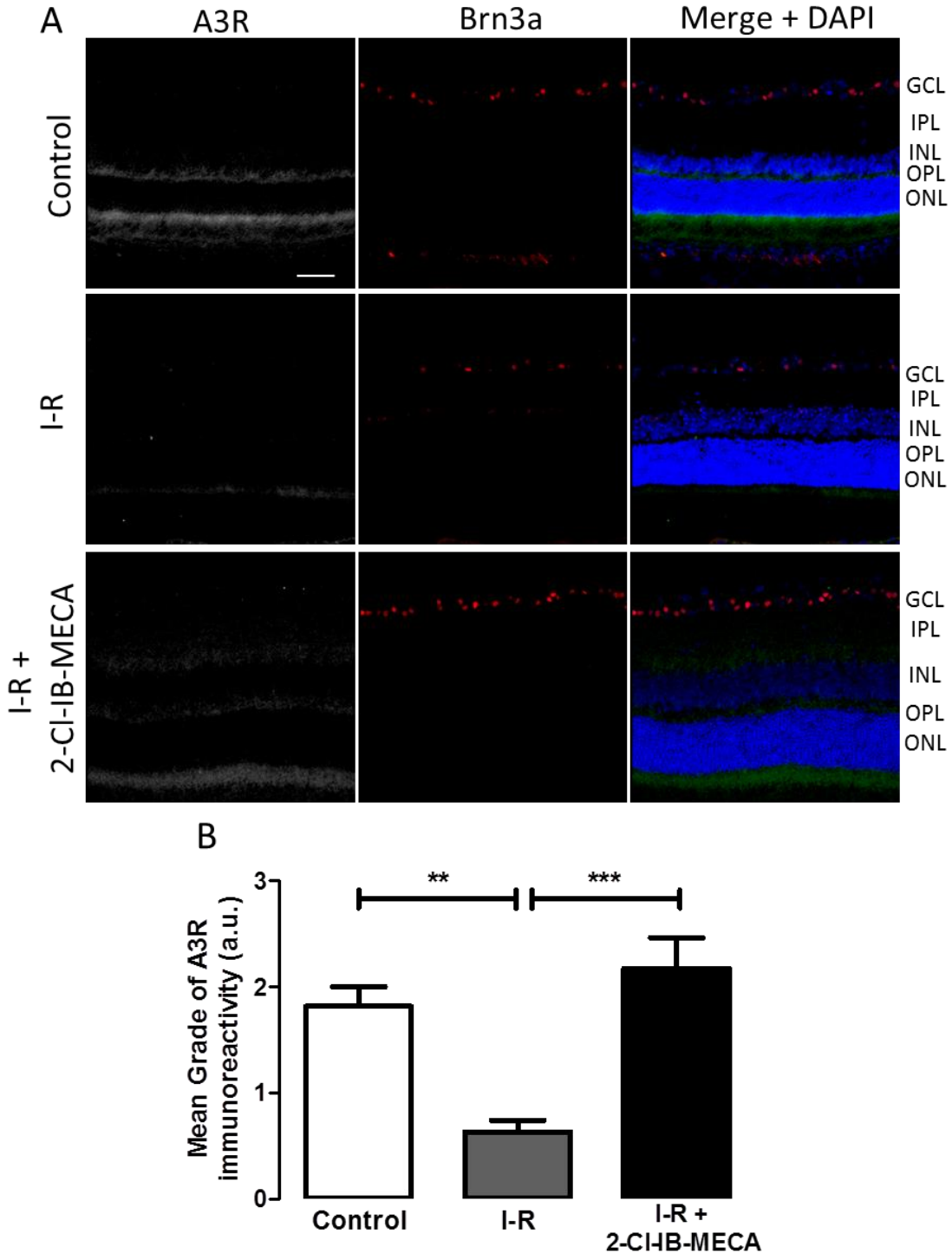

Figure 3.6 - A3 adenosine receptor is down-regulated at the level of RGCs after an ischemia-reperfusion insult. Immunohistochemistry analysis for A3R was performed in retinal slices and shows decreased expression of A3R at the level of RGCs after an ischemia-reperfusion insult (A). The results represent the mean ± SEM, and mean grade of A3R immunoreactivity **p<0.01, compared with control; *** p<0.001, compared with ischemic eyes; One-way ANOVA test followed by Bonferroni post-test (B). Scale bar: 20 µm.

As reported previously, retinal I-R injury induces the loss of RGCs (Fernandez et al., 2009). TUNEL assay was performed in retinal slices of the different groups analysed to evaluate retinal cell apoptosis (Fig 3.7 D, E and F). I-R injury caused a significant increase in the number of TUNEL-positive cells compared with the control (71.5±7.1 TUNEL-positive cells/mm^2 vs. 0.3±0.2 TUNEL-positive cells/mm^2; ***$p<0.001$, Fig 3.7, D and E), in all three nuclear retinal layers (Fig 3.7 D and F). A single intravitreal injection of 2-Cl-IB-MECA significantly inhibited the increase in the number of TUNEL-positive cells in the retina, also in the GCL (1.2±0.2 TUNEL-positive cells/mm^2 vs. 6.0±0.8 TUNEL-positive cells/mm^2; ***$p<0.001$, Fig 3.7 D and F), when compared with I-R group treated with saline.

To evaluate the protective effect of A3R specifically in RGCs, the number of surviving RGCs (Brn3a-immunoreactive cells) was counted (Fig 3.7 A, B and C). Retinal I-R significantly decreased the number of RGCs, compared to the control (contralateral) eye (14.0±2.6 Brn3a-positive cells/mm^2 vs. 33.6±4.6 Brn3a-positive cells/mm^2; **$p<0.01$, Fig 3.7 A and B). Injection with 2-Cl-IB-MECA significantly inhibited the loss of RGCs (21.6±2.0 Brn3a-positive cells/mm; *$p<0.05$, Fig 3.7 A and C) caused by I-R injury.

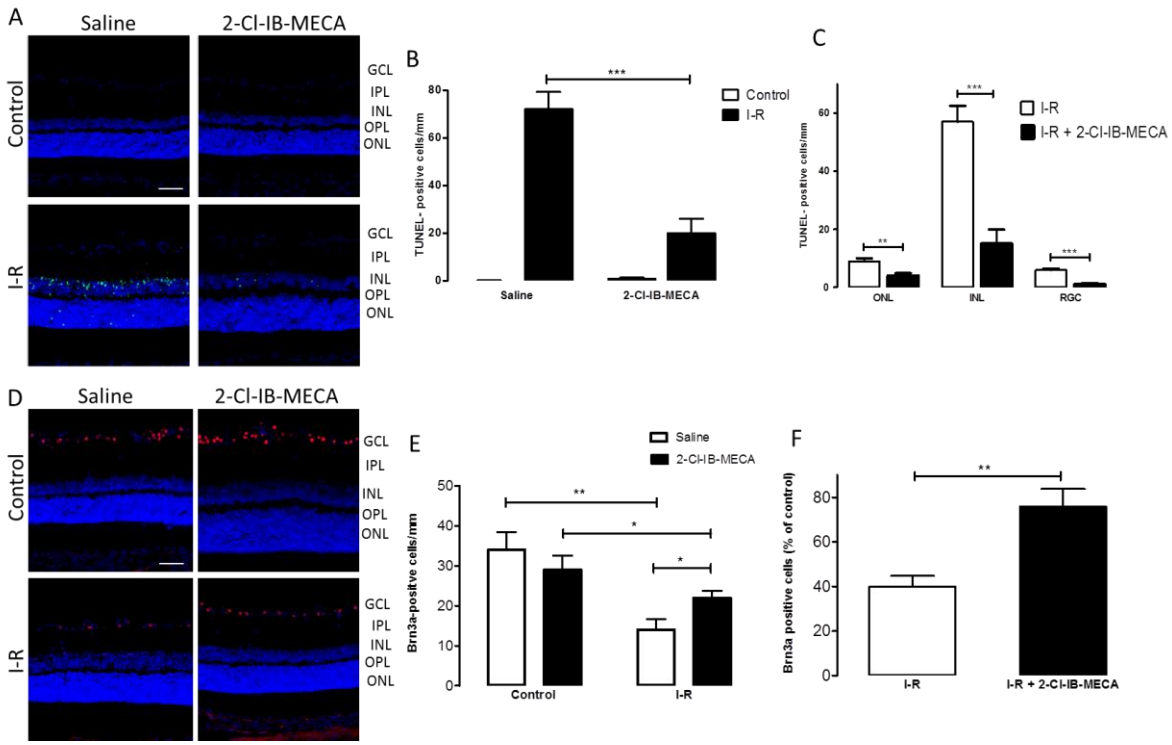

Figura 3.7 - A3 adenosine receptor agonist protects RGCs against an ischemia-reperfusion insult. The number of TUNEL-positive cells was counted in the retina (A). The results are expressed as mean ± SEM, and represent the number of TUNEL-positive cells per mm^2 of retina; ***p<0.001, compared with control eye (B); compared with ischemic eyes (B). The number of TUNEL-positive cells was also assessed in retinal layers; **p<0.01, ***p<0.001 (C). Representative images of TUNEL staining (green) in retinal sections. Nuclei were stained with DAPI (blue) (A). One-way ANOVA test followed by Bonferroni post-test (B,C). The total number of Brn3a-positive cells, representing RGCs, was counted on different retinal slices (D). The results are expressed as mean ± SEM, and represent the number of Brn3a-positive cells per mm^2 of retina; **p<0.01, compared with control eye; * p<0.05, compared with ischemic eye (E). The number of Brn3a-positive cells was also assessed in retinal layers (F). Representative images of Brn3a staining (red) in retinal sections. Nuclei were stained with DAPI (blue) (D). The results are expressed as mean ± SEM, and represent the number of RGCs by mm. One-way ANOVA followed by Bonferroni's multiple comparison test (E, F). Scale bar: 20 µm.

3.5 Discussion

The results presented herein demonstrate that activation of A3 receptors (A3R) protects retinal neurons both *in vitro*, against glutamate excitotoxicity, and in the retina, in two animal models characterized by RGC death, namely DMSO injection into the vitreous and ischemia-reperfusion model. To our knowledge this is the first work using a wide range of experimental models to investigate the neuroprotective effect of A3R activation in the retina.

It was already reported that immunopurified isolated RGCs express A3R mRNA(Zhang et al., 2006a), and functional identification of A3R in cultured RGCs was also demonstrated with 2-Cl-IB-MECA (Zhang et al., 2006a). Here, we showed that immunopurified isolated RGCs are immunoreactive to A3R. Moreover, we also demonstrated that in more complex systems, as retinal organotypic cultures and in retinal cryosections, RGCs are immunoreactive for A3R. To our knowledge, this was the first time that A3R was identified in RGCs by immunofluorescence techniques.

It has been previously proved that activation of A3R protects cells against different insults. A3R agonist (2-Cl-IB-MECA) has a protective role both *in vivo* (in the brain) and *in vitro* (cortical neurons) after hypoxia (Chen et al., 2006). In cortical neurons, the activation of A3R depresses signal transmission by inhibiting glutamate release, providing neuroprotection against excitotoxicity (Brand et al., 2001). Moreover, A3R knock-out mice are more susceptible to ischemic brain injury and increased CO_2-induced neurodegeneration in hippocampus, evidencing a protective role of A3R (Chen et al., 2006).

In the retina, neuroprotective effects of A3R have not been extensively studied. Previous reports have demonstrated that activation of A3R in immunopurified isolated RGC attenuates intracellular calcium concentration increase after NMDA or P2X7 activation (Hu et al., 2010; Zhang et al., 2010, 2006b). The A3R agonist, MRS 3558, prevented RGC loss induced by activation of the P2X7 receptor (Hu et al., 2010). Moreover, the protective effect of ischemic preconditioning (IPC) in cardiac myocytes involved A3R activation with concomitant activation of protein kinase C (PKC) and the opening of K_{ATP} channels in mitochondria leading to p38 MAPK phosphorylation (Leshem-Lev et al.,

2010; Wan et al., 2008). Our results clearly demonstrate protective effects due to the activation of A3R in mixed cultures of retinal neurons upon overactivation of AMPA and kainate receptors. The protection conferred by the activation of A3R appears to be dependent on the type of cells, since A3R activation did not protect cortical neurons from death triggered by kainate and cyclothiazide, albeit the receptor is expressed (Rebola et al., 2005). Moreover, other cells rather than RGCs may also express A3R, which can indirectly contribute to the RGC protection.

Except for the retinal mixed culture, we assessed the neuroprotective effects of A3R activation at the level of GCL. The GCL contains RGCs and displaced amacrine cells, being estimated that 50% of the cells in the GCL of adult rats are amacrine cells (Farah, 2006; Perry, 1981), as well as glial cells, such as Müller cells, astrocytes and microglia. Therefore, dying cells in retinal organotypic cultures and in DMSO and I-R injury models are not likely only RGCs. Nevertheless, in the I-R injury model, RGCs were labelled with an antibody that recognizes Brn3a, a POU domain transcription factor, which is a marker used to label RGCs in the adult rat retina (Nadal-Nicolás et al., 2009).

Our results also showed a decrease in the expression of A3R after I-R. This observation contradicts previous reports in other models showing that this receptor is upregulated in ciliary tissue in eyes with pseudoexfoliation syndrome, in different neoplastic cells, including melanoma, astrocytoma, lymphoma, leukemia and pineal tumour cells (Fishman et al., 2011; Schlötzer-Schrehardt et al., 2005). Furthermore, treatment with A3R agonist prevented the downregulation of A3R induced by I-R and protected RGCs from cell death showing the involvement of this receptor in the neuroprotective effects against ischemia-reperfusion injury.

In summary, our results show that A3R activation protects cells in the GCL, particularly RGCs (identified with an antibody against Brn3a) in different models of cell degeneration induced by excitotoxicity, DMSO or I-R. Therefore, targeting this receptor might be an important step forward to a potential therapy in glaucoma. In fact, it was reported recently that an A3R agonist is already under clinical trial for glaucoma (Gessi et al., 2011), although no extensive studies have been published regarding the protective effects of this drug to RGCs *in vitro* or *in vivo*. Therefore, the main conclusion of this

work is that A3R activation with 2-Cl-IB-MECA is protective to retinal neurons. Our results may have relevance in the treatment of retinal degenerative diseases affecting RGCs, particularly in glaucoma.

3.6 Acknowledgements:

This study was supported by Foundation for Science and Technology, Portugal (Strategic Project PEst-C/SAU/UI3282/2011; fellowship SFRH/BD/47947/2008) and COMPETE-FEDER. We would like to thank Prof. Claire Mitchell, University of Pennsylvania, USA, for general advice for this work. Conflict of Interest: M F Cordeiro – Patent application.

3.7 References

Baltmr, A., Duggan, J., Nizari, S., Salt, T.E., Cordeiro, M.F., 2010. Neuroprotection in glaucoma - Is there a future role? Exp. Eye Res. 91, 554–66.

Barres, B., Silverstein, B.E., Corey, P., Chun, L., 1988a. Electrophysiological Variation among Retinal Ganglion Cells Purified by Panning. Neuron 1, 791–803.

Barres, B., Silverstein, B.E., Corey, P., Chun, L., 1988b. Electrophysiological Variation among Retinal Ganglion Cells Purified by Panning. Neuron 1, 791–803.

Blazynski, C., 1990. Discrete distributions of adenosine receptors in mammalian retina. J. Neurochem. 54, 648–55.

Brand, a, Vissiennon, Z., Eschke, D., Nieber, K., 2001. Adenosine A(1) and A(3) receptors mediate inhibition of synaptic transmission in rat cortical neurons. Neuropharmacology 40, 85–95.

Chang, E.E., Goldberg, 2012. Glaucoma 2.0: neuroprotection, neuroregeneration, neuroenhancement. Ophthalmology 119, 979–86.

Chen, Harvey, B.K., Shen, H., Chou, J., Victor, A., Wang, Y., 2006. Activation of Adenosine A3 Receptors Reduces Ischemic Brain Injury in Rodents. J. Neurosci. Res. 84, 1848–1855.

Cordeiro, M.F., Guo, L., Luong, V., Harding, G., Wang, W., Jones, H.E., Moss, S.E., Sillito, A.M., Fitzke, F.W., 2004. Real-time imaging of single nerve cell apoptosis in retinal neurodegeneration. Proc. Natl. Acad. Sci. U. S. A. 101, 13352–6.

Coxon, K.M., Duggan, J., Guo, L., Cordeiro, M.F., 2010. Retinal Ganglion Cell Apoptosis and Neuroprotection. Encycl. Eye 4, 62–72.

Cunha, R. a, 2005. Neuroprotection by adenosine in the brain: From A(1) receptor activation to A (2A) receptor blockade. Purinergic Signal. 1, 111–34.

Dreyer, E.B., Zurakowski, D., Robert, A., Podos, S.M., Lipton, S.A., 1996. Glutamate the of and. Arch Ophthalmol. 114, 299–305.

Farah, M.H., 2006. Neurogenesis and cell death in the ganglion cell layer of vertebrate retina. Brain Res. Rev. 52, 264–74.

Fedorova, I., Jacobson, M., Basile, A., Jacobson, K., 2011. Behavioral Characterization of Mice Lacking the A3 Adenosine Receptor : Sensitivity to Hypoxic Neurodegeneration. Cell Mol. Neurobiol. 23, 431–447.

Fernandez, D.C., Bordone, M.P., Chianelli, M.S., Rosenstein, R.E., 2009. Retinal neuroprotection against ischemia-reperfusion damage induced by postconditioning. Invest. Ophthalmol. Vis. Sci. 50, 3922–30.

Fishman, P., Bar-Yehuda, S., Liang, B.T., Jacobson, K. a, 2011. Pharmacological and therapeutic effects of A(3) adenosine receptor agonists. Drug Discov. Today 00, 1–8.

Flammer, J., Haeflinger, I., Orgul, S., Resink, T., 1999. Vascular dysregulation: A principal risk factor for glaucoma damage? Journal of Glaucoma.

Gessi, S., Merighi, S., Varani, K., Borea, P.A., 2011. Adenosine receptors in health and disease. Adv. Pharmacol. 61, 41–75.

Gherghel, Gherghel, D., Orgül, S., Prünte, C., Gugleta, K., Lübeck, P., Gekkieva, M., 2004. Interocular differences in optic disc topographic parameters in normal subjects. Curr. Eye Res. 20, 276–282.

Ghiardi, G.J., Gidday, J.M., Roth, S., 1999. The purine nucleoside adenosine in retinal ischemia-reperfusion. Inj. Vis. Res. 39, 2519–2535.

Heijl, A., Leske, M., Bengtsson, Bo, Hyman, L., Bengtsson, Boel, Hussein, M., 2002. Reduction of Intraocular Pressure and Glaucoma Progression. Arch Ophthalmol. 20, 9–12.

Hu, H., Lu, W., Zhang, M., Zhang, X., Argall, A.J., Patel, S., Lee, G.E., Kim, Y.-C., Jacobson, K. a, Laties, A.M., Mitchell, C.H., 2010. Stimulation of the P2X7 receptor kills rat retinal ganglion cells in vivo. Exp. Eye Res. 91, 425–32.

Kvanta, a, Seregard, S., Sejersen, S., Kull, B., Fredholm, B.B., 1997. Localization of adenosine receptor messenger RNAs in the rat eye. Exp. Eye Res. 65, 595–602.

Leshem-Lev, D., Hochhauser, E., Chanyshev, B., Isak, A., Shainberg, A., 2010. Adenosine A(1) and A (3) receptor agonists reduce hypoxic injury through the involvement of P38 MAPK. Mol. Cell. Biochem. 345, 153–60.

Leske, M., Heijl, A., Hussein, M., Bengtsson, B., Hyman, L., Komaroff, E., 2003. Factors for Glaucoma Progression and the Effect of Treatment. Arch Ophthalmol. 121.

Nadal-Nicolás, F.M., Jiménez-López, M., Sobrado-Calvo, P., Nieto-López, L., Cánovas-Martínez, I., Salinas-Navarro, M., Vidal-Sanz, M., Agudo, M., 2009. Brn3a as a marker of retinal ganglion cells: qualitative and quantitative time course studies in naive and optic nerve-injured retinas. Invest. Ophthalmol. Vis. Sci. 50, 3860–8.

Osborne, N.N., Chidlow, G., Layton, C.J., Wood, J.P.M., Casson, R.J., Melena, J., 2004. Optic nerve and neuroprotection strategies. Eye (Lond). 18, 1075–84.

Perry, V.H., 1981. Evidence for an amacrine cell system in the ganglion cell layer of the rat retina. Neuroscience 6, 931–44.

Quigley, 2011. Glaucoma. Lancet 377, 1367–77.

Quigley, Broman, 2006. The number of people with glaucoma worldwide in 2010 and 2020. Br. J. Ophthalmol. 90, 262–7.

Rebola, N., Rodrigues, R.J., Oliveira, C.R., Cunha, R. a, 2005. Different roles of adenosine A1, A2A and A3 receptors in controlling kainate-induced toxicity in cortical cultured neurons. Neurochem. Int. 47, 317–25.

Santiago, A.R., Cristóvão, A.J., Santos, P.F., Carvalho, C.M., Ambrósio, A.F., 2007. High glucose induces caspase-independent cell death in retinal neural cells. Neurobiol. Dis. 25, 464–72.

Schlötzer-Schrehardt, U., Zenkel, M., Decking, U., Haubs, D., Kruse, F.E., Jünemann, A., Coca-Prados, M., Naumann, G.O.H., 2005. Selective upregulation of the A3 adenosine receptor in eyes with pseudoexfoliation syndrome and glaucoma. Invest. Ophthalmol. Vis. Sci. 46, 2023–34.

Varma, R., Lee, P.P., Goldberg, I., Kotak, S., 2011. An assessment of the health and economic burdens of glaucoma. Am. J. Ophthalmol. 152, 515–22.

Wan, T.C., Ge, Z., Tampo, A., Mio, Y., Bienengraeber, M.W., Tracey, W.R., Gross, G.J., Kwok, W., Auchampach, J.A., 2008. The A 3 Adenosine Receptor Agonist CP-532 , 903 [N 6 - (2 , 5- Protects against Myocardial Ischemia / Reperfusion Injury via the Sarcolemmal ATP-Sensitive Potassium Channel 324, 234–243.

Weber, A.J., Harman, C.D., 2008. BDNF preserves the dendritic morphology of alpha and beta ganglion cells in the cat retina after optic nerve injury. Invest. Ophthalmol. Vis. Sci. 49, 2456–63.

Zhang, Budak, M.T., Lu, W., Khurana, T.S., Zhang, X., Laties, A.M., Mitchell, C.H., 2006a. Identification of the A3 adenosine receptor in rat retinal ganglion cells. Mol. Vis. 12, 937–48.

Zhang, Hu, H., Zhang, X., Lu, W., Lim, J., Eysteinsson, T., Jacobson, K. a, Laties, A.M., Mitchell, C.H., 2010. The A3 adenosine receptor attenuates the calcium rise triggered by NMDA receptors in retinal ganglion cells. Neurochem. Int. 56, 35–41.

Zhang, Zhang, M., Laties, A.M., Mitchell, C.H., 2006b. Balance of purines may determine life or death of retinal ganglion cells as A3 adenosine receptors prevent loss following P2X7 receptor stimulation. J. Neurochem. 98, 566–75.

Zhou, Q.Y., Li, C., Olah, M.E., Johnson, R. a, Stiles, G.L., Civelli, O., 1992. Molecular cloning and characterization of an adenosine receptor: the A3 adenosine receptor. Proc. Natl. Acad. Sci. U. S. A. 89, 7432–6.

4 CHAPTER FOUR: Activation of adenosine A3 receptor is neuroprotective against retinal neuronal degeneration in rat models of partial optic nerve transection and ocular hypertension

Table of Contents

4.1 Abstract

Purpose: It has been shown that adenosine can be neuroprotective against retinal insults. However, its potential protective effects to retinal ganglion cells (RGCs) in glaucoma remains to be elucidated. Therefore, the aim of this study was to evaluate the potential neuroprotective effects of adenosine A3 receptor (A3R) activation against RGCs degeneration in animal models of glaucoma.

Methods: Two glaucoma-related rat models, namely the partial optic nerve transection (pONT, n=22) and ocular hypertension (OHT, n=20) models were surgically induced in the left eye of each animal, and the contralateral eyes were used as controls. A3R agonist (2-Cl-IB-MECA, 5 µl, 1.2 µM) or PBS was intravitreally injected into both eyes of each rat. Animals were imaged *in vivo* for RGC apoptosis with DARC technique at baseline and at 7 days after insult for pONT model and 3 weeks for OHT model. Immunohistochemistry analysis was performed for A3R in retinal slices and RGCs were labeled for Brn3a in retina slices and whole-mounts.

Results: A3R agonist significantly decreased RGC apoptosis *in vivo* in both pONT and OHT models ($p<0.01$) and increased RGC survival as evaluated by Brn3a counts in retinal whole-mounts in both models ($p<0.01$ for pONT and $p<0.05$ for OHT). Immunohistochemistry analysis showed that immunoreactivity of the A3R was significantly down-regulated in RGC layer after the insults ($p<0.05$ for pONT and $p<0.001$ for OHT), but treatment with the A3R agonist prevented A3R down-regulation in both models ($p<0.01$ for pONT and $p<0.001$ for OHT).

Conclusions: Our results demonstrate that A3R activation is neuroprotective against RGC death *in vivo* and histologically in two models of RGC degeneration. These results suggest that targeting A3R pathway may have great potential in the management of glaucoma.

4.2 Introduction

Glaucoma, a leading cause of irreversible blindness worldwide, is a degenerative optic neuropathy, characterized by atrophy of the optic nerve and loss of RGCs. By 2020, 80 million people are predicted to be affected by glaucoma and of those 11.1 million are expected to be bilaterally blind (Quigley and Broman, 2006). Lowering of IOP was demonstrated to attenuate RGC death (Heijl et al., 2002; Leske et al., 2003) and is the only pharmacologic treatment currently available. However, by lowering IOP disease progression is not halted in all cases (Chang and Goldberg, 2012). Therefore, novel strategies to save RGCs and prevent vision loss are urgently needed.

Adenosine is a purine nucleoside, being known as a neuromodulator in the central nervous system (CNS). It acts through the activation of inhibitory (A1 and A3) and facilitatory (A2A and A2B) receptors. Modulation of adenosine receptors has been reported to be one of the most promising neuroprotective strategies in the CNS (Cunha, 2005), and their modulation was shown to be neuroprotective against a broad spectrum of brain insults, being in clinical trials for a diverse number of CNS diseases, including Parkinson's and Huntington's disease (Gessi et al., 2011a, 2011b). Moreover, targeting G protein-coupled receptors (GPCR) represents more than 30% to 40% of all the drugs marketed by pharmaceutical industry (Filmore, 2004; Hopkins and Groom, 2002a; Venkatakrishnan et al., 2013). Studies on the retina in several species revealed that the highest adenosine immunoreactivity occurs in RGCs and throughout the inner plexiform layer, where RGCs make synapses with bipolar and amacrine cells. Adenosine A3 receptor (A3R) is also expressed in RGCs and the inner plexiform layer (Zhang et al., 2006a). The mRNA of A3R was identified in RGCs, and the presence of these receptors in RGCs was functionally confirmed in immunopurified isolated RGCs using the selective agonist 2-Cl-IB-MECA (Zhang et al., 2006a). Previous reports demonstrated that A3R activation attenuates calcium rise in RGCs after glutamate, NMDA or P2X activation (Hu et al., 2010; Zhang et al., 2010, 2006b). However, it is unclear if modulation of adenosine receptors could afford RGC neuroprotection in glaucoma.

In this study, we evaluated the neuroprotective effect of the A3R agonist, 2-Cl-IB-MECA, in glaucoma-related animal models and found that A3R activation significantly protected RGCs from degeneration both *in vivo* and histologically.

4.3 Materials and Methods

4.3.1 Animals

Adult male Dark Agouti (DA) rats (250-300 g) were housed in a temperature- and humidity-controlled environment and were provided with standard rodent diet and water *ad libitum* while kept on a 12-h light/12-h dark cycle. All procedures involving animals were in agreement to the ARVO Statement for the Use of Animals in Ophthalmic and Vision Research.

4.3.2 Partial optic nerve transection model

Twenty two DA rats had partial optic nerve transection performed in the left eye, using a previously described technique (Levkovitch-Verbin, 2003). Animals were anesthetized intraperitoneally with ketamine (37.5%) and medetomidine (25% Dormitor; Pfizer Animal Health, Exton, PA, USA) solution at 0.2 ml/100 g, as previously described (Cordeiro et al., 2004). Animals were randomly divided into 4 groups: pONT + PBS, pONT + 2-Cl-IB-MECA, 2-Cl-IB-MECA and PBS. An Intravitreal (IVT) injection of either 1.2 µM 2-CL-IB-MECA (5 µl) or vehicle (PBS) was performed just before pONT was induced. All animals were imaged *in vivo* for RGC apoptosis at 7 days following pONT surgery, by using DARC (Detection of Apoptosing Retinal Cells) technique (Cordeiro et al., 2004). Fluorescently labelled annexin V was intravitreally injected 2 h before DARC imaging.

4.3.3 Ocular hypertension model

Twenty DA rats had IOP surgically elevated in the left eye of each animal under general anaesthesia (see above), using a well-established method (Cordeiro et al., 2004; Guo and Cordeiro, 2008; Morrison et al., 1997). Briefly, OHT was induced by the injection of 50 µl of hypertonic saline solution (1.8 M) into the episcleral veins using a syringe pump (50 µl/min; UMP2; World Precision Instruments, Sarasota, FL, USA) (Cordeiro et al., 2004; Guo et al., 2008; Morrison et al., 1997). A propylene ring, with a 1 mm gap cut out of its circumference, was placed around the equator to prevent injected saline outflow.

Contralateral unoperated eyes served as control. Animals were randomly assigned to OHT + PBS, OHT + 2-Cl-IB-MECA, OHT + 2-Cl-IB-MECA + MRS 1220, 2-Cl-IB-MECA, MRS 1220 and PBS. An IVT injection of 1.2 μM 2-Cl-IB-MECA, 1.2μM MRS 1220 or PBS was performed just before OHT was induced. Three weeks after OHT was induced, fluorescently labelled annexin V was intravitreally injected for imaging RGC apoptosis as described in the previous section.

4.3.4 Measurement of intraocular pressure

The IOP was measured in both eyes under isoflaurane anaesthesia (Merial; Animal Health, Ltd, UK), using Tonolab (Icare, Finland) at approximately the same time of the day. IOP measurements were taken before surgery (baseline), 1h and 1 day after surgery and then at weekly intervals afterwards. Ten IOP readings were taken and averaged. For each animal, integral IOP elevation over time (mmHg/days) was calculated from area under the curve as previously described (Chauhan et al., 2002; Levkovitch-Verbin et al., 2002).

4.3.5 *In Vivo* Imaging of RGC apoptosis

Rats were imaged using HRA Spectralis (Heidelberg Retinal Angiograph, Heidelberg Engineering, Germany) 2h after fluorescently labelled annexin V were intravitreally injected. Based on our previous Staurosporin model, using annexin V to detect RGC apoptosis *in vivo*, 2h was shown to be the time peak of RGC apoptosis, as previsouly elsewhere (Cordeiro et al., 2004). To optimize visualization, eyes were lubricated regularly. Pupils were dilated with one drop each of 2.5% phenylephrine hydrochloride and 1.0% cyclopentolate hydrochloride. During image acquisition, HRA Spetrallis was focused on the retinal nerve fibre layer, as identified in the reflectance mode. The images were collected and RGC labelled with annexin V were counted using the public domain Image J (NHI, Bethesda, USA).

4.3.6 Histological preparation

The eyes of all animals were enucleated immediately after sacrifice. The eyeball was lifted from the eye socket slightly to cut the optic nerve. The eyes were then fixed in 4% PFA (w/v) (paraformaldehyde, Sigma-Aldrich, St. Louis, MO, USA) and kept at 4°C until further processing.

4.3.7 Frozen retinal sections

The lens was removed and the eyes were further fixed in 4% (w/v) PFA overnight. After washing in PBS, the eyes were cryopreserved by placing them in 5% (w/v) sucrose in PBS for 30 min and 3h cycles and then in 30% (w/v) sucrose in PBS overnight at 4°C. Finally, the eyes were embedded in tissue-freezing medium (OCT; Shandon, USA), the frozen blocks were cut in a cryostat into 10 µm thickness sections and the cryosections were then collected on SuperFrost Plus glass slides (Menzel-Glaser, Germany) and stored at -20°C.

4.3.8 Immunofluorescence labelling

Retinal sections were placed overnight at room temperature (RT). After fixing with ice-cold acetone for 10 min at -20°C, the sections were hydrated in PBS until OCT was removed. Sections were permeabilized in 0.25% Triton X-100 for 30 min at RT, and blocked in 1% BSA and 10% normal goat serum (NGS) solution for 30 min in a humidified atmosphere at RT. Sections were then placed overnight at 4°C in a humidified atmosphere with a primary anti-A3R antibody (1:200; Thermo Scientific, UK) in 1% BSA solution. After washing, they were incubated with the corresponding secondary antibody (Alexa Fluor 488, Invitrogen, UK) in 1% BSA solution for 2h at RT. The nuclei were stained with DAPI (1:2000). The sections were mounted using Citifluor mounting medium (Citifluor Ltd, England) and visualized in a laser scanning confocal microscope (Zeiss LSM 710, Germany). Three different images from at least four different eyes were acquired and analysed.

4.3.9 Retina flat-mounts

Retina flat mounts were prepared from the *in vivo* imaged eyes. Eyes were enucleated and retinas were dissected and stored in methanol at -20°C before staining. After removed from methanol, retinas were fixed for 5 min in 4% PFA in PBS and washed in PBS before further use. The retinas were then processed for immunohistochemistry analysis against Brn3a, as previously described (West et al., 2005). Briefly, retinas were blocked in blocking solution (2x PBS, 3% Triton X-100, 1% BSA, 0.5% Tween 20, and 0.1% sodium azide) for 1h at RT, followed by incubation overnight at 4°C with a primary antibody against Brn3a (1:500, Chemicon Millipore, UK). Retinas were washed three times with blocking solution and incubated with the secondary antibody (Alexa fluor 647; Invitrogen, Life Technologies) at RT for 2h. After washing, the retinas were flat-mounted in Mowiol (Sigma, USA), examined under confocal microscope visualization (LSM 710; Carl Zeiss, Germany) and the number of Brn3a-positive cells was counted with image J.

4.4 Results

4.4.1 Partial optic nerve transection and chronic ocular hypertension increase the number of annexin V-positive cells in GCL: *in vivo* evaluation

Using *in vivo* DARC imaging, the number of annexin v-positive cells was evaluated in the GCL in two different models of RGC degeneration. Seven days after pONT, *in vivo* DARC imaging showed an increase in the number of annexin V-positive cells, compared with control group (100.0±17.2 vs 321.7.2±27.1; *** p<0.001; Fig 4.1A, B and C). The results showed increased levels of apoptosis 3 weeks after OHT compared to control (100.0±15.8 vs 411.2±79.1; *** p<0.001; Fig 4.1 D, E and F).

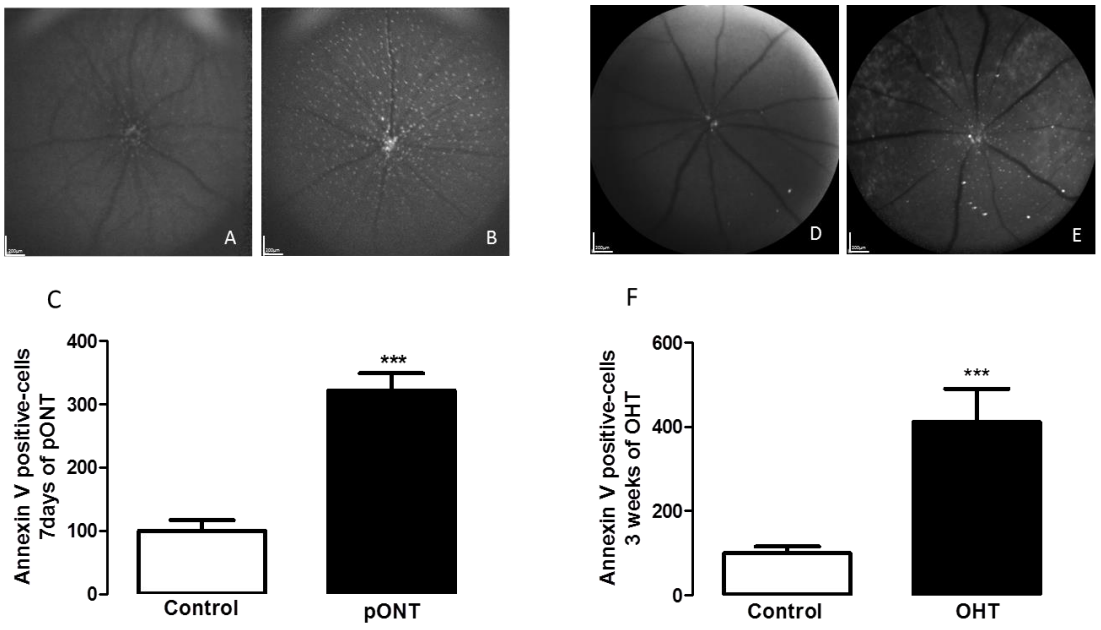

Figure 4.1 - Partial optic nerve transection and ocular hypertension model lead to an increase in RGC apoptosis. *In vivo* DARC images obtained using HRA Spectralis (Heidelberg Engineering, Germany) show white spots representing annexin V-positive cells 2h following IVT injection of fluorescently-labelled annexin V. Partial optic nerve transection for 7 days (B) induced a significant increase (*** p<0.001) in RGCs undertaking apoptosis (C) compared with control (A). Ocular hypertension (OHT) for 3 weeks (E) also induced a significant increase (*** p<0.001) in RGCs undertaking apoptosis (F) compared with control (D). Scale bar 200μm.

4.4.2 Partial optic nerve transection and chronic ocular hypertension decreases the number of retinal ganglion cells

After observing an increase in the number of annexin V-positive cells in the GCL, we histologically assessed the number of Brn3a-positive cells. Brn3a is a transcription factor that in the retina is expressed in RGCs, and therefore can be used as a specific marker of RGCs (Nadal-Nicolás et al., 2009). Seven days after pONT the number of Brn3a-immunoreactive cells decreased as compared with control (Fig 4.2 A, B; 9.72±5.0 vs 100±17.3 % control, 100% representing mean of 17 RGCs per retinal slice; ** $p<0.01$). The number of Brn3a-positive cells was also counted on retina flat-mounts of the retinas imaged with DARC at 3 weeks of OHT. The results show a decrease in the number of Brn3a-positive cells 3 weeks after OHT, compared with control (Fig 4.2 D, E and F; 100.0±2.1 vs 87.3±1.1 % control; ** $p<0.01$).

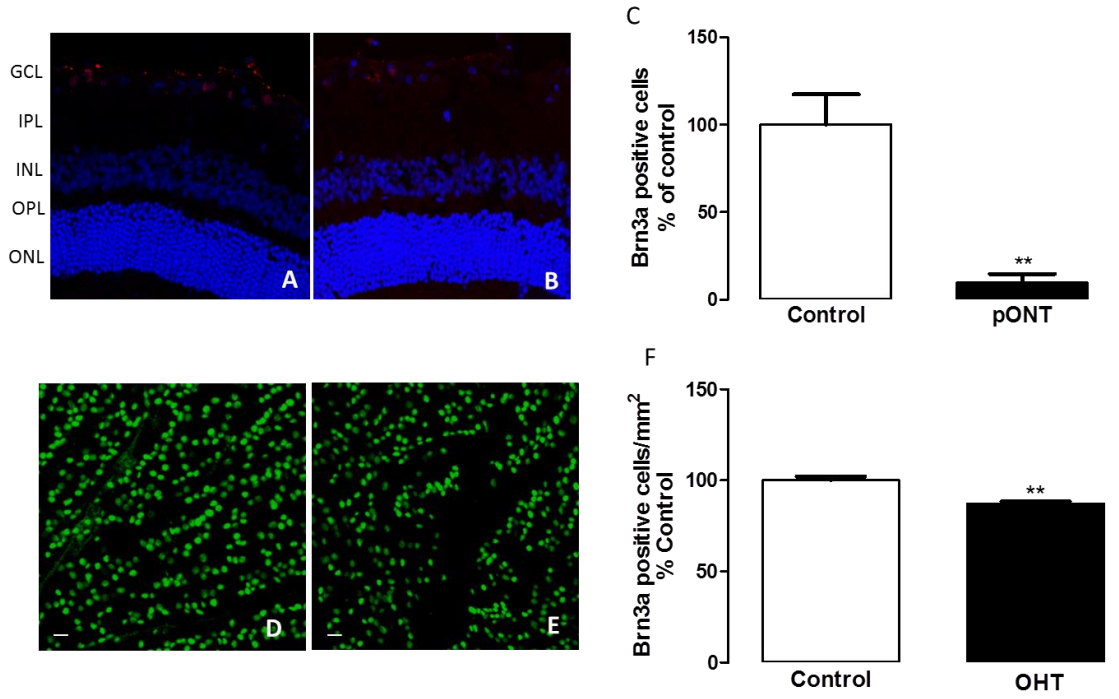

Figure 4.2 - Partial optic nerve transection (7 days) and ocular hypertension (3 weeks) lead to RGC loss. The number of Brn3a-positive cells was counted in retinal slices from eyes collected 7 days after partial optic nerve transection (B) and in the control (A). Partial optic nerve transection (pONT) leads to a decrease (** $p<0.01$) in the number of RGCs compared with control (C).

The total number of Brn3a-positive cells was counted in retinal whole mounts collected 3 weeks after induction of OHT (E) and in age-matched controls (D). OHT led to a decrease (** $p<0.01$) in the number of RGCs (F), compared to control. GCL - Ganglion cell layer; IPL – Inner plexiform layer; INL – Inner nuclear layer; OPL – Outer plexiform layer; ONL – Outer nuclear layer. Scale bar 20µm.

4.4.3 Adenosine A3 receptor is down-regulated following partial optic nerve transection and chronic ocular hypertension. Adenosine A3 receptor activation, prevents A3R down-regulation

The expression levels of A3R at the level of the RGCL were investigated. Retinal sections from eyes with pONT for 7 days and controls were processed for A3R immunoreactivity. pONT induced a significant reduction (** $p<0.01$) in A3R immunoreactivity, especially in the GCL, compared with control group (Fig 4.3A, B and D). Treatment with 2-CL-IB-MECA, completely prevented (*** $p<0.001$) the down-regulation of A3R

immunoreactivity induced by pONT (Fig 4.3C, D). The immunoreactivity of A3R in the pONT eyes treated with the A3R agonist was not significantly different from the immunoreactivity observed in control (PBS injected into the vitreous). A similar analysis was performed in the OHT model after 3 weeks of OHT to evaluate the immunoreactivity of A3R in retinal slices by immunohistochemistry (Fig 4.3F) and age-matched controls (Fig 4.3E). Three weeks of OHT led to a down-regulation of A3R immunoreactivity (***$p<0.001$) in the GCL compared to control eyes (Fig 4.3E, F and H). A single treatment with the A3R agonist prevented the down-regulation (Fig 4.3G, H). The A3R immunoreactivity in OHT animals treated with the A3R agonist was comparable to that observed in control eyes (Fig 4.3D, F). Immunohistochemistry against A3R was also performed in retinal slices of eyes subjected to 6 weeks of OHT and age-match controls. Once again there was a down-regulation of A3R at the level of RGCs (data not shown, * $p<0.05$).

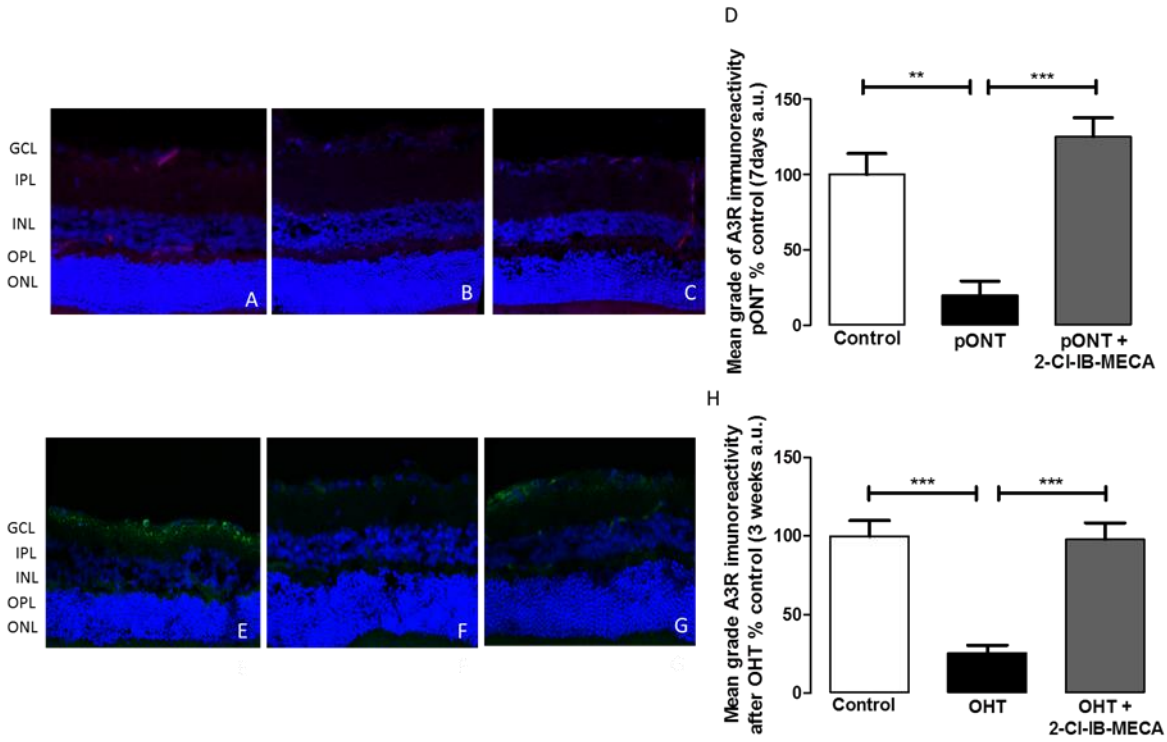

Figure 4.3 - Partial optic nerve transection and chronic ocular hypertension induce a down-regulation of A3R in GCL. Activation of A3R prevents A3R down-regulation after insult. Retinal sections from eyes with pONT or OHT at 7 days or 3 weeks, respectively (pONT and OHT), with A3R agonist treatment (pONT+2-Cl-IB-MECA, OHT+2-Cl-IB-MECA), and controls were processed for A3R immunoreactivity (red - pONT and green- OHT). Nuclei were counterstained with DAPI (blue). Immunohistochemistry images show A3R immunoreactivity in control (A, D, E and H) and injured eyes (B, E, F and H). At 7 days following pONT there was a significant down-regulation (** $p<0.01$) of A3R immunoreactivity (B) compared with control (A). Treatment with the A3R agonist (C) abolished (*** $p<0.001$) the down-regulation on A3R immunoreactivity induced by pONT (B). The immunoreactivity of A3R in pONT eyes treated with the A3R agonist and agonist treatment alone was not significantly different from control group. Retinal sections from eyes with OHT at 3 weeks (F) and controls (E) were processed for A3R immunoreactivity (green). Mean grade of A3R immunostaining significantly decreased at 3 weeks (*** $p<0.001$) of OHT (F) compared to the control eyes (E). Single IVT injection of 2-Cl-IB-MECA prevented A3R down-regulation, (*** $p<0.001$) in the OHT model (F, H). GCL – Ganglion cell layer; IPL – Inner plexiform layer; INL – Inner nuclear layer; OPL – Outer plexiform layer; ONL – Outer nuclear layer.

4.4.4 Activation of adenosine A3 receptor reduces RGC apoptosis induced by partial optic nerve transection and chronic ocular hypertension

We also evaluated the potential neuroprotective effect of the activation of A3R after pONT and OHT. Treatment with A3R agonist, 2-Cl-IB-MECA (1.2 µM; IVT injection), was performed just before pONT. Seven days after pONT plus treatment with the A3R agonist, *in vivo* DARC imaging showed a decrease in the number of annexin V-positive cells, compared with pONT group (171.3±33.5 vs 321.7±27.1 % control, *** $p<0.001$). The number of annexin V-positive cells after treatment with A3R agonist alone was not significantly different from control (175.6±26.4 vs 100.0±24.0 % control). *In vivo* DARC imaging was used to evaluate the level of apoptosis after 3 weeks of OHT with 2-Cl-IB-MECA treatment. The results show that treatment with the A3R agonist decreased (*** $p<0.001$) the levels of apoptosis 3 weeks after OHT (Fig 4.4F, H) compared to OHT without treatment (Fig 4.4E, H). To evaluate whether the protective effects were mediated by A3R activation, treatment with A3R agonist together with a selective antagonist (MRS 1220, 1.2 µM) was performed. Treatment of the OHT model with both the A3R agonist and antagonist showed no significant difference to OHT alone (Fig 4.4H), corroborating that the protective effects observed under treatment with A3R agonist are due to A3R activation rather than other adenosine receptors. Furthermore, there was no effect on IOP after an intravitreal injection of A3R in the OHT model. Nevertheless, a tendency for a decrease in IOP was detected, although this did not reach statistical significance.

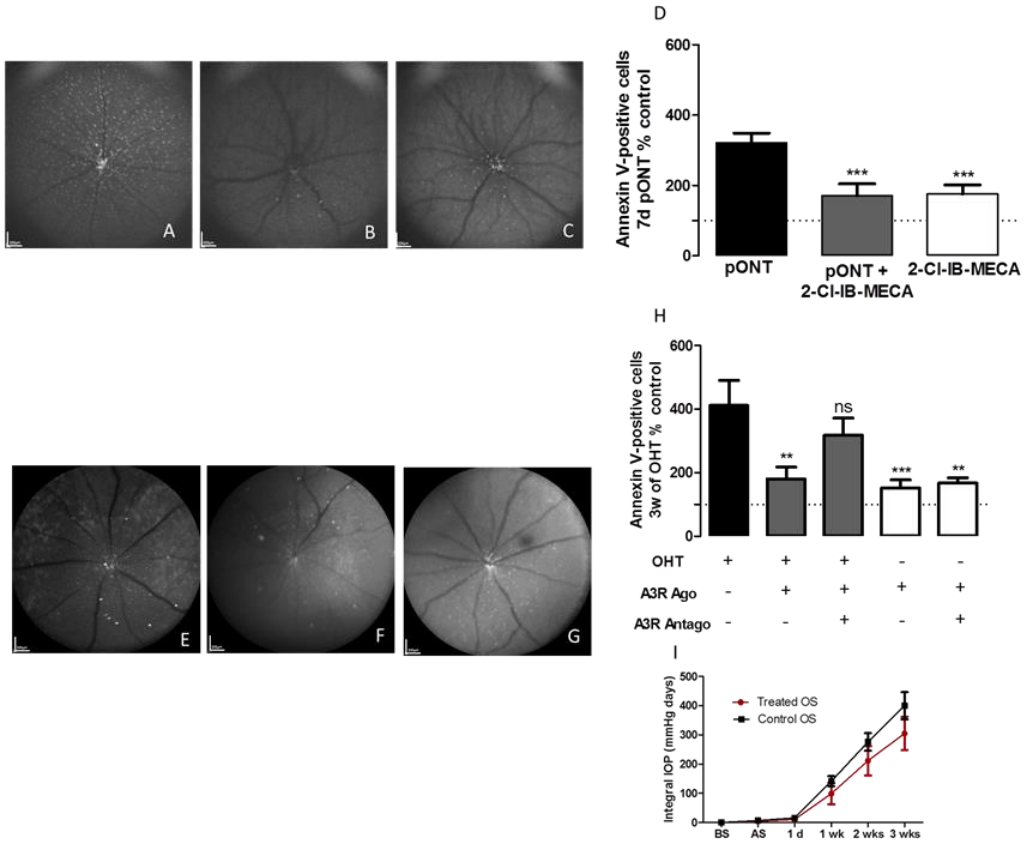

Figure 4.4 - Activation of A3R protects RGC from apoptosis induced by partial optic nerve transection and chronic ocular hypertension as visualized using *in vivo* DARC. *In vivo* DARC images obtained using HRA Spectralis showed white spots representing annexin V-positive cells 2h following IVT injection of fluorescently-labelled annexin V. Treatment with a single IVT injection of the adenosine A3 receptor agonist, 1.2 µM 2-Cl-IB-MECA (C), resulted in a significant reduction (*** $p<0.001$) of RGC apoptosis (D) compared with 7 days pONT (A). Treatment of pONT eyes with the agonist (B) or treatment of normal eyes with 2-Cl-IB-MECA (C) was not significantly different compared to control group. Similarly, in the OHT (E) treatment with a single IVT injection of 1.2 µM 2-Cl-IB-MECA (F) resulted in a significant reduction (**$p<0.01$) of RGC apoptosis (H) compared with OHT group after 3 weeks (E). Agonist treatment of OHT eyes (F) and 2-Cl-IB-MECA injected in non-OHT eyes (G) did not induce significant differences compared to control group. Similarly, treatment of OHT animals with the A3R agonist and antagonist together was not significantly different from OHT (H). The number of apoptotic cells in eyes injected with the A3R agonist alone (A3R Ago) or with the A3R agonist and antagonist together (A3R Ago&Ant) was not significantly different from eyes injected with PBS (H). The IOP was evaluated after application of A3R agonist and it was similar to the control. There was a tendency for a decrease in IOP but did not reach statistical significance (I).

4.4.5 A3 adenosine receptor activation protects retinal ganglion cells after partial optic nerve transection and chronic ocular hypertension

The number of Brn3a-immunoreactive RGCs was assessed in animals treated with the A3R agonist 2-Cl-IB-MECA. The A3R agonist inhibited the decrease in the number of RGCs induced by pONT (Fig 4.5; 67.7±13.8 vs 9.7±5.0 % control). Treatment with the A3R agonist alone was not significantly different from control (98.8±23.1 vs 100±17.3 % control). Moreover, the number of Brn3a-positive cells was also counted on retina flat-mounts of the same retinas imaged with DARC at 3 weeks of OHT. The results show that treatment with a single intravitreal injection of 1.2 µM 2-Cl-IB-MECA significantly inhibited (* $p<0.05$) RGC loss (92.5±0.8 % control) compared with 3 weeks OHT (87.3±1.1 % control). Treatment with the A3R agonist alone was not different from the control (93.9±2.6 vs 100.0±2.1 % control).

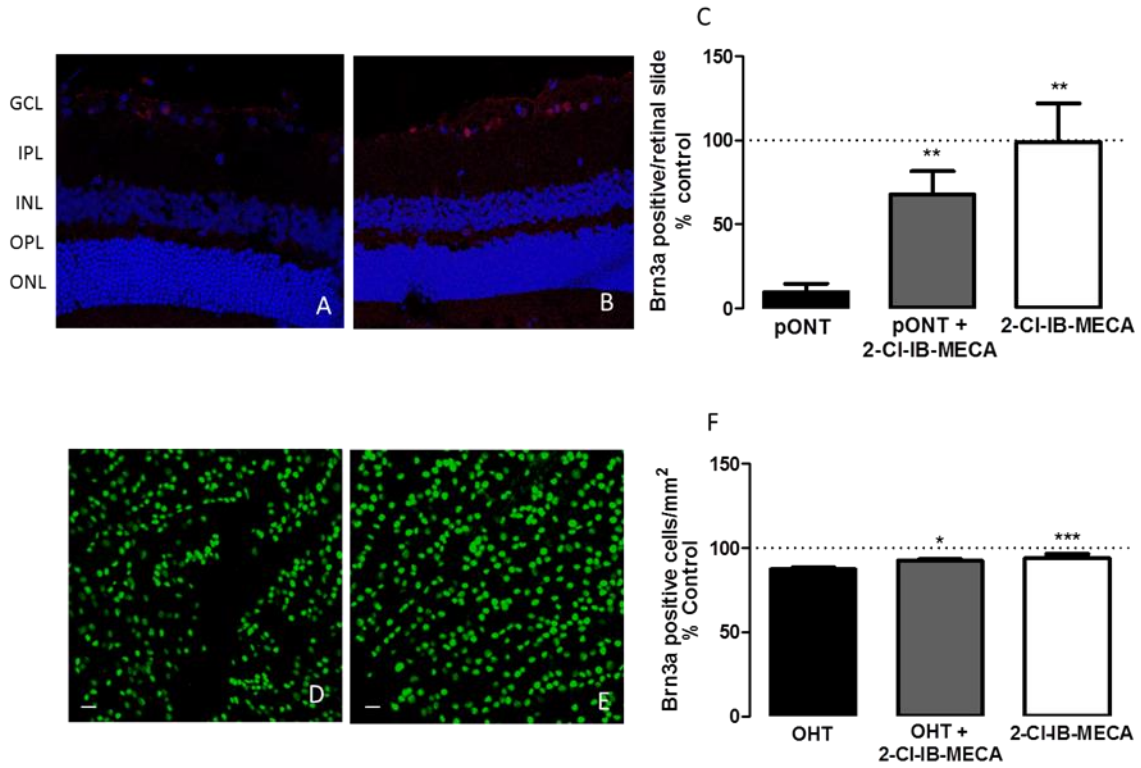

Figure 4.5 - Activation of A3R protects against RGC loss induced by partial optic nerve transection and ocular hypertension. The number of Brn3a-positive cells was counted in retinal slices obtained from animals after 7 days of partial optic nerve transection without (A) and with treatment with the A3R agonist (B). A3R activation (1.2 µM 2-Cl-IB-MECA; pONT+2-Cl-IB-MECA) significantly prevents (** $p<0.01$) RGC loss (C) compared with 7 days of pONT (A). Agonist treatment per se was not significantly different compared to control (C) although it was different to pONT (C).

The total number of Brn3a-positive cells was counted in retinal whole mounts obtained 3 weeks after OHT with (E) and without (D) A3R agonist treatment. Treatment with A3R agonist (OHT+2-Cl-IB-MECA; E) resulted in a significant increase (* $p<0.05$) in the number of RGCs (F) compared with OHT group. Agonist treatment alone was not significantly different from control (F) although it was significantly different from OHT group. GCL – Ganglion cell layer; IPL – Inner plexiform layer; INL – Inner nuclear layer; OPL – Outer plexiform layer; ONL – Outer nuclear layer.

4.5 Discussion

The results presented herein demonstrate that the immunoreactivity of A3 adenosine receptor is down-regulated in the GCL after injury either by partial optic nerve transection or chronic ocular hypertension, and that activation of A3 receptor protects retinal ganglion cells as evaluated either *in vivo* or histologically.

Activation of A3R has been previously shown to protect cells against a different number of insults. A3R activation was reported to be involved in ischemic preconditioning protection of cardiac myocytes (Armstrong and Ganote, 1994; Wang et al., 1997). Transgenic mice over-expressing A3R are protected against post ischemic insult compared with wild type animals, conferring cardioprotection (Cross et al., 2002). The A3R agonist 2-Cl-IB-MECA exerts protective effects in the brain *in vivo,* and in primary cortical culture after a hypoxic insult (Chen et al., 2006). In cortical neurons, the activation of A3R depresses signal transmission by inhibiting glutamate release and provides neuroprotection against excitotoxicity (Brand et al., 2001). In addition, A3R KO mice are more susceptible to ischemic brain injury and CO_2-induced neurodegeneration in hippocampus, suggesting that neuroprotective effects are afforded by A3R (Chen et al., 2006).

Neuroprotective effects of A3R have also been studied in the retina. Activation of A3R was shown to be protective to isolated rat RGCs exposed to NMDA or glutamate. A3R activation by 2-Cl-IB-MECA decreases intracellular calcium concentration increase after glutamatergic (glutamate and NMDA) insult (Zhang et al., 2010). Prevention of excessive increase of the intracellular Ca^{2+} by A3R agonist (MRS 3558) was also shown after P2X7 application *in vitro* (MRS 3558). Protective effects to RGCs after A3R activation were observed both *in vitro* (MRS 3558) and *in vivo* (IB-MECA, 2-Cl-IB-MECA) (Hu et al., 2010; Zhang et al., 2006b). However, it is still unknown whether A3R activation has protective effects on RGCs under glaucomatous conditions. In the present study, we assessed the neuroprotective effect of A3R activation at the level of GCL in two models of experimental glaucoma. GCL contains RGCs, displaced amacrine cells, glial cells, and other cell types, and it is estimated that 50% of the cells in the RGCL of adult rats are displaced amacrine cells (Farah, 2006; Perry, 1981). Brn3a, a POU domain transcription

factor, is only expressed in ganglion cells in the retina, therefore can be successfully used to label RGCs in the rat retina (Nadal-Nicolás et al., 2009). To confirm that the protective effects of A3R were specific for RGCs, we used an antibody against Brn3a to label RGCs. We demonstrated that activation of A3R significantly promote RGC survival following either pONT or chronic OHT. Likewise, we found that a single treatment with 2-Cl-IB-MECA decreases the number of annexin V-positive cells evaluated *in vivo* by DARC technique, 7 days after pONT and 3 weeks after OHT.

The mechanism by which A3R confers neuroprotection in RGCs is still unknown. As mentioned above, it was reported that A3R activation reduces the intracellular calcium concentration increase triggered by P2X7 activation, NMDA or glutamate, in isolated rat RGCs (Zhang et al., 2010, 2006a). Moreover, the protective effect of ischemia pre-conditioning in cardiac myocytes associated with A3R activation was linked to the activation of protein kinase C (PKC) and the opening of K_{ATP} channels in mitochondria leading to phosphorylation of p38 MAPK (Leshem-Lev et al., 2010; Wan et al., 2008).

We have found that both optic nerve injury and chronic IOP elevation induced a down-regulation of A3R in the GCL, suggesting that reduced expression of A3R may be associated with degeneration and loss of RGCs in both models, or that only cells expressing A3R survive after insult. In support of this, our results also show that activation of A3R significantly reduced RGC apoptosis *in vivo* and inhibited RGC degeneration as evaluated histologically.

Upregulation of A3R was found in ciliary tissue in eyes with pseudoexfoliation syndrome and in neoplastic cells, compared to normal cells (Fishman et al., 2011; Schlötzer-Schrehardt et al., 2005). This is in contrast to our findings where we see a down-regulation of A3R immunoreactivity in ganglion cell layer in glaucoma-related insults.

Moreover, in transgenic mice, A3R overexpression confers cardioprotection to these animals compared to wild type animals (Cross et al., 2002). In accordance with these results, we found that treatment with an A3R agonist prevented the downregulation of A3R immunoreactivity induced in both pONT and OHT models and protected RGCs from cell death, demonstrating that activation of A3R in neuroprotective for RGCs.

Modulation of adenosine receptors has been reported to be one of the most promising neuroprotective agents in CNS and targeting G protein-coupled receptors represents more than 30% of all drugs marketed by pharmaceutical industry (Cunha, 2005; Hopkins and Groom, 2002b; Venkatakrishnan et al., 2013). Also important is the fact that there are several on-going clinical trials for a number of diseases related with the modulation of adenosine receptors. In particular, agonists acting on A3R to lower IOP are under clinical trial for glaucoma (Gessi et al., 2011a, 2011b).

The involvement of A3R in controlling the IOP has been previously studied. It has been reported an increase in the IOP after topical application of A3R agonist (Avila et al., 2001; Wang et al., 2007; Yang et al., 2005). Our results show no significant effects of A3R agonist administration, despite a tendency for a decrease in IOP in animals treated with the 2-Cl-IB-MECA. Nevertheless, in this work the A3R agonist was IVT injected while in previous reports it was topically applied, which could explain the difference in the results. For instance, a decrease in IOP was reported in patients with dry eye syndrome when the A3R agonist (IB-MECA, CF101) was orally administered (Avni et al., 2010). The authors also reinforce the fact that in previous studies (Avila et al., 2001; Wang et al., 2007), A3R agonist was topically applied (once) and the IOP was measured immediately after treatment while in their study it was chronically administrated (Avni et al., 2010).

The main conclusion of this work is that A3R activation with 2-Cl-IB-MECA is protective to retinal neurons, and particularly to RGCs, in two different models of RGCs degeneration. To our knowledge, this is the first work using experimental models of glaucoma to investigate the neuroprotective effect of A3R activation. Our results may have relevance in the treatment of patients with glaucoma.

4.6 Acknowledgements:

This study was supported by Foundation for Science and Technology, Portugal (Strategic Project PEst-C/SAU/UI3282/2011; fellowship SFRH/BD/47947/2008) and COMPETE-FEDER. We would like to thank Prof. Claire Mitchell, University of Pennsylvania, USA, for general advice for this work. Conflict of Interest: M F Cordeiro – Patent application.

4.7 References

Armstrong, S., Ganote, C.E., 1994. Adenosine receptor specificity in preconditioning of isolated rabbit cardiomyocytes: evidence of A3 receptor involvement. Cardiovasc. Res. 28, 1049–1056.

Avila, Stone, R. a, Civan, M.M., 2001. A(1)-, A(2A)- and A(3)-subtype adenosine receptors modulate intraocular pressure in the mouse. Br. J. Pharmacol. 134, 241–5.

Avni, I., Garzozi, H.J., Barequet, I.S., Segev, F., Varssano, D., Sartani, G., Chetrit, N., Bakshi, E., Zadok, D., Tomkins, O., Litvin, G., Jacobson, K. a, Fishman, S., Harpaz, Z., Farbstein, M., Yehuda, S.B., Silverman, M.H., Kerns, W.D., Bristol, D.R., Cohn, I., Fishman, P., 2010. Treatment of dry eye syndrome with orally administered CF101: data from a phase 2 clinical trial. Ophthalmology 117, 1287–93.

Brand, a, Vissiennon, Z., Eschke, D., Nieber, K., 2001. Adenosine A(1) and A(3) receptors mediate inhibition of synaptic transmission in rat cortical neurons. Neuropharmacology 40, 85–95.

Chang, E.E., Goldberg, 2012. Glaucoma 2.0: neuroprotection, neuroregeneration, neuroenhancement. Ophthalmology 119, 979–86.

Chauhan, B.C., Pan, J., Archibald, M.L., LeVatte, T.L., Kelly, M.E.M., Tremblay, F., 2002. Effect of intraocular pressure on optic disc topography, electroretinography, and axonal loss in a chronic pressure-induced rat model of optic nerve damage. Invest. Ophthalmol. Vis. Sci. 43, 2969–76.

Chen, Harvey, B.K., Shen, H., Chou, J., Victor, A., Wang, Y., 2006. Activation of Adenosine A3 Receptors Reduces Ischemic Brain Injury in Rodents. J. Neurosci. Res. 84, 1848–1855.

Cordeiro, M.F., Guo, L., Luong, V., Harding, G., Wang, W., Jones, H.E., Moss, S.E., Sillito, A.M., Fitzke, F.W., 2004. Real-time imaging of single nerve cell apoptosis in retinal neurodegeneration. Proc. Natl. Acad. Sci. U. S. A. 101, 13352–6.

Cross, H.R., Murphy, E., Black, R.G., Auchampach, J., Steenbergen, C., 2002. Overexpression of A(3) adenosine receptors decreases heart rate, preserves energetics, and protects ischemic hearts. Am. J. Physiol. Heart Circ. Physiol. 283, H1562–8.

Cunha, R. a, 2005. Neuroprotection by adenosine in the brain: From A(1) receptor activation to A (2A) receptor blockade. Purinergic Signal. 1, 111–34.

Filmore, D., 2004. It;s a GPCR world. Mod. Drug Discov. 24–27.

Fishman, P., Bar-Yehuda, S., Liang, B.T., Jacobson, K. a, 2011. Pharmacological and therapeutic effects of A(3) adenosine receptor agonists. Drug Discov. Today 00, 1–8.

Gessi, S., Merighi, S., Fazzi, D., Stefanelli, A., Varani, K., Borea, P.A., 2011a. Adenosine receptor targeting in health and disease. Expert Opin. Investig. Drugs 20, 1591–609.

Gessi, S., Merighi, S., Varani, K., Borea, P.A., 2011b. Adenosine receptors in health and disease. Adv. Pharmacol. 61, 41–75.

Guo, L., Cordeiro, M.F., 2008. Assessment of neuroprotection in the retina with DARC. Prog. Brain Res. 173, 437–50.

Guo, L., Moss, S.E., Alexander, R.A., Ali, R.R., Fitzke, F.W., Cordeiro, M.F., 2008. Retinal Ganglion Cell Apoptosis in Glaucoma Is Related to Intraocular Pressure and IOP-Induced Effects on Extracellular Matrix. Invest. Ophthalmol. Vis. Sci. 46, 175–182.

Heijl, A., Leske, M., Bengtsson, Bo, Hyman, L., Bengtsson, Boel, Hussein, M., 2002. Reduction of Intraocular Pressure and Glaucoma Progression. Arch Ophthalmol. 20, 9–12.

Hopkins, A.L., Groom, C.R., 2002a. The druggable genome. Nat. Rev. Drug Discov. 1, 727–30.

Hopkins, A.L., Groom, C.R., 2002b. The druggable genome. Nat. Rev. Drug Discov. 1, 727–30.

Hu, H., Lu, W., Zhang, M., Zhang, X., Argall, A.J., Patel, S., Lee, G.E., Kim, Y.-C., Jacobson, K. a, Laties, A.M., Mitchell, C.H., 2010. Stimulation of the P2X7 receptor kills rat retinal ganglion cells in vivo. Exp. Eye Res. 91, 425–32.

Leshem-Lev, D., Hochhauser, E., Chanyshev, B., Isak, A., Shainberg, A., 2010. Adenosine A(1) and A (3) receptor agonists reduce hypoxic injury through the involvement of P38 MAPK. Mol. Cell. Biochem. 345, 153–60.

Leske, M., Heijl, A., Hussein, M., Bengtsson, B., Hyman, L., Komaroff, E., 2003. Factors for Glaucoma Progression and the Effect of Treatment. Arch Ophthalmol. 121.

Levkovitch-Verbin, H., 2003. A Model to Study Differences between Primary and Secondary Degeneration of Retinal Ganglion Cells in Rats by Partial Optic Nerve Transection. Invest. Ophthalmol. Vis. Sci. 44, 3388–3393.

Levkovitch-Verbin, H., Quigley, H. a, Martin, K.R.G., Valenta, D., Baumrind, L. a, Pease, M.E., 2002. Translimbal laser photocoagulation to the trabecular meshwork as a model of glaucoma in rats. Invest. Ophthalmol. Vis. Sci. 43, 402–10.

Morrison, Moore, C.G., Deppmeier, L.M., Gold, B.G., Meshul, C.K., Johnson, E.C., 1997. A rat model of chronic pressure-induced optic nerve damage. Exp. Eye Res. 64, 85–96.

Nadal-Nicolás, F.M., Jiménez-López, M., Sobrado-Calvo, P., Nieto-López, L., Cánovas-Martínez, I., Salinas-Navarro, M., Vidal-Sanz, M., Agudo, M., 2009. Brn3a as a marker of retinal ganglion cells: qualitative and quantitative time course studies in naive and optic nerve-injured retinas. Invest. Ophthalmol. Vis. Sci. 50, 3860–8.

Quigley, H., Broman, 2006. The number of people with glaucoma worldwide in 2010 and 2020. Br. J. Ophthalmol. 90, 262–7.

Schlötzer-Schrehardt, U., Zenkel, M., Decking, U., Haubs, D., Kruse, F.E., Jünemann, A., Coca-Prados, M., Naumann, G.O.H., 2005. Selective upregulation of the A3 adenosine receptor in eyes with pseudoexfoliation syndrome and glaucoma. Invest. Ophthalmol. Vis. Sci. 46, 2023–34.

Venkatakrishnan, a J., Deupi, X., Lebon, G., Tate, C.G., Schertler, G.F., Babu, M.M., 2013. Molecular signatures of G-protein-coupled receptors. Nature 494, 185–94.

Wan, T.C., Ge, Z., Tampo, A., Mio, Y., Bienengraeber, M.W., Tracey, W.R., Gross, G.J., Kwok, W., Auchampach, J.A., 2008. The A 3 Adenosine Receptor Agonist CP-532 , 903 [N 6 - (2 , 5- Protects against Myocardial Ischemia / Reperfusion Injury via the Sarcolemmal ATP-Sensitive Potassium Channel. J. Phamacology Exp. Ther. 324, 234–243.

Wang, Do, C.W., Avila, M.Y., Stone, R. a, Jacobson, K. a, Civan, M.M., 2007. Barrier qualities of the mouse eye to topically applied drugs. Exp. Eye Res. 85, 105–12.

Wang, J., Drake, L., Sajjadi, F., Firestein, G.S., Mullane, K.M., Bullough, D. a, 1997. Dual activation of adenosine A1 and A3 receptors mediates preconditioning of isolated cardiac myocytes. Eur. J. Pharmacol. 320, 241–8.

West, H., Richardson, W.D., Fruttiger, M., 2005. Stabilization of the retinal vascular network by reciprocal feedback between blood vessels and astrocytes. Development 132, 1855–62.

Yang, H., Avila, M.Y., Peterson-Yantorno, K., Coca-Prados, M., Stone, R. a., Jacobson, K. a., Civan, M.M., 2005. The Cross-Species A 3 Adenosine-Receptor Antagonist MRS 1292 Inhibits Adenosine-Triggered Human Nonpigmented Ciliary Epithelial Cell Fluid Release and Reduces Mouse Intraocular Pressure. Curr. Eye Res. 30, 747–754.

Zhang, Budak, M.T., Lu, W., Khurana, T.S., Zhang, X., Laties, A.M., Mitchell, C.H., 2006a. Identification of the A3 adenosine receptor in rat retinal ganglion cells. Mol. Vis. 12, 937–48.

Zhang, Hu, H., Zhang, X., Lu, W., Lim, J., Eysteinsson, T., Jacobson, K. a, Laties, A.M., Mitchell, C.H., 2010. The A3 adenosine receptor attenuates the calcium rise triggered by NMDA receptors in retinal ganglion cells. Neurochem. Int. 56, 35–41.

Zhang, Zhang, M., Laties, A.M., Mitchell, C.H., 2006b. Balance of purines may determine life or death of retinal ganglion cells as A3 adenosine receptors prevent loss following P2X7 receptor stimulation. J. Neurochem. 98, 566–75.

5. CHAPTER Five: General Discussion

Table of Contents

5.1 General Discussion

Glaucoma is a leading cause of irreversible blindness (Quigley and Broman, 2006). Although the primary cause and the pathogenesis of glaucoma are still unclear, elevated IOP is considered to be the most important risk factor, namely for optic nerve head damage and RGC death (Quigley, 2011). Lowering IOP has demonstrated to attenuate the death of RGCs (Heijl et al., 2002; Leske et al., 2003) and that is still to date the only pharmacologic treatment available. However, lowering the IOP does not always stop disease progression (Chang and Goldberg, 2012). Therefore, new and more effective treatments are necessary, and neuroprotection of RGCs is considered to offer potential as an additional therapy. We investigated the potential neuroprotective effects of activation of A3R in different models of RGC degeneration both *in vitro* and *in vivo*.

In the first part of this work (chapter 2), we show that DMSO induces apoptosis in RGCs *in vivo*. High concentrations of DMSO induce toxicity due to plasma membrane pore formation (Aita et al., 2005), but this effect has not been previously observed (in vitro) at concentrations lower than 7 mol % DMSO (de Ménorval et al., 2012; Gurtovenko and Anwar, 2007; Gurtovenko et al., 2008; Notman et al., 2006). We demonstrated that 5 µl of intravitreally administered DMSO solutions at concentrations above 1% (v/v) caused a significant and dose-dependent increase in the number of cells presenting phosphatidylserine externalization *in vivo*. This was determined using the DARC technique to assess the number of annexin V-positive cells (Figure 2.1), and is indicative of cells have entered early stage apoptosis within 2 h of the DMSO insult (Cordeiro et al., 2004; Galvao et al., 2013). This observation is in agreement with previous work (Tsai et al., 2009), where it was reported, using electroretinography, that rat retinal function is impaired by intravitreal administration of 2 µl solutions of DMSO at concentrations greater than 0.6% (v/v).

In vitro, DMSO induces apoptosis in RGCs in a concentration-dependent manner, for concentrations above 2% (v/v). After DMSO exposure, phosphatidylserine is externalise at concentrations equal to or greater than 2% (v/v), whilst increasing the number of cells that underwent chromatin condensation, as visualised using Hoechst staining (Figure 2.2). This observation was supported by a concentration-dependent decrease in cell

viability using the MTT assay, and an increase in TUNEL-positive cells (Figures 2.2 and 2.4) at concentrations above 2 % DMSO (v/v). The *in vitro* observations are in agreement with the existing literature where DMSO concentrations above 2.5% (v/v) are required to induce apoptosis *in vitro* (Liu et al., 2001). We propose that the mechanism by which DMSO induces cell death (Figure 2.7) involves inhibition of mitochondrial respiration leading to decreased oxygen consumption within 4 min of application (Figure 2.3). Moreover, we found that DMSO induces an increase in cytosolic calcium before phosphatidylserine externalization (Figure 2.3). Calcium has been previously implicated in phosphatidylserine flipping (Lee et al., 2013; Mirnikjoo et al., 2009a, 2009b) and is known to induce calpain activation (Norberg et al., 2010; Polster et al., 2005). Calpain acts inducing the release and redistribution of AIF to the nucleus (Norberg et al., 2010; Polster et al., 2005). This could occur through Bax-translocation from the cytosol to the mitochondria (Er et al., 2006; Vieira and Kroemer, 2003). Increased levels of Bax in mitochondrial fractions and decreased levels in the cytosolic fractions are in accordance with Bax oligomerization and pore formation indicating that AIF translocation from mitochondria is via Bax pore formation (Figure 2.5). AIF has also been implicated in phosphatidylserine externalization through the interaction with scramblase Scrm-1 (Wang et al., 2007b) and AIF translocates to the nucleus causing DNA fragmentation and activation of PARP-1 (Figure 2.5 and 2.6) leading to cell death (Figure 2.2).

Since its discovery, numerous studies have employed DMSO as a solvent and vehicle control as it was considered to have low toxicity. In chapter 2, we demonstrate that DMSO is toxic *in vivo* and *in vitro* at low concentrations, and data strongly suggest that care should be taken to consider the toxicity of this molecule when used as a solvent, particularly *in vivo*. The harmful effect of DMSO concentrations as low as 1-2 % (v/v) (140 mM – 280 mM DMSO) can cause cell death via an AIF dependent pathway. As our results demonstrate that DMSO can damage retinal cells, we recommend that the percentage of DMSO used to dissolve drugs should be kept to a minimum (less than 1% v/v injected *in vivo*), with the inclusion of additional controls to allow assessment for DMSO vehicle toxicity. Finally, alternate solvent systems should be considered, with the use of liposome and nanoparticles formulations, promising alternatives for application of non-water soluble drugs to the eye and CNS.

On the second part of this work, we investigated the potential neuroprotective effects of activation of A3R *in vitro* and in animal models of retinal degeneration (Chapters 3 and 4). In chapter 3, we first showed that immunopurified isolated RGCs are immunoreactive to A3R (Figure 3.2). Moreover, we also demonstrated that in more complex systems, as cultured retinal explants and retinal cryosections, RGCs are also immunoreactive for A3R (Figure 3.2). To our knowledge, this was the first time that A3R was identified in RGCs by immunofluorescence techniques. We demonstrated that activation of A3R protects retinal neurons both *in vitro* against kainate and NMDA induced excitotoxicity in retinal mixed cultures (Figure 3.1) and organotypic retinal cultures (Figure 3.3), respectively. The activation of A3R was also demonstrated to have protective effects in two different animal models, either the DMSO-induced retinal degeneration (Figures 3.4 and 3.5) and in an ischemic-reperfusion model (Figure 3.7). Moreover, in chapter 4 we demonstrated that activation of A3 adenosine receptor protected retinal neurons *in vivo* against partial optic nerve transection and in a glaucoma model of ocular hypertension (Figures 4.4 and 4.5).

Activation of A3R has been previously proved to protect cells against a different number of insults. A3R agonist (2-Cl-IB-MECA) was shown to have a protective role both *in vivo*, in the brain, and *in vitro,* in cortical neurons after a hypoxic insult (Chen et al., 2006). Activation of A3R, in cortical neurons, was shown to be neuroprotective against excitotoxicity, inhibiting glutamate release (Brand et al., 2001). Moreover, A3R knock-out mice are more susceptible to ischemic brain injury and increased CO_2-induced neurodegeneration in hippocampus, evidencing a protective role of A3R (Chen et al., 2006). Neuroprotective effects of A3R have not been extensively studied in the retinal tissue both *in vivo* and *in vitro*. In immunopurified isolated RGCs, activation of A3R attenuates intracellular calcium concentration after NMDA or P2X7 activation (Hu et al., 2010; Zhang et al., 2010, 2006). In addition, A3R agonist MRS 3558 prevented RGC loss induced by activation of the P2X7 receptor (Hu et al., 2010).

The involvement of A3R in the intraocular pressure has been extensively studied, and an increase in the IOP after topical application of A3R agonist has been reported (Avila et al., 2001; Wang et al., 2007a; Yang et al., 2005). Our results show that after the intravitreal administration of the A3 agonist there is a tendency for a decrease in IOP,.

The reason for this discrepancy could be the mode of administration of the drug. While we administered A3R agonist intravitreally, others have administered topically. In accordance with our results, a decrease in IOP was reported in patients with dry eye syndrome when A3R agonist (IB-MECA, CF101) was orally administered (Avni et al., 2010). The authors also reinforce the fact that in previous studies (Avila et al., 2001; Wang et al., 2007a), A3R agonist was topically applied (once) and the IOP was measured immediately after treatment while in Avni et al., study was chronically administered (Avni et al., 2010).

Our results show a decreased expression of A3R after different insults (I-R, pONT and OHT). This contradicts some reports (Fishman et al., 2011; Schlötzer-Schrehardt et al., 2005), since in other experimental models this receptor was found to be upregulated. Upregulation of A3R was found in ciliary tissue in eyes with pseudoexfoliation syndrome, and in different neoplastic cells, compared to normal cells (Fishman et al., 2011; Schlötzer-Schrehardt et al., 2005). Future work is needed to fully understand the involvement of this receptor in pathological events in the retina.

To better understand the down-regulatory effect of A3R after an insult, RNA expression for A3R from control samples and after different RGC insults should be evaluated using purified samples of RNA isolated from rat RGC (Veldman et al., 2007). The evaluation of A3R at different time points, would give a better profile of the involvement of this receptor after an insult to RGC.

To further evaluate the protective effects by chronic activation of A3R, intravitreal injection of biodegradable implants, already used for other ocular diseases (Lobo et al., 2010; Yasukawa and Ogura, 2010), containing A3R agonist (2-Cl-IB-MECA), would allow a full assessment of the effects afforded by the activation of this receptor. Pattern ERG, regular measurement of IOP and DARC technique could be used to evaluate RGC function, IOP and RGC survival, respectively, after A3R activation.

Possible further work regarding the results presented herein should fully assess IOP after topical application of A3R agonist/antagonist with an appropriate formulation. Previous reports were based on the use of 2-8% DMSO solutions of A3R antagonist to be applied as eye drops (Avila et al., 2001). Herein, we show that the concentrations of DMSO used

in these formulations induced cell death *in vivo* (intravitreally) and *in vitro* (RGC-5) being not appropriate due to their toxic effects.

Moreover, to evaluate the mechanism by which A3R agonist protects RGCs, purified RGCs could be used to assess the downstream mechanism after A3R activation. It was previously reported that A3R activation protect cardiac cells through opening of mitochondrial ATP channels and p38 MAPK phosphorylation (Leshem-Lev et al., 2010).

Moreover, modulation of all adenosine receptors are under clinical trials for a number of diseases (Gessi et al., 2011a, 2011b). In particular, targeting A3R receptors is an important step forward to a potential IOP control in glaucoma therapy. Recent reports show that an A3R agonist (IB-MECA - CF101) is already under clinical trial for glaucoma (Gessi et al., 2011a, 2011b), although no previous studies have been published regarding the protective effects of this drug in animal models of glaucoma. In fact, modulation of adenosine receptors has been reported to be one of the most promising neuroprotective strategies in CNS and targeting G protein coupled receptors is known to represent by 2002 more than 30% of all the drugs marketed by pharmaceutical industry (Cunha, 2005; Hopkins and Groom, 2002). Nowadays, it has been claimed by some that glaucoma could be a brain disease more than an eye disease (Williams et al., 2013) and adenosine treatment is known to be successfully used in different conditions in the brain (Gessi et al., 2011a; Jacobson and Gao, 2006; Roth, 2004).

Together, this work shows that A3R activation with 2-Cl-IB-MECA is protective to retinal neurons, especially RGCs, in different models of RGC degeneration. To our knowledge, this is the first work using a vast number of models including experimental models of glaucoma to investigate the neuroprotective effect of A3R activation. Our results may have relevance in the treatment of RGCs related diseases, mainly in glaucoma.

5.2 References

Aita, K., Irie, H., Tanuma, Y., Toida, S., Okuma, Y., Mori, S., Shiga, J., 2005. Apoptosis in murine lymphoid organs following intraperitoneal administration of dimethyl sulfoxide (DMSO). Exp. Mol. Pathol. 79, 265–71.

Avila, Stone, R. a, Civan, M.M., 2001. A(1)-, A(2A)- and A(3)-subtype adenosine receptors modulate intraocular pressure in the mouse. Br. J. Pharmacol. 134, 241–5.

Avni, I., Garzozi, H.J., Barequet, I.S., Segev, F., Varssano, D., Sartani, G., Chetrit, N., Bakshi, E., Zadok, D., Tomkins, O., Litvin, G., Jacobson, K. a, Fishman, S., Harpaz, Z., Farbstein, M., Yehuda, S.B., Silverman, M.H., Kerns, W.D., Bristol, D.R., Cohn, I., Fishman, P., 2010. Treatment of dry eye syndrome with orally administered CF101: data from a phase 2 clinical trial. Ophthalmology 117, 1287–93.

Chang, E.E., Goldberg, 2012. Glaucoma 2.0: neuroprotection, neuroregeneration, neuroenhancement. Ophthalmology 119, 979–86.

Chen, Harvey, B.K., Shen, H., Chou, J., Victor, A., Wang, Y., 2006. Activation of Adenosine A3 Receptors Reduces Ischemic Brain Injury in Rodents. J. Neurosci. Res. 84, 1848–1855.

Cordeiro, M.F., Guo, L., Luong, V., Harding, G., Wang, W., Jones, H.E., Moss, S.E., Sillito, A.M., Fitzke, F.W., 2004. Real-time imaging of single nerve cell apoptosis in retinal neurodegeneration. Proc. Natl. Acad. Sci. U. S. A. 101, 13352–6.

Cunha, R. a, 2005. Neuroprotection by adenosine in the brain: From A(1) receptor activation to A (2A) receptor blockade. Purinergic Signal. 1, 111–34.

De Ménorval, M.-A., Mir, L.M., Fernández, M.L., Reigada, R., 2012. Effects of dimethyl sulfoxide in cholesterol-containing lipid membranes: a comparative study of experiments in silico and with cells. PLoS One 7, e41733.

Er, E., Oliver, L., Cartron, P.-F., Juin, P., Manon, S., Vallette, F.M., 2006. Mitochondria as the target of the pro-apoptotic protein Bax. Biochim. Biophys. Acta 1757, 1301–11.

Fishman, P., Bar-Yehuda, S., Liang, B.T., Jacobson, K. a, 2011. Pharmacological and therapeutic effects of A(3) adenosine receptor agonists. Drug Discov. Today 00, 1–8.

Galvao, J., Davis, B.M., Cordeiro, M.F., 2013. In vivo imaging of retinal ganglion cell apoptosis. Curr. Opin. Pharmacol. 13, 123–7.

Gessi, S., Merighi, S., Fazzi, D., Stefanelli, A., Varani, K., Borea, P.A., 2011a. Adenosine receptor targeting in health and disease. Expert Opin. Investig. Drugs 20, 1591–609.

Gessi, S., Merighi, S., Varani, K., Borea, P.A., 2011b. Adenosine receptors in health and disease. Adv. Pharmacol. 61, 41–75.

Gurtovenko, A. a, Anwar, J., 2007. Modulating the structure and properties of cell membranes: the molecular mechanism of action of dimethyl sulfoxide. J. Phys. Chem. B 111, 10453–60.

Gurtovenko, A. a, Onike, O.I., Anwar, J., 2008. Chemically induced phospholipid translocation across biological membranes. Langmuir 24, 9656–60.

Heijl, A., Leske, M., Bengtsson, Bo, Hyman, L., Bengtsson, Boel, Hussein, M., 2002. Reduction of Intraocular Pressure and Glaucoma Progression. Arch Ophthalmol. 20, 9–12.

Hopkins, A.L., Groom, C.R., 2002. The druggable genome. Nat. Rev. Drug Discov. 1, 727–30.

Hu, H., Lu, W., Zhang, M., Zhang, X., Argall, A.J., Patel, S., Lee, G.E., Kim, Y.-C., Jacobson, K. a, Laties, A.M., Mitchell, C.H., 2010. Stimulation of the P2X7 receptor kills rat retinal ganglion cells in vivo. Exp. Eye Res. 91, 425–32.

Jacobson, Gao, Z., 2006. Adenosine receptors as therapeutic targets. Nat. Rev. Drug Discov. 5, 247–264.

Lee, Meng, X.W., Flatten, K.S., Loegering, D. a, Kaufmann, S.H., 2013. Phosphatidylserine exposure during apoptosis reflects bidirectional trafficking between plasma membrane and cytoplasm. Cell Death Differ. 20, 64–76.

Leshem-Lev, D., Hochhauser, E., Chanyshev, B., Isak, A., Shainberg, A., 2010. Adenosine A(1) and A (3) receptor agonists reduce hypoxic injury through the involvement of P38 MAPK. Mol. Cell. Biochem. 345, 153–60.

Leske, M., Heijl, A., Hussein, M., Bengtsson, B., Hyman, L., Komaroff, E., 2003. Factors for Glaucoma Progression and the Effect of Treatment. Arch Ophthalmol. 121.

Liu, Yoshikawa, H., Nakajima, Y., Tasaka, K., 2001. Involvement of mitochondrial permeability transition and caspase-9 activation in dimethyl sulfoxide-induced apoptosis of EL-4 lymphoma cells. Int. Immunopharmacol. 1, 63–74.

Lobo, A.-M., Sobrin, L., Papaliodis, G.N., 2010. Drug delivery options for the treatment of ocular inflammation. Semin. Ophthalmol. 25, 283–8.

Mirnikjoo, B., Balasubramanian, K., Schroit, A.J., 2009a. Mobilization of lysosomal calcium regulates the externalization of phosphatidylserine during apoptosis. J. Biol. Chem. 284, 6918–23.

Mirnikjoo, B., Balasubramanian, K., Schroit, A.J., 2009b. Suicidal membrane repair regulates phosphatidylserine externalization during apoptosis. J. Biol. Chem. 284, 22512–6.

Norberg, E., Orrenius, S., Zhivotovsky, B., 2010. Mitochondrial regulation of cell death: processing of apoptosis-inducing factor (AIF). Biochem. Biophys. Res. Commun. 396, 95–100.

Notman, R., Noro, M., O'Malley, B., Anwar, J., 2006. Molecular basis for dimethylsulfoxide (DMSO) action on lipid membranes. J. Am. Chem. Soc. 128, 13982–3.

Polster, B.M., Basañez, G., Etxebarria, A., Hardwick, J.M., Nicholls, D.G., 2005. Calpain I induces cleavage and release of apoptosis-inducing factor from isolated mitochondria. J. Biol. Chem. 280, 6447–54.

Quigley, 2011. Glaucoma. Lancet 377, 1367–77.

Quigley, Broman, 2006. The number of people with glaucoma worldwide in 2010 and 2020. Br. J. Ophthalmol. 90, 262–7.

Roth, S., 2004. Endogenous neuroprotection in the retina. Brain Res. Bull. 62, 461–6.

Schlötzer-Schrehardt, U., Zenkel, M., Decking, U., Haubs, D., Kruse, F.E., Jünemann, A., Coca-Prados, M., Naumann, G.O.H., 2005. Selective upregulation of the A3 adenosine receptor in eyes with pseudoexfoliation syndrome and glaucoma. Invest. Ophthalmol. Vis. Sci. 46, 2023–34.

Tsai, T.I., Bui, B. V, Vingrys, A.J., 2009. Dimethyl sulphoxide dose-response on rat retinal function. Doc. Ophthalmol. 119, 199–207.

Veldman, M.B., Bemben, M. a, Thompson, R.C., Goldman, D., 2007. Gene expression analysis of zebrafish retinal ganglion cells during optic nerve regeneration identifies KLF6a and KLF7a as important regulators of axon regeneration. Dev. Biol. 312, 596–612.

Vieira, H., Kroemer, G., 2003. Mitochondria as targets of apoptosis regulation by nitric oxide. IUBMB Life 55, 613–6.

Wang, Do, C.W., Avila, M.Y., Stone, R. a, Jacobson, K. a, Civan, M.M., 2007a. Barrier qualities of the mouse eye to topically applied drugs. Exp. Eye Res. 85, 105–12.

Wang, Wang, J., Gengyo-Ando, K., Gu, L., Sun, C.-L., Yang, C., Shi, Yong, Kobayashi, T., Shi, Yigong, Mitani, S., Xie, X.-S., Xue, D., 2007b. C. elegans mitochondrial factor WAH-1 promotes phosphatidylserine externalization in apoptotic cells through phospholipid scramblase SCRM-1. Nat. Cell Biol. 9, 541–9.

Williams, A.L., Lackey, J., Wizov, S.S., Chia, T.M.T., Gatla, S., Moster, M.L., Sergott, R., Spaeth, G.L., Lai, S., 2013. Evidence for widespread structural brain changes in glaucoma: a preliminary voxel-based MRI study. Invest. Ophthalmol. Vis. Sci. 54, 5880–7.

Yang, H., Avila, M.Y., Peterson-Yantorno, K., Coca-Prados, M., Stone, R. a., Jacobson, K. a., Civan, M.M., 2005. The Cross-Species A 3 Adenosine-Receptor Antagonist MRS 1292 Inhibits Adenosine-Triggered Human Nonpigmented Ciliary Epithelial Cell Fluid Release and Reduces Mouse Intraocular Pressure. Curr. Eye Res. 30, 747–754.

Yasukawa, T., Ogura, Y., 2010. Medical devices for the treatment of eye diseases. Drug Deliv. 197, 469–489.

Zhang, Hu, H., Zhang, X., Lu, W., Lim, J., Eysteinsson, T., Jacobson, K. a, Laties, A.M., Mitchell, C.H., 2010. The A3 adenosine receptor attenuates the calcium rise triggered by NMDA receptors in retinal ganglion cells. Neurochem. Int. 56, 35–41.

Zhang, Zhang, M., Laties, A.M., Mitchell, C.H., 2006. Balance of purines may determine life or death of retinal ganglion cells as A3 adenosine receptors prevent loss following P2X7 receptor stimulation. J. Neurochem. 98, 566–75.

6. CHAPTER SIX: Main Conclusions

Table of Contents

The results presented in this thesis, allowed drawing the following main conclusions:

- DMSO induces cell death to retinal neurons both *in vitro* and *in vivo*. The mechanism by which DMSO induces retinal cell death is through mitochondrial respiration inhibition, intracellular calcium increase, AIF translocation from the mitochondria to the nucleus, and calpain and PARP-1 activation.

- A3 adenosine receptor activation protects retinal ganglion cells *in vitro* after an excitotoxic insult to retinal neural cell cultures and cultured retinal explants.

- A3 adenosine receptor activation protects retinal ganglion cells in two acute animal models of retinal degeneration: DMSO and ischemia-reperfusion models.

- A3 adenosine receptor activation protects retinal ganglion cells in two chronic models of retinal ganglion cell degeneration: partial optic nerve transection and ocular hypertension models.

- Altogether, these results may have relevance to develop new potential treatments for patients with glaucoma targeted to A3 receptors.